



University  
of Glasgow

<https://theses.gla.ac.uk/>

Theses Digitisation:

<https://www.gla.ac.uk/myglasgow/research/enlighten/theses/digitisation/>

This is a digitised version of the original print thesis.

Copyright and moral rights for this work are retained by the author

A copy can be downloaded for personal non-commercial research or study,  
without prior permission or charge

This work cannot be reproduced or quoted extensively from without first  
obtaining permission in writing from the author

The content must not be changed in any way or sold commercially in any  
format or medium without the formal permission of the author

When referring to this work, full bibliographic details including the author,  
title, awarding institution and date of the thesis must be given

Enlighten: Theses

<https://theses.gla.ac.uk/>  
[research-enlighten@glasgow.ac.uk](mailto:research-enlighten@glasgow.ac.uk)

**Chorismate synthase**  
**from**  
***Staphylococcus aureus.***



**University  
of  
Glasgow**

**Malcolm James Horsburgh.**

**October 1995.**

ProQuest Number: 10391312

All rights reserved

INFORMATION TO ALL USERS

The quality of this reproduction is dependent upon the quality of the copy submitted.

In the unlikely event that the author did not send a complete manuscript and there are missing pages, these will be noted. Also, if material had to be removed, a note will indicate the deletion.



ProQuest 10391312

Published by ProQuest LLC (2017). Copyright of the Dissertation is held by the Author.

All rights reserved.

This work is protected against unauthorized copying under Title 17, United States Code  
Microform Edition © ProQuest LLC.

ProQuest LLC.  
789 East Eisenhower Parkway  
P.O. Box 1346  
Ann Arbor, MI 48106 – 1346

*Theris*  
10400  
Copy 2



## ACKNOWLEDGEMENTS

There are a great number of people who have been a part of this project and to whom I would like to extend my deep gratitude.

In particular I must thank my supervisor Professor John Coggins for his enthusiasm and inspiration during all parts of the project and also his patience and guidance with protein studies. My collaboration with Zeneca Pharmaceuticals was extremely productive and I am indebted to Dr. Peter Barth for giving me a thorough lesson in the 'art' of molecular biology and supplying me with a few of the tools of the trade. I thank Dr. Wright Nichols for his frequent, helpful discussions, his guidance in the early stages of the project and for his hospitality.

My extended stay at Zeneca Pharmaceuticals was made more enjoyable thanks to Cheryl Gibson for both putting me up and putting up with me; also thanks to Paul Brotherton, Sarah Brockbank and Carl.

I am indebted to Professor Tim Foster from the Moyne Institute, Dublin for his extremely generous gift of plasmid pCOC102. This allowed a great deal more work to be done on *S. aureus* chorismate synthase. I would also like to thank Dr. Anne Moir from the Krebs Institute, Sheffield for her kind gift of plasmid pMAY1, for her hospitality and for helpful discussions.

I thank Dr. Stephen Bornemann, Dr Peter Macheroux and Dr. Roger Thorneley formerly from the University of Sussex now at the John Innes Centre, Norwich for providing expertise and support with kinetic and flavin studies and for their hospitality.

At Glasgow University I thank John Greene for technical expertise and banter. Also John Christie, David Gillooly, David Gourley, John Gilbert, Gillian Muir, Sureka Chackrewarthy and last but not least Tino Krell for his scientific excellence and discussions.

Finally, I would like to thank Alison Turnbull for her support and patience during the last few years and for making it all worthwhile.

*For my Parents and dedicated to the  
memory of the late Dan Horsburgh.*

## CONTENTS

### **CHAPTER 1. INTRODUCTION.**

1.1. The shikimate pathway.	1
1.2. The enzymes and enzymology of the pre-chorismate pathway.	2
1.2.1. DAHP synthase.	3
1.2.2. 3-Dehydroquinate synthase.	5
1.2.3. 3-Dehydroquinate dehydratase.	6
1.2.4. Shikimate dehydrogenase.	6
1.2.5. Shikimate kinase.	7
1.2.6. 5-enolpyruvylshikimate 3-phosphate synthase.	7
1.2.7. Chorismate synthase.	8
1.2.7.1. The role of flavin in enzyme reactions.	9
1.2.7.2. The role of flavin in the chorismate synthase reaction.	9
1.2.7.3. The reaction mechanism of chorismate synthase.	10
1.2.7.4. Enzymology of chorismate synthase.	11
1.2.7.4.1. <i>Escherichia coli</i> .	11
1.2.7.4.2. <i>Bacillus subtilis</i> .	11
1.2.7.4.3. <i>Neurospora crassa</i> .	12
1.2.7.4.4. <i>Euglena gracilis</i> .	12
1.3. Genetics and enzymology of the pre-chorismate pathway.	13
1.4. Beyond chorismate.	15
1.4.1. Phenylalanine and tyrosine pathways.	15
1.4.2. The tryptophan pathway.	16
1.4.3. Other primary metabolites.	17
1.4.4. Secondary metabolites.	18
1.5. Importance and significance of the pathway.	18
1.5.1. Engineering inhibitors/antibiotics.	18
1.5.1.1. Sulphonamides.	18
1.5.1.2. Glyphosate.	19
1.5.1.3. (6S)-6-Fluoroshikimic acid.	19
1.5.2. Aromatic-dependent bacteria as live vaccines.	20
1.6. Flavin reductases.	21
1.7. Aims of the project.	23

**CHAPTER 2. MATERIALS AND METHODS.**

2.0. Chemicals.	24
2.1. Strains and plasmids.	24
2.1.1. Culture media and supplements.	25
2.1.2. Storage of strains.	26
2.1.3. Strain identification.	26
2.2. Purification of genomic DNA from <i>S. aureus</i> .	27
2.3. Polymerase chain reaction (PCR).	27
2.3.1. PCR using Vent polymerase.	28
2.3.2. Recovery of PCR products from reactions.	28
2.4. Plasmid DNA sequencing.	29
2.4.1. Sequencing gel and sample loading.	29
2.5. DNA cloning procedures.	31
2.5.1. Restriction of <i>S. aureus</i> genomic DNA.	31
2.5.2. Restriction of plasmid DNA.	31
2.5.3. Alkaline phosphatase treatment of cut plasmid.	31
2.5.4. Ligation of cut moieties.	31
2.6. Preparation of competent cells and transformation.	32
2.7. Southern hybridisation.	32
2.7.1. Radioactive labelling of DNA.	33
2.8. Expression in pTB361.	34
2.8.1. Expression for protein purification.	35
2.9. λDE3 lysogenization of <i>E. coli</i> GLW40.	36
2.10. Polyacrylamide gel electrophoresis.	36
2.10.1. Protein staining.	37
2.11. Electroblotting proteins onto PVDF membranes.	37
2.12. Western blotting and immunoblotting.	38
2.13. Mutagenesis of chorismate synthase.	38
2.14. Purification of <i>S. aureus</i> chorismate synthase.	40
2.15. Anaerobic UV assay.	41
2.15.1. Preparation of EPSP from its barium salt.	41
2.16. Electrospray mass spectrometry.	42
2.17. Stopped-flow spectrophotometry.	42
2.18. Purification of <i>E. coli</i> flavin reductase.	43
2.19. Flavin reductase assay.	44
2.20. BIACore of <i>E. coli</i> flavin reductase and <i>E. coli</i> chorismate synthase	44
2.21. Chemical cross-linking.	44

**CHAPTER 3. THE MOLECULAR CLONING AND SEQUENCING OF THE *AROC* AND THE *NDK* GENES AND EVIDENCE FOR THE PRESENCE OF THE *GERCC* GENES UPSTREAM FROM *NDK*.**

3.1.	Cloning of the <i>aroC</i> gene.	46
3.1.1.	Restriction mapping of pMJH701.	48
3.1.2.	Subcloning of pMJH701.	48
3.1.3.	Sequencing of plasmids and oligonucleotide primers.	49
3.1.4.	Sequencing of pMJH702.	50
3.2.	Comparison of chorismate synthases.	51
3.3.	Comparison of the N-terminal dehydroquinate synthase fragment with sequences within the Swissprot database.	59
3.4.	Comparison of GerCC with related sequences from the Swissprot database.	59
3.5.	Mapping of the <i>gerC</i> genes in <i>S. aureus</i> .	62
3.6.	Chapter summary.	67

**CHAPTER 4. OVEREXPRESSION ANALYSIS OF *S. AUREU* CHORISMATE SYNTHASE AND NUCLEOSIDE DIPHOSPHATE KINASE AND *E. COLI* FLAVIN REDUCTASE.**

4.1.	Overexpression of <i>S. aureus</i> chorismate synthase.	68
4.1.1.	Lysogenization of <i>E. coli</i> GLW40 for expression.	71
4.2.	Immunological analysis of <i>S. aureus</i> chorismate synthase.	72
4.3.	Overexpression of <i>S. aureus</i> nucleoside diphosphate kinase.	73
4.4.	Overexpression of <i>E. coli</i> flavin reductase.	73
4.5.	Chapter summary.	76

## **CHAPTER 5. PURIFICATION AND CHARACTERISATION OF *S. AUREUS* CHORISMATE SYNTHASE.**

5.1. Purification of <i>S. aureus</i> chorismate synthase.	77
5.2. Protein concentration determination using the extinction coefficient of chorismate synthase.	79
5.3. Molecular weight and subunit structure of chorismate synthase.	79
5.4. pH optimum.	83
5.5. Buffer optimum.	84
5.6. Specific activity with different flavins.	84
5.7. Dependence of chorismate synthase activity on the EPSP and FMN concentration.	85
5.8. Pre-steady state kinetics of <i>S. aureus</i> chorismate synthase.	87
5.8.1. Rapid scanning stopped-flow spectrophotometry.	87
5.8.2. Single wavelength stopped-flow experiments.	91
5.9. Steady state analysis of EPSP analogues.	93
5.10. Preliminary investigation of flavin interaction with <i>S. aureus</i> chorismate synthase.	94
5.10.1. Titration of chorismate synthase with EPSP.	94
5.10.2. Flavosemiquinone formation with 6R-6F-EPSP.	96
5.10.3. Flavosemiquinone formation with EPSP.	97
5.10.4. Dissociation constant for oxidised flavin.	98
5.11. Chapter summary.	99

## **CHAPTER 6. SITE-DIRECTED MUTAGENESIS OF *S. AUREU* CHORISMATE SYNTHASE.**

6.1. Construction and overexpression of site-directed mutants.	100
6.2. Functional test of mutants using complementation.	100
6.3. Specific activities of the crude extracts for the mutants.	104
6.4. Chapter summary.	105

**CHAPTER 7. PURIFICATION AND CHARACTERISATION OF  
*E. COLI* FLAVIN REDUCTASE.**

7.1. Purification of <i>E. coli</i> flavin reductase.	106
7.2. Protein concentration determination using the extinction coefficient of flavin reductase.	109
7.3. Dependence of flavin reductase activity on the concentration of riboflavin, FMN, FAD, NADPH and NADH.	109
7.4. Molecular weight determination of flavin reductase.	113
7.5. Investigation for an interaction between flavin reductase and chorismate synthase.	115
7.6. Chapter summary.	116

**CHAPTER 8. GENERAL DISCUSSION.** 117**REFERENCES.** 135

## LIST OF FIGURES

1.1.	The shikimate or pre-chorismate pathway.	2
1.2.	Pathways to tyrosine, phenylalanine and tryptophan from chorismate.	4
1.3.	The oxidation states of flavin mononucleotide.	8
1.4.	Spectrum of the flavin intermediate formed during the <i>E. coli</i> chorismate synthase reaction.	9
1.5.	Some suggested mechanisms for the enzymic conversion of EPSP to chorismate.	10
1.6.	The aro-trp supraoperon of <i>B. subtilis</i> .	14
1.7.	Enzyme organisation of shikimate pathway enzymes in different organisms.	15
1.8.	Chorismate and beyond, the primary metabolic pathways.	17
2.1.	Map of the expression vector pTB361 showing its main features.	34
2.2.	Site-directed mutagenesis strategy using PCR, based on the method of Higuchi <i>et al.</i> (1988).	39
3.1.	Southern blots of <i>S. aureus</i> 601055 DNA probed with the 350bp <i>Eco</i> RI- <i>Hind</i> III <i>aroC</i> fragment from <i>S. aureus</i> 8325-4.	47
3.2.	Schematic diagram of plasmid pMJH701 showing restriction sites.	48
3.3.	Schematic diagram showing the 5.5kb <i>Clal</i> fragment cloned into pMJH701 and the locations of the putative encoded proteins.	49
3.4.	Schematic diagram of plasmid pMJH702 showing restriction sites and locations of putative encoded proteins.	50
3.5.	Complete nucleotide sequence of pMJH702 and deduced amino acid sequence of encoded proteins.	52
3.6.	Multiple alignment of predicted amino acid sequences of chorismate synthases.	55
3.7.	Dendrogram showing similarity among chorismate synthases from different organisms.	57
3.8.	Multiple alignment of predicted amino acid sequences of nucleoside diphosphate kinases.	58
3.9.	The translated product of the partial <i>S. aureus</i> <i>aroB</i> gene aligned with the N-terminal region of <i>B. subtilis</i> dehydroquinate synthase.	59
3.10.	The translated product of the partial <i>S. aureus</i> <i>gerCC</i> gene aligned with the translated product of the <i>B. subtilis</i> <i>gerCC</i> gene.	60

3.11.	The primary biosynthetic precursors of menaquinones.	60
3.12.	Map of the <i>gerC</i> genes from <i>B. subtilis</i> showing the regions of DNA in pMAY1 used for probing <i>S. aureus</i> genomic DNA.	62
3.13.	Schematic map showing the predicted positions of the <i>gerC</i> genes relative to the <i>aro</i> , <i>ndk</i> region of the <i>S. aureus</i> chromosome.	63
3.14.	Southern blots of <i>S. aureus</i> 601055 DNA probed with an 843bp <i>Dra</i> I- <i>Hind</i> III fragment ( <i>gerCC1</i> ) from pMAY1.	64
3.15.	Southern blots of <i>S. aureus</i> 601055 DNA probed with an 1,215bp <i>Hind</i> III- <i>Ssp</i> I fragment ( <i>gerCAB2</i> ) from pMAY1.	65
3.16.	Southern blots of <i>S. aureus</i> 601055 DNA probed with a 2,252bp <i>Hind</i> III- <i>Hind</i> III fragment ( <i>gerCABC1</i> ) from pMAY1.	66
4.1.	SDS-PAGE showing a time course of protein expression from the <i>aroC</i> clone pMJH7EX2 in two <i>E. coli</i> host strains after induction with IPTG.	69
4.2.	SDS-PAGE showing a time course of protein expression from the <i>aroC</i> clone pMJH7EX2 in <i>E. coli</i> GLW40(DE3) after induction with IPTG.	71
4.3.	Immunoblot of chorismate synthase from <i>E. coli</i> and <i>S. aureus</i> using anti- <i>E. coli</i> chorismate synthase antibodies.	72
4.4.	Protein expression from plasmids pMJH702 and pMJH701 in <i>E. coli</i> DH5 $\alpha$ showing expression of Ndk.	73
4.5.	SDS-PAGE showing a time course of protein expression from the <i>fre</i> clone pFREX2 after induction with IPTG.	75
5.1.	Elution profile of <i>S. aureus</i> chorismate synthase from DEAE-Sephadex.	77
5.2.	Elution profile of <i>S. aureus</i> chorismate synthase from cellulose phosphate.	78
5.3.	Electrospray mass spectrum of <i>S. aureus</i> chorismate synthase.	80
5.4.	Estimation of the native M <sub>r</sub> of chorismate synthase.	81
5.5.	Dimethyl-suberimidate cross-linked chorismate synthase from <i>S. aureus</i> and <i>E. coli</i> .	82
5.6.	Determination of the pH optimum of <i>S. aureus</i> chorismate synthase.	83
5.7.	Determination of apparent K <sub>m</sub> for EPSP.	85
5.8.	Determination of apparent K <sub>m</sub> for FMN.	86
5.9.	The difference spectrum observed during the chorismate synthase reaction.	88

5.10. The difference spectrum observed during the chorismate synthase reaction.	89
5.11. Formation and decay of the flavin intermediate during single turnover rapid scanning stopped-flow spectrophotometry.	90
5.12. Single wavelength stopped-flow titration of EPSP against enzyme.	91
5.13. The increase in $k_1$ with increasing substrate concentration.	92
5.14. Changes to the spectrum of FMN after addition of enzyme followed by the addition of EPSP.	94
5.15. Titration of chorismate synthase with EPSP.	95
5.16. Flavosemiquinone formation in the presence of 6R-6F-EPSP.	96
5.17. Flavosemiquinone formation in the presence of EPSP.	97
6.1. SDS-PAGE showing a time course of protein expression from the <i>aroC</i> clone pMJH7EX2 in <i>E. coli</i> GLW40(DE3)pLysS after induction with IPTG.	101
6.2. Functional tests of mutants and 'wild-type' using complementation on minimal medium.	103
7.1. Elution profile of <i>E. coli</i> flavin reductase from DEAE-Sephadex.	106
7.2. Elution profile of <i>E. coli</i> flavin reductase from phenyl sepharose.	107
7.3. Chromatography of <i>E. coli</i> flavin reductase using S-200 gel filtration.	108
7.4. Determination of apparent $K_m$ for flavins with NADPH as reductant.	110
7.5. Determination of apparent $K_m$ for flavins with NADH as cofactor.	111
7.6. Determination of apparent $K_m$ for NADPH and NADH with riboflavin as substrate.	112
7.7. Electrospray mass spectrum of <i>E. coli</i> flavin reductase.	114
7.8. BIACore analysis.	115
7.9. BIACore analysis.	116
8.1. Schematic diagram representing a map of the <i>gerC</i> , <i>ndk</i> , <i>aro</i> region of the <i>S. aureus</i> chromosome.	120

## LIST OF TABLES

1.1.	The pre-chorismate pathway enzymes of <i>Escherichia coli</i> .	3
1.2.	The pre-chorismate pathway enzymes of <i>Bacillus subtilis</i> .	4
1.3.	Comparison of the properties of chorismate synthases from a number of organisms.	13
2.1.	Bacterial strains and their genotypes.	24
2.2.	Plasmids.	25
2.3.	Supplements to minimal medium.	26
2.4.	Sequencing oligonucleotide primers.	30
2.5.	Primers designed for mutagenesis of the <i>aroC</i> gene.	38
3.1.	Comparison of the translated product from the partial <i>S. aureus</i> <i>gerCC</i> gene with sequences obtained from the Swissprot database.	61
3.2.	Summary of the <i>gerC</i> restriction fragments generated from pMAY1 and used as heterologous probes for Southern blots of <i>S. aureus</i> 601055 DNA.	63
4.1.	N-terminal sequencing data from overexpressed <i>S. aureus</i> chorismate synthase.	70
5.1.	Summary of the purification of <i>S. aureus</i> chorismate synthase from <i>E. coli</i> GLW40(DE3)pMJH7EX2.	78
5.2.	Relative activity of chorismate synthase in different buffers.	84
5.3.	Observed $V_{max}$ for EPSP compared to deutero- and fluoro-analogues of EPSP.	93
6.1.	Complementation test of 'wild-type' and mutants on minimal medium.	102
6.2.	Specific activities of chorismate synthase mutants and 'wild-type' from attempted purifications.	104
7.1.	Summary of the purification of <i>E. coli</i> flavin reductase from <i>E. coli</i> GLW40(DE3)pLysEpFREX2.	108
7.2.	Kinetic parameters for flavins and pyridine nucleotides for <i>E. coli</i> flavin reductase.	113
8.1.	<i>Staphylococcus aureus</i> promoter regions.	118
8.2.	Comparison of the properties of chorismate synthases studied to date.	126

## ABBREVIATIONS

ATP	Adenosine triphosphate.
BIB	Blot incubation buffer.
DAHP	3-deoxy-D- <i>arabino</i> -heptulosonate-7-phosphate.
DEAE	Diethylaminoethyl.
DHQ	3-dehydroquinate.
DMSO	Dimethylsulphoxide.
DNA	Deoxyribonucleic acid.
ddNTP	Dideoxynucleoside triphosphate.
dNTP	Deoxynucleoside triphosphate.
DTT	Dithiothreitol.
$\epsilon$	Extinction coefficient.
E4P	Erythrose 4-phosphate.
ECV	Empty column volume.
EDTA	Ethylene-diamine tetra-acetic acid.
EPSP	5- <i>enol</i> pyruvylshikimate 3-phosphate.
FAD	Flavin adenine dinucleotide.
FMN	Flavin mononucleotide.
FMNH <sub>2</sub>	Flavin mononucleotide - reduced.
GCG	Genetics computer group.
IPTG	Isopropylthiogalactoside.
KIE	Kinetic isotope effect.
K <sub>D</sub>	Dissociation constant.
LB	Luria-Bertani medium.
LMP	Low melting point.
M <sub>r</sub>	Relative molecular weight.
mRNA	Messenger ribonucleic acid.
NAD(P)	Nicotinamide adenine dinucleotide (phosphate).
NAD(P)H	Nicotinamide adenine dinucleotide (phosphate) - reduced.
NDK	Nucleoside diphosphate kinase.
OD	Optical density.
ORF	Open reading frame.
PABA	Para-amino benzoate.
PCR	Polymerase chain reaction.
PHBA	Para-hydroxy benzoate.
PEP	Phosphoenolpyruvate.

PMSF	Phenylmethylenesulphonyl fluoride.
PSI	Pounds per square inch.
RU	Refractive units.
SD	Shine and Dalgarno.
SAM	S-adenosylmethionine.
SDS-PAGE	Sodium dodecyl sulphate polyacrylamide gel electrophoresis.
tRNA	Transfer ribonucleic acid.
U	Unit of (enzyme) activity.

## SUMMARY

The *aroC* gene encoding chorismate synthase and the *ndk* gene encoding nucleoside diphosphate kinase were cloned from *Staphylococcus aureus* by complementation of the Aro<sup>-</sup> phenotype of the *aroC* *E. coli* strain, GLW40. Two partial open reading frames (ORFs) encoding 3-dehydroquinate synthase and a protein which had similarity with the putative *gerCC* gene product from *B. subtilis* were also cloned. In *S. aureus* the *aroC* gene is likely to form the first gene in an operon which includes the *aroB* and *aroA* genes. It has been demonstrated in this study that the *ndk* genes and the *gerCAgerCBgerCC* genes in *S. aureus* are situated upstream from the *aroCaroB* genes; this gene organisation has also been observed in *B. subtilis*.

The *S. aureus* *aroC* gene was expressed from the T7 promoter on plasmid pTB361. This expression system resulted in the accumulation of very high levels of soluble *S. aureus* chorismate synthase and facilitated the purification of the enzyme to near homogeneity, producing 100mg of enzyme from 13g of cells. No detectable immunological cross-reactivity was observed between *S. aureus* chorismate synthase and antibodies raised against *E. coli* chorismate synthase. This contrasts with other chorismate synthases and indicates that there are structural differences between the chorismate synthases from *S. aureus* and *E. coli*. *S. aureus* chorismate synthase was determined to be a homotetramer using gel filtration and chemical crosslinking.

The pH optimum determined for *S. aureus* chorismate synthase was found to be non-symmetrical in MOPS buffer with an optimum of activity around pH 7.0. The apparent K<sub>m</sub> for EPSP of the *S. aureus* enzyme was calculated to be 12.7μM and the apparent K<sub>m</sub> for FMN was calculated to be 4.8μM. The apparent K<sub>m</sub> value for FMN for the *S. aureus* enzyme is two orders of magnitude greater compared to other chorismate synthases, excluding the *B. subtilis* enzyme.

*S. aureus* chorismate synthase was investigated using pre-steady state kinetics and a flavin intermediate was observed during turnover with a difference spectrum resembling that obtained with the *E. coli* enzyme. The spectral characteristics of the *S. aureus* flavin intermediate were different, however, with respect to its maxima, minima and its overall shape. The rate of decay (6.5s<sup>-1</sup>) of the intermediate was eight times slower than that observed for the *E. coli* enzyme (52s<sup>-1</sup>) and this compares well with a 7 fold lower V<sub>max</sub>.

Tyrosine 121 of *S. aureus* chorismate synthase was changed to phenylalanine or alanine using site-directed mutagenesis. The conversion to alanine resulted in a loss of activity while the phenylalanine mutant retained 10% of wild-type activity.

## CHAPTER 1. INTRODUCTION.

---

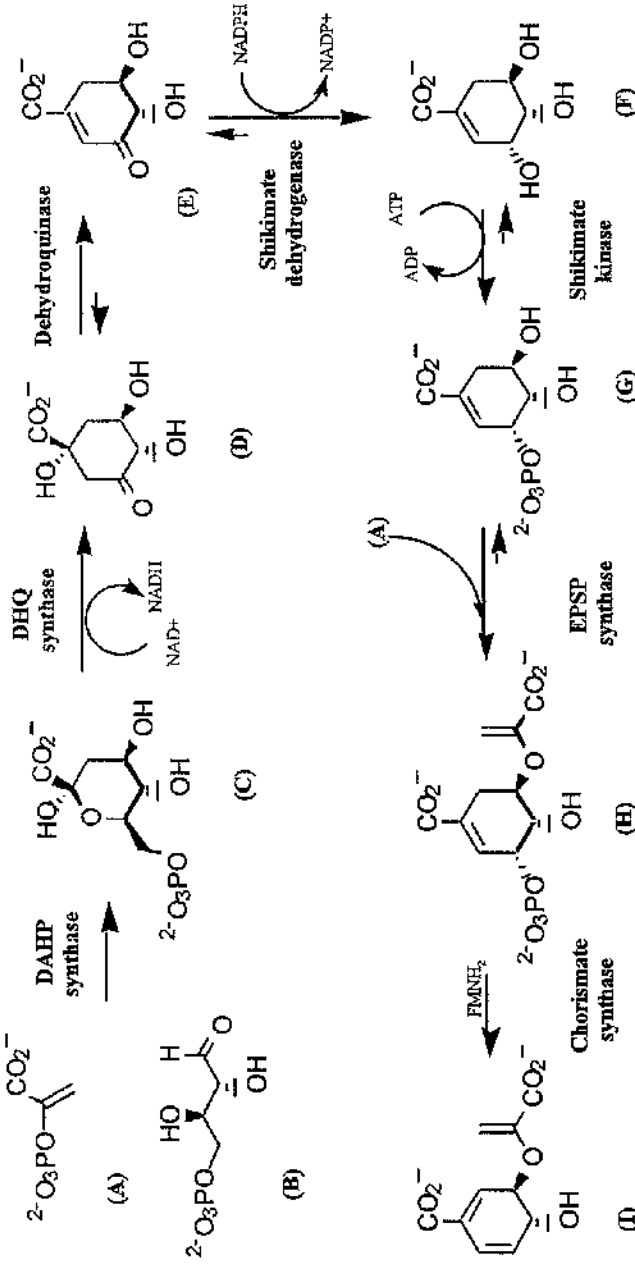
### 1.1. The shikimate pathway.

The genesis of the three aromatic amino acids, phenylalanine, tryptophan and tyrosine, and most of the aromatic compounds found in microorganisms and plants begins with the two carbohydrate precursors, phosphoenolpyruvate and D-erythrose 4-phosphate. These precursors are converted by a seven step enzymic process, the shikimate pathway, via shikimic acid to chorismate (Figure 1.1) (Pittard, 1987; Bentley, 1990; Haslam, 1993).

Shikimic acid was the first intermediate of the pathway to be identified after it was isolated from the fruits of the *Illicium* tree in 1885 by J. F. Eykmann. It was confirmed as a key intermediate of the shikimic acid pathway in the 1950s with the study of auxotrophic mutants of *Escherichia coli* when it was shown to replace the requirement of these mutants for the three aromatic amino acids (Davis, 1955). Similarly, the accumulation by auxotrophs of intermediates preceding blocked steps in the pathway led to the identification of 3-dehydroquinate, 3-dehydroshikimate and shikimate 3-phosphate.

Earlier reactions of the pathway were elucidated with more difficulty. A mutant strain of *E. coli* that accumulated shikimic acid was grown on D-glucose variously labelled with  $^{14}\text{C}$  to determine the distribution of specific carbon atoms from glucose in the shikimate molecule (Sprinson, 1961). It was demonstrated that of the seven precursor carbon atoms entering the pathway, three originated from glycolysis and four from the pentose phosphate pathway. Cell extracts and partially purified enzyme preparations were shown to convert phosphoenolpyruvate (PEP) and erythrose 4-phosphate (E4P) to 3-deoxy-D-arabino-heptulosonate 7-phosphate (DAHP) and 3-dehydroquinate (DHQ). The position of 5-eno/pyruvylshikimate 3-phosphate (EPSP) in the pathway was determined from the conversion of shikimate 3-phosphate and PEP by cell extracts.

Chorismate, the final compound of the classic shikimate pathway was identified only after the production of multiply mutant strains blocked in each of the three aromatic amino acid pathways. While shikimate took its name from the Japanese for the oriental tree from which it was first isolated, chorismate was named after the Greek



(A) Phosphoenolpyruvate (PEP) (B) D-Erythrose 4-phosphate (C) 3-deoxy-D-arabinohexulose 7-phosphate (DAHP)

(D) 3-Dihydroquinate (DHQ) (E) 3-Dehydroshikimate (F) Shikimate (G) Shikimate 3-phosphate

(H) 5-Enolpyruvylshikimate 3-phosphate (EPSP) (I) Chorismate

Figure 1.1. The shikimate or pre-chorismate pathway.

for separation on the assumption that it was the main branchpoint compound of the pathway (Haslam, 1993).

### **1.2. The enzymes and enzymology of the pre-chorismate pathway.**

The first enzyme of the shikimate pathway, DAHP synthase, catalyses the condensation of the carbohydrate precursors phosphoenolpyruvate (PEP) and erythrose 4-phosphate (E4P) to produce DAHP (Figure 1.1). 3-dehydroquinate (DHQ) synthase catalyses the cyclisation of DAHP to give 3-dehydroquinate. The elimination of water by 3-dehydroquinate dehydratase produces 3-dehydroshikimate and introduces the first double bond. Subsequent reduction of the keto group by shikimate dehydrogenase produces shikimate which is phosphorylated by shikimate kinase to give shikimate 3-phosphate. Condensation of PEP and shikimate 3-phosphate catalysed by EPSP synthase yields EPSP, the substrate for the final enzyme of the pathway, chorismate synthase, which introduces the second double bond and produces chorismate.

The seven enzyme pathway described above and shown in Figure 1.1 is now often referred to as the pre-chorismate pathway. The enzyme reactions of the pathway have been shown to be common to every organism in which the pathway has been studied and, furthermore, while present in bacteria, fungi and plants the pathway is absent in animals. Consequently, humans and animals must obtain the three aromatic amino acids and certain cofactors produced by post-chorismate pathways from their diet.

While the intermediates and enzymatic reactions of the pre-chorismate pathway are believed to be identical in all organisms, the genes and operons of the pathway are organised differently in different species possibly reflecting contrasting evolutionary histories and the functional and regulatory constraints experienced by each species (Henner & Yanofsky, 1993). In the following sections differences in the structural, functional, and regulatory features of the pre-chorismate pathway are compared with particular reference to *E. coli* and *Bacillus subtilis*.

### 1.2.1. DAHP synthase.

The condensation of PEP and E4P to produce DAHP is the first committed step in the biosynthesis of aromatic compounds and is catalysed by DAHP synthase. Consequently, the flow of metabolites into the pre-chorismate pathway is controlled by feedback regulation of this enzyme by either intermediates or end-products of the pathway. *E. coli* utilises a different strategy for control from that of *B. subtilis*.

In *E. coli*, there are three DAHP synthase isoenzymes, phenylalanine sensitive DAHP (phe), tryptophan sensitive DAHP (trp) and tyrosine sensitive DAHP (tyr). The three DAHP synthase enzymes display an inhibition pattern in which their activity and rate of synthesis are differentially affected by one of the three aromatic amino acids (Pittard, 1987). Thus each aromatic amino acid influences the flux of the pathway.

Enzyme	Gene	Map pos. (min)	Amino acids	M <sub>r</sub> (calc.)	Quaternary structure
<b>DAHP synthase</b>					
DAHP synthase (tyr)	<i>aroF</i>	57	356	38804	Dimer
DAHP synthase (phe)	<i>aroG</i>	17	350	37997	Tetramer
DAHP synthase (trp)	<i>aroI</i>	37	347	39000	Dimer
3-Dehydroquinate synthase	<i>aroB</i>	75	362	38880	Monomer
3-Dehydroquinate dehydratase	<i>aroD</i>	37	240	26377	Dimer
Shikimate dehydrogenase	<i>aroE</i>	72	272	29380	Monomer
Shikimate kinase <sup>1</sup>	<i>aroL</i>	9	173	18937	Monomer
EPSP synthase	<i>aroA</i>	20	427	46112	Monomer
Chorismate synthase	<i>aroC</i>	51	357	38183	Tetramer

**Table 1.1. The pre-chorismate pathway enzymes of *Escherichia coli*.<sup>2</sup>**

<sup>1</sup> a second shikimate kinase exists encoded by *aroK* but is excluded here for reasons discussed in 1.2.5.

<sup>2</sup> Taken from Haslam, 1993.

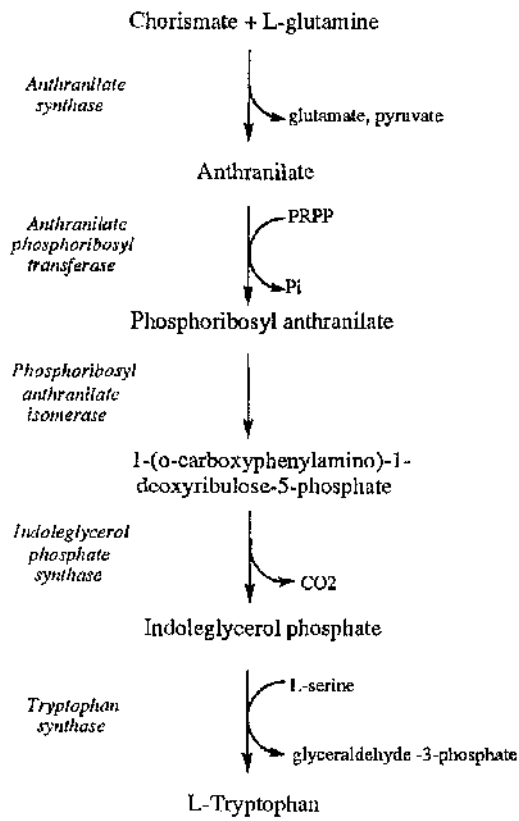
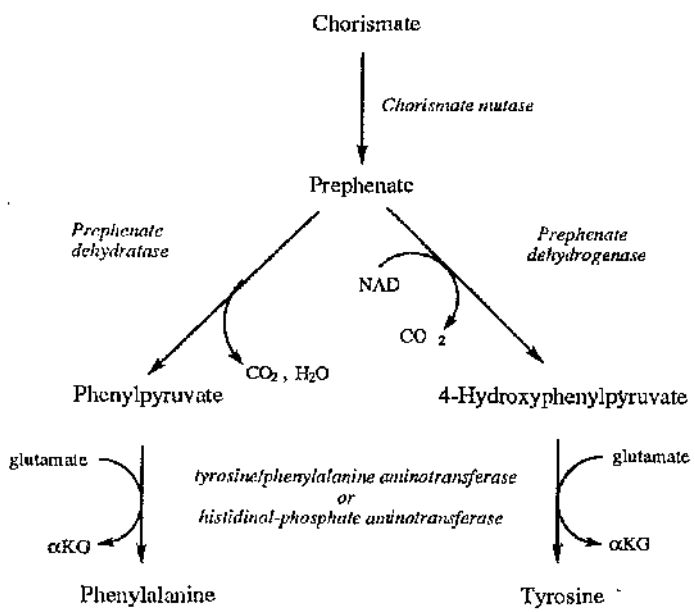


**Figure 1.2. Pathways to tyrosine and phenylalanine (top) and tryptophan (bottom) from chorismate.** Abbreviations:  $\alpha\text{KG}$ ,  $\alpha$ -ketoglutarate; PRPP, phosphoribosyl pyrophosphate.

In *B. subtilis* only one species of DAHP synthase exists which is not inhibited by the aromatic amino acids but rather prephenate, an intermediate of phenylalanine and tyrosine synthesis (Figure 1.2) (Jensen & Nester, 1966; Jensen *et al.*, 1967; Llewellyn *et al.*, 1980). An excess of phenylalanine and tyrosine results in the feedback inhibition of prephenate dehydratase blocking the further conversion of prephenate. The resulting build-up of prephenate inhibits DAHP synthase and reduces the flow of metabolites into the pathway. This sequential feedback strategy could potentially starve the cell for tryptophan, whose synthesis branches from chorismate. However, chorismate mutase, which catalyses the conversion of chorismate to prephenate, is product inhibited by prephenate and this is suggested to be sufficient to channel chorismate into the tryptophan pathway (Henner & Yanofsky, 1993).

Enzyme	Gene	Map pos. <sup>1</sup> ( $\circ$ )	Amino acids	M <sub>r</sub> (calc.)	Quaternary structure
DAHP synthase	<i>aroA</i>	264	358	39,639	Monomer <sup>2</sup>
3-Dehydroquinate synthase	<i>aroB</i>	203	362	40,817	Complex <sup>3</sup>
3-Dhydroquinate dehydratase <sup>4</sup>	<i>aroC</i>	208	255	28,131	nd
Shikimate dehydrogenase	<i>aroD</i>	226	nd	nd	nd
Shikimate kinase	<i>aroI</i>	28	186	21,863	Monomer <sup>2</sup>
EPSP synthase <sup>5</sup>	<i>aroE</i>	202	428	45,240	Monomer
Chorismate synthase	<i>aroF</i>	203	368	39971	Complex <sup>3</sup>

nd, not determined

**Table 1.2. The pre-chorismate pathway enzymes of *Bacillus subtilis*.**

<sup>1</sup> Anagnostopoulos *et al.*, 1993

<sup>2</sup> See section 1.2.5.

<sup>3</sup> Dehydroquinate synthase, chorismate synthase and a flavin reductase form a trifunctional complex.

<sup>4</sup> Sorokin *et al.*, 1993.

<sup>5</sup> Henner *et al.*, 1986.

Some strains of *B. subtilis* have DAHP synthases with different properties. The original Marburg strain of *B. subtilis* has a monofunctional DAHP synthase. Strain 168, which was derived from the Marburg strain by X-ray irradiation, has a bifunctional DAHP synthase which also exhibits chorismate mutase activity (Huang *et al.*, 1974a). The bifunctional enzyme was thought to have arisen from an allosteric site for prephenate being converted to an active site for chorismate mutase activity (Llewellyn *et al.*, 1980). However, recent sequencing of the *aroA(G)* gene of *B. subtilis* 168 and *B. subtilis* Marburg strain has demonstrated they have identical sequences such that the observed differences in DAHP synthase activity were suggested to result from other unspecified changes (Bolotin *et al.*, 1995).

In addition to *Bacillus* species Staphylococci, including *S. aureus*, *S. roseus* and *S. epidermidis*, have been found to use the pattern of sequential feedback inhibition for the control of DAHP synthase activity (Jensen *et al.*, 1967).

### **1.2.2. 3-Dehydroquinate synthase.**

The conversion of DAHP to 3-dehydroquinate requires chemical steps of oxidation,  $\beta$ -elimination, reduction and an intramolecular condensation. This is performed by 3-dehydroquinate (DHQ) synthase in the presence of NAD<sup>+</sup> as cofactor. The enzyme has been purified to homogeneity from both *E. coli* and *B. subtilis*.

In *E. coli* the enzyme is a monofunctional polypeptide of around 40kD, is monomeric and requires NAD<sup>+</sup> and Co<sup>2+</sup> or Zn<sup>2+</sup> for activity (Frost *et al.*, 1984). As with the other remaining enzymes of the pre-chorismate pathway in *E. coli* (with the exception of shikimate kinase) the enzyme is synthesised constitutively. Its synthesis is not repressed by any of the aromatic amino acids.

*B. subtilis* DHQ synthase was purified in association with chorismate synthase and an NADPH-dependent flavin reductase (Hasan & Nester, 1978c). The enzyme was only active when associated with chorismate synthase whereas the presence or absence of the flavin reductase did not affect DHQ synthase activity. The enzyme required NAD<sup>+</sup> and either Co<sup>2+</sup> or Mn<sup>2+</sup> for activity. The molecular weight on SDS-PAGE gels was 24kD, however, the gene has been sequenced and encodes a polypeptide of 41kD.

### **1.2.3. 3-Dehydroquinate dehydratase.**

3-Dehydroquinate (DHQ) dehydratase (3-dehydroquinase) catalyses the third step in the pre-chorismate pathway and is responsible for initiating the process of aromatisation by introducing the first double bond. Two classes of 3-dehydroquinate dehydratase have been identified in organisms to date, type I and type II, which catalyse the reactions with opposite stereochemistry (Kleanthous *et al.*, 1992; Harris *et al.*, 1993). Both *E. coli* and *B. subtilis* possess the type I enzyme which is characterised by forming a Schiff base with the substrate (Shneir *et al.*, 1991). The stereospecific *syn*-dehydration of dehydroquinate results from the conformational change of the substrate due to Schiff base formation.

The *aroD* and *aroC* genes encoding DHQ dehydratase in *E. coli* and *B. subtilis*, respectively, have been sequenced. From the nucleotide sequence of the *E. coli* gene the polypeptide consists of 240 amino acids with a subunit M<sub>r</sub> of 26kD (Duncan *et al.*, 1986). The protein has been purified to homogeneity and exists as a dimer (Table 1.1). The nucleotide sequence of the *B. subtilis* gene encodes a polypeptide of 255 amino acids producing a protein with subunit M<sub>r</sub> of 28kD (Warburg *et al.*, 1984; Sorokin *et al.*, 1993). However, the protein has not been purified from *B. subtilis* and has been studied only in crude extracts.

### **1.2.4. Shikimate dehydrogenase.**

Shikimate dehydrogenase catalyses the reversible reduction of 3-dehydroshikimate to produce shikimate and is an NADP<sup>+</sup> specific dehydrogenase. The *aroE* gene encoding shikimate dehydrogenase in *E. coli* has been sequenced and encodes a polypeptide of 272 amino acids with a subunit M<sub>r</sub> of 29kD. The protein has been purified to homogeneity and exists as a monomer (Table 1.1)(Chaudhuri & Coggins, 1985). The *aroD* gene encoding shikimate dehydrogenase in *B. subtilis* has been mapped but not cloned, although it should soon be sequenced under the *B. subtilis* genome project.

### 1.2.5. Shikimate kinase.

Shikimate kinase catalyses the phosphorylation of shikimic acid to yield shikimate 3-phosphate. The flux through the pre-chorismate pathway is further regulated at this step in both *E. coli* and *B. subtilis* although different mechanisms for control are observed.

*E. coli* synthesises two shikimate kinase enzymes encoded by the *aroL* gene for shikimate kinase II and the *aroK* gene for shikimate kinase I. Shikimate kinase II appears to play the dominant role in the pre-chorismate pathway and is regulated by both the TyrR and TrpR proteins with the amino acids tyrosine and tryptophan as cofactors. The role of shikimate kinase I is less clear. Expression is constitutive and the enzyme has a very much lower affinity for shikimate ( $K_m$  of 20mM compared to 200 $\mu$ M for shikimate kinase II)(Defeyter & Pittard, 1986; Millar *et al.*, 1986). It has been postulated that in *E. coli*, shikimate kinase I has been displaced in importance by the more catalytically active and better regulated shikimate kinase II (Whipp & Pittard, 1995).

In *B. subtilis* 168 there is a single shikimate kinase which forms a complex with the bifunctional DAHP synthase-chorismate mutase as discussed above. The kinase is inactive when dissociated from the complex and the complex is postulated to act as a unit of feedback control (Huang *et al.*, 1974a; Nakatsukasa & Nester, 1972). The situation in the wild-type Marburg strain of *B. subtilis* is unclear since DAHP synthase and chorismate mutase are monofunctional and it has not yet been determined whether shikimate kinase forms part of a complex in this strain.

### 1.2.6. 5-Enolpyruvylshikimate 3-phosphate (EPSP) synthase.

EPSP synthase catalyses the transfer of the enolpyruvyl moiety from phosphoenolpyruvate (PEP) to shikimate 3-phosphate to form 5-enolpyruvylshikimate 3-phosphate and inorganic phosphate. The enzyme has been very extensively studied in a broad range of plants and microorganisms. This is principally due to it being the target of the broad spectrum herbicide glyphosate. Furthermore the *aroA* gene has been a target for the production of live, attenuated vaccines based on *aro* null mutants. Both of these areas are discussed in more detail in a later section.

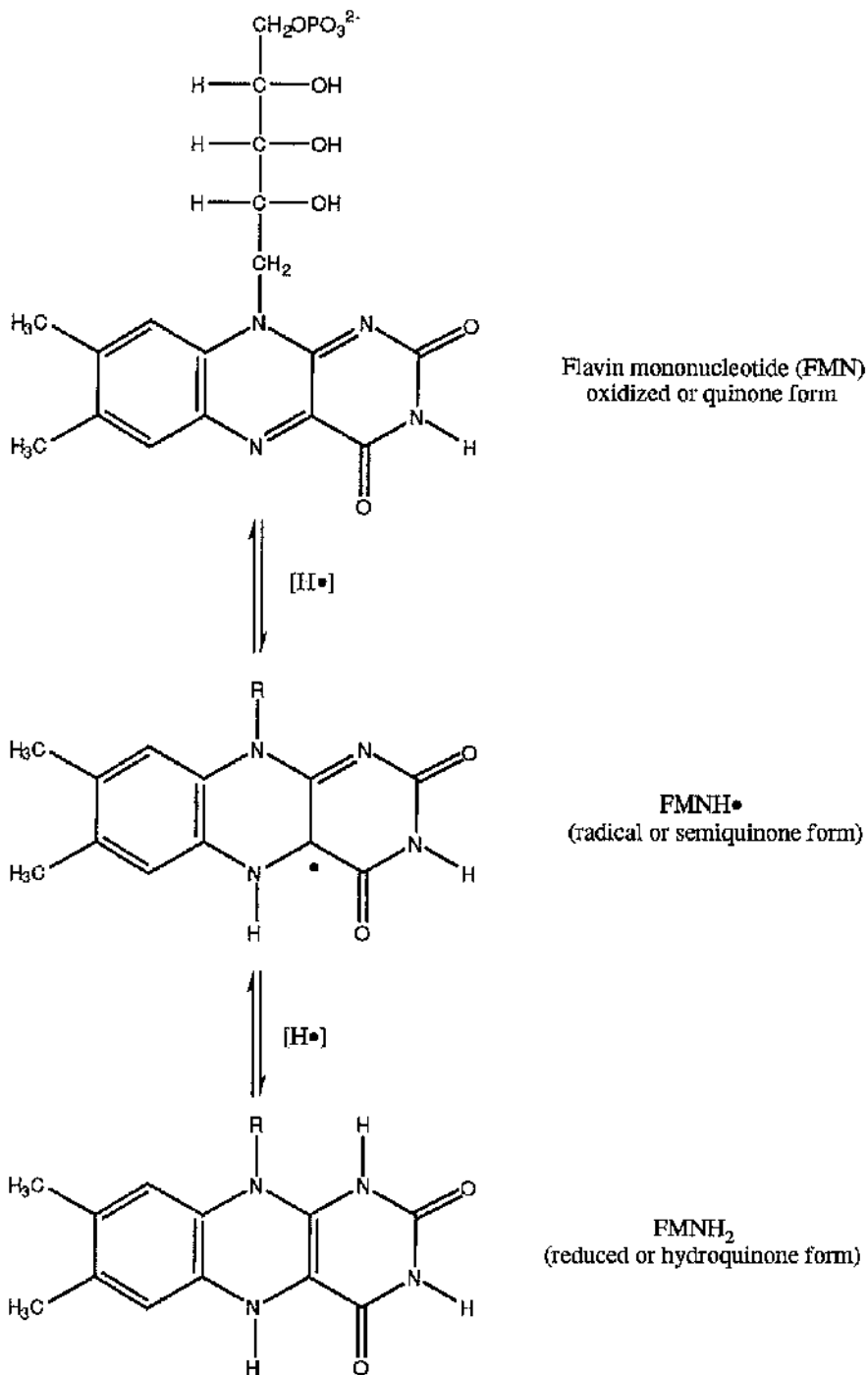


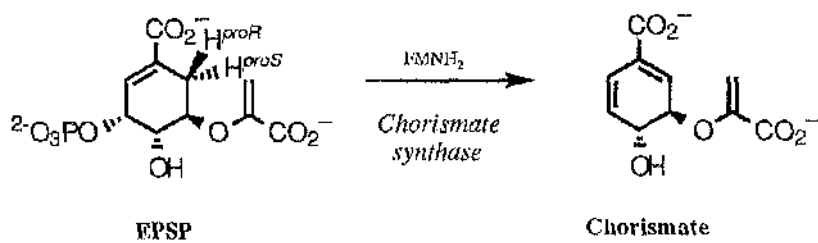
**Figure 1.3. The oxidation states of flavin mononucleotide (FMN).**

The *aroA* gene encoding EPSP synthase in *E. coli* has been sequenced and encodes a polypeptide of 427 amino acids. The protein has a subunit M<sub>r</sub> of 46kD, has been purified to homogeneity, and exists as a monomer (Table 1.1)(Duncan *et al.*, 1984). Similarly, the *aroA* gene has been cloned from *B. subtilis* and encodes a polypeptide of 428 amino acids (Henner *et al.*, 1986). The protein has a subunit M<sub>r</sub> of 45kD, has been purified to near homogeneity and also exists as a monomer. The purified *B. subtilis* enzyme was found to exhibit allosteric behaviour, a feature unique among the EPSP synthases studied to date (Majumder *et al.*, 1995).

### 1.2.7. Chorismate synthase.

Chorismate synthase, the final enzyme of the pre-chorismate pathway, catalyses the conversion of 5-enolpyruvylshikimate 3-phosphate to chorismate. The reaction involves the abstraction of the C-(6pro-R)-hydrogen with the concomitant elimination of phosphate generating the second double bond of the aromatic ring.

The enzyme reaction is unusual in its requirement for a reduced flavin cofactor despite there being no overall change in the redox state. A major difference between the chorismate synthases studied to date is their ability to generate the reduced flavin cofactor required for catalysis. Chorismate synthase from *Neurospora crassa* has been shown to possess an intrinsic NADPH-dependent flavin oxidoreductase activity (Welch



*et al.*, 1974; Boocock, 1983; Henstrand *et al.*, 1995b). However, chorismate synthases purified from other sources, namely the bacteria, *E. coli* (White *et al.*, 1988) and *B. subtilis* (Hasan & Nester, 1978b), the protist, *Euglena gracilis* (Schaller *et al.*, 1991a), and the plant, *Corydalis sempervirens* (Schaller *et al.*, 1990, 1991b), are all

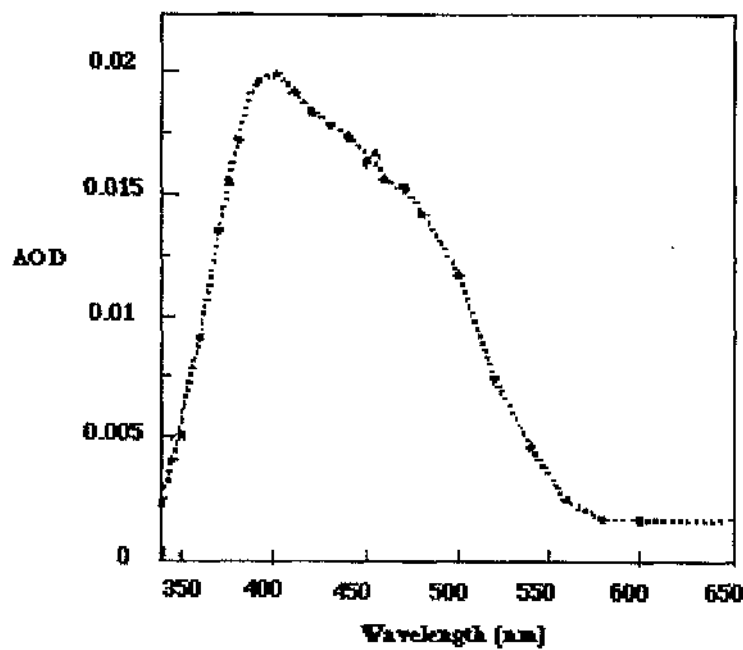


**Figure 1.4. Spectrum of the flavin intermediate formed during the *E. coli* chorismate synthase reaction (Ramjee, 1992).**

monofunctional and must be supplied exogenously with reduced flavin. The enzymes from *B. subtilis* (Hasan & Nester, 1978a) and *E. gracilis* are observed to form enzyme complexes with an NADPH-dependent flavin oxidoreductase. The remaining monofunctional enzymes are postulated to obtain reduced flavin from endogenous flavin reductase activity.

#### **1.2.7.1. The role of flavin in enzyme reactions.**

The flavin molecule is utilised as a cofactor in a wide array of enzyme catalysed reactions in contrast to most other coenzymes which are involved in a more restricted set of chemical events. Flavins are involved, for example, in the dehydrogenation of various different substrates, one-electron transfers, bioluminescence and photobiochemical processes. In the vast majority of enzyme reactions involving flavins there is at some stage a transfer of electrons between the substrate and the flavin itself (Ghisla & Massey, 1989). These electron transfers can on occasions be coupled to the transfer of protons. The flavin molecule may also form covalent intermediates during catalysis such as a C(4a)-adduct and a charge transfer complex.

A feature of the involvement of flavins in redox reactions is their ability to exist in three redox states, quinone, semiquinone and hydroquinone, where semiquinone and hydroquinone states are progressive reductions of the quinone state (Figure 1.3)(Voet & Voet, 1990).

#### **1.2.7.2. The role of flavin in the chorismate synthase reaction.**

The role of the flavin moiety during the chorismate synthase reaction is not yet clear. However, pre-steady state kinetic analysis of the reaction has revealed transient changes in the absorbance spectrum of  $\text{FMNH}_2$  during single turnover experiments with EPSP using a stopped flow spectrophotometer under strict anaerobic conditions (Figure 1.4)(Ramjee *et al.*, 1991). This provides unambiguous spectroscopic evidence of a redox active role for the flavin in the catalytic cycle. Furthermore, the spectrum suggests the presence of a C(4a)-adduct and a charge transfer complex. It has been postulated that the  $\text{FMNH}_2$  does not simply undergo a one or two electron oxidation during turnover (Ramjee *et al.*, 1991)

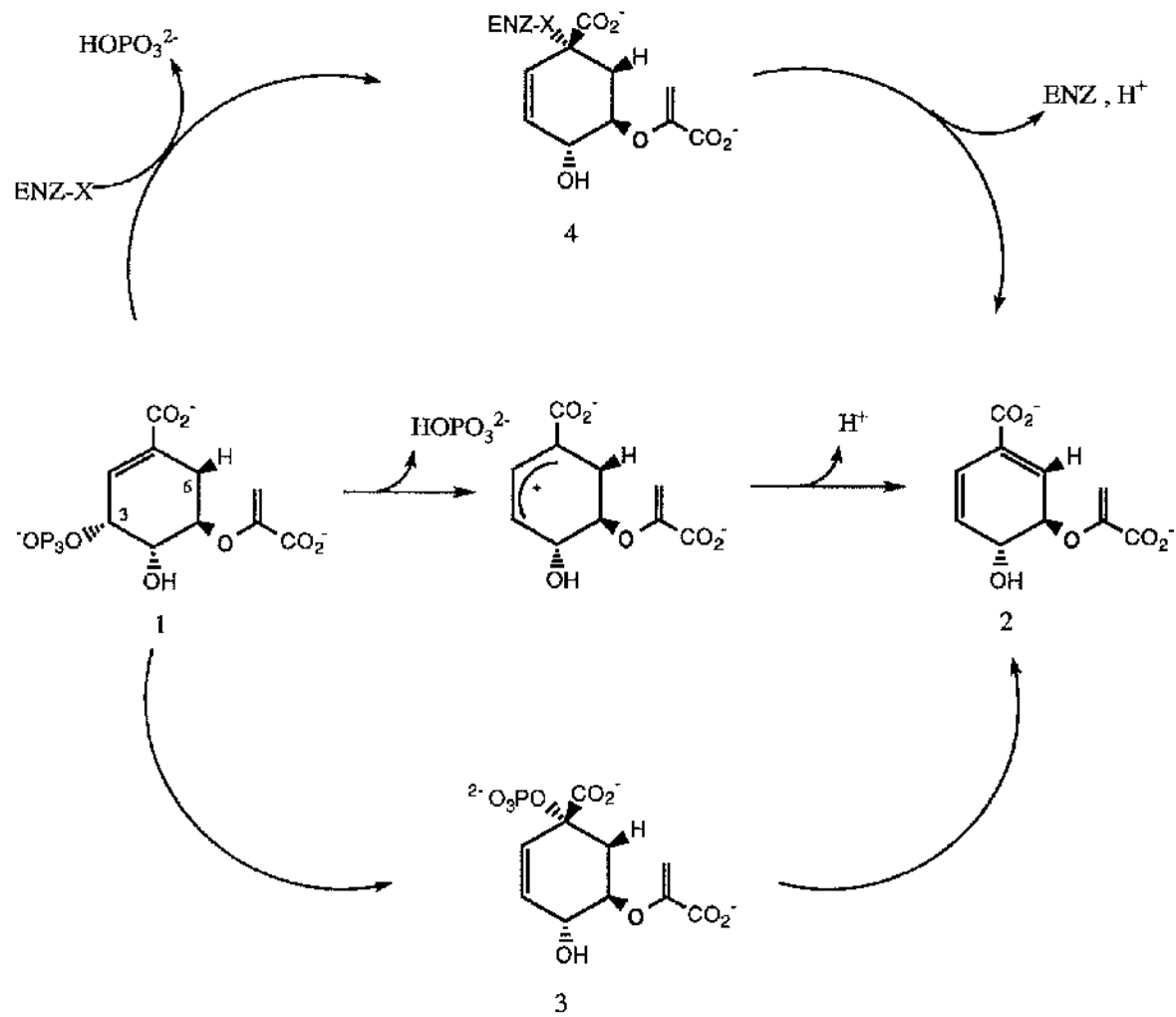


**Figure 1.5. Some suggested mechanisms for the enzymic conversion of EPSP to chorismate. (1) EPSP, (2) chorismate, (3) 'iso-EPSP', (4) enzyme-bound species.**

With the substrate analogue (6R)-6-F-EPSP the FMNH<sub>2</sub> cofactor is quantitatively oxidised to yield a stable flavin semiquinone radical which is not reduced in the presence of dithionite (a strong reducing agent). It has been speculated that the free radical is a transient intermediate during the normal catalytic cycle with EPSP where it does not accumulate (Bornemann *et al.*, 1993). Further evidence for a direct role of flavin in the catalytic cycle has been obtained with the flavin analogue 5-deaza-FMN which binds tightly to *E. coli* chorismate synthase yet exhibits only 1% of the activity obtained with FMN (Bornemann *et al.*, 1993).

Recently, pre-steady state analysis of *E. coli* chorismate synthase with the substrate analogue (6R)-[6<sup>2</sup>H]EPSP has demonstrated a deuterium kinetic isotope effect under single turnover showing that the flavin intermediate forms before the C-(6*pro*R)-H bond is cleaved (Bornemann *et al.*, 1995).

#### **1.2.7.3. The reaction mechanism of chorismate synthase.**

The stereospecific nature of the chorismate synthase reaction was originally demonstrated by growing an *E. coli* mutant blocked both before and after 3-dehydroshikimate with stereospecifically labelled shikimic acid ((6R)-[6<sup>2</sup>H] and (6S)-[6<sup>2</sup>H]) as sole carbon source. Many bacteria have uptake systems for shikimic acid and quinic acid. An analysis of the tyrosine and phenylalanine residues from cellular extracts revealed that only the C-(6 *pro*-R)-hydrogen had been eliminated (Hill & Newkome, 1969; Onderka & Floss, 1969). The reaction was thus shown to proceed via a *trans*-1,4-elimination.

The elimination is thought to proceed by a stereochemically-favoured non-concerted route for which several models have been proposed. These include an X-group mechanism (Floss *et al.*, 1972), an allylic rearrangement of phosphate followed by a 1,2-elimination (Gancin, 1978) and the stepwise loss of phosphate and a proton via a cationic intermediate (Hawkes *et al.*, 1990) (Figure 1.5). However, there is as yet no consensus regarding the overall reaction mechanism.

#### **1.2.7.4. Enzymology of chorismate synthase.**

Chorismate synthase activity has been studied in a number of organisms and the *aroC* gene encoding the enzyme has been cloned from eleven organisms (Figure 3.6). To date the enzyme has been purified and characterised from the bacteria *B. subtilis* (Hasan & Nester, 1978b) and *E. coli* (White *et al.*, 1988), the protist *E. gracilis* (Schaller *et al.*, 1991a), the fungus *N. crassa* (Gaertner & Cole, 1973; Welch *et al.*, 1974; Schaller *et al.*, 1991a; Henstrand *et al.*, 1995a) and the higher plant *C. sempervirens* (Schaller *et al.*, 1990, 1991b). A comparison of these chorismate synthases, excluding the *B. subtilis* enzyme, found they were very similar in terms of cofactor specificity, kinetic properties, isoelectric points and pH optima (Schaller *et al.*, 1991a). The only significant difference was the intrinsic flavin reductase activity shown by the *N. crassa* enzyme (see 1.2.7 & 1.2.7.4.3)

##### **1.2.7.4.1. *Escherichia coli*.**

Chorismate synthase has been overexpressed and purified to homogeneity from *E. coli* and has a subunit molecular weight of 39kD (Ramjee, 1992); the *aroC* gene encoding the enzyme has been cloned and sequenced (White *et al.*, 1988). The enzyme is monofunctional, requiring reduced flavin for catalysis and is generally assayed anaerobically using photoreduced FMN by the method of Ramjee *et al.* (1994). Synthesis of the enzyme is believed to be constitutive and it has been observed that the specific activity of chorismate synthase is only 10-20% that of the preceding enzyme, EPSP synthase (Tribe *et al.*, 1979). The enzyme is compared with other chorismate synthases in Table 1.3.

##### **1.2.7.4.2. *Bacillus subtilis*.**

Chorismate synthase was purified to apparent homogeneity from *B. subtilis* 168 and was observed to form part of a trifunctional complex with the second enzyme of the pathway, dehydroquinate synthase, and an NADPH-dependent flavin oxidoreductase (Hasan & Nester, 1978b). The *aroF* gene, encoding the enzyme, has been sequenced and was found to be the first gene in an operon containing dehydroquinate synthase and chorismate mutase (Henner *et al.*, 1990). Hasan & Nester, (1978b) measured the molecular weights of chorismate synthase, dehydroquinate synthase and flavin reductase to be 24kD, 21kD and 13kD, respectively. However, translation of the

sequenced genes produces proteins with molecular weights of 40kD and 41kD for chorismate synthase and dehydroquinate synthase, respectively. The molecular weight of flavin reductases from a range of organisms is between 20 and 30kD. Clearly a reappraisal of this work would be useful to correct this anomaly.

#### **1.2.7.4.3. *Neurospora crassa*.**

The chorismate synthase from *N. crassa* has been purified to homogeneity and is a bifunctional enzyme having both chorismate synthase and NADPH-dependent flavin reductase activities (Gaertner & Cole, 1973; Welch *et al.*, 1974). The enzyme was observed to be slightly larger than chorismate synthase from other organisms with a subunit molecular weight of 46.4kD (Henstrand *et al.*, 1995a). This larger size was thought to be a consequence of the bifunctional character of the enzyme and the presence of a separate flavin reductase domain. Recently, the gene encoding chorismate synthase was sequenced and was found to have the domain(s) for reduction of the flavin within regions in which homology is shared among monofunctional chorismate synthases (Henstrand *et al.*, 1995a).

#### **1.2.7.4.4. *Euglena gracilis*.**

Chorismate synthase was purified 1200-fold from *E. gracilis* and was observed to be associated with an NADPH-dependent flavin oxidoreductase activity. The study did not unambiguously determine the subunit composition of the purified enzymes or the nature of the association of the flavin reductase activity with the chorismate synthase (Schaller *et al.*, 1991a). The subunit molecular weight of 41.7kD resembles closely that observed for the monofunctional chorismate synthases.

Property	<i>E. gracilis</i>	<i>N. crassa</i>	<i>C. semperflorens</i>	<i>E. coli</i>
Apparent Km (EPSP)	27μM	2.7μM	53μM	1.8μM <sup>1</sup>
Apparent Km (FMN)	76nm	66nM	37nm	
Cofactor specificity	FMN>FAD	FMN>FAD	FMN>FAD	FMN>FAD
Flavin reductase activity	Present	Present	Absent	Absent
Apparent Km (NADPH)	7.4μM	21.4μM		
Mr (native)	110-138kD	198kD	80.1kD	162kD <sup>1</sup>
Mr (subunit)	41.7kD	46.4kD <sup>2</sup>	41.9kD	39kD <sup>1</sup>
No. of subunits	nd	4	2	4
isoelectric point	5.5	4.9	5.0	6.45 <sup>1</sup>
pH optimum	8.2	8.1	8.0	7.5-8.0 <sup>1</sup>

Taken from Schaller *et al.*, 1991a.

**Table 1.3. Comparison of the properties of chorismate synthases from a number of organisms.**

### 1.3. Genetics and enzymology of the pre-chorismate pathway.

The genes and operons responsible for aromatic amino acid biosynthesis are organised differently in the different organisms in which they have been studied. This may well reflect the different evolutionary histories and possibly the regulatory constraints experienced by each species (Henner & Yanofsky, 1993).

*B. subtilis* and *E. coli* differ significantly in the strategies they use to control expression of the genes of aromatic amino acid biosynthesis. In *B. subtilis* many of the genes are organised into common, overlapping, or interdependent transcriptional units, making cross-pathway regulation rather than specific regulation the preferred regulatory strategy. These cross-pathway interactions have resulted in more complex regulatory relationships than are observed for the corresponding genes in enteric bacteria (Nester *et al.*, 1969; Henner & Yanofsky, 1993).

<sup>1</sup> Ramjee, 1992

<sup>2</sup> Henstrand *et al.*, 1995b.

In *E. coli* the genes of the pre-chorismate pathway are scattered widely around the chromosome and the encoded proteins are structurally independent (Pittard & Wallace, 1966; Pittard, 1987). This contrasts with the situation observed in *B. subtilis* where the genes of the pre-chorismate pathway are clustered mainly in one region of the chromosome (Table 1.2) and with many of the other genes for aromatic amino acid biosynthesis. The *aroFBH* operon forms the start of a supraoperon (Figure 1.6) and overlaps the *trp* promoter; the *aroH* stop codon is within the *trp* promoter and the *trp* attenuator is the initial transcription terminator for the *aroFBH* operon (Henner & Yanofsky, 1993). *In vivo* studies have shown that a transcript from the *aroFBH* operon enters the *trp* leader region and it is likely that the *aroFBH* promoter provides a functional *trp* transcript (Henner & Yanofsky, 1993). The *hisH* gene (encoding histidinol phosphate aminotransferase), the *tyrA* gene (encoding prephenate dehydratase) and the *aroE* gene (encoding EPSP synthase) are located immediately downstream from the *trp* genes on the *B. subtilis* chromosome (Henner *et al.*, 1986). The expression of these three genes is subject to tryptophan control being located in a transcription unit with the *trp* genes.

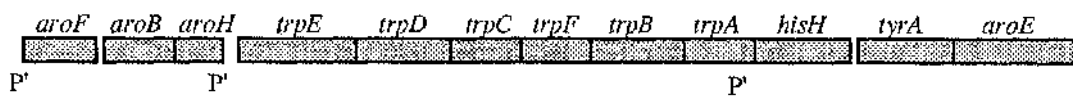


**Figure 1.6. The *aro-trp-aro* supraoperon of *B. subtilis*.** P' indicates identified promoter element and transcription of the genes is from left to right

It has been suggested that the evolution of the pre-chorismate pathway in higher organisms such as plants and fungi has resulted in a decrease in the complexity of the shikimate pathway with the formation of multifunctional enzymes. In the fungi *Neurospora crassa* *Aspergillus nidulans* and *Pneumocystis carinii*, the yeast *Saccharomyces cerevisiae* and the protist *Euglena gracilis* the five central enzymes of the shikimate pathway, DHQ synthase, DHQ dehydratase, shikimate dehydrogenase, shikimate kinase and EPSP synthase are encoded by a single gene (Lumsden & Coggins, 1977, 1978; Gaertner & Cole, 1977; Berlyn & Giles, 1969, Banerji *et al.*, 1993). The expressed protein termed *arom* is a dimer with a subunit molecular weight of around 170kD. It has been suggested that the *arom* complex is the product of gene

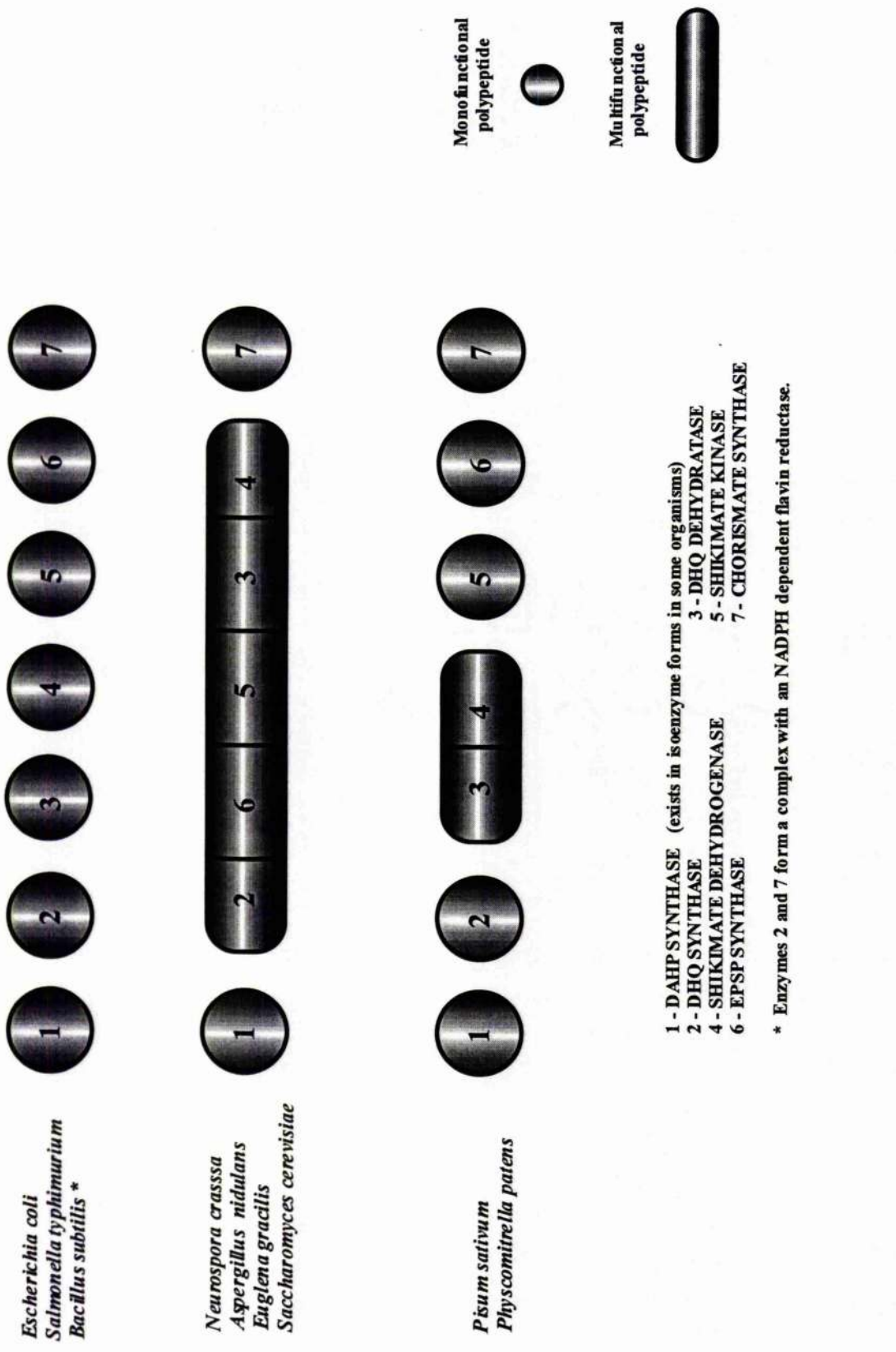


Figure 1.7. Enzyme organisation of shikimate pathway enzymes in different organisms.

fusion events. DHQ dehydratase and shikimate dehydrogenase constitute a bifunctional protein in *Physcomitrella patens* (moss) (Polley, 1978) and *Pisum sativum* (pea seedlings) (Koshiba, 1978; Deka *et al.*, 1994). The structural organisation of the pre-chorismate pathway enzymes in a number of organisms is shown in Figure 1.7.

While many hypotheses exist to explain gene fusions, including the enhancement of catalytic efficiency, substrate channelling and coordinate expression of enzyme activities it would appear that only the latter explanation can be applied to the *arom* polypeptide at present (Coggins *et al.*, 1985; Duncan *et al.*, 1987).

#### **1.4. Beyond chorismate.**

##### **1.4.1. Phenylalanine and tyrosine pathways.**

Both the phenylalanine and tyrosine pathways begin with the conversion of chorismate to prephenate by chorismate mutase (Figure 1.2). In *E. coli* the reaction is catalysed by a bifunctional chorismate mutase which exists as two isoenzymes. One has associated prephenate dehydratase activity, and therefore helps to channel chorismate towards L-phenylalanine synthesis. This enzyme is also subject to feedback inhibition by L-phenylalanine. The second isoenzyme has associated prephenate dehydrogenase activity directing the synthesis of L-tyrosine, and is correspondingly inhibited by L-tyrosine. The isoenzymes are dimers with subunit molecular weights of 40kD (Pittard, 1987).

*B. subtilis* has a monofunctional chorismate mutase which exists as a homodimer of 14.6kD subunits, somewhat smaller than the enzyme from other organisms. The gene encoding the enzyme has been cloned and sequenced (Henner *et al.*, 1986) and the putative encoded sequence bears only minimal similarity with other chorismate mutases. The enzyme is product inhibited by prephenate. Prephenate dehydratase and prephenate dehydrogenase are strongly inhibited by L-phenylalanine and L-tyrosine, respectively in *B. subtilis* (Henner & Yanofsky, 1993).

The phenylalanine and tyrosine pathways correspondingly produce phenylpyruvate and 4-hydroxyphenylpyruvate. The final reaction in both pathways involves the transamination of the respective  $\alpha$ -keto acids with glutamate as the amino group donor. In both *E. coli* and *B. subtilis* several enzymes with broad specificities are capable of catalysing this reaction (Haslam, 1993).

#### 1.4.2. The tryptophan pathway.

The biosynthetic route to tryptophan from chorismate requires seven enzymatic functions, designated A through G. In *E. coli* the seven enzymatic functions necessary for synthesis are encoded in seven genes that constitute a single operon. These functions are performed by two enzyme complexes E<sub>2</sub>(G-D)<sub>2</sub> and B<sub>2</sub>A<sub>2</sub> and a single bifunctional enzyme C-F [dashes indicate covalent linkage] (Haslam, 1993; Pittard, 1987). In *B. subtilis* the seven enzymatic functions are encoded by seven genes which specify the complexes, EG and B<sub>2</sub>A<sub>2</sub> with the remaining enzymes being independent (Henner & Yanofsky, 1993). Again, as in the pre-chorismate pathway the gene designations differ in *B. subtilis* from those in *E. coli*. Six of the seven *trp* genes are present in a supraoperon (section 1.3) while the seventh is located in an operon predominantly concerned with folic acid biosynthesis.

The conversion of chorismate to anthranilate (Figure 1.2), catalysed by anthranilate synthase, is the first step in the pathway and is the major feedback-sensitive enzyme in tryptophan biosynthesis in both *E. coli* and *B. subtilis*. Anthranilate synthase is composed of the TrpE and TrpD polypeptides in *E. coli* and the TrpE and TrpG polypeptides in *B. subtilis* (Pittard, 1987; Henner & Yanofsky, 1993). The reaction involves the amination and aromatisation of chorismate, with either ammonia or glutamine serving as the amino donor.

Phosphoribosyl transferase the next enzyme in the tryptophan pathway is bifunctional in *E. coli*, one domain having amidotransferase activity and the other catalysing the condensation of anthranilate with the ribose-5-phosphate moiety of phosphoribosyl pyrophosphate (Somerville, 1983). In *B. subtilis* the TrpD polypeptide containing phosphoribosyl transferase activity does not associate with anthranilate synthase (TrpEG)(Henner & Yanofsky, 1993).

Phosphoribosyl anthranilate transferase isomerase and indole glycerol phosphate synthase catalyse the Amadori rearrangement of phosphoribosyl anthranilate followed by decarboxylation and ring closure reactions to produce indoleglycerol phosphate, the immediate precursor of tryptophan. These reactions are performed by a bifunctional enzyme in *E. coli* but independent monofunctional enzymes in *B. subtilis* (Somerville, 1983; Henner & Yanofsky, 1993).

Tryptophan synthase the final enzyme in the tryptophan pathway catalyses the pyridoxal-phosphate-dependent conversion of indoleglycerol phosphate and serine to

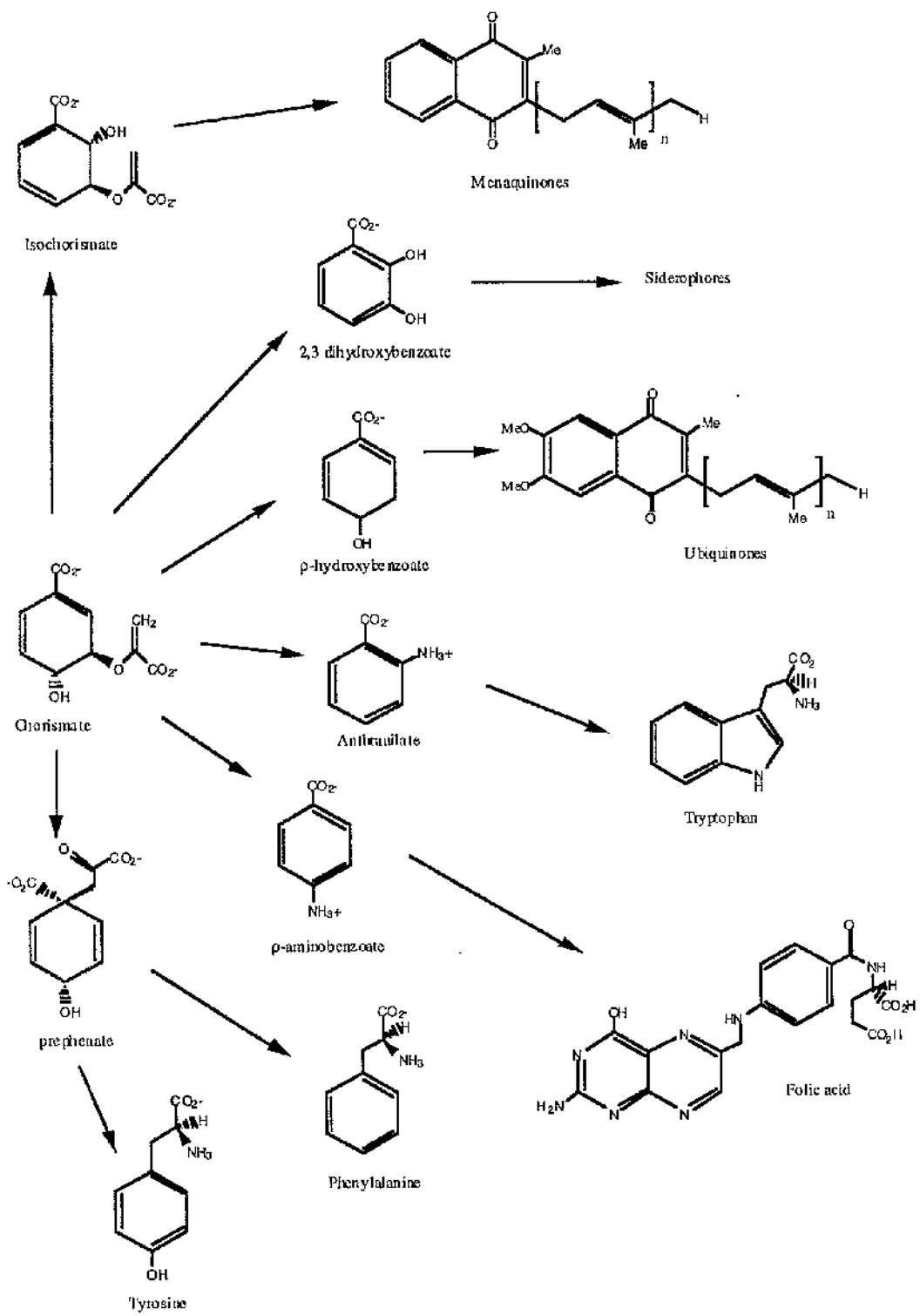


Figure 1.8. Chorismate and beyond, the primary metabolic pathways.

tryptophan and glyceraldehyde-3-phosphate. In both *E. coli* and *B. subtilis* tryptophan synthase is a complex, TrpB<sub>2</sub>A<sub>2</sub> (Somerville, 1983).

#### 1.4.3. Other primary metabolites.

The production of chorismate by the pre-chorismate pathway is only the beginning of the biosynthesis of many other primary metabolites in bacteria. These are listed below in summary and detailed in Figure 1.8. Extensive reviews can be found in Bentley, (1990), Luckner, (1990) and Haslam, (1993).

**p-aminobenzoate and folate coenzymes.** Tetrahydrofolate, synthesised via p-aminobenzoate, holds a central position in one-carbon metabolism. Formyl groups, hydroxymethyl, and methyl groups may be transferred via a number of tetrahydrofolate derivatives. Tetrahydrofolate serves as the acceptor of the  $\beta$ -carbon atom of L-serine when it is cleaved to yield L-glycine (Luckner, 1990). This reaction is of special significance as a source of active 1-carbon atoms required in the synthesis of methionine, thymine, and the purines.

**Quinone biosynthesis.** The lipid-soluble isoprenoid quinones participate in the multienzyme terminal oxidation respiratory complex. The quinones are believed to function in electron relay between other respiratory coenzymes and may have a more direct role in the process of oxidative phosphorylation (Bentley, 1990; Haslam, 1993). The ubiquinones (coenzyme Q) are found universally in nature with the exception of the Gram-positive bacteria and blue-green algae. The menaquinones (vitamin K<sub>2</sub>) are synthesised via isochorismate, have many similarities with the ubiquinones and are found only in bacteria and some fungi (Haslam, 1993).

**Siderophores.** Many organisms synthesise, via 2,3-dihydroxybenzoic acid, a class of compounds to sequester iron ( $Fe^{3+}$ ) under conditions of iron deprivation. These compounds, such as the catechol enterobactins, form one of the two major types of siderophore. The other structural type being the hydroxamates which includes ferrichrome and aerobactin (Luckner, 1990; Bentley, 1990).

#### **1.4.4. Secondary metabolites.**

A vast array of secondary metabolites are biosynthesised from chorismate. These will not be discussed further here but include antibiotics, such as chloramphenicol and vancomycin as well as mycotoxins and phenazines (pigments).

#### **1.5. Importance and significance of the shikimate pathway.**

While the shikimate pathway is of obvious importance to the host microorganism or plant there are a number of important features of the pathway which are of direct benefit to humans and animals and some other features of the pathway which may be exploited for medical benefit. Of immediate importance, and frequently overlooked, is the production of the aromatic amino acids, folic acid and the vitamins K<sub>1</sub> and K<sub>2</sub>. These are essential dietary requirements of humans and animals (with the exception of tyrosine which can be formed from the hydroxylation of phenylalanine) which during the course of evolution have 'lost' the ability to produce these components for themselves. The symbiotic relationship between the commensal gut bacteria in humans and animals is a prominent source of some of these components.

Detailed in the following sections are some of the ways in which man has been able to exploit the pathway for medical benefit.

##### **1.5.1. Engineering inhibitors/antibiotics.**

As mentioned briefly above the shikimate pathway leads ultimately to the production, in some microorganisms, of secondary metabolites which have antimicrobial activity. The absence of the pre-chorismate pathway and its primary metabolic branches from humans has allowed for the possibility of producing synthetic antimicrobials directed towards some of the enzyme reactions.

###### **1.5.1.1. Sulphonamides.**

The sulphonamides are synthetic antibacterial agents which are structural analogues of para-amino benzoic acid (PABA). Sulphonamides interfere with the synthesis of folic acid by inhibiting the condensation of PABA with 2-amino-4-hydroxy-6-

dihydropteridinylmethyl pyrophosphate to form dihydropteroic acid. The sulphonamides compete with PABA in this reaction not simply by occupying the active site on the enzyme but by acting as alternative substrates for dihydropteroate synthase. (Willet, 1988).

### 1.5.1.2. Glyphosate.

Interference with the biosynthesis of aromatic amino acids has been demonstrated with the active component of the nonselective, broad spectrum herbicide glyphosate (N-phosphonomethyl glycine). The primary target of this herbicide is EPSP synthase, although other enzymes are inhibited to a lesser extent in some organisms (Amrhein *et al.*, 1980). Glyphosate has been shown, with all the EPSP synthases studied to date, to be a competitive inhibitor of the substrate phosphoenolpyruvate (PEP). Resistance to glyphosate in microorganisms and plant tissue culture generally occurs as a result of increased levels of sensitive EPSP synthase or the production of an insensitive enzyme. The discovery of glyphosate owes more to serendipity than rational design but demonstrates the specific inhibition of the pre-chorismate pathway (Haslam, 1993).

### 1.5.1.3. (6S)-6-Fluoroshikimic acid.

The (6S)-6-fluoro analogue of shikimic acid was chemically synthesised with the expectation that it would inhibit the biosynthesis of primary aromatic metabolites in bacteria (Sutherland *et al.*, 1989). The compound was shown to be transported into the cytoplasm of the cell by the shikimate transport system and sequentially became a substrate for shikimate kinase, EPSP synthase and chorismate synthase (Davies *et al.*, 1994; Ramjee, 1992; Ewart *et al.*, 1995; Jude *et al.*, unpublished). The original incorporation of a fluorine was based on the rationale that (6S)-6-fluoroshikimate would be biosynthesised through the pre-chorismate pathway to produce a lethal intermediate or end product of a post-chorismate pathway (Davies *et al.*, 1994)

This prediction turned out to be fully realised with the fluoro analogue producing inhibition of  $\rho$ -amino benzoic acid (PABA) synthesis, and thus folic acid production (Davies *et al.*, 1994; Ewart *et al.*, 1995). The success of inhibiting this post-chorismate branch with the sulphonamide class of antibiotics and now (6S)-fluoroshikimate is a consequence of the essential nature of the product of the pathway and the inability of bacteria to obtain PABA from vertebrate tissues (Hoiseth & Stocker, 1981; Davies *et*

*al.*, 1994). (6S)-fluoroshikimate was demonstrated to protect mice against challenge with *E. coli* B (Davies *et al.*, 1994). However, a high frequency of spontaneous resistance to the compound was observed resulting from the loss of activity of the shikimate transport system in these resistant variants (Ewart *et al.*, 1995; Jude *et al.*, unpublished). The frequency of mutation was observed to occur at a level which would be expected to reduce the usefulness of this compound as an antibacterial agent.

The success of (6S)-6-fluoroshikimate as an inhibitor of the shikimate pathway, regardless of the resistance problems, demonstrates the inherent vulnerability of the pathway, and in particular PABA synthesis, to the rational design of selectively toxic inhibitors.

### **1.5.2. Aromatic-dependent bacteria as live vaccines.**

The increasing problem of antibiotic-resistant strains of bacteria in the developed world, and the non-availability of antibiotics and optimal medical care in the developing world has increased the need for the production of prophylactic bacterial vaccines. The ability to produce genetically defined lesions in bacteria has led to the use of live attenuated strains as vaccines. The pre-chorismate pathway has become a major target for the production of just such genetically defined lesions leading to live vaccine production.

Auxotrophic mutants, and in particular PABA-dependent mutants, of salmonellae were first shown to be attenuated in the 1950s (Bacon *et al.*, 1951). However, it was in the 1980s that Stocker demonstrated that an *aroA* lesion in a virulent strain of *S. typhimurium* produced attenuation *in vivo* (Hoiseth & Stocker, 1981). The critical product in this regard was PABA which bacteria are unable to assimilate from vertebrate tissue a feature also demonstrated with the effectiveness of sulphonamide chemotherapy. Thus while the bacteria will colonise a mammalian host, their potential for growth is severely limited by the supplies of PABA. It has subsequently been shown that other genes in the pre-chorismate pathway, including *aroC* and *aroD*, are essential for *in vivo* growth (Chatfield *et al.*, 1992a).

The immunogenicity of an *aroCaroD* deletion strain of *Salmonella typhi* has been tested in humans and shown to be effective. *Aro* mutants have been shown to produce protective immunity against salmonellosis in fowl and calves (Jones *et al.*, 1991; Griffin & Barrow, 1993; Cooper *et al.*, 1992). Furthermore aromatic dependent (*aro*) mutants of the following pathogens have been shown to be avirulent and stimulate protective immunity: *Shigella flexneri* (Verma & Lindberg, 1991; Karnell *et al.*, 1993), *Bordetella pertussis* (Roberts *et al.*, 1990), *Yersinia enterocolitica* (Bowe *et al.*, 1989), *Aeromonas salmonicida* (Vaughan *et al.*, 1993) and *Bacillus anthracis* (Ivins *et al.*, 1990). Attenuated salmonella strains have also been used as experimental oral carriers for the delivery of heterologous antigens to the immune system (Chatfield *et al.*, 1992b; Strugnell *et al.*, 1992; Poirier *et al.*, 1988). These experimental vaccines are attractive as salmonellae are effective carriers inducing secretory and humoral antibodies and various cell mediated responses (Chatfield *et al.*, 1992a).

### 1.6. Flavin reductases.

All chorismate synthases have an essential requirement for a reduced flavin cofactor for activity. However, the ability to reduce the flavin cofactor differs markedly between the enzymes. The *N. crassa* enzyme has an intrinsic NADPH-dependent flavin reductase activity while chorismate synthase from *B. subtilis* and *E. gracilis* are found associated with enzymes having flavin reductase activity. These enzymes can all be assayed aerobically by monitoring diene formation at 275nm. The lack of associated flavin reductase activity with the monofunctional chorismate synthases from *E. coli* and *C. sempervirens* means that the flavin cofactor must be reduced by chemical or photochemical means or alternatively by enzymic means with the addition of a flavin reductase.

NAD(P)H-dependent flavin oxidoreductases catalyse the reduction of flavins, flavin mononucleotide (FMN), flavin adenine dinucleotide (FAD) or riboflavin, by reduced pyridine nucleotides, NADPH or NADH. Flavin reductases have been purified from a number of microorganisms: *E. coli* (Fontecave *et al.*, 1987), *B. subtilis* (Hasan & Nester, 1978a), *Pseudomonas aeruginosa* (Halle & Meyer, 1992), *Vibrio harveyi* (Lei *et al.*, 1994; Jablonski & DeLuca, 1978) and *Entamoeba histolytica* (Lo & Reeves, 1980).

The purified enzymes have a number of characteristics in common. Most flavin reductases are cytosolic enzymes consisting of one polypeptide chain with molecular weights in the range of 20-30kD. With the exception of the *V. harveyi* enzyme they are not flavoproteins i.e. do not have flavin bound to the enzyme. Rather the polypeptide chain has an active site which allows both the reduced pyridine nucleotide and the flavin to transiently bind allowing a rapid electron transfer to proceed (Fontecave *et al.*, 1994). The enzymes can act on a variety of flavin electron acceptors, although the respective affinities for each vary ( $K_m$  between 1 and 40 $\mu$ M). Flavin reductases may also be divided into three groups: one including enzymes specific for NADH, another for enzymes specific for NADPH, and a third for enzymes accepting both NADH and NADPH.

Several flavin reductases may be present in some microorganisms. Two flavin reductases have been purified from *E. coli* and the *fre* gene encoding one of these has been cloned and sequenced (Spry *et al.*, 1991). Similarly two flavin reductases have been cloned and purified from *V. harveyi* (Lei *et al.*, 1994; Zenno & Saigo, 1994; Watanabe & Hastings, 1982).

Another interesting feature of the flavin reductases is that they have been found to be associated with other biological processes requiring reduced flavins. A flavin reductase from *B. subtilis* has been shown to be associated with the pre-chorismate pathway enzymes chorismate synthase and dehydroquinate synthase (Hasan & Nester, 1978a). The enzyme was found to be 13kD as discussed in section 1.2.7.4.2, but if this mass was underestimated by around half then the enzyme would be of similar molecular weight to those previously characterised.

Each of the purified flavin reductases from *Vibrio harveyi* have been postulated to be capable of forming a complex with luciferase (Jablonski & DeLuca, 1978; Duane & Hastings, 1975; Hastings *et al.*, 1985). Bacterial luciferase catalyses the oxidation of reduced FMN by oxygen in the presence of a long-chain aldehyde with the emission of light (bioluminescence). It was suggested that the flavin reductases were supplying reduced flavin to the luciferase reaction *in vitro* since coupling the reductase reaction to light emission decreased the apparent  $K_m$  of the enzyme for NADH, NADPH and FMN (Jablonski & DeLuca, 1978). However, a decrease in the apparent  $K_m$  was not seen when the reductase reaction was monitored directly in the presence of the luciferase reaction. Only when the coupled luciferase reaction was monitored could changes in the  $K_m$  for the flavin reductase be observed.

The best studied interaction of a flavin reductase with other enzymes is that with the complex multiprotein system that catalyses the transformation of an inactive form of ribonucleotide reductase into an active enzyme, containing a radical on Tyr-122 (Fontecave *et al.*, 1987, 1989). The function of the flavin reductase is to reduce the non-heme ferric centre of ribonucleotide reductase and is followed by the formation of the tyrosyl radical with the reaction of the reduced iron centre with molecular oxygen (Fontecave *et al.*, 1989; Fontecave *et al.*, 1994). The flavin reductase was in this context suggested to provide a mechanism for regulating ribonucleotide reductase and thus DNA synthesis (Fontecave *et al.*, 1994)

### **1.7. Aims of the project.**

**To clone and sequence the gene encoding chorismate synthase from the pathogenic bacterium *Staphylococcus aureus*.** At the time the project was started there were no sequences from Gram-positive bacteria known and of the four chorismate synthase sequences identified only two were bacterial and were from the evolutionarily related enteric bacteria *Escherichia coli* and *Salmonella typhi*.

**Maximally overexpress *S. aureus* chorismate synthase to facilitate subsequent purification of the enzyme in 100mg quantities.** The high overexpression of *E. coli* chorismate synthase using the *tac* promoter (White *et al.*, 1988) had enabled Ramjee, (1992) to purify 140mg of enzyme to around 95% purity from 20g of cells.

**Characterise the purified *S. aureus* enzyme in terms of subunit structure and native molecular weight and also investigate the enzyme using both steady state and pre-steady state kinetic techniques.** A comparison of the enzyme with the well characterised enzyme from *E. coli* would be undertaken. The use of pre-steady state techniques had resulted in the observation of a transient flavin intermediate during turnover of the *E. coli* enzyme (Ramjee *et al.*, 1991). The *S. aureus* enzyme would be investigated to determine whether such an intermediate was similarly observed.

---

**CHAPTER 2. MATERIALS AND METHODS.**


---

**2.0. Chemicals.**

Chemicals and biochemicals were generally Analar grade or the highest grade available and unless stated were from Sigma Chemical Company, England or Fisons Chemicals, England. Individual manufacturers of reagents and enzymes are indicated in the text, where appropriate.

**2.1. Strains and plasmids.**

The bacteria used during this project are detailed in Table 2.1. *Staphylococcus aureus* 601055, *Escherichia coli* BL21(DE3) and *Escherichia coli* HMS174(DE3) were obtained from Zeneca Pharmaceuticals Ltd. *Escherichia coli* GLW40, a *recA* strain of AB2849 (Pittard & Wallace, 1966) was obtained from Dr. I. Hunter, Laboratory of Genetics, University of Glasgow.

The plasmids used during this project are detailed in Table 2.2. Plasmid pCOC102 was the very kind gift of Professor Tim Foster, Moyne Institute, Dublin. Plasmid pTB361 was the kind gift of Dr. Peter Barth, Zeneca Pharmaceuticals Ltd. Plasmid pMAY1 was the kind gift of Dr. Anne Moir, Dept. of Molecular Biology and Biotechnology, University of Sheffield.

---

Bacterial Strain	Genotype
<i>Staphylococcus aureus</i> 601055	wild type clinical isolate
<i>Escherichia coli</i> DH5 $\alpha$	F $^+$ $\phi$ 80dlacZ $\Delta$ M15 <i>recA1 endA1 gyrA96 thi-1 hsdR17(rk<math>^-,</math>mk<math>^+</math>) supE44 relA1 deoR</i> $\Delta$ ( <i>lacZYA-argF</i> )U169
<i>Escherichia coli</i> GLW40	<i>aroC recA13 thi</i> (from AB2849)
<i>Escherichia coli</i> BL21(DE3)	F $^+$ <i>ompT rB<math>^-,</math>mb<math>^-</math> λ<sub>DE3</sub></i>
<i>Escherichia coli</i> HMS174(DE3)	F $^+$ <i>recA rk12<math>^-,</math>mk12<math>^+</math> Rif<math>^R</math> λ<sub>DE3</sub></i>
<i>Escherichia coli</i> AB1321	<i>aroA2 proA2 his4 thi lacY1</i>

---

Table 2.1. Bacterial strains and their genotypes.

### 2.1.1. Culture media and supplements.

The bacteria listed above were routinely cultured in Luria-Bertani medium (Bacto-tryptone 10g<sup>-1</sup>, yeast extract 5g<sup>-1</sup>, NaCl 10g<sup>-1</sup>) and grown overnight at 37°C with shaking. For culture on solid media, Bacto agar (Difco, Detroit, USA) was added at 1.5% w/v to the above medium. For culture on slopes, Bacto agar was added at 1% w/v to the medium.

For growth in minimal medium bacteria were cultured in M9S (NH<sub>4</sub>Cl 1g<sup>-1</sup>, MgSO<sub>4</sub>.7H<sub>2</sub>O 130mg<sup>-1</sup>, KH<sub>2</sub>PO<sub>4</sub> 3g<sup>-1</sup>, Na<sub>2</sub>HPO<sub>4</sub> 6g<sup>-1</sup>) with 12ml per litre of sterile glucose solution (D-glucose AR 15g and 7.5 ml of 100mM CaCl<sub>2</sub> made to 90ml with water). For the preparation of minimal agar 250ml of 2xM9S was autoclaved separately from an equal volume of water containing 2% w/v Oxoid N°1 (Oxoid Ltd., Basingstoke, England); this prevented the precipitation of the salts. When hand-hot, 6ml of glucose solution was added to the M9S solution together with the appropriate amino acids and vitamins detailed in Table 2.3. The agar solution and the M9S solution were then mixed before the plates were poured.

Plasmid	Remarks	Reference
pUC18	general cloning vector	Yanisch & Peron, 1982
pBluescript SKII	general cloning vector	Short, J.M <i>et al.</i> , 1988
pCOC102	<i>S. aureus</i> 8325-4	O' Connell <i>et al.</i> , 1993
	<i>aroA</i> <i>aroB</i> partial <i>aroC</i>	
pMAY1	<i>Bacillus subtilis</i> <i>gerCA</i> <i>gerCB</i> <i>gerCC</i> genes	Yazdi, 1989
pGM605	<i>aroC</i> overexpression plasmid	White <i>et al.</i> , 1988
pTB361	T7 expression plasmid	Dr. Peter Barth
pLysS	T7 lysozyme plasmid	Moffat & Studier, 1987
pLysE	T7 lysozyme plasmid	Moffat & Studier, 1987
pMJH701	<i>S. aureus</i> 601055 <i>ndk</i> , <i>aroC</i> <i>aroB</i> <i>aroA</i> genes	This study
pMJH702	<i>S. aureus</i> 601055 <i>ndk</i> , <i>aroC</i> genes	This study
pMJH7EX2	<i>aroC</i> overexpression plasmid	This study

Table 2.2. Plasmids.

Antibiotics were added to the culture medium at the following concentrations: ampicillin  $100\mu\text{g ml}^{-1}$ , tetracycline  $12.5\mu\text{g ml}^{-1}$ , chloramphenicol  $17\mu\text{g ml}^{-1}$  (all from Sigma). Stock solutions were made up in water or ethanol as appropriate and filter sterilised.

### 2.1.2. Storage of strains.

The long-term storage of bacteria was accomplished by making glycerol stocks of exponential or stationary phase cultures with the addition of sterile 80% v/v glycerol to a final concentration of 15% v/v. These were stored at  $-80^{\circ}\text{C}$  and never defrosted. For inoculation an upper piece of the frozen culture was chipped or melted off. For medium-term storage agar slopes were prepared and stored in a cool, dark place. Short-term storage was accomplished with the use of agar plates sealed with lasso tape and maintained at  $4^{\circ}\text{C}$ .

Supplement to minimal medium	Concentration
L-histidine	$50\text{ mg l}^{-1}$
L-proline	$150\text{ mg l}^{-1}$
L-tryptophan	$200\text{ mg l}^{-1}$
L-phenylalanine	$400\text{ mg l}^{-1}$
L-tyrosine	$200\text{ mg l}^{-1}$
PABA	$320\text{ mg l}^{-1}$
PHBA	$320\text{ mg l}^{-1}$
Thiamine-HCl	$2\text{ mg l}^{-1}$

Table 2.3. Supplements to minimal medium.

### 2.1.3. Strain identification

*Staphylococcus aureus* 601055 was a clinical isolate from Zeneca Pharmaceuticals culture collection. The strain was confirmed as *Staphylococcus aureus* using the apiSTAPH strain identification system (Bio Merieux, France) using the manufacturer's protocol and the accompanying computer software package. The organism was first subcultured on LB agar for 18 hours at  $37^{\circ}\text{C}$  and checked for purity by Gram stain and wet-film

microscopy. A homogenous suspension of the culture was made in an ampoule of apiSTAPH medium using 6 colonies before inoculating the test strip as directed and incubating at 37°C for 18 hours. A Staphylase test (Oxoid Diagnostic Reagents, England) was used as a supplementary and confirmatory test for *S. aureus* identification. As directed 3 colonies were smeared on the test strip and completely resuspended before adding 1 drop of test or control suspension. Clumping of the test suspension, rabbit fibrinogen sensitised sheep red blood cells, indicated a positive test.

## 2.2. Purification of genomic DNA from *S. aureus*.

A 50ml overnight culture was harvested by centrifugation at 10,000rpm (Sorvall RC-5B, SS-34) for 10 min. The cells were resuspended in 5ml of TE (10mM Tris-HCl pH7.2, 1mM EDTA) and lysostaphin (Sigma) was added to give a final concentration of 100µg/ml. This was incubated at 37°C for 15min. 1ml of 0.5M EDTA, pH8.0 was added and the solution mixed before adding 1ml of 10% w/v SDS with further mixing to obtain a clear viscous solution.

An equal volume of TE saturated phenol was added and the solution mixed well before centrifuging at 3,000rpm for 10min. The aqueous layer was extracted with another equal volume of phenol and spun again. Two further organic extractions were performed using TE saturated phenol/chloroform and then chloroform. The aqueous layer was removed and the DNA precipitated with the addition of 1/10th volume of 1M NaCl and an equal volume of isopropanol. After mixing, the DNA was centrifuged at 5,000rpm for 10min. The pellet of DNA was washed in 70% v/v ethanol, drained, vacuum desiccated and redissolved in water overnight at 4°C.

## 2.3. Polymerase Chain Reaction (PCR).

This was performed in PCR tubes using a reaction volume of either 25µl or 100µl. Both Taq polymerase (Promega, USA) and Vent polymerase (New England Biolabs, USA) were used. Vent polymerase was used in instances where a greater fidelity was required. Taq polymerase was mainly used for the amplification of genomic DNA from *S. aureus* using multiply degenerate primers.

### 2.3.1. PCR using Vent polymerase.

Vent polymerase PCR reactions were performed in 100 $\mu$ l volumes and were prepared by adding the following sequentially: 10 $\mu$ l of 10 x Vent buffer, water, 10 $\mu$ l of 10 x dNTPs (3mM), 100ng template DNA and 100pmol of each primer.

The annealing temperature for the primers in the Vent PCR reaction was generally required to be lower than for Taq PCR in contrast to previous reports (Ceasc *et al.*, 1994). The typical cycle profile used was 94°C for 1min, 50°C for 1min and 72°C for 70sec per kb of DNA to be amplified, with 20-30 cycles being performed.

### 2.3.2. Recovery of PCR products from reactions.

20 $\mu$ l of PCR product was run on a 1% w/v agarose gel to determine whether the PCR reaction had produced the desired amplicon and whether other secondary PCR products were present. When only the desired amplicon was observed after agarose gel electrophoresis a Wizard PCR clean-up kit (Promega, USA) was used with elution of the DNA into sterile distilled water. When secondary bands were observed after agarose gel electrophoresis, the desired DNA band was excised from the gel and purified using either a Geneclean kit (BIO-101, USA), a Spin-X column (Costar, France) or phenol/ chloroform extraction.

For phenol/chloroform extraction the PCR product was first separated on a low melting point agarose gel and the band excised. An approximately equal volume of TE, pH7.2 was added together with an equal volume of TE-saturated phenol, pH7.2 and heated to 65°C for 5min, vortexed and spun at full speed for 5min. The aqueous layer was then promptly removed and further extractions of the aqueous layer with phenol, TE-saturated phenol/chloroform and TE-saturated chloroform were performed. The DNA was recovered by adding an equal volume of isopropanol and 1/10th volume of 1M NaCl, vortexing and spinning at full speed in a microfuge for 15min. The pellet was then dried and resuspended in a small volume of sterile, distilled water.

## 2.4. Plasmid DNA sequencing.

Plasmid DNA sequencing was performed on DNA isolated using a Qiagen plasmid kit (Qiagen, Germany). Typically 2.5-3 $\mu$ g of DNA was used for each sequencing reaction using a Sequenase 2.0 kit (Amersham, England).

To denature the DNA; for each reaction, 8 $\mu$ l of plasmid DNA (i.e. total volume contains 2.5-3 $\mu$ g) and 2 $\mu$ l of 1M NaOH, 1mM EDTA were mixed in an eppendorf tube and incubated at room temperature for 5min. 3 $\mu$ l of 3M NaAc, 17 $\mu$ l distilled water and 30 $\mu$ l of isopropanol were then added. The tubes were centrifuged at full speed for 15min, drained, vacuum desiccated and the DNA dissolved in 7 $\mu$ l of water. For each annealing reaction, 2 $\mu$ l of Sequenase reaction buffer and 1 $\mu$ l of primer (1-2 pmol/ $\mu$ l) was added. This was heated at 100°C for 1min before transferring the tubes to a 37°C waterbath for 20min to allow the primers to anneal.

For the sequencing reactions: the ddNTP mixes were dispensed into wells of a microtitre plate (Nunc plates are heat resistant). For 4 reactions 10 $\mu$ l of ddNTP mix and 1 $\mu$ l of DMSO were mixed together with 2.5 $\mu$ l amounts dispensed per well. The labelling mixture (L) was made up by adding, for four reactions, 2 $\mu$ l of labelling mixture, 1 $\mu$ l of DMSO and 7 $\mu$ l of water. To each template/primer mix 1 $\mu$ l of 0.1M DTT, 0.5 $\mu$ l of  $\alpha^{35}$ S[dATP] and 2 $\mu$ l of mixture L was added. The enzyme mixture (S), for 4 reactions, was prepared by mixing 10.6 $\mu$ l of enzyme dilution buffer and 1.4 $\mu$ l of Sequenase enzyme. 2 $\mu$ l of this was then dispensed into each template/primer/label mix and incubated at room temperature for 5min. Finally, 3.5 $\mu$ l of the complete mixture was dispensed into the 4 corresponding ddNTP wells for each reaction and incubated at 37°C for 5min. 4 $\mu$ l of stop/loading dye was added and mixed before storing at -20°C until loading.

### 2.4.1. Sequencing gel and sample loading.

A BRL S0 sequencing gel kit was used for sequencing with gels being poured the day before running and stored at 4°C overnight. A 6% sequencing gel was prepared by mixing 63g of urea, 22.5ml of 40% w/v acrylamide solution, 15ml of 10 x TBE (900mM Tris-HCl, 900mM boric acid, 25mM EDTA pH8.3) made to 150ml with distilled water. 750 $\mu$ l of 10% w/v ammonium persulphate and 125 $\mu$ l of TEMED were then added, the solution mixed and poured without degassing.

The samples were heated to 75-80°C and placed on ice immediately before loading. 3µl of sample was loaded per well and the gel run at 40mA for 4 hours or until the bromophenol blue reached the base of the gel. After electrophoresis the gel was fixed for 30min in 2 litres of 10% v/v methanol, 10% v/v acetic acid then transferred to a sheet of 3MM Whatman paper and dried at 80°C under vacuum on a gel drier. An autoradiograph was then set up using Hyperfilm MP (Amersham, England) with exposure for around 18 hours and development using a Kodak X-Omat.

Primer	Sequence	Location in pMJH702
CHOR 16	CCTGCAGCAAGTATCGTC	2171-2188
CHOR 17	TATGATCGTAAATTAGAT	1854-1872
CHOR 19	GTTTTCGCTTCATCAAT	1768-1751
CHOR 20	GTCGTAGCGGTGGGTGCA	1562-1580
CHOR 22	AGTAATATACATAAACCT	182-200
CHOR 23	AGCATGTGCCGGTCTTGG	1463-1481
CHOR 24	ATCTAATTACGATCATA	1854-1872
CHOR 25	TGTGCATTCATAAATGTT	1076-1058
CHOR 26	ATTTGCAGGTACACCTTC	1214-1196
CHOR 27	GGAGAATCACATGGACCT	1159-1177
CHOR 28	TGGATAATTGTTGAAGG	2372-2354
CHOR 29	TGTTTCTCTGGCAGATGA	1555-1537
CHOR 30	GAACACCAAGGTAAACCA	374-392
CHOR 31	AATATACAAGCTATATT	841-823
CHOR 32	CACGGTTCAGATTCTTAA	565-583
CHOR 33	ACCAATTAGATITCTTTG	281-263

**Table 2.4. Sequencing oligonucleotide primers.**

## 2.5. DNA cloning procedures.

### 2.5.1. Restriction of *S. aureus* genomic DNA.

Genomic DNA was generally cut in a 50 $\mu$ l volume with a relatively high number of units of restriction enzyme to ensure complete digestion. 2 $\mu$ g of genomic DNA would be cut with 10-20U of enzyme for 2 hours at 37°C in the appropriate buffer before adding a further 10-20U of enzyme with incubation for 3 hours. The restriction enzymes were inactivated, where possible and when appropriate, by incubation at 65°C for 20min.

### 2.5.2. Restriction of plasmid DNA.

The two general purpose cloning vectors, pUC18 and pBluescript SKII, were used for cloning procedures. For genomic DNA cloning pBluescript was exclusively used. 5 $\mu$ g of plasmid DNA was digested in a 50 $\mu$ l volume with 10-20U of restriction enzyme in the corresponding buffer at 37°C for 1 hour.

### 2.5.3. Alkaline phosphatase treatment of cut plasmid.

Calf intestinal alkaline phosphatase (CIAP) was added to the digested plasmid at the concentration of 1.0U per pmol of 3' or blunt ends and 0.1U per pmol of 5' ends. The molar amount of plasmid ends was calculated according to the following formula:

$$\text{g of plasmid} \times \text{No. of bases} / M_r \quad (M_r \text{ of a base } \sim 660)$$

The CIAP was added directly to the restriction buffer without inactivating the restriction enzymes, when possible. CIAP buffer was added and the volume made up to 100 $\mu$ l and incubated at 37°C for 1 hour. All of the enzymes were then subsequently removed using a Magic DNA cleanup column (Promega) with elution of the purified DNA in water.

### 2.5.4. Ligation of cut moieties.

Prior to ligation, concentrations of DNA were either measured accurately by spectrophotometry or by estimation from gel electrophoresis. Generally, several ratios of vector DNA and insert DNA were used in separate ligations. The ligations were performed in 10 $\mu$ l volumes with 1-3 Weiss units of T4 DNA ligase and incubated

overnight at 4°C. To facilitate blunt-ended cloning either twice this concentration of T4 DNA ligase was used or 0.025% v/v Nonidet P-40 was added.

## 2.6. Preparation of competent cells and transformation.

Competent cells were made on the day they were required. A single colony of the appropriate strain of *E. coli* was picked from an agar plate or a loop was used to melt a small amount of culture from the top of a glycerol stock. This was used to inoculate 20ml of LB medium which was incubated at 37°C overnight with shaking.

30ml of fresh LB medium was inoculated with 600µl of overnight culture and incubated at 37°C for around 2 hours until the OD<sub>600</sub> reached around 0.3. The cells were then spun down at 3,000g for 5min and completely resuspended in one half volume of ice-cold sterile 100mM CaCl<sub>2</sub>. The cells were left on ice for around 20min followed by centrifugation at 3,000g, 4°C for 5min with resuspension in one tenth volume of ice-cold 100mM CaCl<sub>2</sub>. The cells were usually left on ice for several hours prior to transformation.

For transformation of the cells, 5µl of ligation mix was diluted with 45µl of sterile, ice-cold TNE buffer (50mM Tris-HCl pH7.5, 50mM NaCl, 1mM EDTA) on ice and 100µl of competent cells were added. Transformation controls were performed at the same time and were made up to an equal volume. The mixture was incubated for 30min ensuring the contents were thoroughly mixed. The tubes were then transferred to a 37°C waterbath for 90s without agitation then immediately returned to ice for a further 30min. 1ml of L-broth was added and the tubes were incubated for 1-2 hours to allow expression of antibiotic resistance. Suitable aliquots were then plated onto selective plates and incubated overnight at 37°C.

## 2.7. Southern hybridisation.

DNA fragments from genomic DNA digests were transferred onto Hybond-N (Amersham, England) nylon membranes as described by Southern, (1975) with DNA being fixed to the membrane by baking the filter at 80°C for 2 hours. The membranes were blocked by incubating the membrane in prehybridisation buffer (50% v/v formamide, 6x SSC, 0.5% w/v SDS, 0.1% w/v NaPPi, 5x Denhardt's ) (50x Denhardt's is 1% w/v Ficoll, 1% w/v polyvinylpyrrolidone, 1% w/v bovine serum albumin) for 3-4 hours at 42°C. The prehybridisation buffer was discarded and changed to hybridisation

buffer which was the same as prehybridisation buffer but had no Denhardt's present. The radioactive probe was boiled for 5-10min to denature it before adding it to the hybridisation buffer. The membrane was hybridised at the highest possible stringency (42°C for homologous probes) for 12-14 hours. The membrane was then washed at room temperature in 2xSSC, 0.5% w/v SDS for 5min followed by a subsequent wash in fresh 2xSSC, 0.5% w/v SDS for 15min. The filter was given two subsequent washes in 2xSSC, 0.5% w/v SDS for 15min followed by a stringent wash, if required (at 65°C in 0.1xSSC, 0.1% w/v SDS for 1 hour if homologous probe). An autoradiogram was then set up using two intensifying screens and left overnight at -70°C.

For heterologous probing experiments, prehybridisation was done in 6xSSC, 5xDenhardt's, 0.1% w/v NaPPi, 0.5% w/v SDS at 50°C. Hybridisation was done in the same buffer without Denhardt's. Washes of the membranes were done as above with the most stringent wash at 50°C in 1xSSC, 0.25% w/v SDS.

#### 2.7.1. Radioactive labelling of DNA.

Specific fragments of DNA that were used as radioactive probes were labelled to high specific activity using a Megaprime DNA labelling kit (Amersham, England). The method used was essentially as described in the manufacturers protocol. The subsequent labelling reaction was performed after melting the agarose containing the DNA without further purification.

The radioactive probe was purified to remove unincorporated nucleotides using a Sephadex-100 mini-column. This was prepared by filling the base of a 1ml syringe barrel, to a depth of roughly 1cm, with siliconised glass wool. The syringe barrel was filled with a solution of Sephadex-100 such that the top began to dry. The syringe barrel was then centrifuged at 3,000g for 3min and 100µl of TE added before centrifuging at 3,000g for 3min. Another addition of 100µl TE was made and the centrifugation repeated. The radioactive probe, made up to a volume of 100µl, was added to the column and centrifuged for 3min at 3,000g with an Eppendorf tube placed underneath to collect the labelled DNA. 1µl of the labelled DNA was counted in a scintillation counter.

## 2.8. Expression in pTB361.

The expression plasmid pTB361 is a *cer*, *tet<sup>R</sup>*, plasmid which contains a consensus T7 promoter immediately upstream from a multiple cloning site (Figure 2.1). The plasmid was obtained from Dr. Peter Barth, Zeneca Pharmaceuticals and its use is described in Brockbank & Barth (1993).

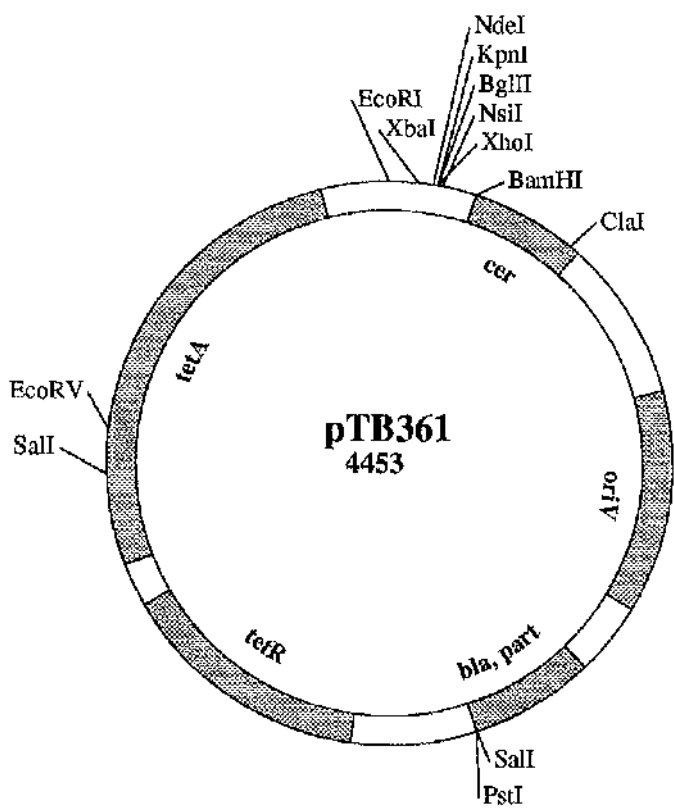


**Figure 2.1. Map of the expression vector pTB361 showing its main features.** The T7 promoter is located immediately upstream from the *NdeI* restriction site which marks the start of the multiple cloning site.

A number of host *E. coli* strains were used during studies on the expression of genes using the T7 expression plasmids. Initially JM109(DE3) (Promega, USA) was used, however, BL21(DE3) and HMS174(DE3) were found to give better expression. These latter strains were also used in conjunction with the pLysS and pLysE plasmids.

The inclusion of the gene for T7 lysozyme (which binds and inhibits T7 RNA polymerase) on plasmids pLysS and pLysE provides a means of controlling the basal levels of expressed protein prior to induction with IPTG. pLysE provides higher levels of T7 lysozyme by virtue of having the T7 lysozyme gene expressed from a *tet* promoter and thus lower basal levels of the target mRNA. The pLysS plasmid has the T7 lysozyme gene inserted in the inverse direction to the *tet* promoter producing lower levels of enzyme and allowing greater mRNA production (Studier & Moffat, 1986). These plasmids are compatible with pTB361 and confer chloramphenicol resistance. These host strains offer a number of advantages over the JM109(DE3) strain, notably BL21(DE3) is *ompT*, *lon* and HMS174(DE3) is *ompT* which may help to circumvent proteolysis during purification. The lysozyme produced from the pLysS and pLysE plasmids is sufficient to enable lysis with either freeze-thaw or mild Triton treatment.

For expression 20ml of an overnight culture was grown in LB with glucose plus antibiotic(s). 50ml of fresh LB with glucose plus antibiotic(s) was then inoculated with 5ml of overnight culture and grown to an OD<sub>600</sub> of 0.7-1.0. The culture was then made 0.4mM with respect to IPTG and grown for a further 4-5 hours removing 1ml samples at time-points. The OD<sub>600</sub> of the samples were measured and then they were centrifuged at full speed for 1min in a microcentrifuge. The cells were resuspended in 10µl of sample buffer for every 0.1OD unit and boiled for 5min before loading 20µl per well for a large gel or 5µl for a mini-gel.

To determine whether the overexpressed protein was soluble a sample of culture was pelleted by centrifugation and resuspended in a half final volume of TE buffer pH7.2. 100µg/ml of lysozyme was added and the cells incubated for 15min at 37°C. An equal volume of 2x sample buffer was added before centrifuging for 2min at full speed. The supernatant was then carefully removed and set aside and the pellet resuspended in a volume equal to the supernatant of sample buffer and both samples were boiled for 5min before loading.

### **2.8.1. Expression for protein purification**

Large scale growth of bacteria for subsequent enzyme purification was accomplished by growing 500ml cultures in 2l flasks in a flat-bed box shaker at 37°C. Typically 25-50ml of overnight culture was inoculated into 500ml of LB containing 0.4% w/v glucose and appropriate antibiotics. Growth for 2 hours at 37°C was usually sufficient before induction with 0.4mM IPTG and growth for a further 4-5 hours at 37°C was sufficient

for expression. Plasmids were transformed into *E. coli* expression strains prior to growth of cells for expression. This was required because of the low stability of the plasmids on storage.

### 2.9. $\lambda$ DE3 lysogenization of *E. coli* GLW40.

The site specific integration of the  $\lambda$ DE3 prophage into the chromosome of *E. coli* GLW40 was achieved using a commercially available  $\lambda$ DE3 lysogenization kit (Novagen Inc., Madison, WI). The production of GLW40(DE3) obviates the problem of having *E. coli* chorismate synthase present during purification of the *S. aureus* chorismate synthase as the lysogenized host was used to express target genes cloned into the T7 promoter vector, pTB361.

Lysogenization was accomplished in a three way infection with  $\lambda$ DE3, the helper phage, B10, and the selection phage, B842.  $\lambda$ DE3 cannot integrate into or be excised from the chromosome due to a defective *int* gene. The helper phage provides the *int* function that  $\lambda$ DE3 lacks but cannot form a lysogen by itself as it has a defective *cI* gene. The selection phage kills a major class of  $\lambda$ DE3 host range mutants that otherwise would be among the surviving cells but can neither integrate into susceptible cells (*cI*<sup>r</sup>) nor kill  $\lambda$ DE3 lysogens as it has the same immunity.

Specifically, lysogenization was achieved as follows. *E. coli* GLW40 was grown at 37°C to an OD<sub>600</sub> of 0.5 in LB supplemented with 0.2% w/v maltose, 10mM MgSO<sub>4</sub>. 5μl of  $\lambda$ DE3, 3μl of helper phage, and 3μl of selection phage were mixed with 7μl of *E. coli* GLW40 and incubated at 37°C for 20min to allow the phage to adsorb to the host. The cells were then plated onto LB plates and incubated at 37°C overnight.  $\lambda$ DE3 lysogens were screened by their ability to express chorismate synthase from pMJH7EX2.

### 2.10. Polyacrylamide gel electrophoresis

Sodium dodecyl sulphate polyacrylamide gel electrophoresis (SDS-PAGE) was performed essentially as described by Laemmli (1970). 3% stacking and 10% separating gels were routinely run in buffer comprising Tris-HCl (3g l<sup>-1</sup>), Glycine (15g l<sup>-1</sup>), and SDS (1g l<sup>-1</sup>). Samples were denatured by boiling for 5min after dilution in loading buffer comprising 60mM Tris-HCl pH6.8, 2% w/v SDS, 20% v/v glycerol, 10% v/v β-mercaptoethanol and 0.0025% w/v bromophenol blue.

### 2.10.1. Protein staining.

Protein was visualised on polyacrylamide gels after staining with Coomassie blue. The Coomassie reagent was prepared with 0.1% (w/v) Coomassie brilliant blue R-250 in 10% (v/v) glacial acetic acid, 25% (v/v) methanol. Destaining was performed with several changes of a 10% (v/v) glacial acetic acid, 10% (v/v) methanol solution.

### 2.11. Electroblotting proteins onto PVDF membranes.

A conventional 10% SDS-polyacrylamide gel was poured and 'aged' overnight at 4°C. Prior to electrophoresis the top buffer tank was made 0.1mM with respect to sodium thioglycollate (a free-radical scavenger). Both of these measures were designed to reduce the risk of N-terminal blockage of the protein. Proteins were electroblotted by a modification of the method of Matsudaira, (1987) onto polyvinylidenefluoride (PVDF).

The gel was trimmed using a scalpel blade and soaked in 400ml of electroblotting buffer (10mM CAPS/KOH pH11, 10% v/v methanol) for 30min. The mats and twelve pieces of Whatman No.3 paper, of approximately the same size as the mats, were soaked in electroblotting buffer. PVDF (Problott, Applied Biosystems) membrane was pre-treated by soaking in 100% methanol for a few seconds followed by 50% v/v methanol before leaving in electroblotting buffer. A BIO-RAD Trans-Blot electrophoresis transfer cell was connected with the cassette prepared as follows:

→ cassette /paper /mat /paper/ gel /PVDF /paper /mat /paper /cassette + ←

The gel was electroblotted at 100V constant voltage for 90min at 4°C. After transfer the cassette was dismantled and rinsed with deionised water for 5min followed by methanol for a few seconds. The PVDF was stained using Coomassie blue (0.1% w/v Coomassie R-250 in 50% v/v methanol) for 30sec and immediately destained in 50% v/v methanol, 10% v/v acetic acid. Destaining was done for only 3-4min to minimise acid hydrolysis. PVDF was rinsed in several changes of distilled water and air dried overnight.

### 2.12. Western blotting and immunoblotting.

Samples were separated on a 10% polyacrylamide gel. Afterwards the gel was rinsed in distilled water before setting up a blot similar to blotting onto PVDF (described above) except blotting onto nitrocellulose membrane (0.45 $\mu$ M, Schleicher & Schuell). After transfer the nitrocellulose membrane was blocked overnight with BIB (25mM Tris-HCl pH7.2, 12.5mM NaCl) and Tween 20 (0.5% v/v)(BIB+T). The nitrocellulose was incubated in 100ml of BIB+T containing 1% v/v polyclonal rabbit anti-chorismate synthase antibody raised against denatured enzyme and 5% v/v polyclonal donkey serum (SAPU) for 90 min at 23°C. This was followed with 4 washes in 100ml of BIB/T then 1 wash in BIB, each for 12min each. The nitrocellulose was then incubated in 100ml of 0.5% donkey anti-rabbit horse-radish peroxidase conjugated IgG (SAPU) for 90min at 23°C. This was followed by 4 washes in BIB over 1 hour. The membrane was developed with a 5min wash with 1-chloronaphthol solution.

### 2.13. Mutagenesis of chorismate synthase.

The mutation which was to be attempted was the conversion of tyrosine 121 of the *S. aureus* chorismate synthase to either phenylalanine or alanine. Tyrosine 121 corresponds to tyrosine 130 in the multiple sequence lineup (Figure 3.6).

Primer	Sequence	Length
CHOR 34	5'GGCATATGAGATACTAACATCAGGA <sup>3'</sup>	26
CHOR 35	5'GGAGATCTTAAACTCAATATTAAATTG3'	28
CHOR Y36F	5'GGCGGTATGAAATTAAATCATCGTGACTTACG <sup>3'</sup>	32
CHOR Y37F	5'CGTAAGTCACGATGATTAAATTICATACCGCC <sup>3'</sup>	32
CHOR Y38A	5'GGCGGTATGAAAGCTAATCATCGTGACTTACG <sup>3'</sup>	32
CHOR Y39A	5'CGTAAGTCACGATGATTAGCTTCATACCGCC <sup>3'</sup>	32

**Table 2.5. Primers designed for mutagenesis of the *aroC* gene.**

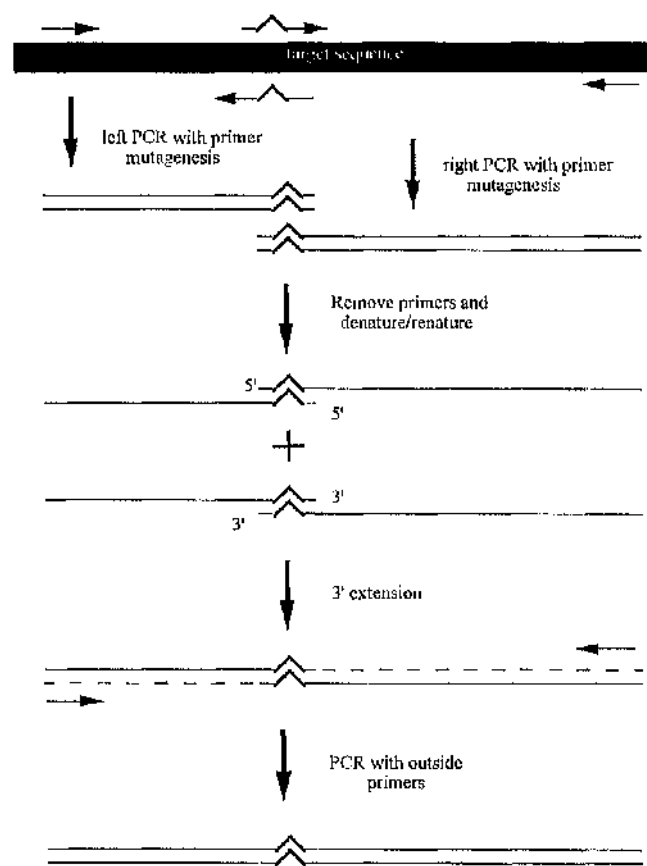


**Figure 2.2. Site-directed mutagenesis strategy using PCR, based on the method of Higuchi *et al.* (1988).**

The protocol followed was similar to that described in Higuchi *et al.*, (1988). Primary PCR reactions were set up as illustrated in Figure 2.2 using Vent polymerase. The standard Vent PCR reaction protocol was followed as described in 2.3.2 using 100 pmol of the primers CHOR 34 + CHOR Y36F, CHOR 35 + CHOR Y37F, CHOR 34 + CHOR Y38A or CHOR 35 + CHOR Y39A with 30 cycles at 94°C for 1min, 50°C for 1min and 72°C for 50sec. 2mM and 3mM MgSO<sub>4</sub> both gave identical results.

The PCR products obtained from the reaction were excised from an LMP gel to remove the primers and existing template. The DNA was cleaned up using phenol/chloroform extraction and around 100ng of each PCR moiety was added to a second PCR reaction. This contained 100pmol of primers CHOR 34/CHOR 35 and the temperature profile

used was the same as above except only 20 cycles were performed with an extension time of 1.75min.

The final PCR reactions were cleaned up using a Wizard PCR cleanup kit (Promega, USA). The purified DNA was digested with *Nde*I and *Bgl*II for 7.5 hours before cleaning up the DNA, this time with a Magic DNA cleanup kit. The DNA was finally ligated into pTB361 (Figure 2.1).

#### **2.14. Purification of *S. aureus* chorismate synthase.**

*E. coli* GLW40 pMJH7EX2 (13g wet weight) was thawed passively at room temperature and 10ml of buffer A\* (20% v/v glycerol, 50mM KCl, 50mM Tris-HCl pH 7.5 at 4°C, 1mM Benzamidine, 1.2mM PMSF, 1.3mM EDTA, 0.4mM DTT) was added. The cell paste was subjected to 2 passes through a French Press at 1000psi and then made up to 80ml with buffer A\*. 0.5mg of DNaseI was added and the mixture incubated for 30min at 4°C before spinning at 28,000g for 30min at 4°C.

A 120ml DEAE sephacel (Sigma) column (4cm i.d. x 15cm) was equilibrated with 3 ECVs of buffer A\*. The column was loaded at 40mlhour<sup>-1</sup> with the protein and the column washed with buffer A\* until the OD<0.3. The enzyme was then eluted with a gradient of 300ml of buffer A1 (20% v/v glycerol, 50mM KCl, 50mM Tris-HCl pH 7.5 at 4°C, 1.2mM PMSF, 1.3 mM EDTA, 0.4mM DTT) and 300ml of A2 (A1 with 500mM KCl) with 10ml fractions being collected. The pooled chorismate synthase activity was dialysed against 2 x 2l (3h then overnight) of buffer B1 (20% v/v glycerol, 10mM KPi pH6.6 @ 4°C, 0.45mM PMSF, 1.3mM EDTA, 0.4mM DTT).

A 60ml cellulose phosphate (Whaiman, England) column (4cm i.d. x 15cm) was prepared using NaOH and HCl as instructed in accompanying literature. The cellulose phosphate was resuspended in 200ml of 0.5M KPi pH6.6 at 4°C and the pH adjusted with KOH. The column was washed with 2ECVs of buffer B1 before loading (20mlhour<sup>-1</sup>) the dialysed protein and then washed with buffer B1 until OD<0.3. The chorismate synthase activity was eluted with a gradient of 200ml of buffer B1 and 250 ml of buffer B2 (A1 with 400mM KPi) with 5ml fractions being collected.

Chorismate synthase was concentrated using 80% w/v ammonium sulphate with 10% glycerol. This was then spun at 28,000g with resuspension in the minimum volume of

50mM Tris-HCl pH7.5, 0.4mM DTT, 1.2mM PMSF and 50% glycerol for long term storage.

### **2.15. Anaerobic UV Chorismate Synthase Assay.**

The assay was performed essentially as described by Ramjee *et al.* (1994). To begin the assay 20ml of buffer, 50mM MOPS, pH 7.5, 100mM NaCl was sparged with nitrogen gas for around one hour. This was done in a small flask stoppered with a No. 37 Subaseal stopper. A flushing needle (0.8mm i.d. x 70mm) was inserted into one end of a 30cm length of Portex tubing (0.5mm i.d.) and to the other end a second needle (0.4mm i.d. x 40mm) with a female luer was attached. The tubing allowed the buffer to be moved from the gas supply. The flask was vented by using a second needle.

Anhydrous potassium oxalate ( $\text{COOK}_2$ ) [184mg] was weighed out into an eppendorf tube and closed with a No.17 subaseal stopper; the solid was sparged for at least 10 min. 1ml of the sparged MOPS buffer was added to the potassium oxalate using anaerobic technique (i.e. syringe flushed with  $\text{N}_2$  dead space in vial then flushed with buffer). Once the  $\text{COOK}_2$  was dissolved 19 $\mu\text{l}$  was added to the MOPS buffer.

Standard assay constituents were: 50mM MOPS pH7.5, 100mM NaCl, 1mM Oxalate, 25 $\mu\text{M}$  FMN and 50 $\mu\text{M}$  EPSP. These were added separately using gas-tight syringes with 7cm needles to a sparged cuvette via a gas tap and Subaseal assembly. The cuvette was kept under a stream of  $\text{N}_2$ , with venting, by a length of portex tubing which was attached to a needle with female luer fitting. The other end of the tubing was inserted into a needle which was inserted through the Subaseal.

The FMN was photochemically reduced using a Schott LK1500 microscope lamp at full power setting for 3min. The photoreduction of the flavin was calibrated spectrophotometrically at 445nm. The cuvette was equilibrated at 25°C and assays were initiated with the addition of enzyme.

#### **2.15.1. Preparation of EPSP from its barium salt.**

EPSP was available in the laboratory as the barium salt,  $\text{Ba}_2(\text{EPSP})\cdot 2\text{H}_2\text{O}$  (Gibson, 1970). For assays this was converted to the potassium salt by first dissolving the barium salt in distilled water and adding an equal volume of 100mM potassium

sulphate. After a few minutes the sample was spun at full speed in a microfuge and the supernatant collected. The concentration of the substrate was ultimately determined spectrophotometrically by enzymatic conversion using  $\epsilon_{275}=2630\text{M}^{-1}\text{cm}^{-1}$ .

#### **2.16. Electrospray mass spectrometry.**

Mass spectrometry was performed on a VG platform quadropole mass spectrometer fitted with a pneumatically assisted electrospray source and controlled using the VG Mass-Lynx software (VG Biotech, Ltd, Altrincham, Cheshire, UK). The carrier solvent (1:1 (v/v) acetonitrile/water) infusion was controlled at a flow rate of 10 $\mu\text{l}/\text{min}$  using a Harvard syringe pump (Harvard Apparatus, South Natic, MA, USA). Capillary voltages were between 2.8 and 3.2kV, extraction cone voltages 20-30V and the focusing cone voltage offset by +10V. The source temperature was set at 65°C and the nebulising gas flow at 10 lhour $^{-1}$ . Lens stack voltages were adjusted to give maximum ion currents. Before use the instrument was calibrated over the molecular weight range of the protein of interest with horse heart myoglobin (Sigma).

Desalting of samples was carried out before analysis using Centricon-10 filtration units and HPLC grade water with concentration by centrifugation. For analysis samples were diluted with an equal volume of 4% (v/v) formic acid in acetonitrile and 10-20 $\mu\text{l}$  aliquots were injected directly into the carrier stream. The MaxEnt deconvolution procedure was applied for quantitative analysis of the raw data using 1.0Da peak width and 1 Da/channel resolution.

#### **2.17. Stopped-flow spectrophotometry**

Stopped-flow experiments were performed at the University of Sussex, and were carried out using a Hi-Tech Scientific SF-51 stopped flow spectrophotometer (Hi-Tech Ltd, UK) installed and operated in an anaerobic glove box as described previously (Ramjee, 1992). The apparatus was temperature controlled at 25°C using a C-400 Thermostatted Liquid Circulator (Techne, UK). Spectra of reaction intermediates were obtained using a Hi-Tech Scientific MG-6000 rapid-scanning photodiode array coupled to the stopped-flow sample handling unit. Rapid scanning experiments were carried out using a Xenon lamp with a 20mm slit width and single wavelength experiments were carried out using a Tungsten lamp with a 1.8nm slit width. Kinetic data was fitted using the Hi-Tech Scientific IS-2 v2.3b0 software.

A 100 $\mu$ l volume from each syringe was mixed (200 $\mu$ l final volume) with one syringe containing 40 $\mu$ M EPSP in 50mM Mops pH 7.0, 100mM NaCl and the other syringe containing 40 $\mu$ M chorismate synthase, 40 $\mu$ M FMN and either 1mM potassium oxalate or sodium dithionite in the same buffer. Where potassium oxalate was used as the reductant, FMN was reduced photochemically using a Schott LK1500 for 3min before the syringes were loaded. Glycerol concentrations were maintained at equality between the two syringes to minimise mixing problems. The glove box was operated and maintained at ~1ppm oxygen concentration using nitrogen gas as described previously (Ramjee, 1992).

#### 2.18. Purification of *E. coli* flavin reductase.

The protocol for purification of *E. coli* flavin reductase was based upon the procedure previously described by Fontecave *et al.* (1987), with a number of modifications. In particular, DEAE-Trisacryl was substituted by DEAE-Sephadex followed by phenyl sepharose chromatography. ACA 54 gel filtration chromatography was replaced with S-200 gel filtration chromatography and succeeded the phenyl sepharose step. The final FPLC protocol was omitted and glycerol was included in all purification buffers.

14g (wet weight) of *E. coli* BL21(DE3)pLysEpFREX2 was thawed passively at room temperature and resuspended in 20ml of ice cold buffer A (20% glycerol, 50mM HEPES pH8, 1.3mM EDTA, 0.4mM DTT, 1.2mM PMSF, 1mM benzamidine). The cells were lysed with three passes through a French press at 1,000 psi. The crude extract was made up to 80ml with buffer A before adding 0.5mg of DNaseI and stirring on ice for 30min. The extract was clarified by centrifuging at 16,000rpm (Sorvall SS-34) for 45 min and the supernatant was loaded at 40mlhour<sup>-1</sup> onto a 50 ml DEAE sephadex (Sigma) column (4cm i.d. x 15cm) pre-equilibrated with buffer A. The column was then washed with approximately 12 column volumes of buffer A before eluting the protein with a gradient of 300ml each of buffer A and buffer A2 (buffer A but 300mM NaCl) with 10ml fractions collected.

The pooled fractions containing flavin reductase were made 0.5M with respect to KCl by adding solid KCl. The pool was then loaded at 20mlhour<sup>-1</sup> onto a 25ml phenyl sepharose CL-4B (Sigma) column (4cm i.d. x 15cm) pre-equilibrated with buffer B (20% glycerol, 50mM Tris-HCl pH7.5, 0.4mM DTT, 1.3mM EDTA and 1.2mM PMSF) containing 0.5M KCl. The column was washed with a gradient of 150 ml each of 0.5M-0M KCl buffer B before finally eluting the enzyme with a step of buffer B\*

(10mM Tris HCl pH7.5, 0.4mM DTT, 1.3mM EDTA and 1.2mM PMSF) with 5ml fractions being collected.

The enzyme was precipitated using ammonium sulphate and was then resuspended in 10% glycerol, 50mM Tris-HCl, 0.4mM DTT. The enzyme was loaded at 10mlhour<sup>-1</sup> onto a 350ml S-200 gel filtration column (2cm i.d. x 1100cm) previously equilibrated with buffer C (10% glycerol, 50mM Tris-HCl pH7.5, 0.5M KCl, 0.4mM DTT). The column was run in buffer C and 5ml fractions collected. The enzyme was stored in buffer C with the inclusion of glycerol to 50% for long term storage.

#### **2.19. Flavin reductase assay.**

*E. coli* flavin reductase was assayed as described previously by Fontecave *et al.* (1987) except that a unit of activity was changed to correspond to the oxidation of 1μmol of NAD(P)H per min rather than 1nmol per min. The amount of activity obtained here was several orders of magnitude greater than has previously been obtained. Activity was assayed by following the time-dependent disappearance of NAD(P)H absorbance at 340nm. Assays were performed in a 1ml, 1cm path length cuvette containing 50mM Tris-HCl pH7.5, 0.25mM NAD(P)H and 3μM riboflavin. Incubation was made in air and at room temperature. Oxidation of NAD(P)H was calculated from the slope of the recorded change with one unit of activity corresponding to the oxidation of 1μmol of NADPH ( $\epsilon_{340}=6200\text{M}^{-1}\text{cm}^{-1}$ ) per min under the above conditions with specific activity as units per mg of protein.

#### **2.20. BIACore of *E. coli* flavin reductase and *E. coli* chorismate synthase.**

Possible interactions between *E. coli* flavin reductase and *E. coli* chorismate synthase were investigated using a BIACore 2000 instrument essentially as described in the users manual. The BIACore instrument enables one particular enzyme to be immobilised to a sensor chip allowing the interaction of a second enzyme with the first to be measured. This is made possible by immobilising the first enzyme to carboxyl groups which have been activated in the presence of a mixture of succinimide (NHS) and carbodiimide (EDC) to form active esters which react spontaneously with amine groups on the enzyme. Interaction of the second enzyme with the first is measured by changes in refractive index close to the surface of the sensor chip. These experiments were performed in collaboration with Mr. Tino Krell, University of Glasgow.

For the assay *E. coli* flavin reductase was immobilised onto the pre-activated sensor chip in coupling buffer consisting of 50mM NaAc pH4.2. 5 $\mu$ l of the flavin reductase (1.3mgml<sup>-1</sup>) in 50mM MOPS pH7.5 was mixed with 95 $\mu$ l HBS coupling buffer and 35 $\mu$ l loaded into the machine at a flow rate of 5 $\mu$ lmin<sup>-1</sup>. Interaction was tested using *E. coli* chorismate synthase. 25 $\mu$ l of 7.7mgml<sup>-1</sup> enzyme in 50mM MOPS pH7.5 was diluted in 800 $\mu$ l of HBS coupling buffer and 10 $\mu$ l was loaded with a flow rate of 5 $\mu$ lmin<sup>-1</sup>. The interaction of chorismate synthase with flavin reductase was also tested in the presence of 50 $\mu$ M FAD 50 $\mu$ M EPSP, or 50 $\mu$ M NADH.

The order of the interaction was also altered such that the *E. coli* chorismate synthase was immobilised and interaction of the flavin reductase measured. In this case 50 $\mu$ M EPSP and 50 $\mu$ M FAD were included throughout to counteract the problem of precipitation.

### **2.21. Chemical cross-linking.**

Cross-linking of chorismate synthase was achieved using dimethyl-suberimidate. Typically, 50 $\mu$ l of 2mg/ml enzyme was added to 50 $\mu$ l of freshly prepared cross-linking solution. Cross-linking solution was prepared by adding 4ml of 0.5M Triethanolamine pH8.0, 800 $\mu$ l of 1M NaOH and 109mg dimethyl-suberimidate made up to 10ml with 0.4M NaCl.

---

**CHAPTER 3. THE MOLECULAR CLONING AND SEQUENCING OF THE *AROC* AND THE *NDK* GENES, AND EVIDENCE FOR THE PRESENCE OF THE *GERCC* GENES UPSTREAM FROM *NDK*.**

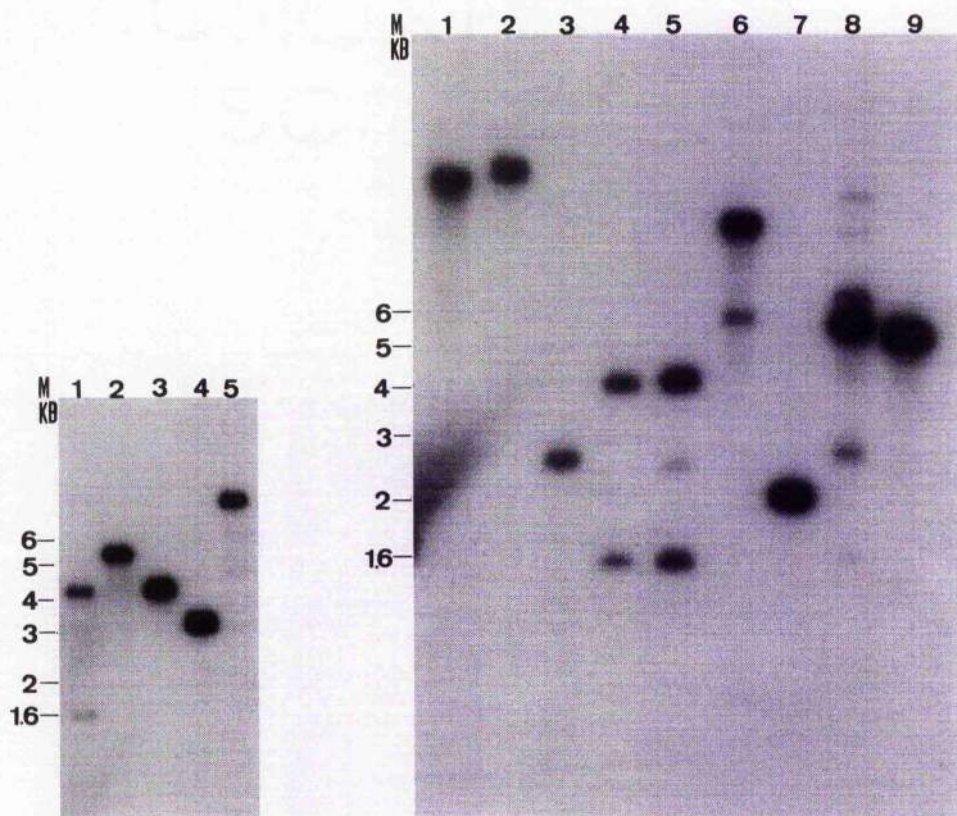
---

This chapter details the cloning and sequencing strategy used for isolating the *aroC* gene, encoding chorismate synthase, from *Staphylococcus aureus*. Sequence comparisons of the gene and the encoded protein are presented together with details of other genes which were isolated during the cloning of the *aroC* gene.

### **3.1. Cloning of the *aroC* gene.**

Chromosomal DNA from *S. aureus* 601055 was digested with a number of restriction enzymes and blotted onto Hybond-N membrane. The blot was probed with a 350bp *EcoRI-HindIII* DNA fragment from the plasmid, pCOC102, which contains part of the *aroC* gene. This plasmid also contains the complete *aroA* and *aroB* genes from *S. aureus* 8325-4 (O'Connell *et al.*, 1993). A 5.5kb *ClaI* fragment was observed after hybridisation (Figure 3.1) and from examination of the restriction map around the *aroA* region sequenced by O' Connell *et al.* (1993) was expected to contain the complete *aroC* gene. A plasmid library was therefore prepared by ligating *ClaI* digested chromosomal DNA into *ClaI* cut pBluescript.

The 5.5kb *ClaI* restriction fragment was cloned using its ability to complement the Aro<sup>-</sup> phenotype of the *aroC* strain of *E. coli*, GLW40. The *ClaI* library was transformed into *E. coli* GLW40 and the cells were plated directly onto minimal medium agar containing the appropriate supplements (Table 2.3). 12 colonies were obtained after incubation of the plates for 40 hours at 37°C. Small-scale plasmid isolations from each of the 12 colonies revealed the presence of plasmid containing a 5.5kb *ClaI* fragment and which produced identical restriction patterns following digestion with *EcoRI/HindIII*. One of the 12 clones was picked and the isolated plasmid, pMJH701, used to confirm the presence of the *aroC* gene by transforming *E. coli* GLW40 again and plating the cells onto minimal medium agar. As expected, many colonies were now visible after incubation for 40 hours at 37°C. The plasmid pMJH701 was similarly shown to complement the Aro<sup>-</sup> phenotype of the *aroA* strain of *E. coli*, AB1321. The complete coding region for *aroA*, the gene for 5-enolpyruvylshikimate 3-phosphate (EPSP) synthase is also contained within the 5.5kb *ClaI* fragment.



Lane M: DNA markers.  
 Lane 1: *AccI* digest  
 Lane 2: *Clal* digest.  
 Lane 3: *HindIII* digest.  
 Lane 4: *NdeI* digest.  
 Lane 5: *PstI* digest.

Lane M: DNA markers.  
 Lane 1: *SacI-SalI* digest.  
 Lane 2: *SacI* digest.  
 Lane 3: *NdeI-AccI* digest.  
 Lane 4: *AccI* digest.  
 Lane 5: *AccI-BamHI* digest.  
 Lane 6: *KpnI-BamHI* digest.  
 Lane 7: *EcoRI-Clal* digest.  
 Lane 8: *Clal* digest.  
 Lane 9: *Clal-BamHI* digest.

**Figure 3.1.** Southern blots of *S. aureus* 601055 DNA probed with the 350bp *EcoRI-HindIII aroC* fragment from *S. aureus* 8325-4.

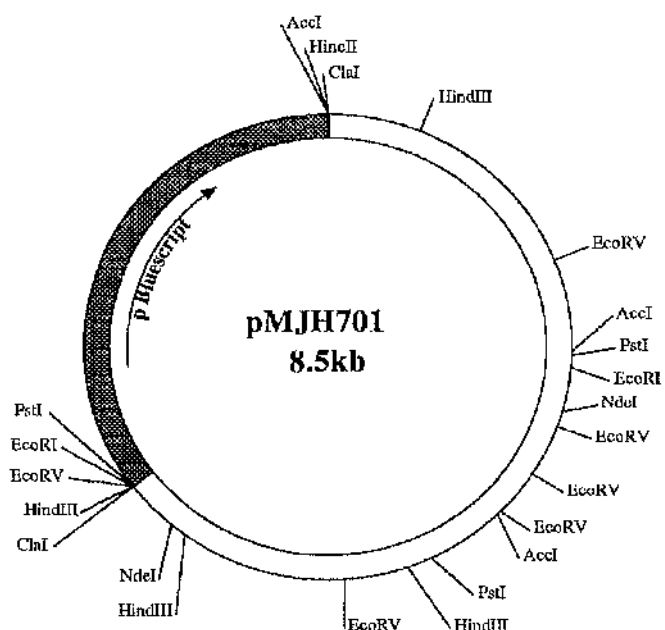


**Figure 3.2 Schematic diagram of plasmid pMJH701 showing restriction sites.**

### 3.1.1. Restriction mapping of pMJH701.

Plasmid pMJH701 was mapped with a number of restriction enzymes. Similarities were observed between pMJH701 and pCOC102 with respect to the position of many restriction enzyme sites although some differences were observed and are likely to be the result of strain differences. The similarities in the maps meant that the location of the *aroC* gene could be deduced with some degree of certainty.

### 3.1.2. Subcloning of pMJH701.

Plasmid pMJH701 (Figure 3.2) was subcloned to produce a number of plasmids for sequencing with the polylinker sequencing primers SK and KS (Stratagene) and primers designed from pUC18 sequence. A 2.5kb *NdeI-ClaI* fragment from pMJH701 was cloned into *NdeI-AccI* digested pUC18 to produce pMJH702 (Figure 3.4) and a 2.2kb *EcoRI-ClaI* fragment from pMJH701 was cloned into *EcoRI-ClaI* cut pBluescript producing pMJH703. Plasmid pMJH703 was subcloned further by

digesting the *Eco*RI-*Cla*I insert with *Dra*I and four of the resulting fragments were purified and cloned into *Sma*I digested pBluescript to produce pMJH706, pMJH707, pMJH708 and pMJH709. In addition, 1.4kb *Eco*RV-*Sal*I and 1.6kb *Nsi*I-*Sal*I fragments from pMJH701 were cloned into pBluescript and pGEM5, respectively, to produce plasmids pMJH710 and pMJH711. The variety of subclones produced may be of use for gene replacement work for the *aroC* gene similar to that performed by O'Connell et al. (1993) for the *aroA* gene.

### 3.1.3. Sequencing of plasmids and oligonucleotide primers.

The subclones produced were sequenced from each end using the appropriate primer derived from vector sequences. From the information generated it was determined that the entire *aroC* gene would reside completely within the 2.5kb *Nde*I-*Cla*I fragment of pMJH702 and consequently the complete sequence of pMJH702 was determined. Synthetic oligonucleotide primers spaced around 250bp apart along the template and based on previously sequenced regions were produced to complete the sequence of pMJH702 on both strands.

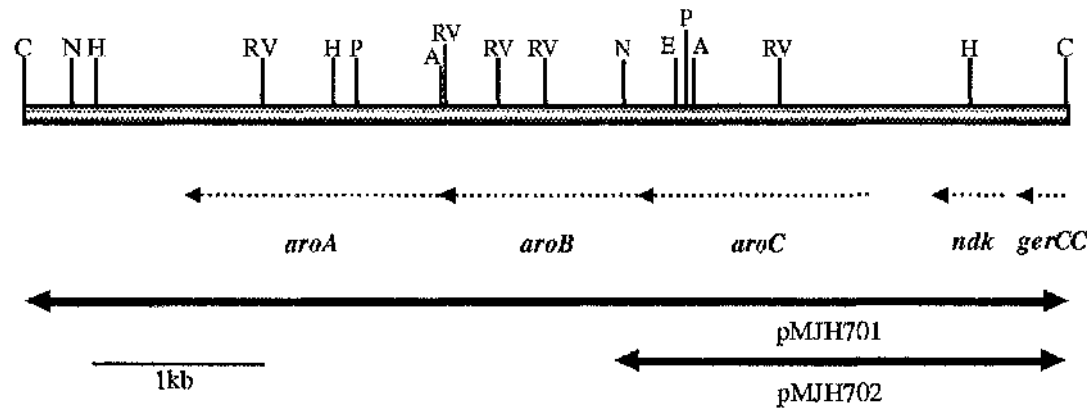


**Figure 3.3. Schematic diagram showing the 5.5kb *Cla*I fragment cloned into pMJH701 and the locations of the putative encoded proteins.** The locations of the *aroA* and *aroB* genes are included using the similarity in restriction maps generated from pCOC102 (O'Connell et al., 1993) and that of pMJH701. The locations of the *aroC*, *ndk* and partial *gerCC* genes were obtained from sequencing. Restriction enzymes are abbreviated: A, *Acc*I; C, *Cla*I; E, *Eco*RI; RV, *Eco*RV; H, *Hind*III; N, *Nde*I; P, *Pst*I.

### 3.1.4. Sequencing of pMJH702.

The DNA sequence together with the deduced amino acid sequence of the encoded proteins is shown in Figure 3.5. Two complete open reading frames (ORFs) were located by DNA sequencing. The predicted polypeptide from the larger of the two ORFs consisted of 388 amino acids and was 61% identical to the *aroF* gene product of *B. subtilis* and 37% identical to the *aroC* gene product from *E. coli*. The second complete ORF is situated some 500 base pairs upstream from *aroC* and the predicted polypeptide from this consisted of 149 amino acids and had 62% and 45% homology with the *ndk* gene products from *B. subtilis* and *E. coli*, respectively.

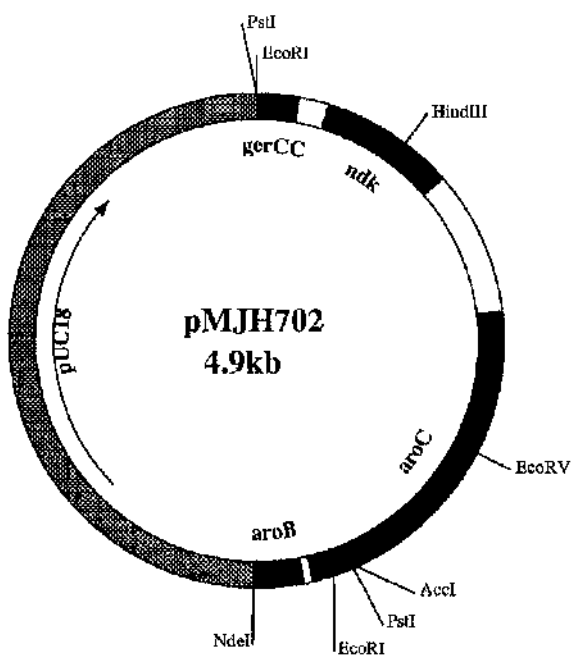


**Figure 3.4. Schematic diagram of plasmid pMJH702 showing restriction sites and relative locations of genes (*gerCC* 1-132, *ndk* 224-673, *aroC* 1142-2308, *aroB* 2343-2501).**

Contained within the 2.5kb of DNA sequenced in pMJH702 are two partial ORFs. Situated 25bp downstream from the TAA stop codon of *aroC* is the 5' end of an ORF (Figure 3.9) which has similarity with the *aroB* gene of *B. subtilis*. The *aroB* gene of *B. subtilis* encodes dehydroquinate synthase, the second enzyme of the shikimate

pathway. The 3' end of the second partial ORF immediately precedes the *ndk* gene and the translated product from this has similarity with the putative *gerCC* gene product from *B. subtilis* (Figure 3.10).

Immediately upstream from both the *aroC* and *ndk* genes are putative promoter sequence elements. These regions -66 to -42 ATGAAT (18 bases) TATTAT and -63 to -47 TTGAAA (17 bases) TAATAT, respectively are similar to the *E. coli*  $\sigma^{70}$ /*B. subtilis*  $\sigma^A$  promoter sequence. The codon usage pattern for the sequenced genes is strongly biased toward A- or U-rich codons, reflecting the relatively low G+C content of *S. aureus* DNA. The value of 33% for the 2.5kb sequenced region matches the value of de Ley (1970) for the *S. aureus* chromosome. Work with *E. coli* and *B. subtilis* has demonstrated a likely correlation between expression level of a gene and its codon usage pattern (Grantham *et al.*, 1981; Ikemura & Ozeki, 1983). More highly expressed genes display a non-random pattern of codon usage, utilising a restricted set of codons that are recognised by the major species of isoacceptor tRNAs, unlike genes expressed at low levels which display a random codon usage pattern. The codon AUA (isoleucine) which is rarely used in highly expressed genes in *E. coli* and *B. subtilis* is biased against in the *ndk* gene (0 of 12) but is present in *aroC* (5 of 35). Fitting in with this data is the fact that Ndk is known to be a highly expressed protein in contrast to chorismate synthase. Ignoring methionine (AUG) and tryptophan (UGG) for which there are only single codons, an A or U is found in the wobble (3') position of a codon 84% of the time in the sequenced genes.

### 3.2. Comparison of chorismate synthases.

Chorismate synthase from *S. aureus* was compared with the sequences of other chorismate synthases using the PILEUP program of the GCG package (Figure 3.6) and a consensus sequence was produced. A dendrogram was created using the same program (Figure 3.7) and revealed that the chorismate synthase sequences were divided into two groups, the first containing the Gram-positive bacterial sequences and the second group containing the other bacterial, plant and fungal sequences.

**Figure 3.5. Complete nucleotide sequence of pMJH702 and deduced amino acid sequence of encoded proteins.** The putative promoter -35 and -10 regions, ribosome binding sites and protein translations are indicated. Regions of amino acid sequence which have been confirmed from protein sequencing experiments are underlined. Nucleotides are numbered from the first base of the AccI/Clal combined site of the 2.5kb NdeI-Clal fragment in pMJH702.

1 ATCGATGAAGCTAAGGCAGTAAGTTCGAAGTATCTAAGTAAAGCTTGGA  
 I D E A K A V S S K Y L S K A L D

51 TTGATTTCTGAGTTGCCAGATGGACATCCAAAATCACTACTTTAACCTT  
 L I S E L P D G H P K S L L L S L  
 -35

101 TGACGAAAAAAATGGGTCAAGAACACACATAGTATTATGAAAAGTATTG  
 T K K M G S R N T •  
 -10

151 AAAGCGCTTACCAACCTGTTAATATAATACATAATACATAAACCTA

*ndk*

201 TTAAACACAGGGGATACATAAAGTGGAACGTACATTAAATGATTAAA  
 M E R T F L M I K

251 CCAGACGCAGTACAAAGAAATCTAATTGGTGAAGTAATTCAAGAATTGA  
 P D A V Q R N L I G E V I S R I E

301 AAGAAAAGGACTAAAACCTGTCGGTGGTAAATTAAATCCAAGTACCAATGG  
 R K G L K L V G G K L M Q V P M E

351 AACTTGCTGAAACACATTATGGTGAACACCAAGGTAAACCATTATAAT  
 L A E T H Y G E H Q G K P F Y N

401 GATTTAATTTCATTTATTACATCAGCACCAGTGTTCGAATGGTAGTTGA  
 D L I S F I T S A P V F A M V V E

451 AGGTGAAGATGCAGTTAATGTATCTAGACATATTATGGCAGCACCAATC  
 G E D A V N V S R H I I G S T N P

501 CTTCAAGCTTCACCAAGGATCATTAGAGGTGATTTAGGTTAACCTGTT  
 S E A S P G S I R G D L G L T V

551 GCTAGAAATATCATCACGGTTAGATTCTAGAGTCTGCTGAACGTGA  
 G R N I I H G S D S L E S A E R E

601 AATTAAATTATGGTTAATGAAAATTACTAGCTATGCTTCACCAAC  
 I N L W F N E N E I T S Y A S P R

651 GTGATGCTTGGTTATCGAATAAAATATAAGCTATAATCTTCTGATT  
 D A W L Y E •

701 ATAAAAGGAAAAAGGGTTTGTATGTGGTTAGTGATTGACCAATTCA

751 TAACAAAGCCCTATTTTATACGGACTGATTAACCTTATAAAAAATAATC

801 AGTCCATTTCCTTTATTAAGAAATATAAGCTTGTATATTATTATTACG

851 TGGTTAGCTACGATTATATGCGGTATAAGTGTTCGAATAATTAAAT

901 TTTCAAATGGTTGTTAAACAATCTAACATATTAGAAATTCAATAACT

951 TTTCTCGTTGTGAATATATTATAATGAATCTTAGTTCTGTTAATATTAAG

1001 ATAATTCTGACATTAAAAAGAGATATAATCAATTCTTAATTGAGCTT

-35

1051 GAAAACAAACATTATGAATGCACAAATGAATATGATAAGATTAACACAT

-10-

aroc

1101 ATTATAATGTTATCGTGGAAAGTATGAAAGGAGCGAGTGTGATGAGATAC  
M R Y

1151 CTAACATCAGGAGAATCACATGGACCTCAATPAACAGTTATTGTTGAAGG  
L T S G E S H G P O L T V I V E G

1201 TGTACCTGCAAATTTAGAACCTAACGGTTGAGGATATTAAATAAAAGAAATGTT  
V P A N L E V K V E D I N K E M F

1251 TTAAGCGTCAGGCAGGTTACGGACGCTGGACGTCGTATGCAAATTGAAAAAA  
K R Q G G Y G R G R R R M Q I E K

1301 GATACAGTGGAGATTGTTTGGGTGTAAGAAATGGTTATACATTAGGTAG  
D T V E I V S G V R N G Y T L G S

1351 CCCTATTACAATTGTTACTAATGATGATTACACATTGGCGAAAAAA  
P I T I V V T N D D F T H W R K I

1401 TTATGGGGCGTGCGCCAATAAGCGACGAAGAACCGAGAAAATATGAAACGT  
M G R A P I S D E E R E N M K R

1451 ACAATTACGAAGCCAAGACCGGACATGCAGATTACTTGGCGGTATGAA  
T I T K P R P G H A D L V G G M K

1501 ATATAATCATCGTACTTACGAAATGTATTAGAACGTTCATCTGCCAGAG  
Y N H R D L R N V L E R S S A R E

1551 AACAGCAGCACGTGTAGCGGTGGTGCACATGCAAAGTTTATTAGAA  
T A A R V A V G A L C K V L L E

1601 CAATTAGATATCGAAATATACAGTCGTGTTGTTGAGATAGGTGGCATTAA  
Q L D I E I Y S R V V E I G G I K

1651 AGATAAAGATTTTATGATTCAAGAACATTAAAGCAAACCTTGATCGAA  
D K D F Y D S E T F K A N L D R N

1701 ATGACGTCCGTGTAATTGATGATGGCATCGCACAGCAATGCGCGATAAA  
D V R V I D D G I A Q A M R D K

1751 ATTGATGAAGCGAAAAACGATGGTATTCAATAGGGCCCGTAGTTCAAGT  
I D E A K T D G D S I G G V V Q V

1801 TGTAGTTGAAATATGCCCTGGTGTAGGTAGTTATGTACATTATGATC  
V V E N M P V G V G S Y V H Y D R

1851 GTAAATTAGATGGAAGAATAGCACAGGGTGTGTTAGTATTAAATGCATT  
K L D G R I A Q G V V S I N A F

1901 AAAGGTGTAAGTTGGAGAAGGATTAAAGCAGCTGAAAAGCCTGGTAG  
K G V S F G E G F K A A E K P G S

1951 CGAAATTCAAGACGAAATTCTCTACAATACTGAATTGGGCTATTATCGTG  
E I Q D E I L Y N T E L G Y Y R C

2001 GGTCAAATCACTTAGGTGGTTAGAACGGCGGTATGTCAAATGGAATGCCA  
S N H L G G L E G G M S N G M P

2051 ATTATCGTTAATGGTGTAAATGAAACCAATTCCAACGTTATATAAACCAATT  
I I V N G V M K P I P T L Y K P L

2101 AAATTCAGTAGACATTAATACTAAAGAAGACTTAAAGCAACAATTGAAC  
N S V D I N T K E D F K A T I E R

2151 GTTCTGATAGTTGTGCTGTCCTGCAGCAAGTATCGTCGTGAACATGTC  
S D S C A V P A A S I V C E H V

2201 GTAGCATTGAAATTGCAAAAGCATTATTGAGAAGAATTCCAATCAAATCA  
V A F A I A K A L L E E F Q S N H

2251 TA'TTGAGCAACTAAACAACAAATTATTGAGCGCAGACAATTAAATATTG  
I E Q L K Q Q I I E R R Q L N I E  
*aroB*

2301 AGTTTTAACAAACAAGAACAAATTGAGGTGTAATCATGAAATTACAACAAAC  
F \* M K L Q T T

2351 ATACCCTTCAAACAATTATCCAATATATGTTGAACACGGTGCATCAAGT  
Y P S N N Y P I Y V E H G A I K Y

2401 ATATAGGCACATATTTAAATCAATTGACCAAAGTTCTTGTAAATTGAT  
I G T Y L N Q F D Q S F L L I D

2451 GAATATGTAAATCAATATTTGCGAATAAATTGATGAATTATCATA  
E Y V N Q Y F A N K F D D I L S Y

2501 TG

---

**Figure 3.6. Multiple alignment of predicted amino acid sequences of chorismate synthases.** The alignment was created using the GCG PILEUP program (Genetics Computer Group, 1991). Gaps were introduced by PILEUP to optimize the alignment using the following parameters: gap weight=3; gap length=0.1. Amino acids which were completely conserved are highlighted with uppercase letters in the row labelled CHOR. Amino acids which occurred in at least 10 of the 12 sequences are highlighted with lowercase letters.

bsu	<i>Bacillus subtilis</i>
sau	<i>Staphylococcus aureus</i>
sty	<i>Salmonella typhi</i>
eco	<i>Escherichia coli</i>
van	<i>Vibrio anguillarum</i>
hin	<i>Haemophilus influenzae</i>
les	<i>Lycopersicon esculentum</i>
cse	<i>Corydalis sempervirens</i>
syn	<i>Synechocystis PCC6803</i>
see	<i>Saccharomyces cerevisiae</i>
ncr	<i>Neurospora crassa</i>

	1	50
bsu	M..... RYLTAGESHG PQLTTIIEGV PAGLYITEED INFELARRQK	
sau	M..... RYLTSGESHG PQLTVIVEGV PANLEVVKVED INKEMFKRQG	
sty	MAGNTIGQLF RVTTFGESHG LAVGGIVDGV PPGTIPLTEAD LQHDLDRRRP	
eco	.AGNTIGQLF RVTTFGESHG LALGCIIVDGV PPGTIPLTEAD LQHDLDRRRP	
van	MAGNSIGQHF RVMTFGESHG IALGCIIVDGC PPGLEITEAD LQIDLDRRRP	
hin	MAGNTIGQLF RVTTFGESHG IALGCIIVDGV PPNELESEKD IQPDLDRRRP	
les2	.AGSTPGNYF RVTTFGESHG GGVGCIIDGC PPRPLPLSESAD MQVELDRRRP	
les1	.AGNTPGNYF RVTTFGESHG GGVGCIIDGC PPRPLPLSESAD MQVELDRRRP	
cse	.SGSSPGKVF QVTTYGESHG GGVGCVIDGC PPRFPISEAD IQSDLDRRRP	
syn	M.GNTFGSLF RITTFGESHG GGVGVIIDGC PPRLEISPEE IQVDLDRRRP	
sce	M..STFGKLF RVTTYGESHC KSVGCIIVDGV PPGMSLTEAD IQPQLTRRRP	
ncr	M..STFGHYF RVTTYGESHC KSVGCIIVDGV PPGMELTEDD IQPQMTRRRP	
CHOR	..... r..T.GESHg ...g.i.dG. Pp.....e.d .q..l.rRrp	
	51	100
bsu	GHGRGRRMGI EKDQAKIMSG VRHARTLCSP IALVVENNDW KHWTKIMGAA	
sau	GYGRGRRMGI EKDTVEIVSG VRNGYTLGSP ITIVVTNDDF THWRKIMGRA	
sty	GTSRYTTQRR EPDQVKILSG VFDGVTGTS IGLLIENTD. ....	
eco	GTSRYTTQRR EPDQVKILSG VFEQVTTGTS IGLLIENTD. ....	
van	GTSRYTTPRR EADEVKILSG VFEQVTTGTS IGLLIENTD. ....	
hin	GTSRYTTPRR EDDEVQILSG VFEQVTTGTS IGMITKNGD ....	
les2	GQSRITTTPRK ETDTCKISSG TADGLTTGSP IKVEVPNTD. ....	
les1	GQSRITTTPRK ETDTCKIYSG TADGLTTGSP IKVEVPNTD. ....	
cse	GQSKITTPRK ETDTCKIYSG VADGFTTGSP IHISVPNTD. ....	
syn	GQSKLSTPRD EKDRVEIQSG TEFGKTLGTP IAMMIKNED. ....	
sce	GQSAITTPRD EKDRVIIQSG TEFGKTLGTP IGMIVMNED. ....	
ncr	GQSAITTPRD EKDRVIIQSG TEFGVTLGTP IGMIVMNED. ....	
CHOR	G.s...t.r. E.D...I.SG ...g.T.G.. I....N.D. ....	
	101	150
bsu	PITEDEEKEM KROISRPRPG HADLNGAIKY NIIRDMLRNVL RSSARETTVR	
sau	PISDEERENM KRTITKPRPG HADLVCGMKY NHRLDRRNVL RSSARETAAR	
sty	..QRSQDYSA ..IKDVFRPG HADTYEQKY GLRDYRGG.G RSSARETAMR	
eco	..QRSQDYSA ..IKDVFRPG HADTYEQKY GLRDYRGG.G RSSARETAMR	
van	..QRSTDYSD ..IKDKFRPG HADTYHQKY GIRDYRGG.G RSSARETAMR	
hin	..QRSQDYGD ..IKDRFRPG HADFTYQQKY GIRDYRGG.G RSSARETAMR	
les2	..QRGNDYSE ..MSLAYRPS HADATYDFKY GVRSVQGG.G RSSARET1GR	
les1	..QRGNDYSE ..MSLAYRPS HADATYDFKY GVRSVQGG.G RSSARETIGR	
cse	..QRGNDYSE ..MAKAYRPS HADATYDFKY GVRSVQGG.G RSSARETIGR	
syn	..ARSQDYNE ..MAVKYRPS HADATYEAKY GIRNWQGG.G RSSARETIGR	
sce	..QRPHDYS ..MDKFPRPS HADFTYSEKY GIKASSGG.G RASARETIGR	
ncr	..OPPKDYGK KTMDIYPRPS HADWTYLEKY GVKASSGG.G RSSARETIGR	
CHOR	.....dy.. .....RP. HAD.ty..KY g.r...gg.g RsSARET..R	
	151	200
bsu	VAAGAVAKKI LSE.LGIKVA GHVLQIGAV. .... .KAEKTGY	
sau	VAVGALCKVL LEQ.LDIEIY SRVVEIGGI. .... .KDK..,DF	
sty	VAAGAIAKKY LAEKFGIEIR GCLTQMIDP L. ....	
eco	VAAGAIAKKY LAEKFGIEIR GCLTQMIDP L. ....	
van	VAAGAIAKKY LKQEFGVETR AYLSQMGDVC I. ....	
hin	VAAGAIAKKY LREHFGIEVR GFLSQIGNIK.I. .... .APQK	
les2	VAAGAVAKKI LKLYSGAEVL AYVSQVHQVV L. .... .PEDLID	
les1	VAAGAVAKKI LKLYSGTEIL AYVSQVHNVV L. .... .PEDLVD	
cse	VAAGALAKKI LKAYAGTEVL AYVSQAHKV L. .... .PEGLVD	
syn	VAAGAIAKKI LAQFNGVEIV AYVKSICDI. .... .EATVD	
sce	VASGAIAEKF LAQNSNVEIV AFVTQIGEIK M. .... .NR DSFDPEFQHL	
ncr	VAAGAIAKKY LKPRYGVETR AFVSSVGSEH LFPPTAEHPS PSTNPEFLKL	
CHOR	VAaGA.a.k. L....g.e.. ....	

	201	250
bsu	TSIEDLQRVT EESPVRCYDE EAGKKMMAAI DEAKANGDSTI GGI	VIVEVG
sau	YDSETFKANL DRNDVRVIDD GIAQAMRDKI DEAKTDGDSI GGVVQVVEN	
sty	.EIKDWROVE LN.PFFCPDA DKLDALDELM RALKKEGDSI GAKVTVMASG	
eco	.DIKDWSQVE QN.PFFCPDP DKIDALDELM RALKKEGDSI GAKVTVMASG	
van	.DKVWDNEIE NN.AFFCPDA DKVAAFDQLI RDLKKEGDSI GAKIQVATN	
hin	VGQIDWEKVN SN.PFFCPDE SAVEKFDEL RELKKEGDSI GAKLTVIAEN	
les2	HQNVTLEQIE SNI.VRCPDP EYAEKMIAAI DAVRVRGDSV GGVVTCIVRN	
les1	NQIVTLEQIE SNI.VRCPNP EYAEKMIGAI DYVRVRGDSV GGVVTCIVRN	
cse	HETLSSLQIE SNI.VRCPDS EYAEKMIAAI DAVRVKGDSV GGVVTCIMRN	
syn	SNTVTLEQVE SNI.VRCPDE ECAEKMIERI DQVLRQKDSTI GGVVECAIRN	
sce	LNTITREKVD SMGPIRCPDA SVAGLMVKEI EKYRGNKDSI GGVVTCVVRN	
ncr	VNSITRETVD SFLPVRCPDA EANKRMEDLI TKFRDNHDSI GGTVTCVIRN	
CHOR	.....cpd. .... DS. Gg.v.....	
	251	300
bsu	MPVGVGSSYVH YDRKLDSKLA AAVLSINAFK GVEFGIGFEA AGRNGSEVHD	
sau	MPVGVGSSYVH YDRKLDGRIA QGVVSINAFK GVSFGEGLKA AEKPGSEIQT	
sty	VPAGLGEPVF ..DRLDADIA HALMSINAVK GVEIGEGFNV VALRGSQNRD	
eco	VPAGLGEPVF ..DRLDADIA HALMSINAVK GVEIGDGFDV VALRGSQNRD	
van	LPVGLGEPVF ..DRLDADIA HALMSINAVK GVEIGDGFDV VQQKGSQHRD	
hin	VPVGLGEPVF ..DRLDADLA HALMGINAVK GVEIGDGFAV VEQRGSEHRD	
les2	LPRGLGTPVF ..DKLEAELA KACMSLPAVK GFEFGSGFAG TFMTGSEHND	
les1	VPRGLGTPVF ..DKLEAELA KACMSLPAVK GFEFGSGFAG TFMTGSEHND	
cse	VPRGLGSQPF ..DKLEAELA KACMSLPAVK GFEFGSGFSG TFLTGSEHND	
syn	APKGLGEPVF ..DKLEADLA KAMMSLPAVK GFEFGSGFAG TLLTGSQHND	
sce	LPTGLGEPCF ..DKLEAMLA HAMLSJ.PASK GFEIGSGFQG VSVPGSKHND	
ncr	VPSGLGEPAF ..DKLEAMLA HAMLSIPATK GFEVGSGFGG CEVPGSIHND	
CHOR	.P.G1G.p.f ..d.L.a..A .a..S..A.K G.e.G.GF.. ....GS...D	
	301	350
bsu	EIIWDEEKGY TRA..... .TNRLGGLE GGMMTGMPIV	
sau	EILYNTELGY YRG..... .SNHLGGLE GGMSNGMPII	
sty	EITAQG..... FQSNHAGGIL GGISSGQHIV	
eco	BITKDQ..... FQSNHAGGIL GGISSGQQII	
van	PLTPNG..... FRSNHAGGIL GGISTGQDIV	
hin	PLTPNH..... FRSNHAGGIL GGISTGQDIV	
les2	EFYMDEHG..... RIR TRTNRSGGIQ GGISNGEVIN	
les1	EFFMDEHD..... QIR TKTNRSGGIQ GGISNGEIIN	
cse	EFYTDENG..... RIR TRTNRSGGIQ GGISNCEIIN	
syn	EYYLDEAG..... EWR TRTNRSGGVQ GGISNGEPII	
sce	PFYFEKETN..... RLR TKTNNSSGGVQ GGISNGENIY	
ncr	PFVSAENTEI PPSVAASCAA RNGIPRKLT TKTNFSGGIQ GGISNGAPIY	
CHOR	..... N..GG.. GGis.G..I.	
	351	400
bsu	VRGVMKPIPT LYKPLKSVDI ETKEPFS.AS IERSDSCAVP AASVVAE...	
sau	VNGVMKPIPT LYKPLNSVDI NTKEDFK.AT IERSDSCAVP AASIVCEHV	
sty	AHMALKPTSS ITVPGRТИNR MG.EEVEMIT KGRHDPCVGI RAVPIAEAML	
eco	AHMALKPTSS ITVPGRТИNR FG.EEVEMIT KGRHDPCVGI RAVPIAEAML	
van	ASTALKPTSS ITVPGDTITR TG.EPTQLIT KGRHDPCVGI RAVPIAEAML	
hin	ATIALKPPTSS ITIPGRSINL NG.EAVEVVT KGRHDPCVGI RAVPIAEAMV	
les2	MRIGFKPTST ISRKQQTVTR DK.HETELIA RGRHDPCVVP RAVPMVEAMV	
les1	MRVAFKPTST IARKQHTVSR DK.HETELIA RGRHDPCVVP RAVPMVEAMV	
cse	MRIAFKPTST IGKKQNTVTR ER.EEIELIA RGRHDPCVVP RAVPMVEAMV	
syn	MRIAFKPTAT IGQEQLIVSN IG.EETTLAA KGRHDPCVLP RAVPMVEAMA	
sce	FSVPFKSVAT ISQEQTATY DG.EEGILAA KGRHDPAVTP RAIPIVEAMT	
ncr	FRVGFKPAAAT IGQEQTATY DGTSEGVLAA KGRHDPSVVP RAVPIVEAM	
CHOR	....Kp... i....t... .... .gRhDp.v.. rA.p..E...	

	401	450
bsu	ALSLGKLQPS LNNSD.....	.....
sau	AFAIAKALLE EFQSNHIEQL KQQIERRQL NIEF.....	.....
sty	AIVLMDHLLR HRAQNADVKT EIPRW.....	.....
eco	AIVLMDHLLR QRAQNADVKT DIPRW.....	.....
van	AIVLMDHLLR HRGQNFAVQT ETPKI.....	.....
hin	AIVLMDHLLR FKAQCK.....	.....
les2	ALVLVDQLMA QYSQCMMFPI NPELQEPLQS SPESAEVTL.....	.....
les1	ALVLVDQLMT QYAQCMLFPV NLTLQEPLQP STTKSA.....	.....
cse	ALVLLDQLML QHAQGNLFSI NPALQEPLSE TVSSAAASLQ GV.....	.....
syn	ALVLCDDHLLR FQAQCKTL.....	.....
sce	ALVIADALLI QKARDFSRSV VH.....	.....
ncr	ALVIMDAVLA HEARVTAKSL LPPLKQTINS GKDTVGNGVS ENVQESDLAQ	
CHOR	A.vl.d.l.....	

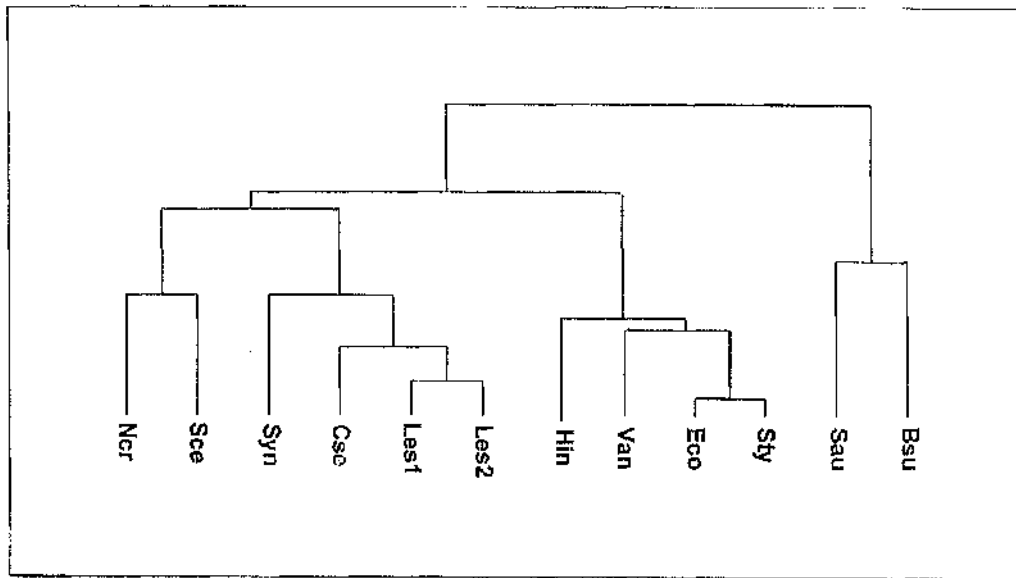


**Figure 3.7. Dendrogram showing similarity among chorismate synthases from different organisms.** The dendrogram was derived using the PILEUP program of the GCG package (Genetics Computer Group, 1991) with the SWISSPROT entries for each protein being used.

**Figure 3.8. Multiple alignment of predicted amino acid sequences of nucleoside diphosphate kinases.** The alignment was created using the GCG PILEUP program (Genetics Computer Group, 1991). Gaps were introduced by PILEUP to optimize the alignment using the following parameters: gap weight penalty=3; gap length penalty=0.1. Amino acids which were completely conserved are highlighted with uppercase letters in the row labelled NDK. Amino acids which occurred in at least 7 of 9 of the sequences are highlighted with lowercase letters.

Eco	<i>Escherichia coli</i>
Mxa	<i>Myxococcus xanthus</i>
Bsu	<i>Bacillus subtilis</i>
Sau	<i>Staphylococcus aureus</i>
Psa	<i>Pisum sativum</i>
Sol	<i>Spinacia oleracea</i>
Osa	<i>Oryza sativa</i>
Sce	<i>Saccharomyces cerevisiae</i>
Ddi	<i>Dictyostelium discoideum</i>

### 3.3. Comparison of nucleoside diphosphate kinases.

Nucleoside diphosphate kinase (Ndk) from *S. aureus* was compared with the sequences of other nucleoside diphosphate kinases using the PILEUP program of the GCG package (Figure 3.8) and a consensus sequence was produced. The putative encoded Ndk from *S. aureus* shows a high degree of similarity with other Ndks. There was no obvious grouping of the Ndk sequences when a dendrogram was produced in contrast to chorismate synthase. This may be a consequence of the greater degree of conservation between the sequences.

1	50
Eco	.....MAIER TFSIIKPNAV AKNVIGNIFA RFEAAAGFKIV GTKMLHLTVE
Mxa	.....AIER TLSIIKPDGL EKGVIICKIIS RFEEKGLKPV AIRLQHLSQA
Bsu	.....MMEK TFIMVKPDGV QRQLIGDIILS RFERKGLQLA GAKLMRVTEQ
Sau	.....MER TFLMIKPDAV QRNLIGEVIS RIERKGLKLV GGKLMQVPME
Psa	.....MAEQ TFIMIKPDGV QRGLVGEIIS RFEKKGFYLK GLKFVNVERA
Sol	.....MEQ TFIMIKPDGV QRGLVGEIIS RFEKKGFSLK ALKFVNVDRP
Osa	.....MEQ SFIMIKPDGV QRQLIGDIIS RFEKKGFYLR GMKFMNVERS
Sce	...MSSQTER TFIAVKPDGV QRGLVSQILS RFEKKGYKLV AIKLVKADDK
Ddi	MSTNKVNKER TFLAVKPDGV ARGLVGEIIA RYEKKGFVLL GLKQLVPTKD
NDK	.....E. tf...KPdgv .r.l.g.i.. R.E.KG..1. ...k.....
 51	
Eco	QARGFYAEHD GKPFDFDGLVE FMTSGPIVVS VLEGENAVQR HRDLLGATNP
Mxa	QAEQFYAVHK ARPFFKDLVQ FMISGPVVL M VLEGENAVLA NRDIRGATNP
Bsu	MAEKHYAEHQ GKPFPGELVE FITSGPVFAM VWEGENVIEV TRQLIGKTNP
Sau	LAETHYGEHQ GKPFYNDIIS FITSAPVFAM VWEGEDAVNV SRHTIGSTNP
Psa	FAEKHYADLS AKPFFSGLVD YIISGPVVAM IWECKNVTT GRKLIIGATNP
Sol	FAEKHYADLS AKPFFNGLVE YIVSGPVVAM VWECKGVVAT GRKLIIGATNP
Osa	FAQQHYADLS DKPFFPGLVE YIISGPVVAM VWECKDVVAT GRRIGATRP
Sce	LLEQHYAEHV GKPFPPKMVS FMKSGPILAT VWECKDVVRQ GRTILGATNP
Ddi	LAESHYAEHK ERPFFGGLVS FITSGPVVAM VFECKGVVAS ARLMIGVTNP
NDK	.a..hYa... .KPFI...v. ...SgPv.am v.EG...v... .R..1G.TnP
 101	
Eco	ANALAGTLRA DYADSLTENG THGSDSVESA AREIAYFFGE GEV..CPRTR
Mxa	AQAAEGTIKR DFATSIDKNT VHGSDSLENA KIEIAYFFRE TEIHSYPYQK
Bsu	KEALPGTIKG DYGMFVGKNI IHGSDSLESA EREINIFFKN EELVSYQQLM
Sau	SEASPGSIRG DLGLTVGRNI IHGSDSLESA EREINLWFNE NEITSYASPR
Psa	AQSEPGTIKG DFAIDIGRNV IHGSDAVESA NKEIALWF.P EGAANWESSL
Sol	LASEPGTIKG DFAIDIGRNV IHGSDAVDSA TKEIALWF.P DGVVHWQSSL
Osa	WEAAPGTIRA DYAVEVGRNV IHGSDSDVNG KKEIALWF.P EGLAEWRSNL
Sce	LGSAPGTIRG DFGIDLGRNV CHGSDSDVDSA EREINLWFKK EELVDWESNQ
Ddi	LASAPGSIRG DFGVDVGRNI IHGSDSVESA NREIALWFKP EELLT.EVKP
NDK	.....Gtir. D.....g.N. .HGSDS.... .EI...F... ....
 151	
Bsu	AGWIY..
Sau	DAWLVE
Psa	HSWIYE
Scl	HSHWIYE.
Osa	HPWIYES
Sce	AKWIYE.
Ddi	NPNLYE.

### **3.4. Comparison of the N-terminal 3-dehydroquinate synthase fragment with sequences within the Swissprot database.**

The *aroB* fragment located downstream from *aroC* was translated and compared with other 3-dehydroquinate synthase sequences in the Swissprot database. The degree of identity was found to be low. The N-terminal region of this protein would appear to be poorly conserved among the sequences examined. There is no doubt, however, that the protein is a 3-dehydroquinate synthase as the 3' end of the *aroB* gene has been sequenced and shows identity with other 3-dehydroquinate synthases and, furthermore, a plasmid containing the region 5' of *aroA* and 3' of *aroC* complements the *aroB* mutation of *E. coli* AB2847 (O'Connell *et al.*, 1993). The N-terminal region of the *S. aureus* 3-dehydroquinate synthase is shown aligned with *B. subtilis* 3-dehydroquinate synthase in Figure 3.9.

**Figure 3.9.** The translated product of the partial *S. aureus aroB* gene aligned with the N-terminal region of *B. subtilis* 3-dehydroquinate synthase. The symbol (|) indicates identical amino acids and (•) indicates conserved amino acids.

### 3.5 Comparison of GerCC with related sequences from the Swissprot database.

The partial *gerCC* gene of *S. aureus* was identified by virtue of its homology with the *B. subtilis* *gerCC* gene and an ORF from *B. stearothermophilus* (Figure 3.10). Although only a small portion of the *S. aureus* *gerCC* gene sequence was known a significant level of identity was observed (39%) with each of the *Bacillus* genes. A comparison of the protein sequence matches obtained from a search of the Swissprot database with the partial *S. aureus* sequence revealed identity with a broad family of proteins including geranylgeranyl pyrophosphate synthetases and hexa- and heptaprenyl pyrophosphate synthetases (Table 3.1).

**Figure 3.10.** The translated product of the partial *S. aureus* gerCC gene aligned with the translated product of the *B. subtilis* gerCC gene and the *B. stearothermophilus* ORF3 protein. The symbol (|) indicates identical amino acids and (•) indicates conserved amino acids.

The *B. stearothermophilus* ORF3 gene has recently been demonstrated to encode one subunit of a heterodimeric heptaprenyl pyrophosphate synthetase (Koike-Takeshita *et al.*, 1995). The ORF3 gene has 65% identity with the *B. subtilis* *gerCC* gene such that the *gerCC* gene of *B. subtilis* is likely to similarly encode a heptaprenyl pyrophosphate synthetase. Heptaprenyl pyrophosphate synthetase functions to produce the polypropenyl side-chain precursor of the respiratory quinone in *B. subtilis* and *B. stearothermophilus* (Takahashi *et al.*, 1980). The respiratory quinone in Gram-positive organisms is menaquinone which is produced via a post-chorismate pathway. The primary biosynthetic precursors of menaquinones are shown in Figure 3.11.

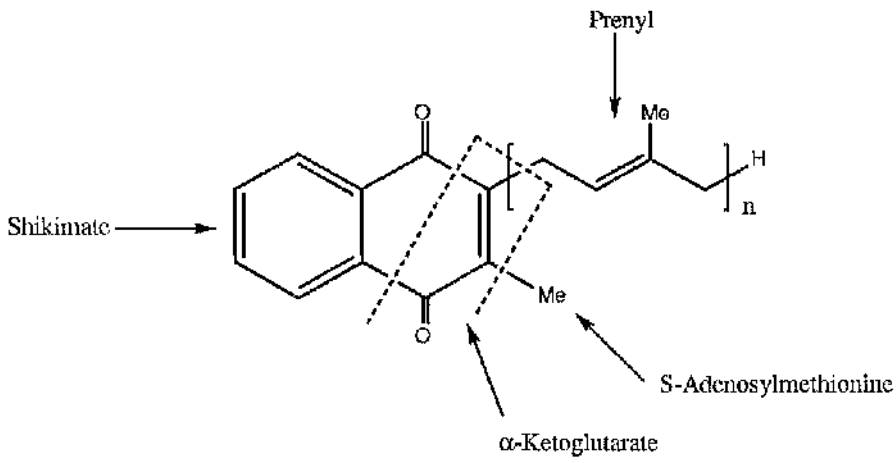


**Figure 3.11.** The primary biosynthetic precursors of menaquinones.

Sequence	Protein	Organism	Accession number	% ident.	% simil.
SauGerCC	Putative heptaprenyl pyrophosphate synthetase	<i>Staphylococcus aureus</i>	U31979	-	-
BsuGerCC	Putative heptaprenyl pyrophosphate synthetase	<i>Bacillus subtilis</i>	M80245	38.6	59.1
BstORF3	Heptaprenyl pyrophosphate synthetase	<i>Bacillus stearothermophilus</i>	D49976	38.6	53.0
NcrGGPP	Geranylgeranyl pyrophosphate synthetase	<i>Neurospora crassa</i>	p24322	18.2	52.3
EcoGGPs	Hypothetical geranylgeranyl pyrophosphate synthetase	<i>Escherichia coli</i>	p19641	18.6	39.5
ScsHps	Hexaprenyl pyrophosphate synthetase	<i>Saccharomyces cerevisiae</i>	p18900	32.6	48.8
CpaGGPs	Geranylgeranyl pyrophosphate synthetase	<i>Cyanophora panophora</i>	p31171	20.9	44.2
RcaGGPs	Geranylgeranyl pyrophosphate synthetase	<i>Rhodobacter capsulatus</i>	p17060	20.5	40.9
EcoGTT	Geranyl transtransferase	<i>Escherichia coli</i>	p22939	18.6	46.5
EurGGPs	Geranylgeranyl pyrophosphate synthetase	<i>Erwinia uredovora</i>	p21684	28.9	55.3

**Table 3.1. Comparison of the translated product from the partial *S. aureus gerCC* gene with sequences obtained from the GenEMBL and Swissprot databases.** Values for percentage identity and similarity between the sequences were obtained using the GAP program of the GCG package (Genetics Computer Group, 1991).

### 3.6. Mapping of the *gerC* genes in *S. aureus*.

To examine the possibility that the *gerCA* and *gerCB* genes immediately precede *gerCC*, as is observed in *B. subtilis*, and to confirm that the partial 3' ORF in pMJH702 was *gerCC*, *S. aureus* DNA was hybridized against selected radioactively labelled fragments from pMAY1 (Figure 3.12) using reduced stringency conditions. The plasmid pMAY1, which contains the complete coding sequences for the *gerC* genes from *Bacillus subtilis*, was obtained from Dr. Anne Moir, University of Sheffield. Southern blots of *S. aureus* DNA were probed using a number of different restriction fragments from pMAY1 as detailed in Table 3.2 and shown in Figure 3.12.

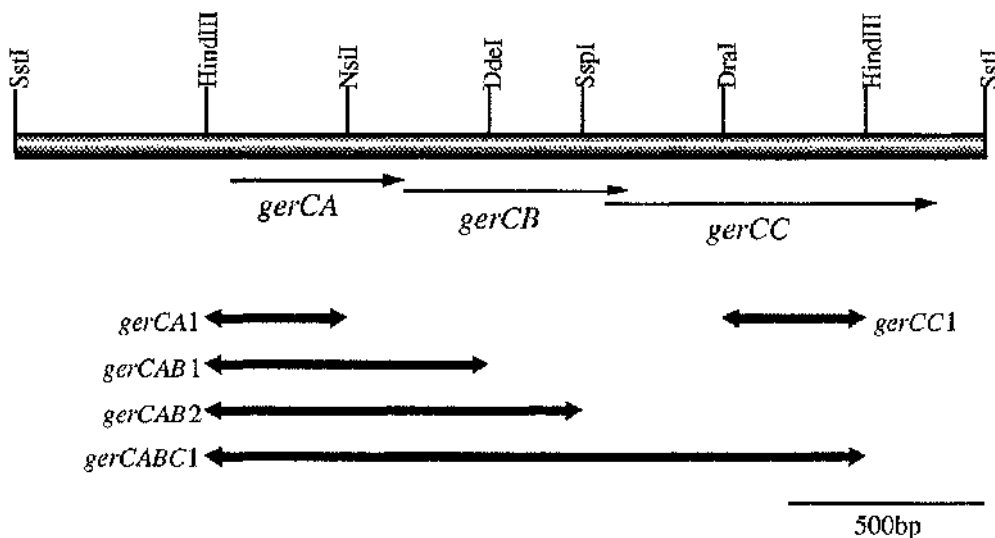


**Figure 3.12.** Map of the *gerC* genes from *B. subtilis* showing the regions of DNA in pMAY1 used for probing *S. aureus* genomic DNA.

Examination of the Southern blots generated using the *gerCAB2*, *gerCC1* and *gerCABC1* probes (Figures 3.14, 3.15, 3.16) demonstrated that the *gerC* genes were likely to be present in some form in *S. aureus*. The heterologous probes bound with differing efficiency but did mostly reveal discrete bands. The pattern of restriction fragments generated using the *gerCC1* probe was compared with the restriction pattern generated previously using the *aroC* probe (Figure 3.1 and Figure 3.14) and was found to match closely with these blots and with the restriction map generated previously for the *aroC* and *ndk* genes (Figure 3.3). This agreement between the restriction patterns allowed a restriction map to be produced for the region 5' to the

*ndk* gene and encompassing the region where the *gerCA* and *gerCB* genes might be expected to reside if their location matched that observed in *B. subtilis*.

Fragment from pMAY1	Restriction sites	length (bp)
<i>gerCAgerCBgerCC</i>	<i>Hind</i> III- <i>Hind</i> III	2,252
<i>gerCAgerCB</i>	<i>Hind</i> III- <i>Ssp</i> I	1,215
<i>gerCAgerCB</i>	<i>Dde</i> I- <i>Hind</i> III	906
<i>gerCA</i>	<i>Hind</i> III- <i>Nsi</i> I	452
<i>gerCC</i>	<i>Dra</i> I- <i>Hind</i> III	843

**Table 3.2.** Summary of *gerC* restriction fragments generated from pMAY1 and used as heterologous probes for Southern blots of *S. aureus* 601055 DNA.

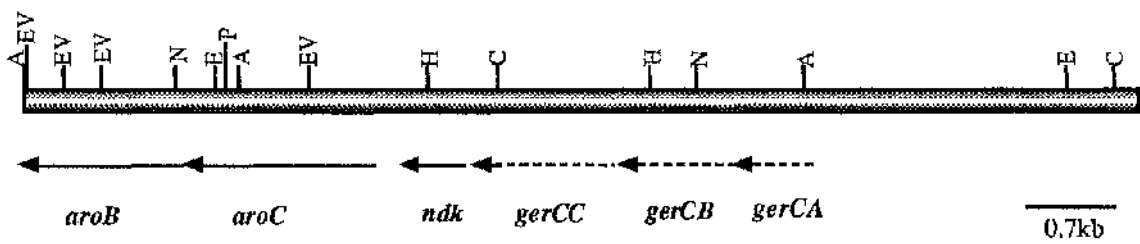
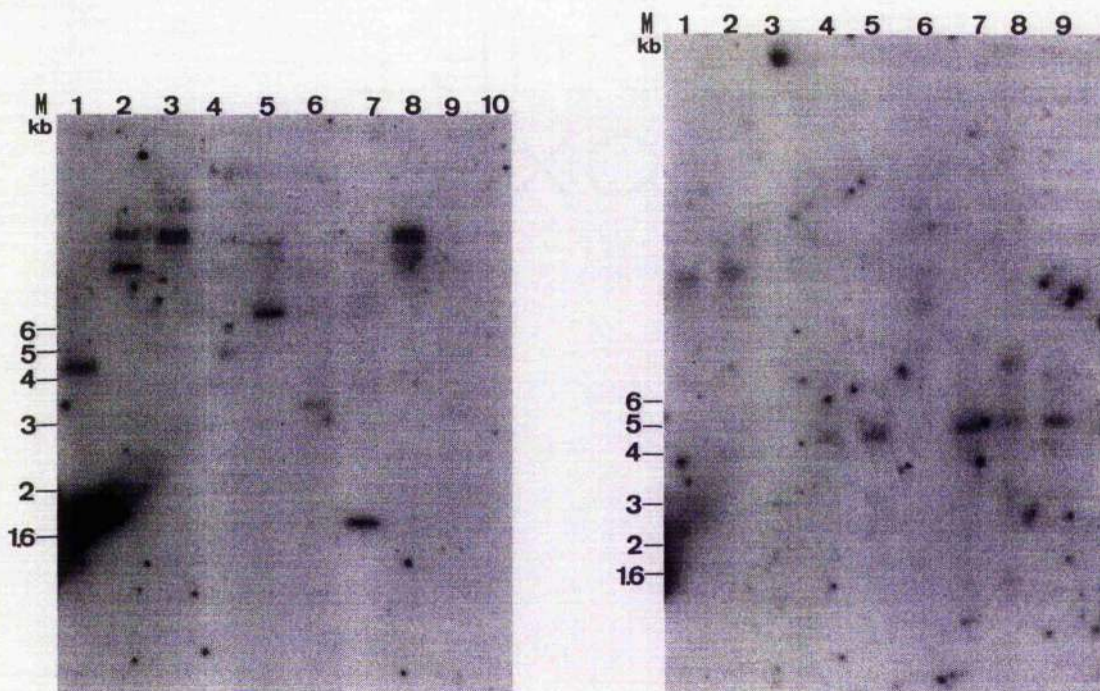


**Figure 3.13.** Schematic map showing the predicted positions of the *gerC* genes relative to the *aro*, *ndk* region of the *S. aureus* chromosome. The positions of the *gerC* genes are shown by dashed lines indicating approximate locations based on the hybridisation data presented here and using the sizes of the genes from *B. subtilis*. The restriction endonucleases are abbreviated: A, *Acc*I; C, *Cla*I; E, *Eco*RI; RV, *Eco*RV; H, *Hind*III; N, *Nde*I; P, *Pst*I.

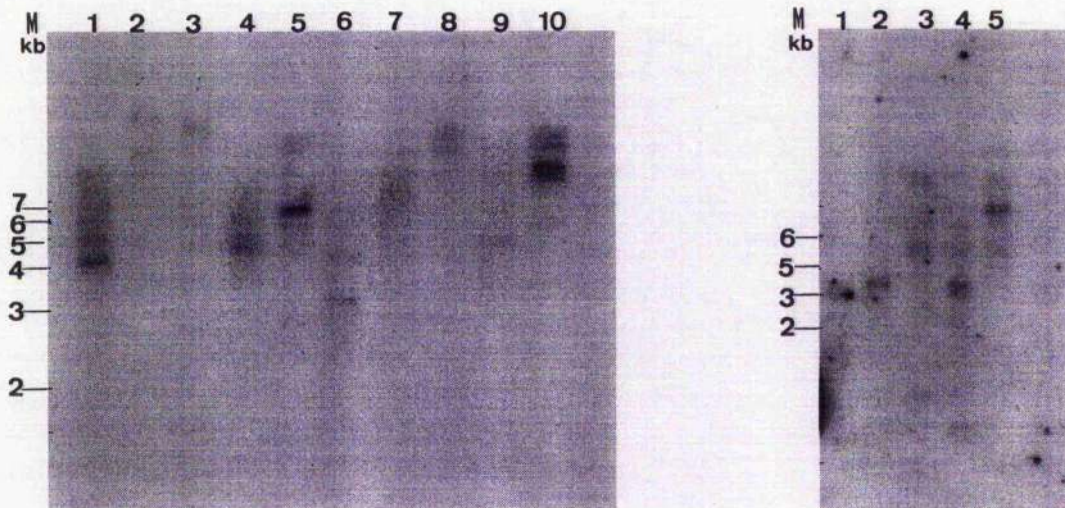
Comparison of the restriction patterns produced with the *gerCAB2* and *gerCABC1* probes with the restriction patterns produced using the *aroC* and *gerCC* probes enabled the mapping of the *gerCA* and *gerCB* genes in the region 5' to the *aroC* and *ndk* genes (Figures 3.15 & 3.16 cf. Figures 3.14 & 3.1). The *gerCAgerCBgerCC* genes are likely to reside almost exclusively on a 4.5kb *Cla*I fragment; the 3' end of *gerCC* resides on the 5.5kb *Cla*I fragment which constitutes pMJH701 (Figure 3.13).



Lane M: DNA markers.  
 Lane 1: *AccI* digest.  
 Lane 2: *BamHI* digest.  
 Lane 3: *BglII* digest.  
 Lane 4: *Clal* digest.  
 Lane 5: *EcoRI* digest.  
 Lane 6: *HincII* digest.  
 Lane 7: *HindIII* digest.  
 Lane 8: *KpnI* digest.  
 Lane 9: *NdeI* digest.  
 Lane 10: *PstI* digest.

Lane M: DNA markers.  
 Lane 1: *SacI-SalI* digest  
 Lane 2: *SacI* digest.  
 Lane 3: *NdeI-AccI* digest.  
 Lane 4: *AccI* digest.  
 Lane 5: *AccI-BamHI* digest.  
 Lane 6: *KpnI-BamHI* digest.  
 Lane 7: *EcoRI-Clal* digest.  
 Lane 8: *Clal* digest.  
 Lane 9: *BamHI-Clal* digest.

**Figure 3.14.** Southern blots of *S. aureus* 601055 DNA probed with an 843bp *DraI-HindIII* fragment (*gerCC1*) from pMAY1.



Lane M: DNA markers.

Lane 1: *AccI* digest

Lane 2: *BamHI* digest.

Lane 3: *BglII* digest.

Lane 4: *ClaI* digest.

Lane 5: *EcoRI* digest.

Lane 6: *HincII* digest.

Lane 7: *HindIII* digest.

Lane 8: *KpnI* digest.

Lane 9: *NdeI* digest.

Lane 10: *PstI* digest.

Lane M: DNA markers.

Lane 1: *AccI* digest.

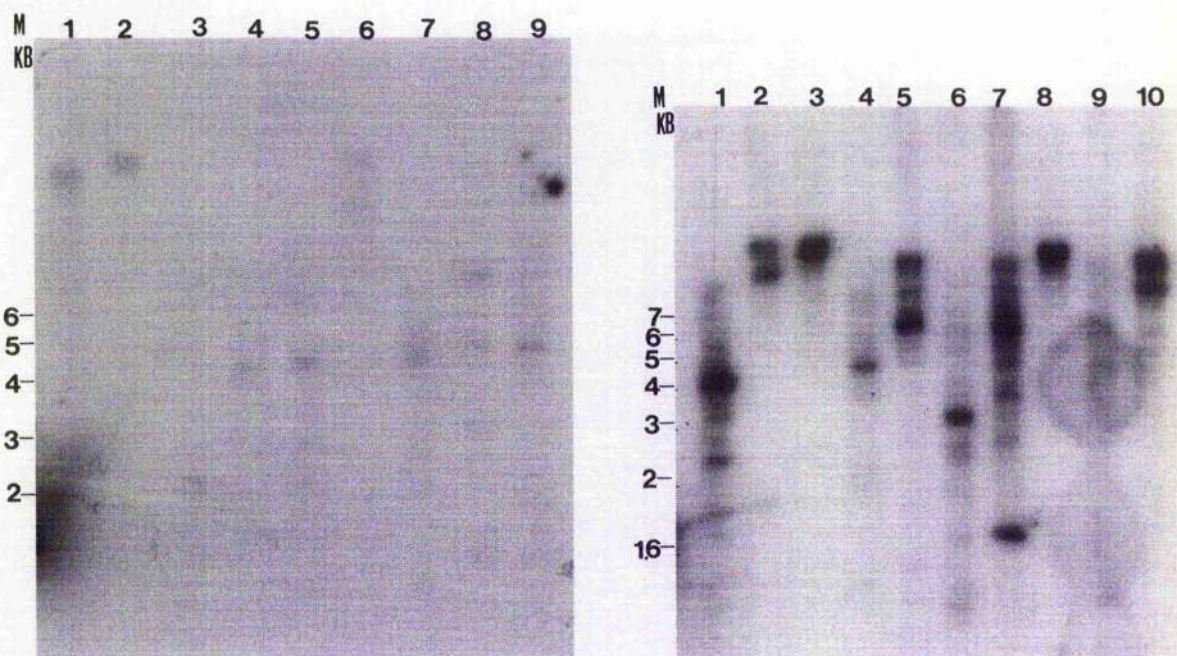
Lane 2: *ClaI* digest.

Lane 3: *HindIII* digest.

Lane 4: *NdeI* digest.

Lane 5: *PstI* digest.

**Figure 3.15.** Southern blots of *S. aureus* 601055 DNA probed with a 1,215bp *HindIII-SspI* fragment (*gerCAB2*) from pMAY1.



Lane M: DNA markers.  
 Lane 1: *SacI-SalI* digest  
 Lane 2: *SacI* digest.  
 Lane 3: *NdeI-AccII* digest.  
 Lane 4: *AccI* digest.  
 Lane 5: *AccI-BamHI* digest.  
 Lane 6: *KpnI-BamHI* digest.  
 Lane 7: *EcoRI-Clal* digest.  
 Lane 8: *Clal* digest.  
 Lane 9: *BamHI-Clal* digest.

Lane M: DNA markers.  
 Lane 1: *AccI* digest.  
 Lane 2: *BamHI* digest.  
 Lane 3: *BglII* digest.  
 Lane 4: *Clal* digest.  
 Lane 5: *EcoRI* digest.  
 Lane 6: *HincII* digest.  
 Lane 7: *HindIII* digest.  
 Lane 8: *KpnI* digest.  
 Lane 9: *NdeI* digest.  
 Lane 10: *PstI* digest.

**Figure 3.16. Southern blots of *S. aureus* 601055 DNA probed with a 2,252bp *HindIII-HindIII* fragment (*gerCABC1*) from pMAY1.**

### 3.6. Chapter summary.

The *aroC* gene encoding chorismate synthase was cloned from *Staphylococcus aureus* by complementation of an *aroC* strain of *Escherichia coli*. Sequencing upstream of the cloned gene revealed a putative promoter sequence indicating that the *aroC* gene may form an operon with the downstream *aroB* and *aroA* genes identified previously (O'Connell *et al.*, 1993). A comparison of the *S. aureus* chorismate synthase sequence with other known chorismate synthase sequences demonstrated that the enzymes from *S. aureus* and *Bacillus subtilis* form a sequence group which is distinct from that formed by the other bacterial, plant and fungal enzymes.

Sequencing upstream from the *aroC* gene of *S. aureus* revealed the presence of the complete *ndk* gene encoding nucleoside diphosphate kinase. The encoded protein had a high level of sequence similarity with other known Ndks. Sequencing of the plasmid containing the *aroC* gene also revealed partial open reading frames encoding the 5' end of the *aroB* gene, encoding 3-dehydroquinate synthase, and the 3' end of a *gerCC* homologue. The N-terminal region of the *S. aureus* 3-dehydroquinate synthase had a low level of sequence identity to other 3-dehydroquinate synthases. The *gerCC* gene from *B. subtilis* is believed to encode a heptaprenyl pyrophosphate synthetase by virtue of its high degree of similarity with the ORF3 gene from *Bacillus stearothermophilus* which encodes a heptaprenyl pyrophosphate synthetase involved in menaquinone biosynthesis.

In *B. subtilis* the *gerCC* gene is the final gene in an operon with *gerCB* and *gerCA*. Similarly the ORF3 gene of *B. stearothermophilus* resides in a three gene operon which has a high degree of identity with the *B. subtilis gerC* genes. Southern hybridisation experiments were performed using fragments of the *gerC* genes from *B. subtilis* to probe for the *S. aureus gerC* genes. This revealed that the *gerCB* and *gerCA* genes were similarly situated upstream from *gerCC* in *S. aureus*. Furthermore it demonstrated that the *gerC* genes were linked to the *aroBaroA* genes in both *S. aureus* and *B. subtilis*.

---

## CHAPTER 4. OVEREXPRESSION ANALYSIS OF *S. AUREUS* CHORISMATE SYNTHASE AND NUCLEOSIDE DIPHOSPHATE KINASE AND *E. COLI* FLAVIN REDUCTASE.

---

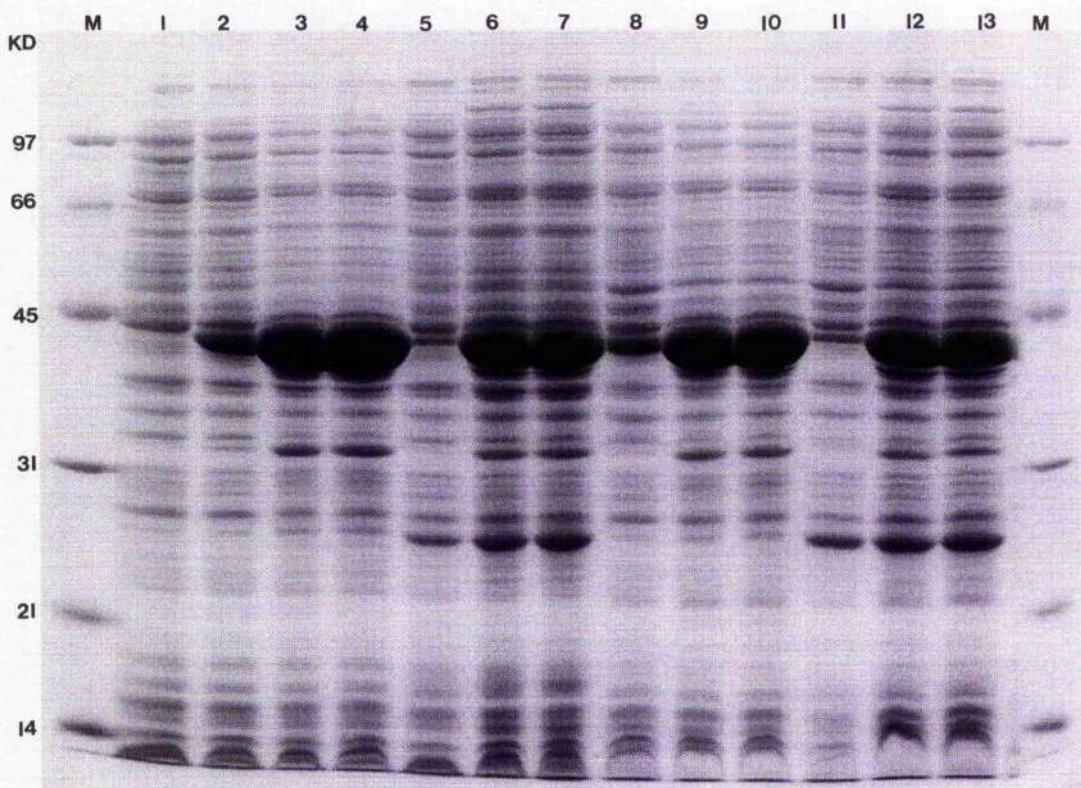
This chapter describes the maximal overexpression of *S. aureus* chorismate synthase and its verification by N-terminal sequencing. In addition the overexpression of an *E. coli* flavin reductase is detailed. This enzyme was overexpressed to examine possible interactions between this flavin reductase and *E. coli* chorismate synthase.

### 4.1. Overexpression of *S. aureus* chorismate synthase.

Expression analysis of the plasmids pMJH701 and pMJH702 suggested that chorismate synthase was expressed from its native promoter in *E. coli* DH5 $\alpha$  (Figure 4.4). However, the level of expression was relatively low and to maximise expression the *aroC* gene was cloned downstream from a strong promoter and ribosome binding site.

The *S. aureus* *aroC* gene was amplified using PCR with oligonucleotide primers. The oligonucleotide CHOR 34 5'GGCATATGAGATACTAACATCAGGA<sup>3'</sup> had an *Nde*I restriction site (underlined) incorporated to facilitate cloning, and this was followed by the 5' end of the *aroC* gene sequence. Similarly, the oligonucleotide CHOR 35 5'GGAGATCTAAAACTCAATTTAATTG3' had a *Bgl*II restriction site incorporated and this was followed by the 3' end of the *aroC* gene sequence. The *aroC* gene was amplified using the proofreading, thermostable enzyme Vent polymerase and the number of cycles of PCR was minimised to reduce the likelihood of misincorporation during the reaction. The amplified *aroC* gene product was cloned into the T7 promoter containing vector, pTB361, producing the plasmid pMJH7EX2, which was sequenced and found to match the template sequence.

The plasmid pMJH7EX2 was transformed into *E. coli* BL21(DE3) and HMS174(DE3) and expression was monitored over time before and after induction with 0.4mM IPTG (Figure 4.1). Chorismate synthase was observed to accumulate to levels around 50% of total protein (using gel scanning densitometry) after a period of 5 hours post induction. The protein was also shown to be soluble by lysing the cells with lysozyme and separating the soluble material from insoluble material by centrifugation. PAGE revealed chorismate synthase to be located in the soluble (supernatant) fraction.



- Lane M: Molecular weight markers.  
Lane 1: BL21(DE3)pTB361.  
Lanes 2-4: BL21(DE3)pMJH7EX2 - 0, 4, 5 hours.  
Lanes 5-7: BL21(DE3)pLysSpMJH7EX2 - 0, 4, 5 hours.  
Lanes 8-10: HMS174(DE3)pMJH7EX2 - 0, 4, 5 hours.  
Lanes 11-13: HMS174(DE3)pLysSpMJH7EX2 - 0, 4, 5 hours.

**Figure 4.1. SDS-PAGE showing a time course of protein expression from the *aroC* overexpression clone pMJH7EX2 in two *E. coli* host strains after induction with IPTG.**

In addition to the 43kD band expected for *S. aureus* chorismate synthase, a second band of 33kD was observed on the gel. The presence of this band was thought to arise from the larger expressed protein and to confirm this a gel with the overexpressed proteins was blotted onto polyvinylidenefluoride (PVDF). N-terminal sequencing, by Edman degradation, was used to obtain the sequence of both the main 43kD species and the 33kD sub-species (Table 4.1). The 43kD species matched the N-terminal amino acid

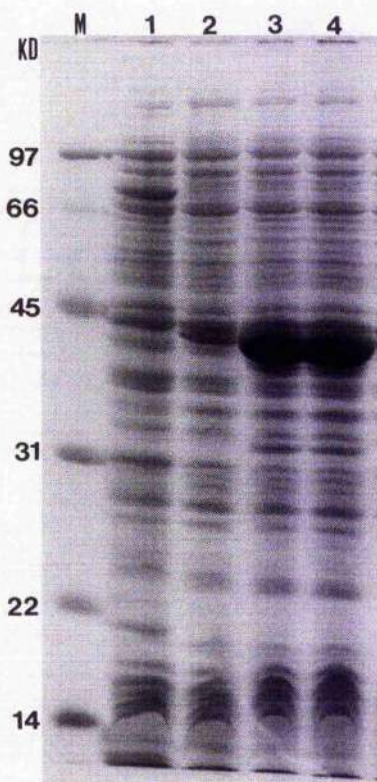
sequence predicted from translation of the *aroC* gene sequence including the initiating methionine. The sequence of the 33kD band matched an internal region of chorismate synthase and also began with a methionine. Examination of the DNA sequence immediately upstream from this methionine revealed the presence of a potential, weak ribosome binding site. The 33kDa band thus appears to be due to translational start events were occurring within the *aroC* mRNA. This was presumably a result of the large amounts of mRNA present when expression to such high levels was initiated.

Cycle	43kD band		33kD band	
	Amino acid	pmol	Amino acid	pmol
1	M	72.85	M	22.72
2	R	72.53	K	21.3
3	Y	68.19	R	39.69
4	L	65.18	T	11.52
5	T	41	I	17.66
6	S	22.1	T	10.23
7	G	45.5	K	16.5
8	E	39.1	P	13.16
9	S	15.2	R	29.68
10	H	20.4	P	11.17
11	G	26.7	G	13.05
12	P	26.4	H	17.71
13	Q	20.9	A	10.93
14	L	22.9	D	15.23
15	T	12.8	L	11.36
16	V	20.9	V	11.6
17	I	19.6	G	11.16
18	V	15.6	G	2.2
19	R	10.4		
20	G	14.7		
21	V	16.3		
22	P	17.9		
23	A	30.8		
24	N	27.5		
25	L	15.6		
26	E	5.84		
27	V	19.3		
28	K	9.4		

**Table 4.1. N-terminal sequencing data from overexpressed *S. aureus* chorismate synthase.**

#### 4.1.1. Lysogenization of *E. coli* GLW40 for expression.

The lysogenization of *E. coli* GLW40 with the  $\lambda$ DE3 prophage to produce an expression system which would be free from endogenous contaminating chorismate synthases was thought to be advantageous since the *E. coli* chorismate synthase purification protocol would be the starting point for subsequent enzyme purification. Consequently, *E. coli* GLW40 was lysogenized with  $\lambda$ DE3 and a suitable lysogen was selected by virtue of its ability to direct the overexpression of chorismate synthase.



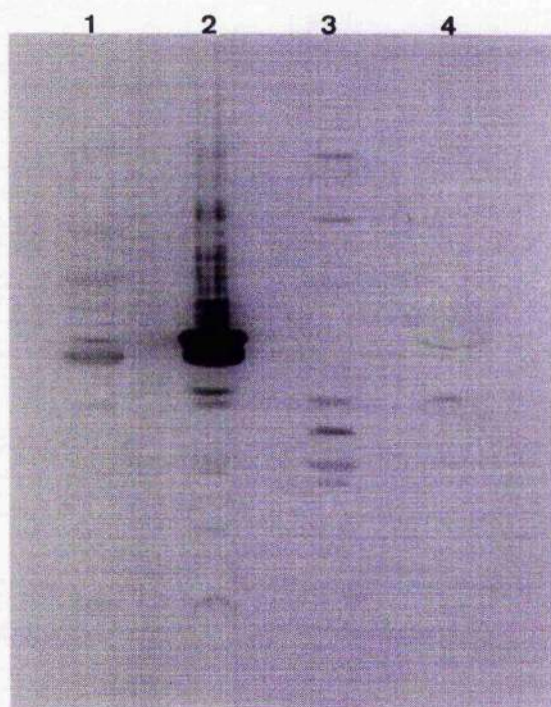
- Lane M: Molecular weight markers.  
Lane 1: GL W40(DE3).  
Lanes 2-4: GL W40(DE3)pMJH7EX2 - 0, 4, 5 hours.

**Figure 4.2.** SDS-PAGE showing a time course of protein expression from the *aroC* overexpression clone pMJH7EX2 in *E. coli* GLW40(DE3) after induction with IPTG.

The level of overexpression using *E. coli* GLW40(DE3) was less than that observed with *E. coli* BL21(DE3). This contrasts with the expression of *E. coli* EPSP synthase where levels of overexpression were comparably high in both *E. coli* AB2849(DE3) and *E. coli* BL21(DE3) (Shuttleworth *et al.*, 1992). However, the level of overexpression was sufficiently high to warrant using the *aroC* lysogen strain to obviate the problem of *E. coli* chorismate synthase contaminating the *S. aureus* preparation.

#### 4.2. Immunological analysis of *S. aureus* chorismate synthase.

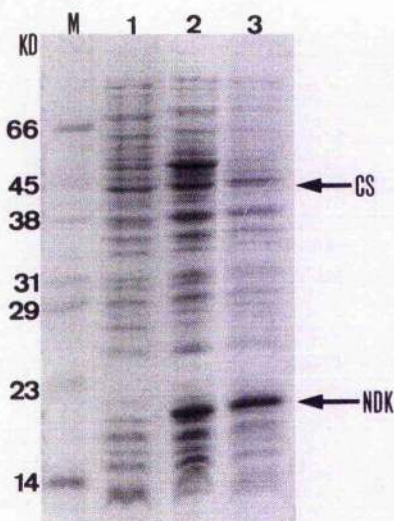
Crude extracts of *S. aureus* 601055, *E. coli* BL21(DE3)pMJH7EX2, *E. coli* AB2849pGM605, and *E. coli* AB2849 were separated by SDS-PAGE. The gel was then blotted onto nitrocellulose membrane and the membrane incubated with polyclonal rabbit anti-*E. coli* chorismate synthase antibodies generated against denatured enzyme.



- Lane 1: *E. coli* AB2849.
- Lane 2: *E. coli* AB2849pGM605.
- Lane 3: *S. aureus* 601055.
- Lane 4: *E. coli* BL21(DE3)pMJH7EX2.

**Figure 4.3. Western blot of chorismate synthase from *E. coli* and *S. aureus* using rabbit anti-*E. coli* chorismate synthase antibodies.**

Development of the nitrocellulose membrane revealed that the antibodies had bound to two main proteins in both of the *E. coli* AB2849 lanes, the larger of the two proteins being *E. coli* chorismate synthase (Figure 4.3). The lane containing *S. aureus* 601055 revealed no band at the molecular weight of the *E. coli* enzyme, as expected. Furthermore, the lane containing the overexpressed *S. aureus* chorismate synthase showed only a faint band corresponding to *E. coli* chorismate synthase but no band at the molecular weight corresponding to the *S. aureus* enzyme. This lack of immunological cross-reactivity provides evidence for structural differences between *S. aureus* chorismate synthase and *E. coli* chorismate synthase.



Lane M: Molecular weight markers.

Lane 1: *E. coli* DH5 $\alpha$ .

Lane 2: *E. coli* DH5 $\alpha$ pMJH702.

Lane 3: *E. coli* DH5 $\alpha$ pMJH701.

**Figure 4.4. Protein expression from plasmids pMJH702 and pMJH701 in *E. coli* DH5 $\alpha$  with arrows showing expression of chorismate synthase and nucleoside diphosphate kinase.**

#### 4.3. Overexpression of *S. aureus* nucleoside diphosphate kinase.

Examination of protein expression from the plasmids pMJH701 and pMJH702 revealed the presence of a second protein in addition to chorismate synthase (Figure 4.4). This protein had an estimated molecular weight from SDS-PAGE of 16.5kD. The molecular

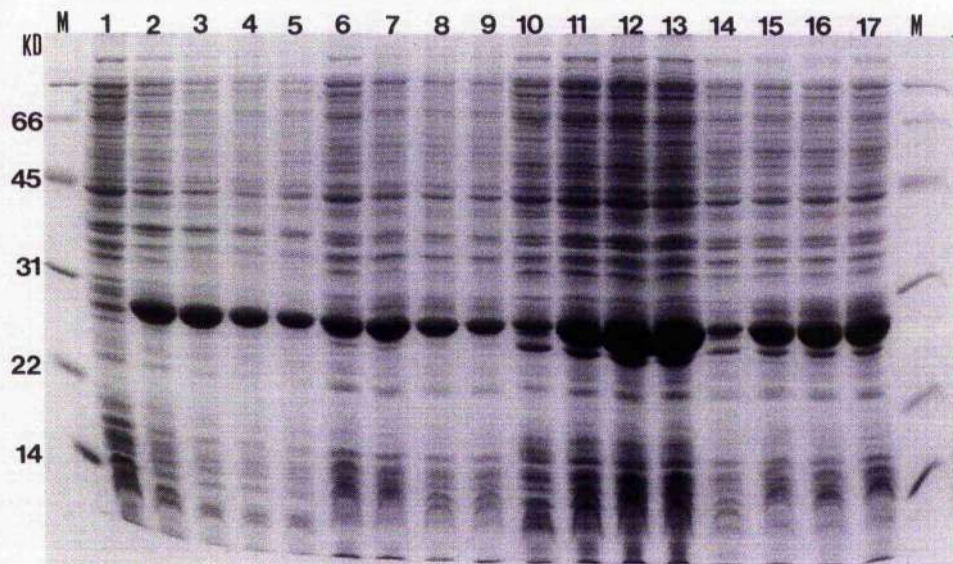
weight of nucleoside diphosphate kinase (Ndk) from translation of its gene sequence is 16.6kD. Confirmation that the protein was Ndk by N-terminal sequencing was not possible due to extremely poor blotting of the protein onto PVDF. The presence immediately upstream from the *ndk* gene of what would appear to be a strong ribosome binding site supports the proposal that the second expressed protein is Ndk. The level of expression was unaffected by the addition of IPTG to growing cells harbouring the plasmids as judged by SDS-PAGE.

#### 4.4. Overexpression of *E. coli* flavin reductase.

The *E. coli* *fre* gene, encoding flavin oxidoreductase, was amplified from *E. coli* K-12 genomic DNA using PCR with oligonucleotide primers based upon the gene sequence published previously by Spry *et al*, 1991. The oligonucleotide FLRD1 5'GAGAAAGCATATGACAACCTTAAGCTGTAAA<sup>3'</sup> had an *Nde*I restriction site (underlined) incorporated to facilitate cloning, and this was followed by the 5' end of the *fre* gene sequence. Similarly, the oligonucleotide FLRD2 5'TCTCCCAGATTTATCAGATAAATGCAAACGCATC<sup>3'</sup> had a *Bgl*II restriction site incorporated and this was followed by the 3' end of the *fre* gene sequence with an extra stop codon TAA placed after the TGA stop codon. The *fre* gene was amplified using the proofreading thermostable enzyme Vent polymerase as described for the *aroC* gene and required 4mM MgSO<sub>4</sub> for extension. The amplified *fre* gene product was cloned into the T7 promoter containing vector, pTB361, producing the plasmid pFREX2, which was sequenced and found to match the published sequence.

The plasmid pFREX2 was transformed into *E. coli* BL21(DE3) and BL21(DE3)pLysS to examine expression of the flavin reductase. The growth of the strains on L-agar was observed to be significantly retarded, especially BL21(DE3)pFREX2 which grew extremely slowly. Growth in L-broth was similarly poor and the strains grew around 2-3 times slower compared with the expression of chorismate synthase. Protein expression was monitored after induction with IPTG by SDS-PAGE (Figure 4.5).

The level of expression of the flavin reductase was observed to be high and a notable feature of the cells obtained was their distinctly pale colour, presumably a consequence of flavins in the cell mostly being reduced.



- Lane M: Molecular weight markers.  
Lane 1: BL21(DE3)pTB361.  
Lanes 2-5: BL21(DE3)pFREX2 - 0, 2, 3, 4 hours.  
Lanes 6-9: BL21(DE3)pLysSpFREX2 - 0, 2, 3, 4 hours.

**Figure 4.5.** SDS-PAGE showing a time course of protein expression from the *fre* overexpression clone pFREX2 after induction with IPTG.

#### 4.5. Chapter summary.

Chorismate synthase from *S. aureus* was maximally overexpressed by placing the coding region of the *aroC* gene optimally spaced downstream of a T7 promoter. Expression was performed using both the *E. coli* strain BL21(DE3) and by lysogenising GLW40, an *aroC* strain of *E. coli*. Lysogenisation of GLW40 was performed to remove the presence of contaminating endogenous *E. coli* chorismate synthase during the purification of the *S. aureus* enzyme. Antibodies previously generated against *E. coli* chorismate synthase were found not to cross-react with the *S. aureus* enzyme. This highlights further the differences between the Gram-positive chorismate synthases and the enzymes from other bacteria, plant and fungi which show strong inter-species cross-reactivity.

Overexpression from the *aroC* overexpression clone pMJH7EX2 revealed two bands after SDS-PAGE. The N-terminal sequence of the main band matched that predicted to be the N-terminus of the protein. The N-terminal sequence of the second, minor band revealed that an internal start event had occurred during overexpression. *S. aureus* nucleoside diphosphate kinase was found to overexpress presumably from its native promoter in pMJH701 and pMJH702.

The flavin reductase from *E. coli* encoded by the *fre* gene was maximally overexpressed with the same vector system used for *S. aureus* chorismate synthase. The *E. coli* flavin reductase was overexpressed to allow the investigation of possible interactions with *E. coli* chorismate synthase which are detailed in chapter 7.

## CHAPTER 5. PURIFICATION AND CHARACTERISATION OF *S. AUREUS* CHORISMATE SYNTHASE.

This chapter describes the purification of *S. aureus* chorismate synthase to near homogeneity. In addition details of the enzyme with respect to its subunit molecular mass, its native structure and its kinetic properties are presented.

### 5.1. Purification of *S. aureus* chorismate synthase.

*S. aureus* chorismate synthase was purified from 13g (wet weight) of *E. coli* GLW40(DE3) pMJII7EX2 using two chromatographic steps of DEAE-Sephacel and cellulose phosphate, principally as described by White *et al.*, 1988 and incorporating some minor alterations (Ramjee, 1992). The purification yielded around 100mg of enzyme with a purity of 95% as judged by SDS-PAGE. The chromatographic profiles of the enzyme on the two columns are shown in Figures 5.1 and 5.2 and Table 5.1 summarises the purification.

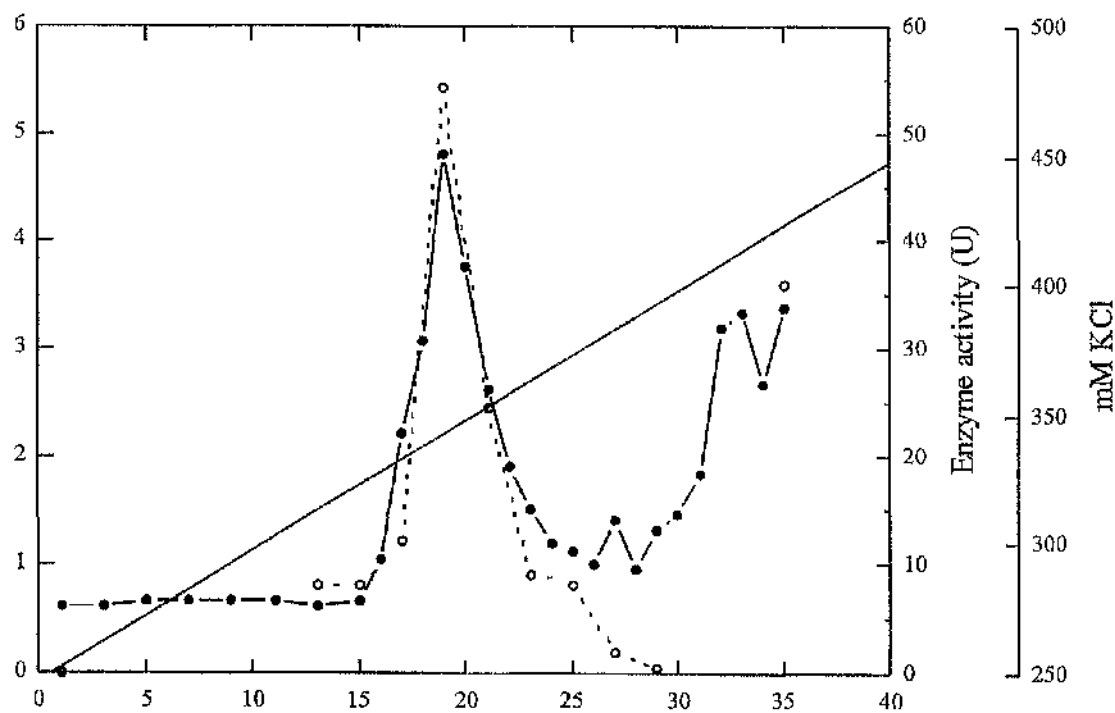


**Figure 5.1.** Elution profile of *S. aureus* chorismate synthase from DEAE-Sephadex. OD<sub>280</sub> (●), enzyme activity(○).

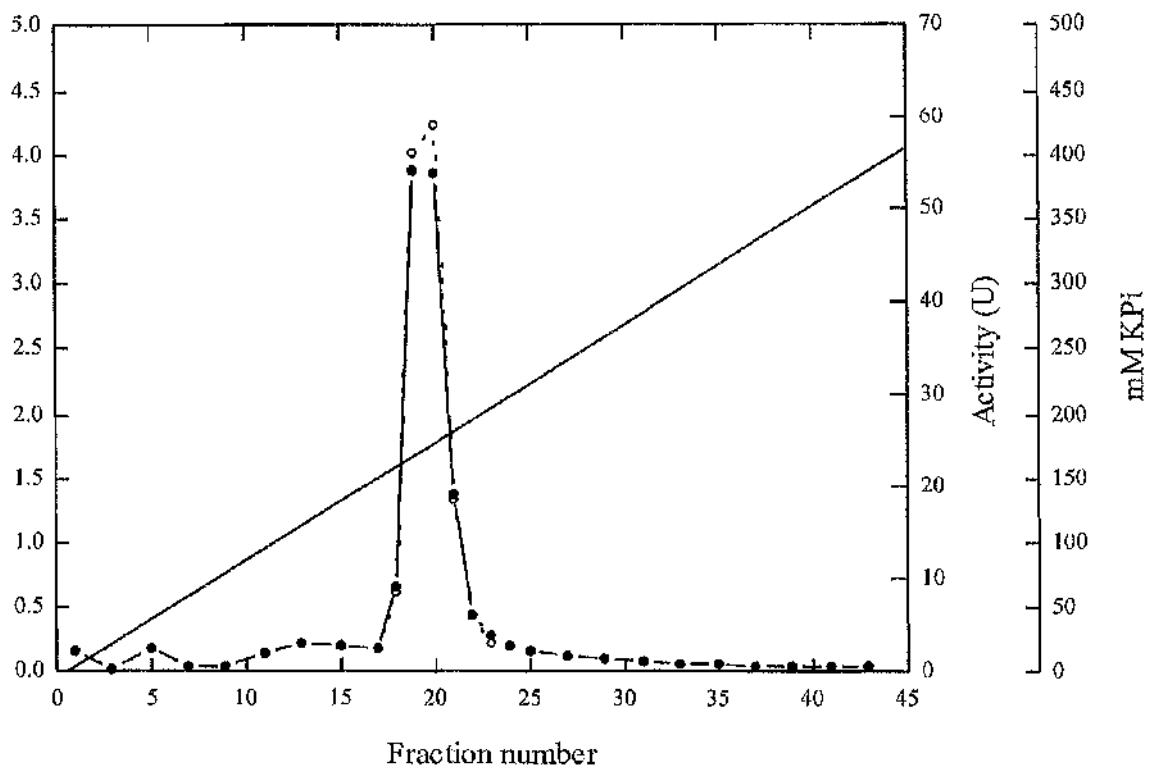


Figure 5.2. Elution profile of *S. aureus* chorismate synthase from cellulose phosphate. OD<sub>280</sub> (●), Activity (○).

Step	Total protein (mg)	Total activity (U)	Specific activity (U mg <sup>-1</sup> )	Yield (%)	Purification (-fold)
Crude extract	1210	416	0.34	100	1
DEAE-Sephadex	592	317	0.54	76	1.6
Cellulose phosphate	98.5	248	2.5	60	7.4

Table 5.1 Summary of the purification of *S. aureus* chorismate synthase from *E. coli* GLW40(DE3)pMJH7EX2.

*S. aureus* chorismate synthase was ultimately resuspended in the minimum volume of 50mM Mops pH7.0, 0.4 mM DTT, 1.2mM PMSF, 50% glycerol after ammonium sulphate precipitation and was stored at -20°C. The enzyme was concentrated greatly using this procedure with the most concentrated sample produced being around 40mgml<sup>-1</sup>. The stability of *S. aureus* chorismate synthase in this buffer was good with no obvious loss of activity after six months as judged by UV assay. The specific activity of chorismate synthase from *S. aureus* was significantly lower than that from *E. coli* such that purification of the enzyme using the UV assay was made more difficult. The volume of sample being added was above the optimum for the UV assay meaning that significant amounts of oxygen were added to the system resulting in the underestimation of specific activity. A significantly higher specific activity was obtained after DEAE-Sephacel chromatography when the flavin on the enzyme was photoreduced for 1 min in the absence of oxalate before addition to the assay.

### **5.2. Protein concentration determination using the extinction coefficient of chorismate synthase.**

The concentration of chorismate synthase was determined spectrophotometrically at 280nm using the method described by Gill and Von Hippel, 1989. The extinction coefficient was calculated using the number of tyrosine, tryptophan and cysteine residues present and determining the absorbance of the protein in water and 6M guanidine hydrochloride.  $\epsilon_{M,N}$  at the calculated extinction coefficient for chorismate synthase in water was determined to be 23,100 M<sup>-1</sup>cm<sup>-1</sup>.

### **5.3. Molecular weight and subunit structure of chorismate synthase.**

The subunit molecular weight ( $M_r$ ) of *S. aureus* chorismate synthase was measured by electrospray mass spectrometry as 43,024 ± 3.8 (Figure 5.3), consistent with the migration position observed with SDS-PAGE. The predicted mass of the enzyme from translation of the DNA sequence was 43,027 which is in good agreement with the mass determined by electrospray mass spectrometry.

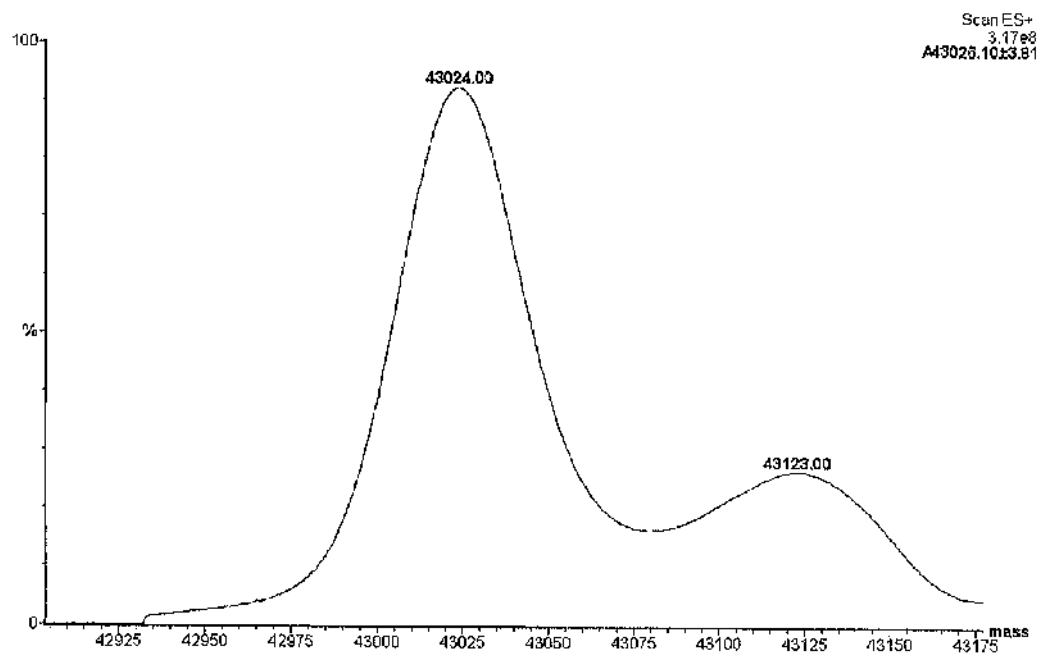
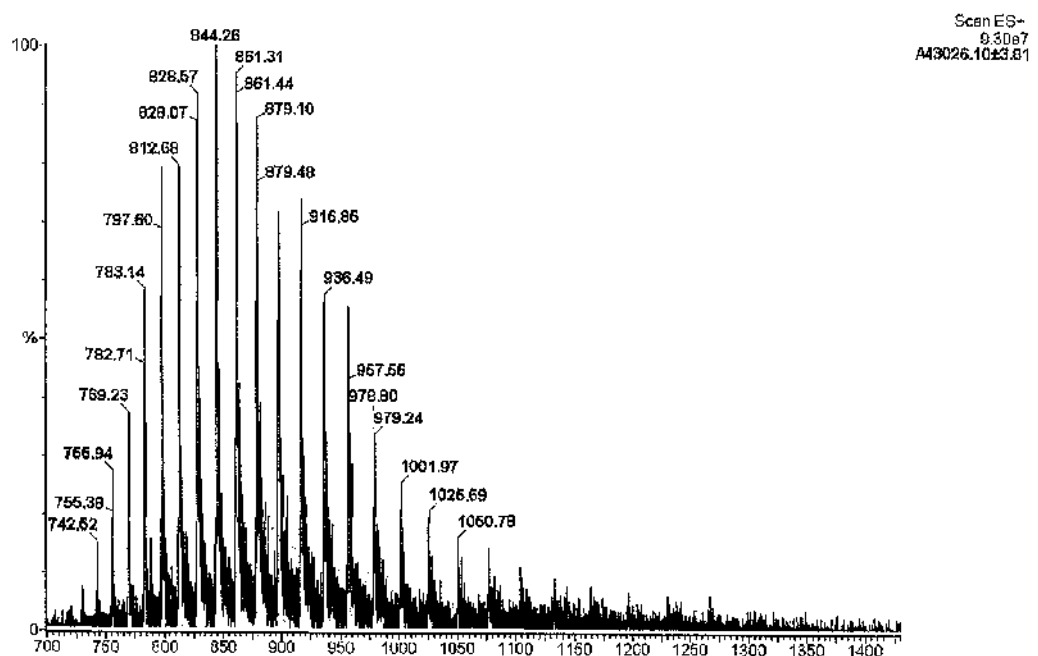


**Figure 5.3.** Electrospray mass spectrum of *S. aureus* chorismate synthase. The spectrum over the  $M_r$  range shown (42,000–44,000) was obtained using the MaxEnt deconvolution programme on the raw data, top.

The native ( $M_r$ ) was determined using gel filtration chromatography, with reference to several standard proteins of known  $M_r$ . Active chorismate synthase eluted between catalase ( $M_r$  232,000) and haemoglobin ( $M_r$  68,000) with an apparent  $M_r$  of  $186,800 \pm 7,000$  (Figure 5.4). Chemical cross-linking of the subunits of chorismate synthase was achieved using dimethyl-suberimidate. A gel of the crosslinked enzyme (Figure 5.5) suggests that chorismate synthase is a homotetramer with a molecular weight of  $182,400 \pm 12,500$ , which is similar to the mass obtained by gel filtration.

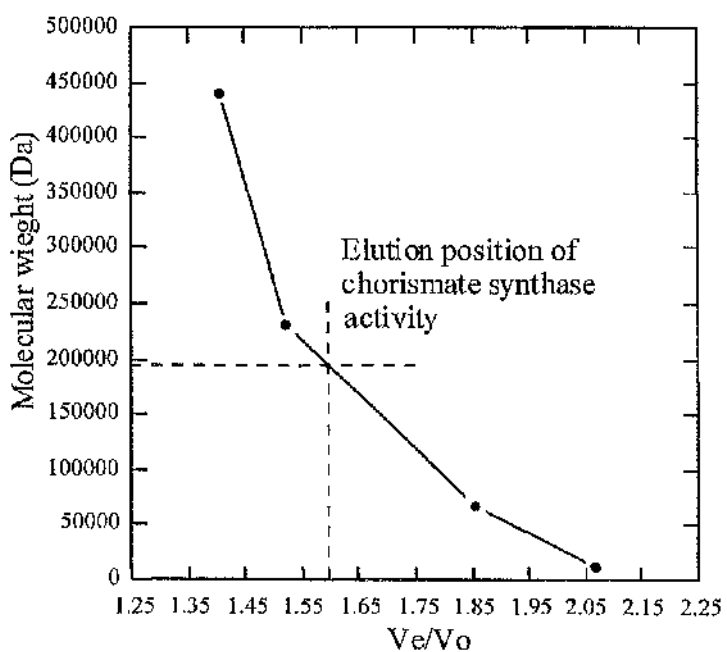
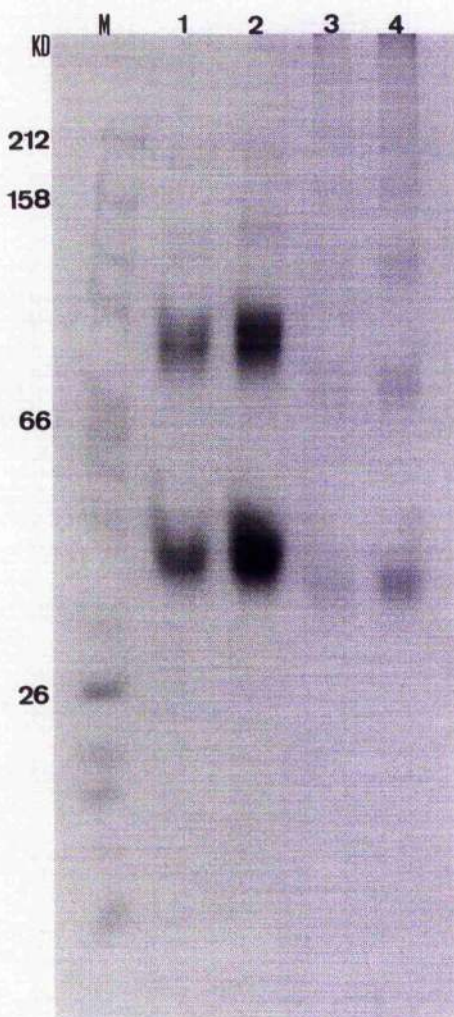


**Figure 5.4. Estimation of the native  $M_r$  of chorismate synthase.** The native  $M_r$  of active chorismate synthase was estimated by gel filtration using a superose-12 FPLC column with reference to standard proteins of known  $M_r$ .  $V_e$  - Elution volume,  $V_o$  - Void volume.



- Lane M: Molecular weight markers.  
Lanes 1, 2: *S. aureus* chorismate synthase (18, 27 $\mu$ g).  
Lanes 3, 4: *E. coli* chorismate synthase (8, 12 $\mu$ g)

**Figure 5.5. Dimethyl-suberimidate cross-linked chorismate synthase from *S. aureus* and *E. coli*.** 5% SDS polyacrylamide gel stained with Coomassie blue.

#### 5.4. pH optimum.

The pH optimum for the chorismate synthase reaction catalysed by the *S. aureus* enzyme was determined by measuring activity using the UV assay, with substrate levels as in the standard assay, in 50mM MOPS, 100mM NaCl with the pH adjusted between 6.5 and 8.5 with KOH. Initial experiments revealed a slight curvature in the traces when FMN was at a concentration of 10 $\mu$ M. This was eliminated when the FMN concentration was increased to 25 $\mu$ M. Maximal activity in MOPS buffer was observed between pH 6.0 and pH 7.25, however, increasing pH above 7.25 resulted in a progressive loss of activity up to pH 8.5, where only 8% of activity remained (Figure. 5.6).

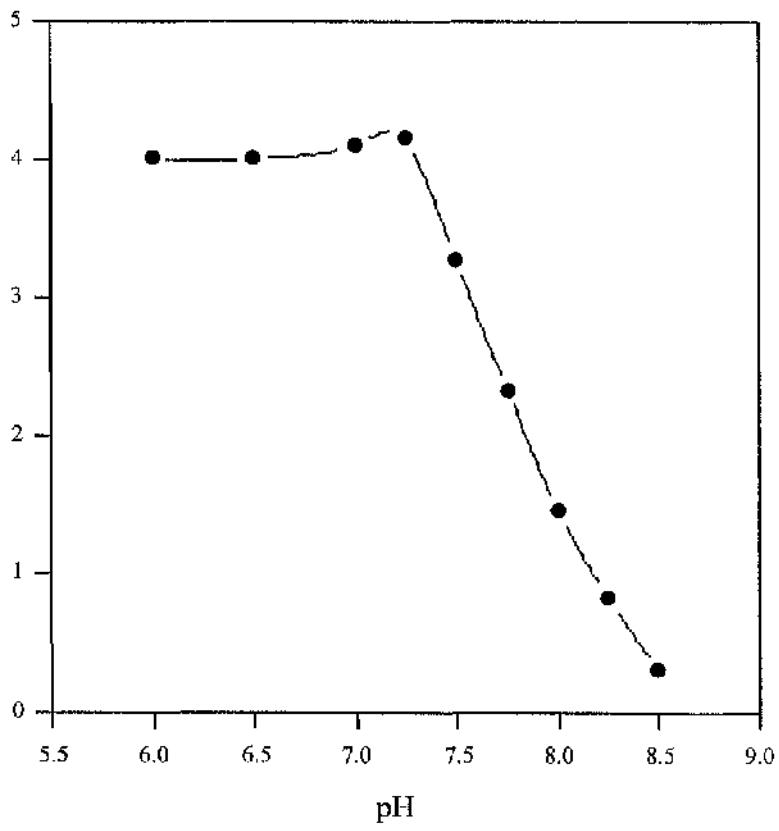


**Figure 5.6. Determination of the pH optimum of *S. aureus* chorismate synthase.** Graph shows the change in specific activity with changing pH in 50mM MOPS, 100mM NaCl buffer.

### 5.5. Buffer optimum.

The optimum buffer for the chorismate synthase reaction catalysed by the *S. aureus* enzyme was determined by measuring activity with substrate and FMN levels as in the standard assay, in 50mM buffer pH7.5, 100mM NaCl. MOPS buffer was found to give maximum activity while only 26% of maximal activity was observed in Tris-HCl buffer (Table 5.3).

Buffer	Relative activity
MOPS	1.0
Tricine	0.82
Triethanolamine	0.46
KPi	0.34
Tris-HCl	0.26

1.0 corresponds to 29.27U; 7.3 $\mu$ g of enzyme per assay

**Table 5.3. Relative activity of chorismate synthase in different buffers.**

### 5.6 Specific activity with different flavins.

Chorismate synthase from different organisms has been shown to utilise FMN, FAD and riboflavin as cofactor with a pronounced preference for FMN. *S. aureus* chorismate synthase was assayed using the standard assay with each of the three flavins at 25 $\mu$ M. The highest specific activity was obtained when FMN was the cofactor with a value of 4.01  $\mu$ molesmin $^{-1}$ mg $^{-1}$  (100%) ; FAD gave a specific activity of 0.52  $\mu$ molesmin $^{-1}$ mg $^{-1}$  (13%) ; and riboflavin gave a specific activity of 0.10  $\mu$ molesmin $^{-1}$ mg $^{-1}$  (2.4%).

### 5.7. Dependence of chorismate synthase activity on the EPSP and FMN concentration.

Apparent  $K_m$  values were determined from steady-state kinetic analyses using 50mM MOPS pH 7.0, 100mM NaCl buffer.  $K_m$  values were calculated from double reciprocal plots as shown in Figures 5.7 and 5.8.

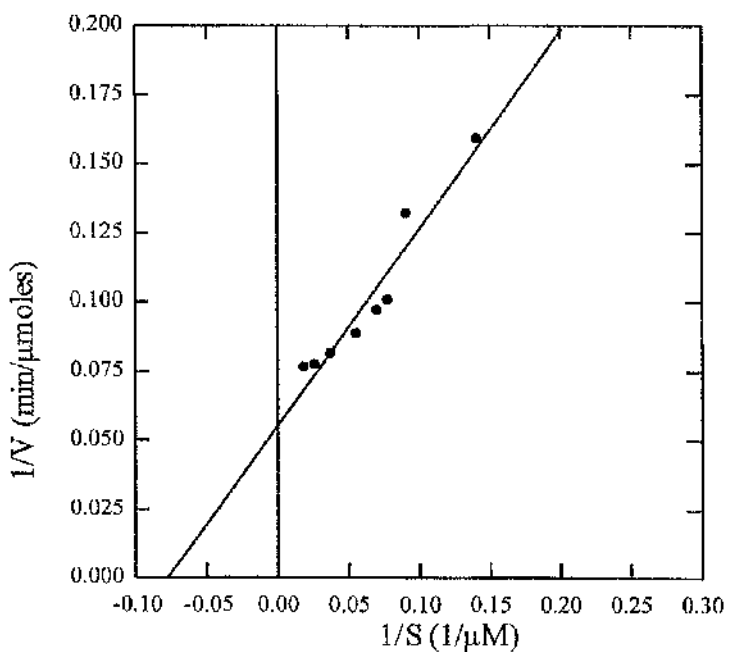


**Figure 5.8. Determination of apparent  $K_m$  for EPSP.** A double reciprocal plot showing the dependence of chorismate synthase activity on the EPSP concentration. Standard assays were performed as described in 'Materials and Methods' with varying EPSP concentration in 50mM MOPS pH7.0, 100mM NaCl. Assays were initiated with 0.2 $\mu$ l (7.3 $\mu$ g) of enzyme.

Linear regression of the data gave the equation  $y = 0.7109x + 0.0558$  and a value for  $r$ , the correlation coefficient, of 0.9623. The apparent  $K_m$  for EPSP was  $12.7 \pm 0.5$   $\mu$ M a value in accordance with most of the other chorismate synthases studied.

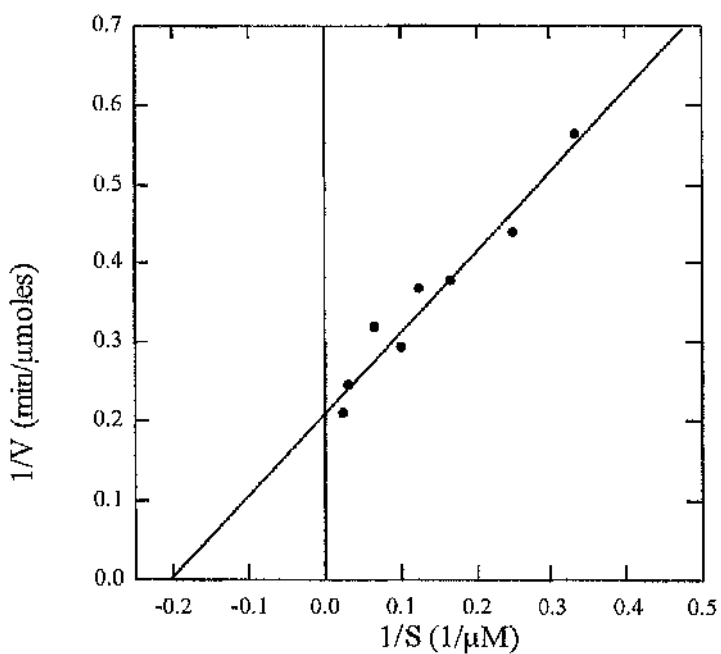


**Figure 5.8. Determination of apparent  $K_m$  for FMN.** A double reciprocal plot showing the dependence of chorismate synthase activity on the FMN concentration. Standard assays were performed as described in 'Materials and Methods' with varying FMN concentration in 50mM MOPS pH7.0, 100mM NaCl. Assays were initiated with 0.2 $\mu$ l (7.3 $\mu$ g) of enzyme.

Linear regression of the data gave the equation  $y = 1.0221x + 0.2125$  and a value for  $r$ , the correlation coefficient, of 0.9741. The apparent  $K_m$  for FMN was  $4.8 \pm 0.5 \mu\text{M}$  which is approximately two orders of magnitude greater than other chorismate synthases studied.

### 5.8. Pre-steady state kinetics of *S. aureus* chorismate synthase.

A series of experiments investigating the transient absorbance changes during the *S. aureus* chorismate synthase reaction were performed at the University of Sussex, Brighton in collaboration with Dr. Stephen Bornemann.

Single turnover experiments with rapid scanning stopped-flow spectrophotometry were used to observe the difference spectrum of any intermediate(s) formed during the *S. aureus* chorismate synthase reaction. The FMN cofactor provides a convenient chromophore for stopped flow spectrophotometry with its three oxidation states having distinct spectra. The difference spectrum obtained for the reaction intermediate(s) was then used to select a single wavelength for the analysis of the chorismate synthase reaction during multiple turnover experiments. The reaction of the enzyme with (6S)-6-F-EPSP and possible kinetic isotope effects using (6R)-[6<sup>2</sup>H]-EPSP and (6S)-[6<sup>2</sup>H]-EPSP were also investigated.

#### 5.8.1 Rapid scanning stopped-flow spectrophotometry.

Figure 5.9. shows the difference spectrum between 350nm and 700nm of the transient flavin intermediate formed during single turnover of chorismate synthase. The spectrum was produced by subtraction of a spectrum of reduced flavoenzyme with no substrate. The spectral features of the intermediate observed consists of a maximum at 390nm with a secondary maximum at 450nm separated by a trough which has a minimum at 425nm. An isosbestic point exists at 355nm. The flavin intermediate is formed extremely rapidly and decays more slowly as detailed in Figure 5.11. Analysis of the spectrum shown in Figure 5.9 at 390nm was used to produce first order rate constants to describe the rate of formation and decay of the flavin intermediate (Figure 5.11). This gave values of 12.1s<sup>-1</sup> for k<sub>1</sub> and 6.0s<sup>-1</sup> for k<sub>2</sub>.

In addition to photochemically reducing FMN in the presence of oxalate, dithionite mediated reduction of the cofactor was performed as a comparison, where 50μM sodium dithionite replaced potassium oxalate, in a stopped-flow experiment set up essentially as indicated above. Dithionite mediated reduction obviates the problem of small amounts of dissolved oxygen remaining in the solutions, however, the dithionite ion absorbs strongly in the UV region of the spectrum and consequently spectra produced were less smooth. A difference spectrum was generated against a

control of enzyme, dithionite and FMN in buffer (Figure 5.10) and gave rate constants describing the formation and decay of the intermediate which closely matched those obtained when FMN was reduced photochemically with values of  $12.6\text{s}^{-1}$  for  $k_1$  and  $6.4\text{s}^{-1}$  for  $k_2$ .

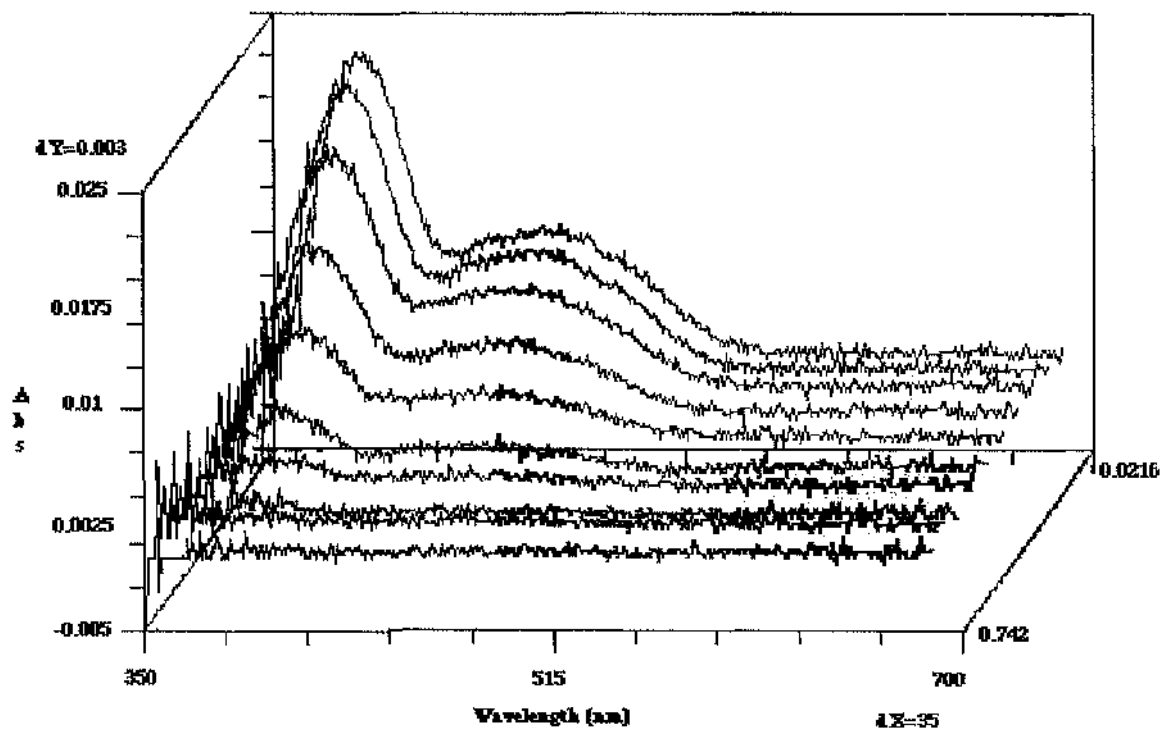


**Figure 5.9.** The difference spectrum observed during the chorismate synthase reaction. Syringe A contained  $40\mu\text{M}$  FMN,  $40\mu\text{M}$  chorismate synthase and  $1\text{mM}$   $(\text{COOK})_2$  in  $50\text{mM}$  Mops pH7.0,  $100\text{mM}$  NaCl. Syringe B contained  $40\mu\text{M}$  EPSP and trace FMN in  $50\text{mM}$  Mops pH7.0,  $100\text{mM}$  NaCl. The run time of the experiment was 1.92 sec.

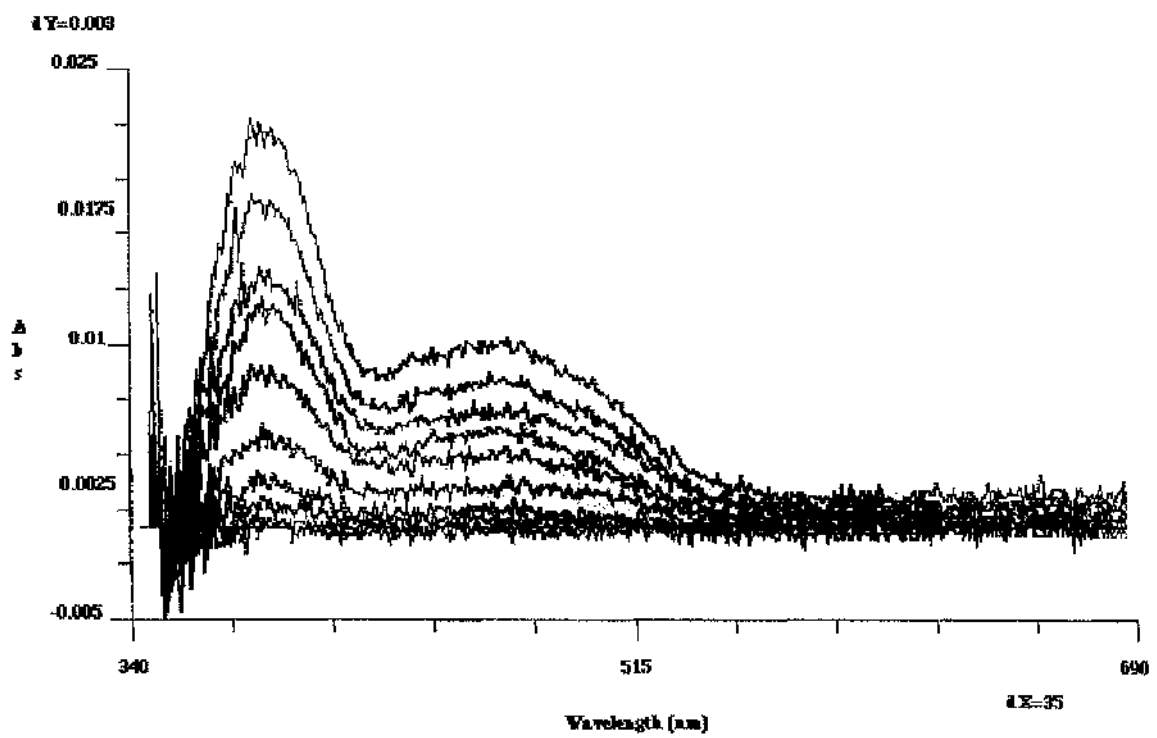


**Figure 5.10.** The difference spectrum observed during the chorismate synthase reaction. Syringe A contained 40 $\mu$ M FMN, 40 $\mu$ M chorismate synthase and 1mM sodium dithionite in 50mM Mops pH7.0, 100mM NaCl. Syringe B contained 40 $\mu$ M EPSP in 50mM Mops pH7.0, 100mM NaCl. The run time of the experiment was 9.6 sec.

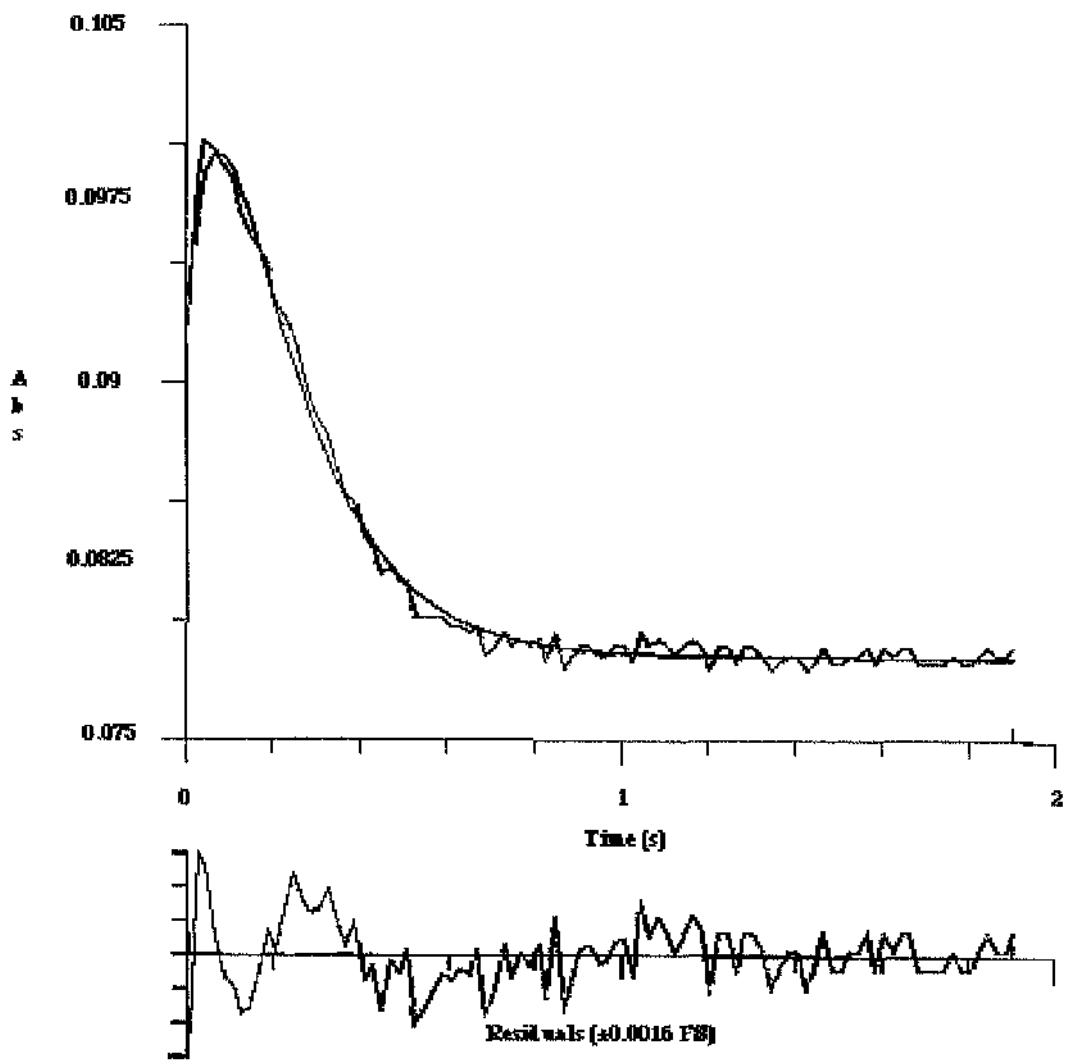


**Figure 5.11.** Formation and decay of the flavin intermediate during single turnover rapid scanning stopped-flow spectrophotometry. Two exponentials were fitted to the data obtained at 390nm to obtain the rate constants  $k_1$  and  $k_2$ .

### 5.8.2. Single wavelength stopped-flow experiments.

Single wavelength (390nm) stopped flow experiments were performed to obtain a more accurate measurement for the kinetics of flavin intermediate formation during turnover with EPSP. The kinetics of the intermediate were further investigated with respect to the substrate analogues (6S)-[6<sup>2</sup>H]-EPSP, (6R)-[6<sup>2</sup>H]-EPSP and (6S)-6F-EPSP.

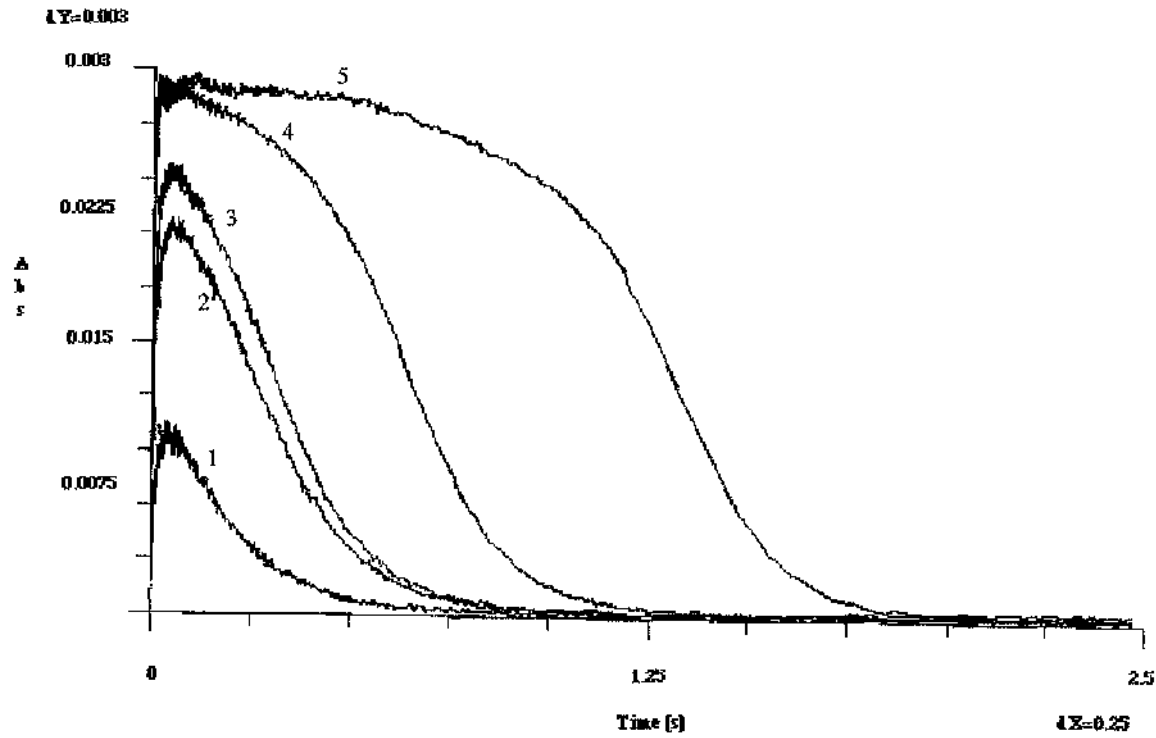


**Figure 5.12. Single wavelength stopped-flow titration of EPSP against enzyme.** Syringe A: chorismate synthase 40μM, FMN 40μM and dithionite 1mM in 50mM Mops pH7.0, 100mM NaCl. Syringe B: EPSP at (1) 10μM, (2) 20μM, (3) 30.8μM, (4) 80μM and (5) 160μM in 50mM Mops pH7.0, 100mM NaCl. 25 C, 1.8nm slit width, tungsten lamp.  $k_1$  for (1) 72s<sup>-1</sup> (2) 106s<sup>-1</sup> (3) 122s<sup>-1</sup> (4) 186s<sup>-1</sup> (5) 313s<sup>-1</sup>.  $k_2$  for (1) 6.6s<sup>-1</sup> (2) 6.6s<sup>-1</sup> (3) 6.3s<sup>-1</sup> (4) 6.6s<sup>-1</sup> (5) 6.5s<sup>-1</sup>. The errors for  $k_1$  and  $k_2$  were calculated to be ±10% and ±0.1s<sup>-1</sup>, respectively.

EPSP was titrated against enzyme and the kinetics of flavin intermediate formation were determined from one quarter to four times turnover of the enzyme (Figure 5.12). When EPSP concentration was increased an increase in the rate of formation of the flavin intermediate was observed (Figure 5.13). This contrasts with *E. coli* chorismate synthase where the rate of flavin intermediate formation is independent of substrate concentration. Furthermore, it was not possible to fit two exponentials to describe the rates of formation and decay of the intermediate above one quarter to one half times turnover. The latter part of flavin intermediate decay did fit to an exponential for each of the substrate concentrations and revealed a similar rate of decay at each concentration.

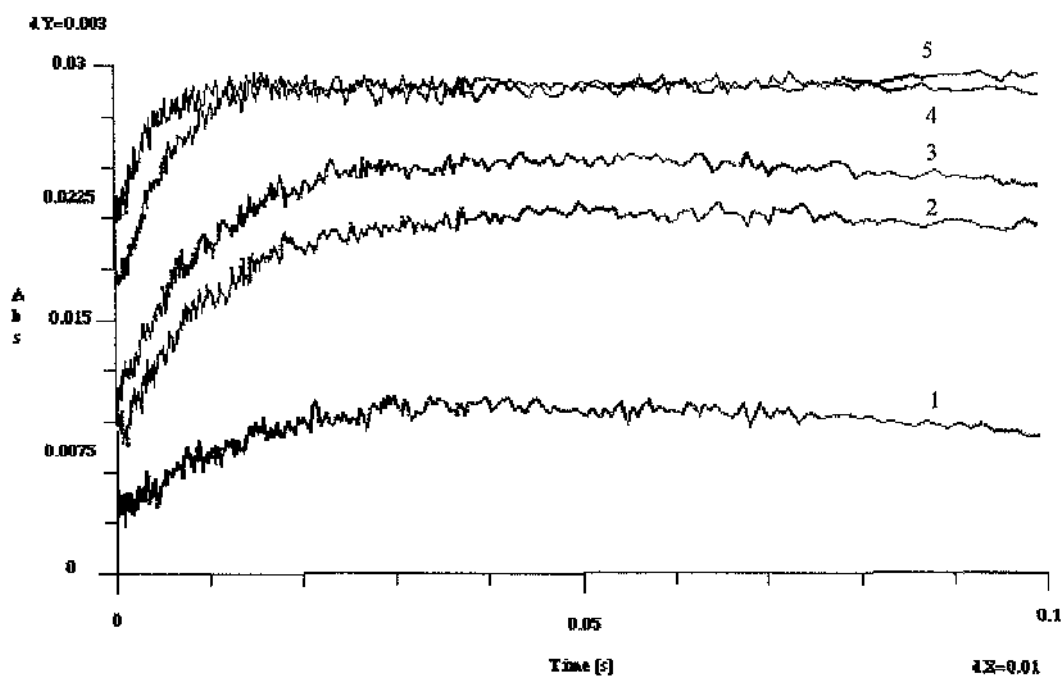


**Figure 5.13. The increase in  $k_1$  with increasing substrate concentration.**  
Derived from Figure 5.12.

Further stopped-flow kinetic analysis of chorismate synthase was performed using the substrate analogues (6S)-[ $^6$ H]-EPSP and (6R)-[ $^6$ H]-EPSP to determine whether there were kinetic isotope effects (KIE) on either the pro-S or pro-R hydrogen bonds during the *S. aureus* chorismate synthase reaction i.e. establish if C-H bond cleavage

was rate-limiting during catalysis. The error in fitting two exponentials to the data as demonstrated above meant that the pre-steady state analysis of a KIE produced an unacceptably large error. This was a problem for what appeared to be a very small KIE; instead steady-state kinetic analysis was used to investigate a possible kinetic isotope effect.

### 5.9 Steady state analysis of EPSP analogues.

Steady-state assays with deutero- and fluoro-substituted EPSP were performed using the standard anaerobic assay containing 25 $\mu$ M FMN, 50 $\mu$ M EPSP and 7.3 $\mu$ g *S. aureus* chorismate synthase (36.5 $\mu$ g for (6S)-6F-EPSP and its control assay) in 50mM Mops pH 7.0, 100mM NaCl. Assays were carried out using a Shimadzu MPS2000 multipurpose recording spectrophotometer.  $V_{max}$  was determined for each of the analogues as detailed in Table 5.3. The kinetic isotope effect at the pro-*R* hydrogen was determined to be  $1.02 \pm 0.06$  and  $1.00 \pm 0.09$  at the pro-*S* hydrogen. It was observed, however, that there was a great deal of curvature in the traces during the deutero analogue assays and consequently the very beginning of the traces were used to calculate the rates.

The rate of product formation was judged to be approximately 130 times slower for the fluoro analogue when compared to EPSP. However, pronounced curvature of the trace was observed initially with the rate apparently increasing before remaining linear for the majority of the assay.

Substrate	$V_{max}$ ( $\text{Umg}^{-1}$ )	Error
EPSP	4.22	$\pm 0.10$
(6 <i>R</i> )-[62H]-EPSP	4.15	$\pm 0.17$
(6 <i>S</i> )-[62H]-EPSP	4.20	$\pm 0.28$
EPSP	4.45	$\pm 0.10$
(6 <i>S</i> )-6F-EPSP	0.034	$\pm 0.007$

**Table 5.3. Observed  $V_{max}$  for EPSP compared to deutero- and fluoro-analogues of EPSP.**

### 5.10. Preliminary investigation of flavin interaction with *S. aureus* chorismate synthase.

Experiments designed to investigate the interaction of the flavin cofactor with chorismate synthase were done at the University of Sussex, Brighton in collaboration with Dr. Peter Macheroux. Spectrophotometry was done using an HP 8452A diode array spectrophotometer linked to a Vectra 386/33N PC.

#### 5.10.1. Titration of chorismate synthase with EPSP.

A spectrum of FMN, 14 $\mu$ M in 50mM MOPS, 100mM NaCl pH 7.0, was taken prior to and after the addition of *S. aureus* chorismate synthase to 15 $\mu$ M. Further spectra were then taken after additions of 3, 6, 9, 12, 15, 18 and 27 $\mu$ M EPSP (Figure 5.14).

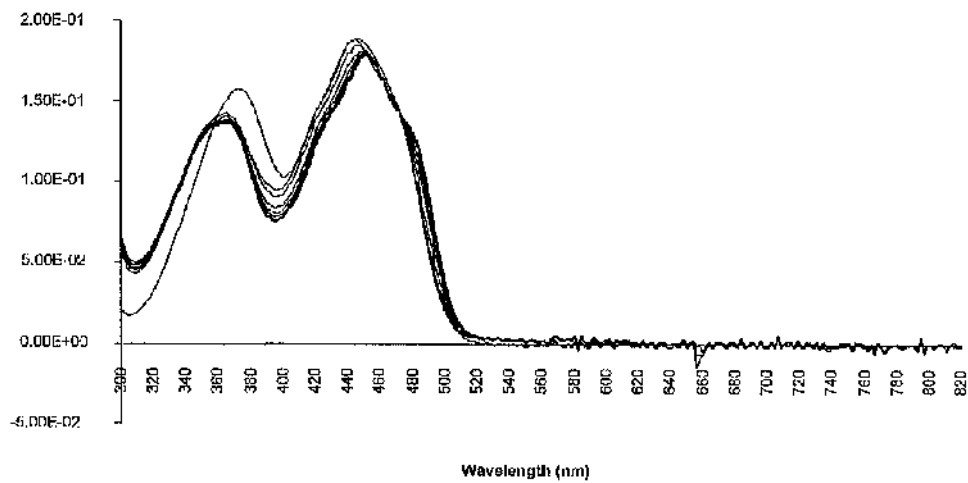


**Figure 5.14. Changes to the spectrum of FMN after addition of enzyme followed by the addition of EPSP.** A large change in the spectrum is observed upon addition of enzyme (largest change in spectrum is in the region 300-400nm). Each addition of EPSP changes the spectrum slightly (reduction in the spectrum in the region 300-480nm and increase in the spectrum between 480 and 520nm)

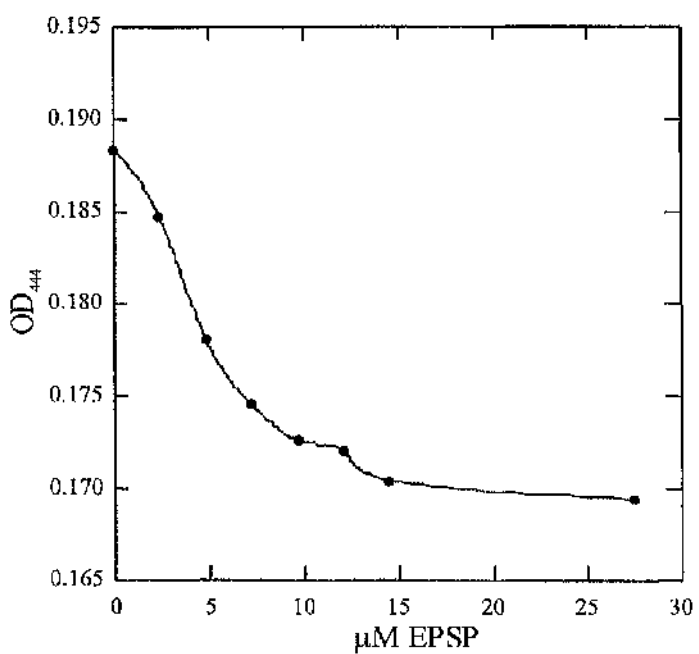


**Figure 5.15. Titration of chorismate synthase with EPSP.** Graph generated from data obtained from Figure 5.14.

Values obtained from changes in the FMN spectrum at 444nm before and after the addition of EPSP were plotted (Figure 5.15). Extrapolation of the curve to obtain the concentration of EPSP where there was essentially no further change in the flavin spectrum at 444nm gave a value around 15 $\mu$ M. This matched the concentration of enzyme present in the titration and indicated stoichiometric binding of the EPSP to *S. aureus* chorismate synthase. Figure 5.14 shows the spectra obtained during the titration. A large change in the FMN spectrum between 300 and 400nm was observed when enzyme was added to the FMN displaying that the enzyme was binding the oxidised FMN and shifting its spectrum. This contrasts with the *E. coli* enzyme where no change to the flavin spectrum is observed upon addition of the enzyme to the FMN (P. Macheroux, personal communication). Further changes in the spectrum were then observed as EPSP was added suggesting conformational changes to the enzyme-flavin complex.

### 5.10.2. Flavosemiquinone formation with 6R-6F-EPSP.

The following two experiments were performed using a quartz cuvette which had a side-arm in the neck and which could be stoppered with a Subaseal stopper to allow an anaerobic environment to be produced by cycles of vacuum and nitrogen. After a baseline was recorded for buffer (50mM MOPS pH7.0, 100mM NaCl) the spectrum of 14 $\mu$ M FMN, 15 $\mu$ M *S. aureus* chorismate synthase and 30 $\mu$ M 6R-6F-EPSP in buffer was recorded. 2mM oxalate was then added to the other components by mixing the contents of the cuvette with the side arm. After photoreduction of the oxalate for 10s using a Schott LK1500 lamp at full power setting a spectrum was taken. Further spectra were then recorded after 10, 20, 35, 50, 70, 130, 430s.

Examination of the spectra produced (Figure 5.16) revealed photoreduction of the flavin, as evinced by a decrease in the maxima at 360nm and 444nm, furthermore, there was evidence for the formation of a flavosemiquinone (radical) [broad peak between 500 and 650 nm with a maximum of 594nm]. The flavosemiquinone was formed extremely rapidly, however, complete reduction of the FMN (flavosemiquinone to hydroquinone) was very slow.

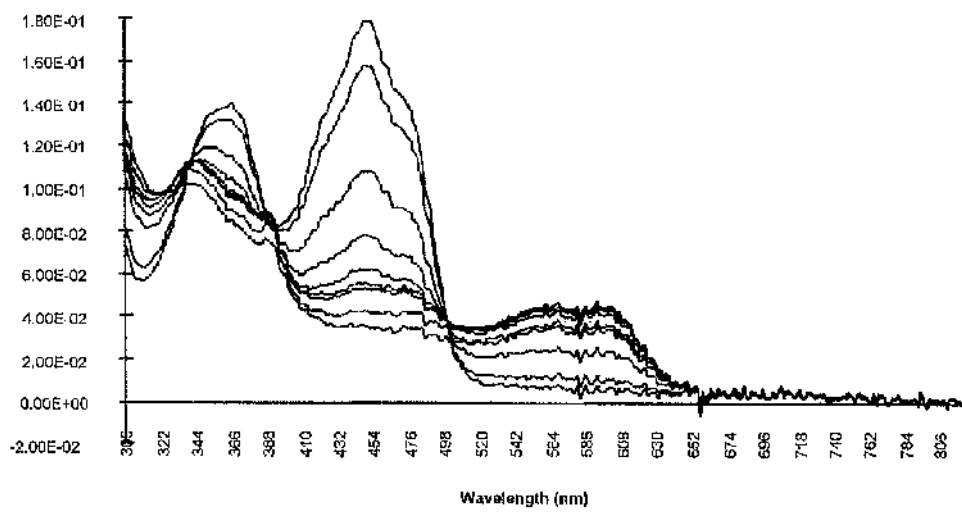


**Figure 5.16. Flavosemiquinone formation in the presence of 6R-6F-EPSP.**  
Photoreduction of the flavin is shown by decrease in the maxima at 360nm and 444nm from the spectrum of FMN+enzyme+6R-6F-EPSP. Flavosemiquinone formation, 500 to 600nm, was rapid and was followed by its slow disappearance with further photoreduction to produce hydroquinone.

### 5.10.3. Flavosemiquinone formation with EPSP.

This experiment was performed in a similar way to the above experiment. A baseline of buffer was taken before recording a spectrum of  $15\mu\text{M}$  FMN,  $15\mu\text{M}$  enzyme and  $2\text{mM}$  oxalate in  $50\text{mM}$  MOPS pH7.0,  $100\text{mM}$  NaCl. The FMN was then photoreduced for 5, 15, 35, 55, 115 and  $175\text{s}$  with spectra taken at each time-point. EPSP was added via the side arm,  $150\mu\text{M}$  final concentration, and spectra were recorded after 15, 90 and  $210\text{s}$  (Figure 5.17).

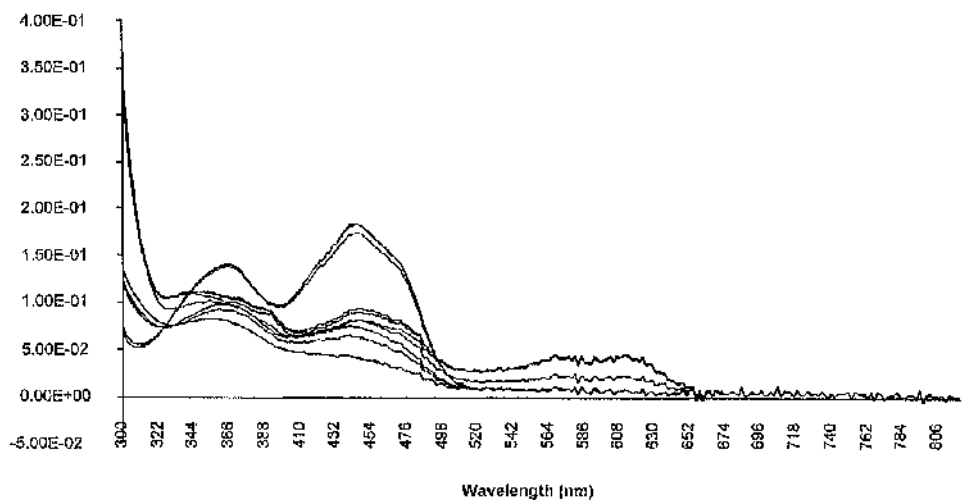


**Figure 5.17. Flavosemiquinone formation in the presence of EPSP.** The spectra reveal photoreduction of the FMN with decreases in the maxima at 360 and 444nm. Flavosemiquinone formation shown by the broad peak between 500 and 650nm occurred after addition of EPSP; the addition of a small amount of oxygen at the same time resulted in oxidation of some flavin with a concomitant increase in the spectrum. Chorismate formation is noted by the dramatic increase in absorbance at the 300nm region for several of the spectra.

Flavosemiquinone was formed in the presence of chorismate with a shift in the maximum to  $610\text{nm}$ , compared to the maximum of  $594\text{nm}$ , observed for (6R)-6F-EPSP. The same spectral shift was observed for *E. coli* chorismate synthase (P. Macheroux, personal communication) and is thought to result from chorismate not

being released from the enzyme-flavin complex. Chorismate is more hydrophobic than EPSP, due to loss of the phosphate group, and would create a more apolar environment around the flavin perturbing the flavosemiquinone spectrum. Furthermore, the spectrum is characteristic of the anionic reduced form of FMN (Muller *et al.*, 1972)

#### 5.10.4. Dissociation constant for oxidised flavin.

The dissociation constant,  $K_D$ , for oxidised FMN ( $FMN_{ox}$ ) was calculated after incubating *S. aureus* chorismate synthase, 15 $\mu$ M, with FMN, 14 $\mu$ M, in 50mM MOPS pH7.0, 100mM NaCl and separating free flavin from enzyme bound flavin using a centricon-10 concentrator. The  $OD_{444}$  was calculated for the free flavin in the eluate and for the enzyme bound flavin in the concentrated protein fraction. The  $K_D$  was then obtained from the following equation:

$$K_D = [FMN]_{FREE} \cdot [Enzyme]_{FREE} / [Enzyme-FMN]$$

The  $K_D$  for  $FMN_{ox}$  in the presence of EPSP was similarly calculated with 50 $\mu$ M EPSP added after incubation of the enzyme with FMN. The values obtained for  $K_D$   $FMN_{ox}$  were 7.15 $\mu$ M without EPSP and 2.42 $\mu$ M in the presence of 50 $\mu$ M EPSP. These values indicate that oxidised flavin is bound tightly by the enzyme in contrast to the *E. coli* enzyme which has a  $K_D$  for  $FMN_{ox}$  of >100 $\mu$ M. It also shows that oxidised flavin is bound more strongly when EPSP is present. This has implications for crystallography where the FMN can be retained on the enzyme in the presence of EPSP to produce holoenzyme.

### 5.11. Chapter summary.

Chorismate synthase was purified to near homogeneity producing nearly 100mg of enzyme from 13g (wet weight) of *E. coli* GLW40(DE3)pMJH7EX2. The enzyme was judged to be a homotetramer using cross-linking with dimethyl-suberimidate. The subunit molecular mass was determined to be 43,024 by electrospray mass spectrometry and this closely matched the value of 43,027 determined from translation of the gene sequence.

The pH optimum of the enzyme was found to be non-symmetrical in MOPS buffer with an optimum of activity around pH 7.0. The apparent  $K_m$  for EPSP of the *S. aureus* enzyme was calculated to be 12.7 $\mu$ M and the apparent  $K_m$  for FMN was calculated to be 4.8 $\mu$ M.

*S. aureus* chorismate synthase was further investigated using stopped-flow methods to examine the pre-steady state kinetics of the enzyme. A flavin intermediate was observed during turnover with a difference spectrum which resembled that obtained previously with the *E. coli* enzyme. The spectral characteristics of the *S. aureus* flavin intermediate were different, however, with respect to its maxima, minima and overall shape. The rate of decay ( $6.5\text{s}^{-1}$ ) of the intermediate was eight times slower than that observed previously for the *E. coli* enzyme ( $52\text{s}^{-1}$ ) and this compared well with a seven fold lower  $V_{max}$ .

## CHAPTER 6. SITE-DIRECTED MUTAGENESIS OF *S. AUREUS* CHORISMATE SYNTHASE.

---

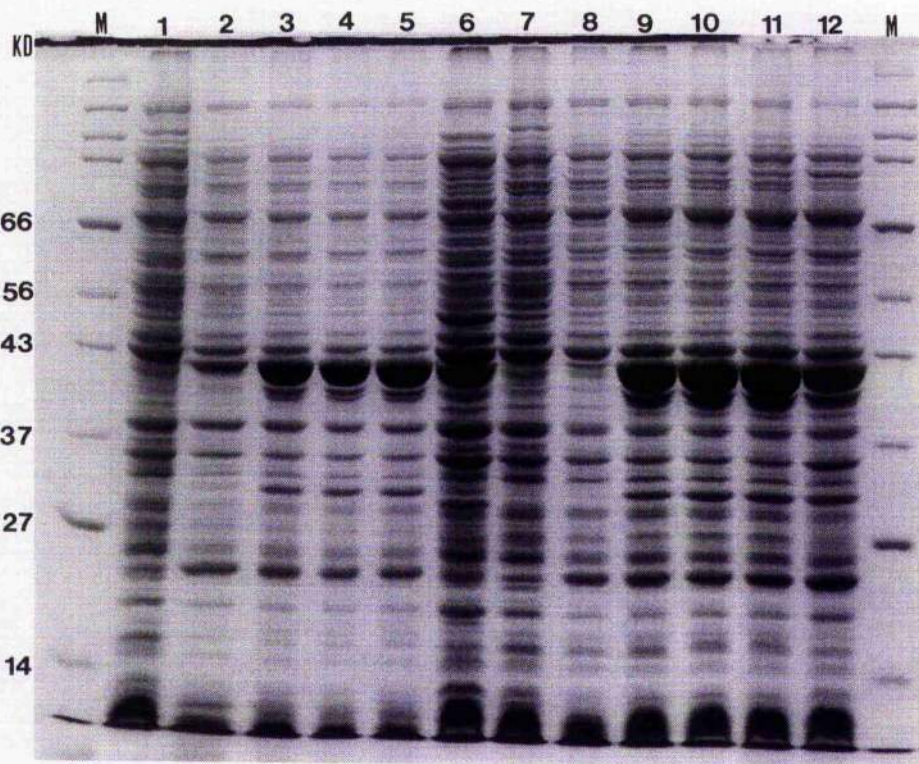
The mutagenesis of *S. aureus* chorismate synthase was attempted without structural information for the enzyme. The mutagenesis of tyrosine 121 (130 in multiple lineup, Figure 3.6) in the *S. aureus* sequence was based upon the premise that tyrosine residues are known to be important for flavin binding in a variety of flavin-cofactor requiring enzymes and that a lineup of the chorismate synthase sequences known to date revealed only one tyrosine residue which was completely conserved.

### 6.1. Construction and overexpression of site-directed mutants.

The tyrosine residue was substituted by phenylalanine and by alanine in *S. aureus* chorismate synthase using the PCR method of Higuchi *et al.* (1988) as described in section 2.17. The final mutagenised PCR products were cloned into pTB361 and when sequenced were found to match the original template except for the desired mutations. The two resulting plasmids pMJHY121F and pMJHY121A were transformed into *E. coli* GLW40(DE3)pLysS and protein expression monitored over time (Figure 6.1). The host strains containing the two mutant plasmids were observed to grow more slowly than the 'wild type', pMJH7EX2 containing host strain but did produce large amounts of overexpressed enzyme. Expression of the mutants in *E. coli* BL21(DE3) or GLW40(DE3) when the pLysS plasmid was absent was poor and cell growth was significantly retarded. The reason for this is not at all clear but suggested that the mutations had produced some change which was detrimental to the cell.

### 6.2 Functional test of mutants using complementation.

The chorismate synthase free background of the host strain *E. coli* GLW40(DE3) was used to express the tyrosine mutants with growth on minimal medium. The ability to complement the Aro<sup>-</sup> phenotype of this strain has been shown to be a sensitive procedure for cloning *aroC* genes (this study, Millar *et al.*, 1988), testing deletion mutants for chorismate synthase activity (Henstrand *et al.*, 1995b) and should by the same argument provide a sensitive test for the activity of site-directed mutants of chorismate synthases.



Lane M: Molecular weight markers

Lanes 1,7: *E. coli* GLW40(DE3)pLysS

Lanes 2-6: *E. coli* GLW40(DE3)pLysSpY121F 0, 2, 3, 4, 14 hr

Lanes 8-12: *E. coli* GLW40(DE3)pLysSpY121A 0, 2, 3, 4, 14 hr

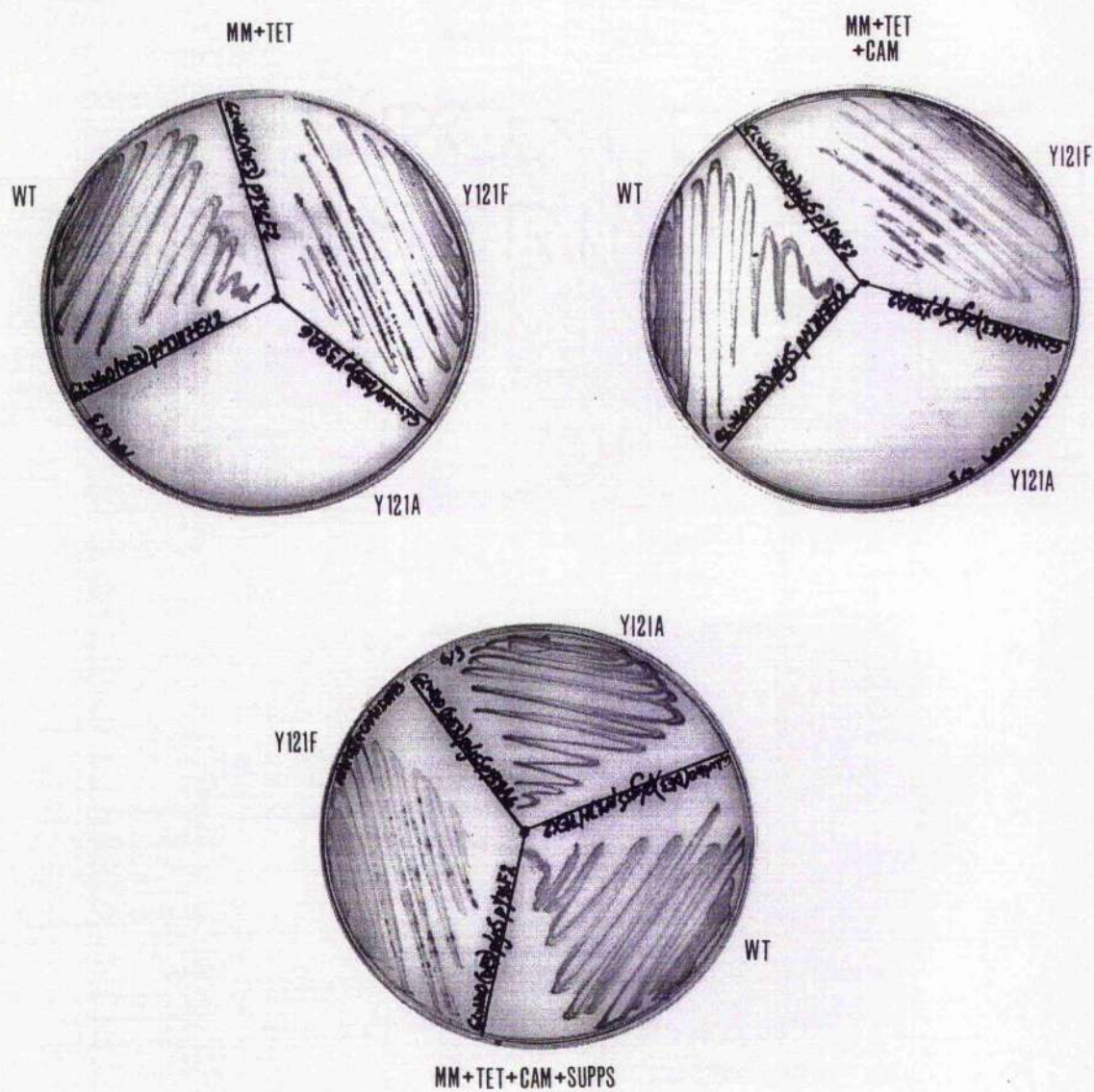
**Figure 6.1. SDS-PAGE showing a time course of protein expression from the *aroC* clones pY121F and pY121A in *E. coli* GLW40(DE3) pLysS after induction with IPTG. The 10% SDS gel was stained with Coomassie blue.**

The plasmids pMJH7EX2, pMJHY121F and pMJHY121A were each transformed into GLW40(DE3) and GLW40(DE3)pLysS and plated onto LB plates containing antibiotics where appropriate. Following growth on rich medium for 12 hours, minimal medium plates containing antibiotics and supplements where appropriate were streaked. The minimal medium plates were then incubated for 24 hours and checked for growth with a further check for growth after 60 hours. The results are summarised in Table 6.1 and a number of the plates are shown in Figure 6.2.

Plasmids in <i>E. coli</i> GLW40(DE3)	MM	MM+ TET	MM+TET +CAM	MM+ SUPPS	MM+TET+ CAM+SUPPS
pMJH7EX2	+++	+++	+++	+++	+++
pMJHY121F	++	+++	+++	+++	+++
pMJHY121A	-	-	-	+++	+++
pLysSpMJH7EX2	+++	+++	+++	+++	+++
pLysSpMJHY121F	+++	+++	++	++	++
pLysSpMJHY121A	-	-	-	-	+++

**Table 6.1. Complementation test of 'wild-type' and mutants on minimal medium.** +++ indicates strong growth, ++ indicates medium growth, + indicates poor growth and - indicates no growth after 60 hours. MM minimal medium, TET tetracycline [ $12.5\mu\text{g ml}^{-1}$ ], CAM chloramphenicol [ $17\mu\text{g ml}^{-1}$ ]. SUPPS [tyrosine ( $200\text{mg l}^{-1}$ ), tryptophan ( $200\text{mg l}^{-1}$ ), phenylalanine ( $400\text{mg l}^{-1}$ ), para-aminobenzoate ( $320\mu\text{g l}^{-1}$ ), para-hydroxybenzoate ( $320\mu\text{g l}^{-1}$ ), thiamine-HCl ( $3\text{mg l}^{-1}$ )]. Chloramphenicol was included in plates when the pLysS plasmid was present.

The 'wild-type', pMJH7EX2, produced a positive control with growth on minimal medium with or without antibiotics and/or aromatic supplements. The phenylalanine mutant was capable of growth on minimal medium suggesting a functional chorismate synthase. However, the alanine mutant was particularly distinctive using the complementation test due to its inability to grow on minimal medium with or without the appropriate antibiotics. It was capable of growth on supplemented minimal medium indicating that the plasmids were present and the host strain was viable.



W.T. is *E. coli* GLW40(DE3)pMJH7EX2.

Y121F is *E. coli* GLW40(DE3)pMJHY121F.

Y121A is *E. coli* GLW40(DE3)pMJHY121A.

**Figure 6.2. Functional tests of mutants and 'wild-type' using complementation on minimal medium.** MM indicates minimal medium, TET+CAM indicates the inclusion of tetracycline ( $12.5\mu\text{gml}^{-1}$ ) and chloramphenicol ( $17\mu\text{gml}^{-1}$ ). SUPPS indicates the inclusion of aromatic supplements as detailed in the legend for Table 6.1. CAM was added to plates when pLysS was present with pMJH plasmids.

### 6.3. Specific activities of the crude extracts for the mutants.

Unsuccessful attempts were made to purify both of the mutant *S. aureus* chorismate synthases. The purification of 'wild-type' chorismate synthases, generally, is made more difficult by the reduced solubility of the apoenzyme. Flavin dissociates from the enzyme during purification ( $K_D$  for oxidised flavin with EPSP absent is  $7.15\mu M$  for the *S. aureus* enzyme) and the flavin is completely removed during absorption of the enzyme to cellulose phosphate in the final affinity chromatography step of purification. The enzyme can be stabilised during purification by the addition of glycerol as a co-solvent.

The crude extract of the alanine mutant was noticeably less yellow than the crude extracts of the phenylalanine mutant and the 'wild-type'. Furthermore during purification the pool of chorismate synthase activity obtained after DEAE-Sephacel chromatography was colourless compared to the light yellow coloured enzyme pool obtained with the phenylalanine mutant and the more obviously yellow coloured pool obtained with the 'wild-type'. Enzyme activity was lost dramatically upon dialysis of the DEAE-Sephacel pool from the alanine mutant in 10mM KPi buffer, pH6.6 due to precipitation of the enzyme. Millar, (1988) observed that during the attempted purification of *E. coli* chorismate synthase from a strong overproducer at least 90% of activity was lost during the dialysis, a problem overcome by Ramjee, (1992) with the inclusion of glycerol.

Plasmid	Volume (ml)	Protein (mg)	Activity (U)	Specific activity (Umg <sup>-1</sup> )
pMJH7EX2	80	1210	416	0.34
pMJHY121F	80	748	23.2	0.031
pMJHY121A	70	1390	2.94	$2.12 \times 10^{-3}$

**Table 6.2. Specific activities of chorismate synthase mutants and 'wild-type' from attempted purifications.** Specific activities were determined using the standard assay and values were also examined by adding enzyme before the photoreducing step to avoid the addition of large volumes of sample and thus dissolved oxygen.

As a consequence of these problems, the *S. aureus* mutants were not successfully purified past chromatography on DEAE-Sephacel. The mutants were compared instead by examining the specific activity of crude extracts as detailed in Table 6.2. The specific activity of the alanine mutant was at least 150 fold less than the 'wild-type' while that of the phenylalanine mutant was around 10 fold less. The mutant enzymes were known to be soluble in the crude extracts as evinced by their presence in the soluble supernatant fraction after lysis with lysozyme.

#### 6.4. Chapter summary.

Tyrosine 121 of *S. aureus* chorismate synthase was changed to either phenylalanine or alanine using the PCR mutagenesis strategy of Higuchi *et al.* (1988). The two mutant enzymes were expressed to high levels, however, the levels of expression achieved were observed to be lower than those observed for the wild-type *S. aureus* chorismate synthase.

Activity of the two mutants was determined by their ability to complement the Aro<sup>-</sup> phenotype of *E. coli* GLW40. While both the wild-type and phenylalanine mutant enzymes were able to complement the *aroC* mutation the alanine mutant was not. Changes to the activity of the mutant chorismate synthases was confirmed by an observed reduction in the specific activities of the mutant enzymes compared to wild-type enzyme when assayed in crude extracts.

## CHAPTER 7. PURIFICATION AND CHARACTERISATION OF *E. COLI* FLAVIN REDUCTASE.

This chapter describes the purification and characterisation of a flavin reductase from *E. coli*. This enzyme was purified to analyse possible interactions between *E. coli* chorismate synthase and flavin reductase.

### 7.1. Purification of *E. coli* flavin reductase.

*E. coli* flavin reductase was purified from 14g (wet weight) of *E. coli* BL21(DE3)pLysEpFREX2 using three chromatographic steps of DEAE-Sephacel, phenyl sepharose and S-200 gel filtration. The protocol was similar to the method previously published by Fontecave *et al.* (1987) for purification from wild-type *E. coli* C600 but included a number of changes as detailed in section 2.23. The purification yielded around 20mg of enzyme which was apparently homogeneous as judged by Coomassie-stained SDS-PAGE. The chromatographic profiles of the enzyme on the two columns are detailed in Figures 7.1, 7.2 and 7.3 while Table 7.1 summarises the purification.

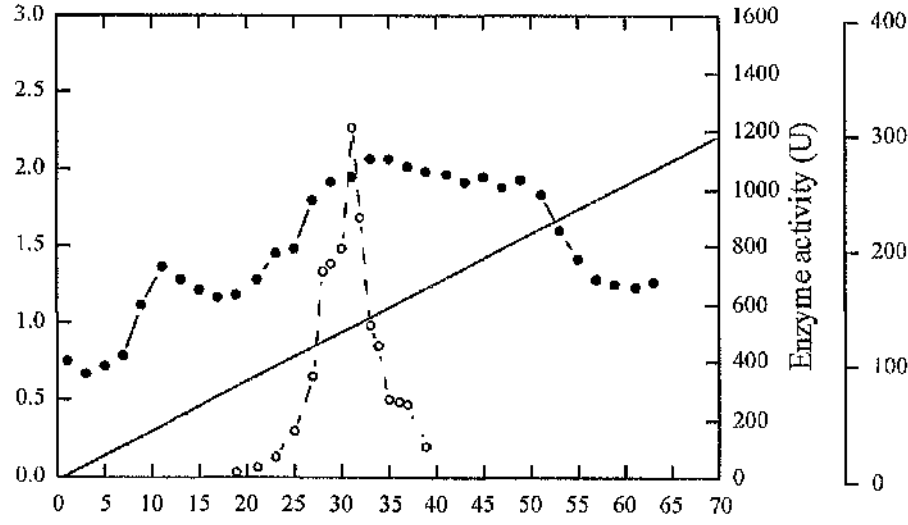


**Figure 7.1.** Elution profile of *E. coli* flavin reductase from DEAE-Sephadex. OD<sub>280</sub> (●), Activity (○).

The pLysE plasmid was incorporated into the expression system for the expression of *E. coli* flavin reductase to relieve the problem of extremely slow cell growth. This may be a consequence of the possibly detrimental reduction of most of the free flavins within the cell and/or NAD(P)H being shunted through the flavin reductase reaction depleting cellular 'energy' reserves. In addition, NAD(P)H:flavin reductase has been demonstrated to be a selective superoxide radical generator under aerobic conditions (Gaudu *et al.*, 1994) and it may be the toxicity of this which was retarding growth. Cells after overexpression were observed to be very pale in colour in contrast to the usual golden colour.

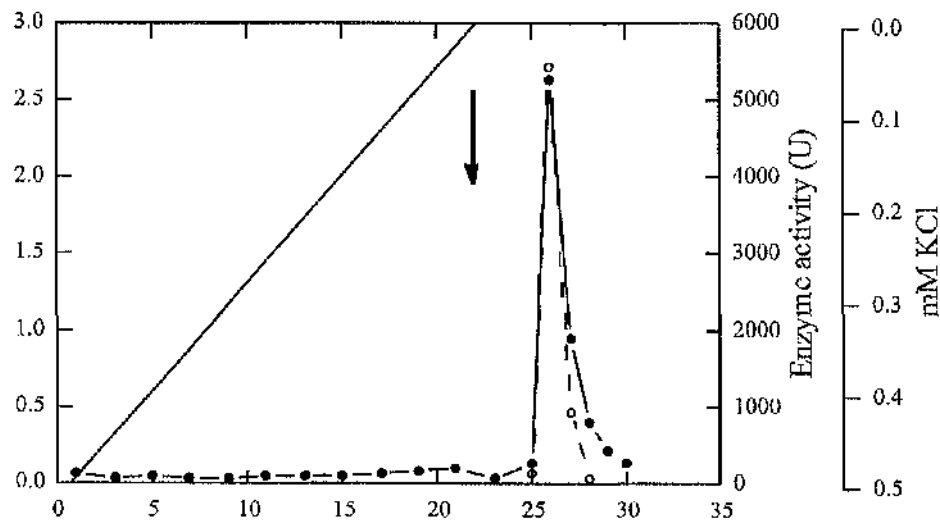


**Figure 7.2. Elution profile of *E. coli* flavin reductase from phenyl sepharose.** Arrow indicates elution of the enzyme using a step of 10mM Tris-HCl pH7.5 from 50mM Tris-HCl pH7.5. OD<sub>280</sub> (●), Activity (○).

Step	Total protein (mg)	Total activity (U)	Specific activity (U mg <sup>-1</sup> )	Yield (%)	Purification (-fold)
Crude extract	987	1,612	1.63	100	1
DEAE-Sephadex	192	4,322	23.74	268	14.6
Phenyl sepharose	79.5	6,378	80.2	396	49.2
S-200	19.2	3,513	183	218	112.3

**Table 7.1** Summary of the purification of *E. coli* flavin reductase from *E. coli* GLW40(DE3)pLysEpFREX2. Assays for activity were performed as per standard assay (section 2.19) with riboflavin as substrate and NADPH as cofactor.

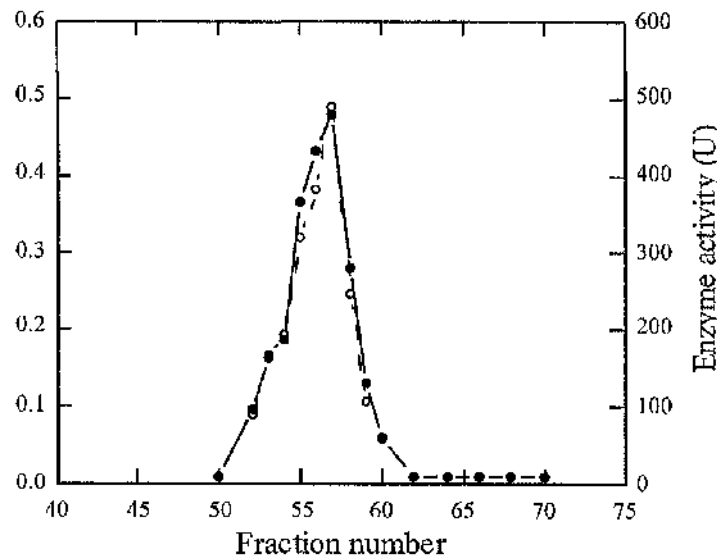


**Figure 7.3.** Chromatography of *E. coli* flavin reductase using S-200 gel filtration. OD<sub>280</sub> (●), Activity (○).

*E. coli* flavin reductase was ultimately resuspended in the minimum volume of 50mM Tris-HCl pH7.5, 0.4mM DTT, 1.2mM PMSF, 50% glycerol after ammonium sulphate precipitation and stored at -20°C. The purification of *E. coli* flavin reductase yielded around 20mg of apparently pure enzyme and this was despite expression being minimised with the inclusion of the pLysE plasmid. The use of the pLysS plasmid would be more useful for obtaining large yields of enzyme for more detailed kinetic analysis or crystallography.

### **7.2. Protein concentration determination using the extinction coefficient of flavin reductase.**

The concentration of flavin reductase was determined spectrophotometrically at 280nm using the method described by Gill & Von Hippel, (1989). The extinction coefficient was calculated using the number of tyrosine, tryptophan and cysteine residues present and determining the optical density of the protein in water and 6M guanidine hydrochloride.  $\epsilon_{M,Nat}$  the extinction coefficient of flavin reductase in water was calculated to be 23,800 M<sup>-1</sup>cm<sup>-1</sup>.

### **7.3. Dependence of flavin reductase activity on the concentration of riboflavin, FMN, FAD, NADPH and NADH.**

Although the aim of purifying the flavin reductase was to investigate possible interactions with *E. coli* chorismate synthase a re-evaluation of the steady-state kinetics was thought to be necessary since earlier work with the enzyme was done using enzyme which was only 25% pure. The dependence of flavin reductase activity on the concentration of the substrates, riboflavin, FMN or FAD and on the concentration of cofactor, NADPH or NADH is shown in Figures 7.4, 7.5 and 7.6. The  $V_{max}$  of the enzyme with each of the flavins and cofactors was also determined. The purity of the enzyme in the previous study had been too low to permit these calculations. Comparison of the apparent  $K_m$ s obtained in this study with those of the previous study were in broad agreement but generally lower overall. The  $V_{max}$  of the enzyme was considerably greater than had been suggested in the earlier study as shown in Table 7.2 and reveals the enzyme to have a very high value for  $k_{cat}/K_m$ , the measure of catalytic efficiency.

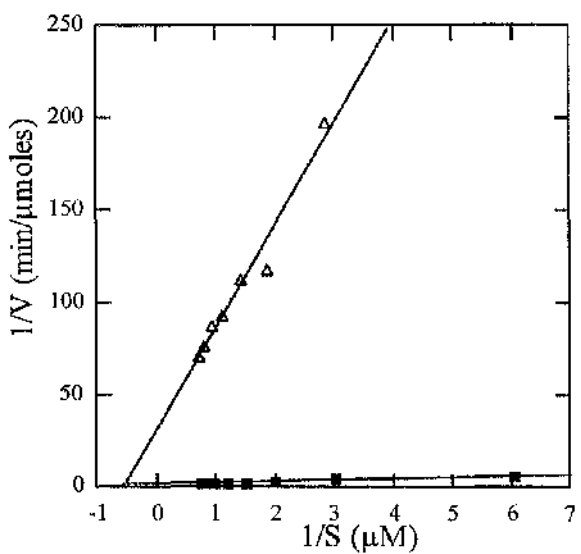


**Figure 7.4. Determination of apparent  $K_m$  for flavins with NADPH as reductant.**  
A double reciprocal plot showing the dependence of flavin reductase activity on the flavin concentration with 0.25mM NADPH. Standard assays were performed as described in 'Materials and Methods' with varying riboflavin (■) or FMN(Δ) concentration in 50mM Tris-HCl pH7.5. Assays were initiated with 0.13μg and 6.356μg of enzyme, respectively.

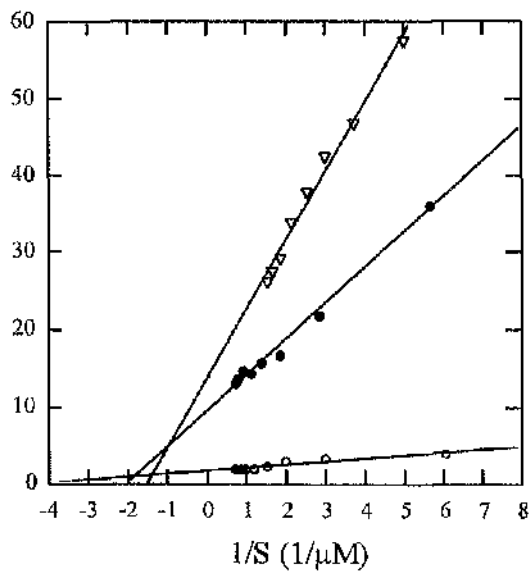


**Figure 7.5. Determination of apparent  $K_m$  for flavins with NADH as cofactor.** A double reciprocal plot showing the dependence of flavin reductase activity on the flavin concentration with 0.25mM NADH. Standard assays were performed with varying riboflavin (○), FMN (●) or FAD (Δ) concentration in 50mM Tris-HCl pH7.5. Assays were initiated with 0.13μg, 0.32μg and 0.64μg of enzyme, respectively.

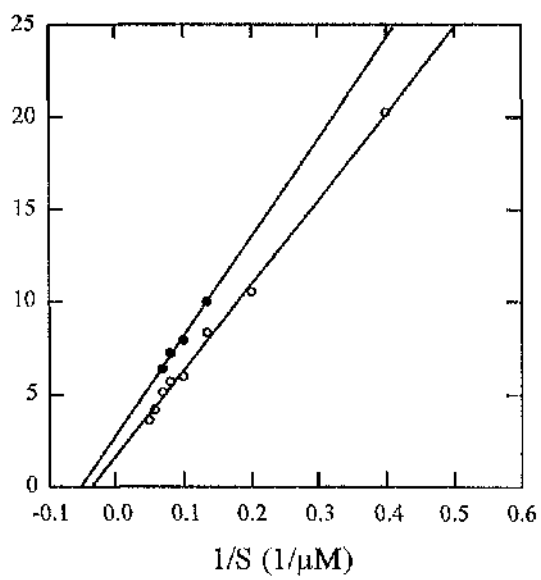


**Figure 7.6. Determination of apparent  $K_m$  for NADPH and NADH with riboflavin as substrate.** A double reciprocal plot showing the dependence of flavin reductase activity on the NADPH (○) or NADH (●) concentration with  $0.3\mu\text{M}$  riboflavin. Standard assays were performed as described in 'Materials and Methods' with varying NADPH or NADH concentration in 50mM Tris-HCl pH7.5. Assays were initiated with  $0.095\mu\text{g}$  of enzyme.

Substrate	Second substrate	Apparent K <sub>m</sub> (μM)	k <sub>cat</sub> (s <sup>-1</sup> )	k <sub>cat</sub> /K <sub>m</sub> (M <sup>-1</sup> s <sup>-1</sup> )	V <sub>max</sub> (Umg <sup>-1</sup> )
Riboflavin	NADH	0.23	42.1	1.8 x 10 <sup>8</sup>	96.4
FMN	NADH	0.51	25.5	5 x 10 <sup>7</sup>	58.4
FAD	NADH	0.67	17.0	2.5 x 10 <sup>7</sup>	38.9
Riboflavin	NADPH	0.96	76.5	7.97 x 10 <sup>7</sup>	175.2
FMN	NADPH	1.89	9.4	4.97 x 10 <sup>6</sup>	21.6
FAD	NADPH	-	-	-	-
NADH	Riboflavin	19.9	nd	nd	nd
NADPH	Riboflavin	28.4	nd	nd	nd

**Table 7.2. Kinetic parameters for flavins and pyridine nucleotides for *E. coli* flavin reductase.** nd indicates not determined.

#### 7.4. Molecular weight determination of flavin reductase.

The molecular weight (M<sub>r</sub>) of *E. coli* flavin reductase was measured by electrospray mass spectrometry as 26,115.00 ± 0.82 (Figure 7.7), consistent with the migration position observed with SDS-PAGE. The predicted M<sub>r</sub> of the enzyme from translation of the DNA sequence with the N-terminal methionine removed is 26,113. The N-terminal methionine was shown to be removed from the protein in the previous study of Spry *et al.* (1991).

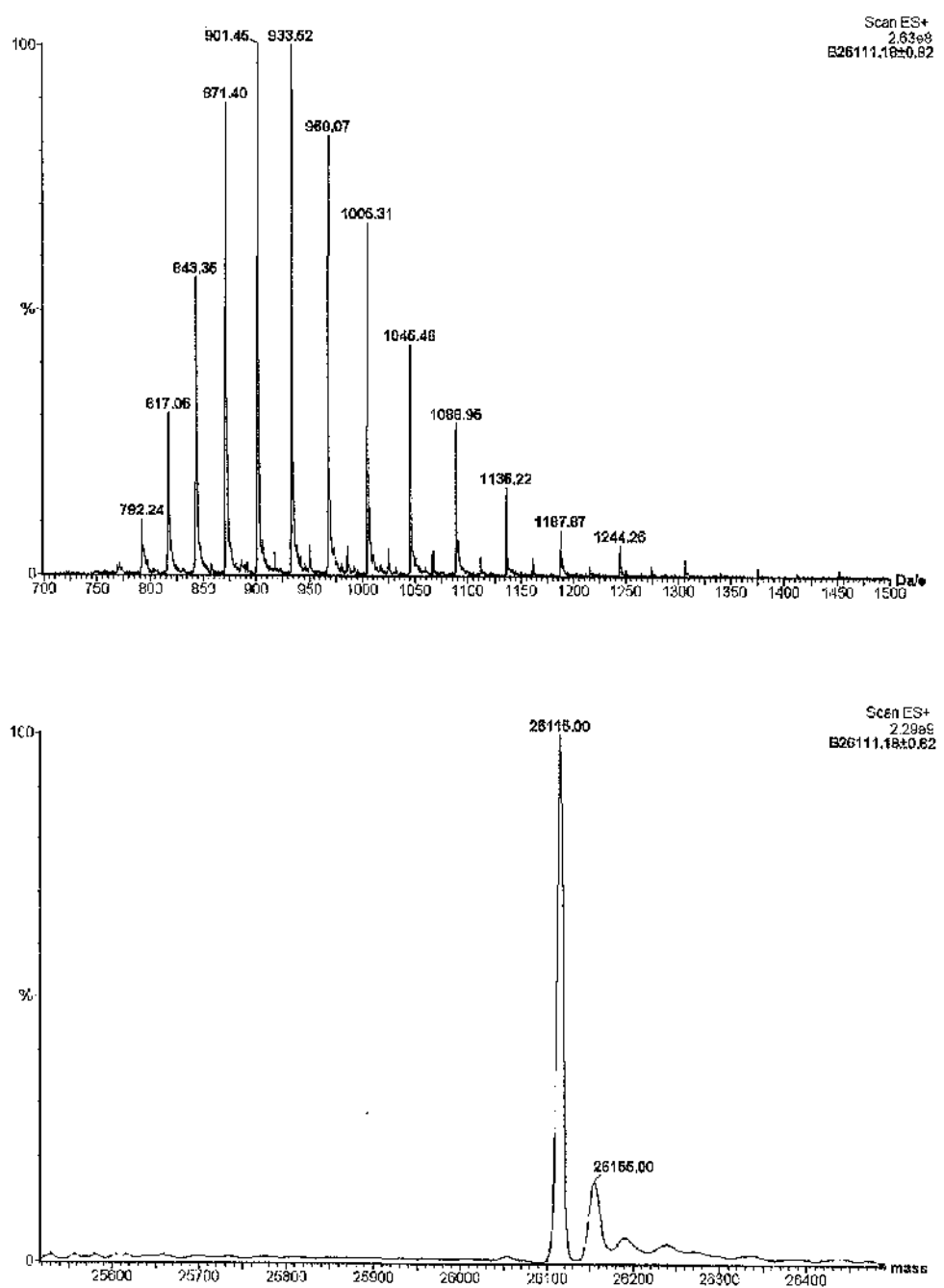


**Figure 7.7. Electrospray mass spectrum of *E. coli* flavin reductase.** The lower spectrum over the  $M_r$  range shown (25,500-26,500) was obtained using the MaxEnt deconvolution programme on the raw data (upper spectrum).

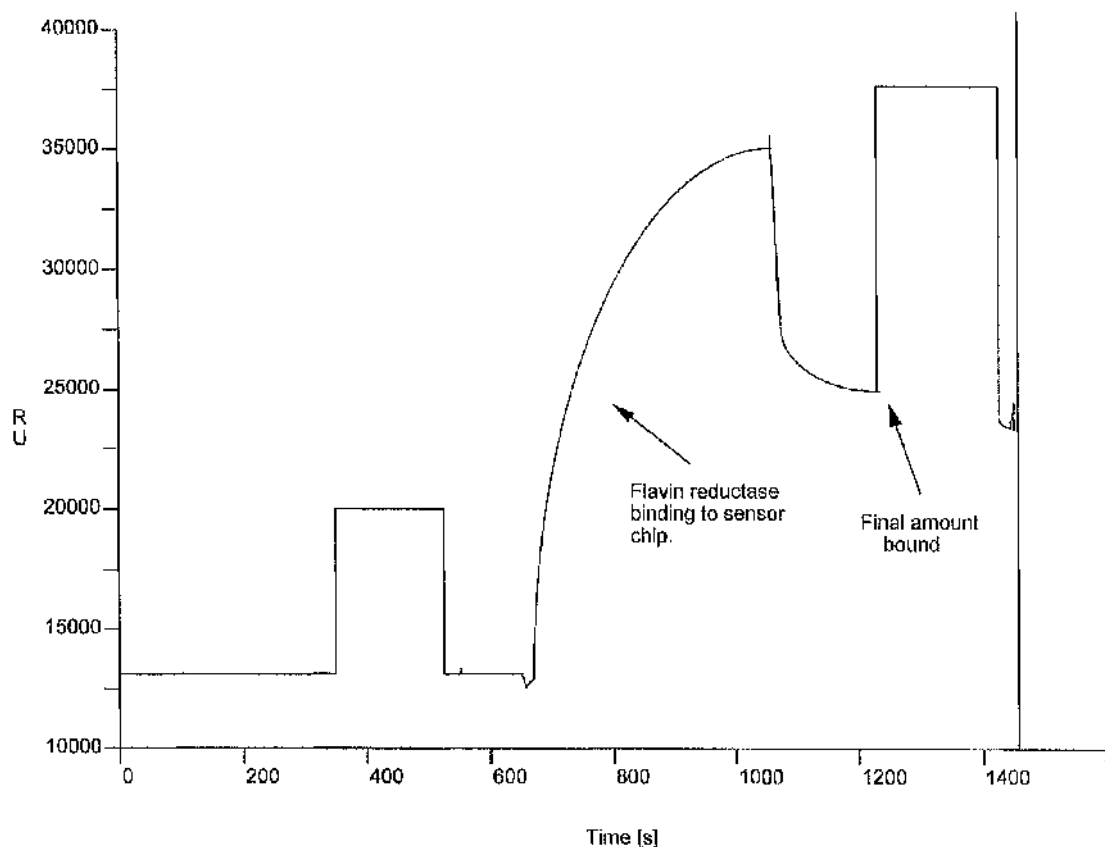


**Figure 7.8. BIAcore analysis.** Flavin reductase binding to the sensor chip with a corresponding increase in refractive units (RU) from 13,500 to 23,721.

### 7.5. Investigation for an interaction between flavin reductase and chorismate synthase.

*E. coli* flavin reductase was immobilised to the sensor chip using coupling buffer, sodium acetate pH 4.2, followed by washing of the chip with the same buffer (Figure 7.8). The final amount of enzyme that was bound corresponded to an increase of 10,221 refractive units. *E. coli* chorismate synthase was tested for binding (Figure 7.9) in the absence of any other ligand and in the presence of FMN, EPSP or NADH. The experiment was also repeated with chorismate synthase first immobilised onto the sensor chip and binding tested with flavin reductase. This reversed order produced essentially the same result. The lack of an increase in the number of refractive units after each addition of enzyme/and ligand (large increase in RU) and washing (drops back to start point) of the chip demonstrated the lack of any binding between the two enzymes.

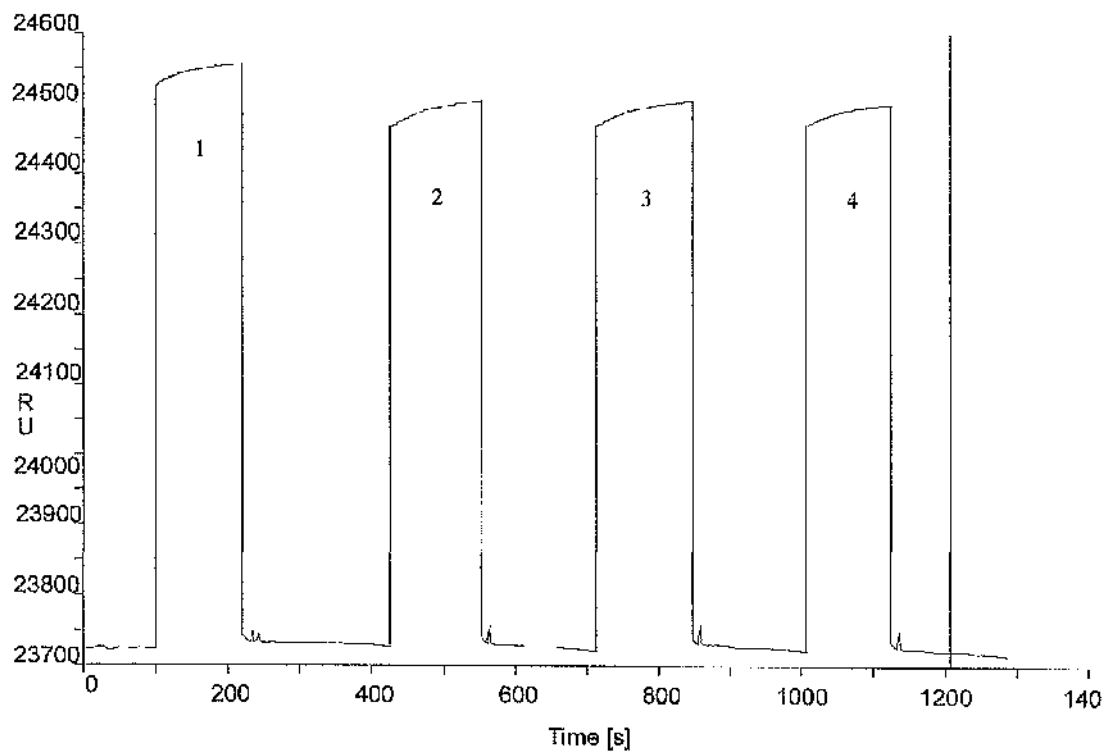


**Figure 7.9. BIAcore analysis.** Chorismate synthase ( $50\mu\text{M}$ ) was tested for binding to immobilised flavin reductase ( $50\mu\text{M}$ ) in the absence of any other ligands (1) and in the presence of stoichiometric amounts of FMN (2), EPSP (3) or NADH (4) relative to chorismate synthase.

#### 7.6. Chapter summary.

*E. coli* flavin reductase encoded by the *fre* gene was purified to homogeneity in three steps. Nearly 20mg of enzyme was obtained with a specific activity of  $183 \text{ Umg}^{-1}$  in the standard assay. This value was higher than that previously estimated for the enzyme from a partially pure preparation (Fontecave *et al.*, 1987). The  $K_m$  of the enzyme for riboflavin, FMN and FAD were very similar to those demonstrated in the same study. The subunit molecular mass of the enzyme was determined to be 26,115, which is consistent with a predicted mass of 26,113 from translation of the gene with the N-terminal methionine having been removed.

Biacore analysis was used to demonstrate that *E. coli* chorismate synthase does not interact intimately with the *E. coli* flavin reductase encoded by the *fre* gene. This confirms that *E. coli* chorismate synthase does not require intimate contact with this, the main, flavin reductase to obtain reduced flavins.

---

**CHAPTER 8. GENERAL DISCUSSION.**

---

The aim of this project was to clone the gene encoding chorismate synthase from the pathogen *Staphylococcus aureus* and subsequently express the encoded protein to high levels for purification. Thereafter the enzyme would be investigated kinetically with both steady-state and pre-steady-state techniques in order to compare the pure enzyme with other chorismate synthases studied to date. As detailed in the preceding chapters the gene encoding chorismate synthase was cloned together with the gene encoding nucleoside diphosphate kinase and two partial open reading frames encoding regions of 3-dehydroquinate synthase and a heptaprenyl pyrophosphate synthetase. Chorismate synthase was successfully purified to near homogeneity and was studied kinetically in some detail.

The *aroC* gene encoding chorismate synthase and the *ndk* gene encoding nucleoside diphosphate kinase were cloned from a clinical isolate of *Staphylococcus aureus* by complementation of the Aro<sup>-</sup> phenotype of the *aroC E. coli* strain, GLW40. The genes were isolated on a 5.5kb *Cla*I restriction fragment forming plasmid pMJH701. This plasmid was also found to complement the Aro<sup>-</sup> phenotype of the *aroA E. coli* strain AB1321. Subsequent restriction mapping of pMJH701 and its comparison with pCOC102 demonstrated that it contained the complete *aroC* gene and the complete *aroA* and *aroB* genes which had been identified previously (O'Connell *et al.*, 1993). A 2.5kb *Nde*I-*Cla*I restriction fragment from pMJH701 which was expected to contain the *aroC* gene was cloned to form pMJH702 and the complete nucleotide sequence of this was determined.

Sequencing of pMJH702 confirmed the presence of the complete coding sequence for chorismate synthase and revealed that the complete open reading frame for nucleoside diphosphate kinase was located around 500bp upstream from the *aroC* gene. In addition two partial open reading frames (ORFs) were contained within pMJH702. The 5' end of an ORF which had similarity with the *aroB* gene, encoding 3-dehydroquinate synthase, of *B. subtilis* was located immediately downstream of the *aroC* gene. Immediately upstream from the *ndk* gene was the 3' end of a second partial ORF, the translated product of which had similarity with the putative *gerCC* gene product from *B. subtilis*.

The low G+C content of the sequenced DNA was consistent with the value of 33% determined for the *S. aureus* chromosome (de Ley, 1970) and the codon usage pattern of the *aroC* and *ndk* genes was also consistent with the low G+C content. The codon usage further supported observations made with *E. coli* and *B. subtilis*. In these bacteria more highly expressed genes are observed to display a non-random pattern of codon usage, utilising a restricted set of codons that are recognised by the major species of isoacceptor tRNAs, whereas genes expressed at low levels display a random codon usage pattern (Grantham *et al.*, 1981; Ikemura & Ozeki, 1983). The AUA codon (isoleucine) is rarely used in highly expressed genes in *E. coli* and *B. subtilis*. The gene encoding nucleoside diphosphate kinase is known to be highly expressed in the organisms in which it has been studied and the *S. aureus* *ndk* gene contains no AUA codons (0 of 12) while *aroC* contains 5 (of 35) AUA isoleucine codons. The gene encoding chorismate synthase belongs to the group of lowly expressed genes.

Promoter region	-35	-10
pT181 <i>repC</i>	ATTAGA	TGTTAT
pT181- <i>ct</i>	TCTTGA	TTTAAT
pT181 <i>pre</i>	TATTAA	TAGACT
pT181 <i>tet</i>	AGCGAA	AACAAA
<i>agr-P2</i>	TAATGA	TCGTAT
pI258 <i>blaZ</i>	TTGACA	TATTAT
<i>spa</i>	TTGCAA	TATGAT
<i>hla</i>	TTGATT	TATTTT
<i>aroC</i>	ATGAAT	TATTAT
<i>ndk</i>	TTGAAA	TAATAAT
<i>E. coli</i> consensus $\sigma^{70}$	TTGACA	TATAAT
<i>B. subtilis</i> consensus $\sigma^A$	TTGACA	TATAAT

Taken from Novick (1990).

Table 8.1. *Staphylococcus aureus* promoter regions.

Putative promoter sequence elements and ribosome binding sites were located upstream from both the *aroC* and *ndk* genes. Novick, (1990) reported a variety of sequences corresponding to -35 and -10 promoter regions for *S. aureus*. Many of these were from plasmid encoded genes with few being chromosomally encoded. The putative promoter sequence elements identified in this study matched more closely those obtained for chromosomally encoded genes and were also similar to the -35 and -10 consensus regions of *E. coli*  $\sigma^{70}$  and *B. subtilis*  $\sigma^A$  promoters (Table 8.1).

In *S. aureus* the *aroC* gene is likely to form the first gene in an operon which includes the *aroB* and *aroA* genes. Evidence to support this includes, firstly, the demonstration by O'Connell *et al.*, (1993) that temperature sensitive plasmids which were forced to integrate into the chromosome 5' to *aroA* produced an Aro<sup>-</sup> phenotype. Secondly, in this study a putative consensus promoter was identified 5' to the *aroC* gene while no such sequences were observed 5' to the *aroB* gene (this study) or the *aroA* gene (O'Connell *et al.*, 1993). A further piece of evidence which may support an *aroCaroBaroA* operon in *S. aureus* comes from a comparison with the gene organisation of the *B. subtilis* chromosome. In *B. subtilis* the *aroF*, *aroB* and *aroH* genes encoding chorismate synthase, dehydroquinate synthase and chorismate mutase, respectively, form the start of an *aro-trp-aro* 'supraoperon' of thirteen genes concerned with the biosynthesis and transport of aromatic amino acids. In the absence of tryptophan the *aroFaroBaroH* genes are transcribed as a unit (Henner & Yanofsky, 1993). This *aro* operon is preceded by the *cheR* and *ndk* genes and the *gerCAgerCBgerCC* operon. In this study the *ndk* gene and the *gerC* genes of *S. aureus* were located upstream from the *aroC*, *aroB* and *aroA* genes. As shown in Figure 8.1 there are obvious similarities in gene organisation in these regions of the *S. aureus* and *B. subtilis* chromosomes. This similarity in gene organisation between the two organisms may also extend to transcription of the genes such that the *S. aureus* *aro* genes are also transcribed as a unit.

Physical mapping experiments with *S. aureus* have shown that *aroA* (and thus *aroB* and *aroC*) are linked to *tyrB* (O'Connell *et al.*, 1993) while the *trp* operon is linked to *tyrA* which maps some distance from *tyrB* (Pattee, 1981). The *cheR* gene which is situated between *ndk* and *aroF* in *B. subtilis* was not observed in *S. aureus*. The *cheR* gene encodes a receptor-methylating enzyme involved in motility and transfers methyl groups from S-adenosylmethionine (SAM) to the methylation chemotaxis proteins. *S. aureus* is a non-motile organism and the absence of the *cheR* gene is likely to reflect this.

Although there is no similar *aro-trp-aro* 'supraoperon' in *S. aureus* it has been demonstrated in this study that the *ndk* genes and the *gerCAgerCBgerCC* genes are situated upstream from the *aroC**aroB* genes as is observed in *B. subtilis*.

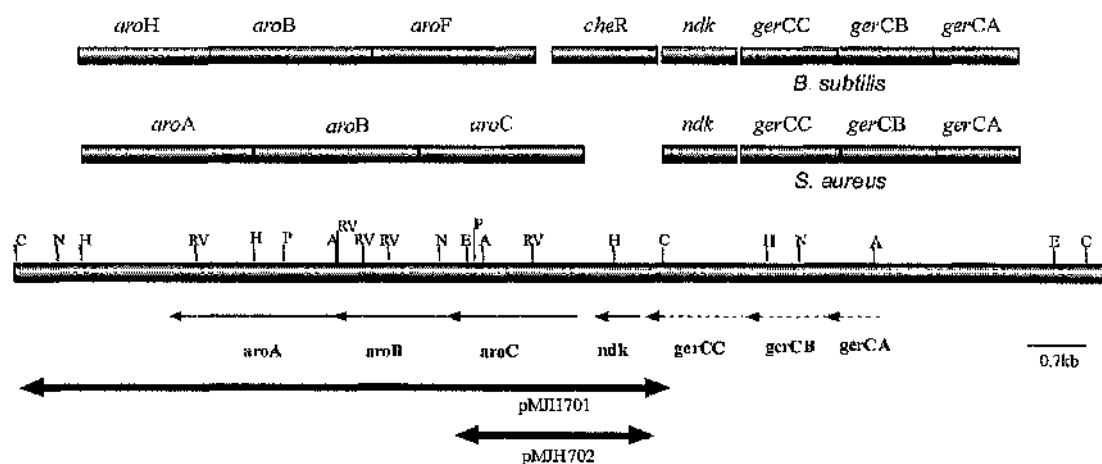


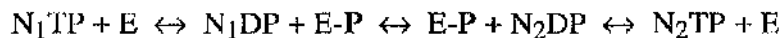
**Figure 8.1. Schematic diagram representing a map of the *gerC*, *ndk*, *aro* region of the *S. aureus* chromosome.** The positions of the *ndk* and the *aro* genes were determined from the DNA sequencing data obtained in this study and from the previous work of O'Connell *et al.* (1993). The positions of the *gerC* genes are shown by dashed arrows indicating approximate locations based on hybridisation analysis data obtained in this study and using the sizes of the *B. subtilis* genes (Henner *et al.*, 1986). The map also indicates the positions of the inserts of pMJH701 and pMJH702. The restriction enzymes are abbreviated as follows: A, *Acl*; C, *Clal*; E, *EcoRI*; RV, *EcoRV*; H, *HindIII*; N, *NdeI*; P, *Pst* I.

The observed linkage between the *gerC* and the *aro* genes in *S. aureus* and *B. subtilis* may have a functional explanation. The *gerCC* gene of *B. subtilis* has 65% identity with an open reading frame (ORF3) in *Bacillus stearothermophilus* which encodes heptaprenyl pyrophosphate synthetase (Koike-Takeshita *et al.*, 1995). This heptaprenyl pyrophosphate synthetase has been demonstrated to be involved in the synthesis of the polyprenyl side-chain of menaquinone in this organism (Koike-Takeshita *et al.*, 1995; Takahashi *et al.*, 1980). The high level of identity observed between the genes from *B. subtilis* and *B. stearothermophilus* suggests that the *gerCC* gene of *B. subtilis* similarly encodes the heptaprenyl pyrophosphate synthetase involved in menaquinone

biosynthesis. Since menaquinone biosynthesis is a post-chorismate pathway the close linkage of the *gerC* genes and the *aro* genes may reflect the greater clustering of aromatic pathway genes in these organisms. It would be of interest to determine whether the *gerC* genes of *B. stearothermophilus* are located upstream of *aro* genes.

The *S. aureus* *ndk* gene encodes a protein with a high level of identity to other known Ndk sequences. The *ndk* gene belongs to the class of highly biased genes in *E. coli* and is highly expressed in all of the bacteria in which it has been studied. It is the only enzyme responsible for the phosphorylation of nucleotides other than ATP in *Salmonella typhimurium* (Ginther & Ingraham, 1974). The initiating methionine codon of the *S. aureus* *ndk* gene was found to be GUG. In *E. coli* the use of a non-AUG codon serves to limit expression of a gene at the translational level. However, this situation does not appear to be reflected in *B. subtilis* and other clostridial branch Gram-positive organisms where nearly 30% of genes have non-AUG initiation codons. Instead it has been suggested that translational efficiency is controlled more by the strength of the Shine-Dalgarno (SD) sequence and as strength of the SD sequence increases differences between AUG, GUG and UUG in terms of translational efficiency is moderated (Vellanoweth, 1993). Consequently the ribosome binding site of the *S. aureus* *ndk* gene may be of more importance to translational efficiency than the GUG codon.

Nucleoside diphosphate (NDP) kinases are ubiquitous enzymes that catalyse the transfer of the  $\gamma$ -phosphate of nucleoside triphosphates to nucleoside diphosphates. These enzymes show very little specificity for the base and the sugar. Any ribonucleotide triphosphate (NTP), deoxyribonucleotide triphosphate, ribonucleotide diphosphate (NDP) or deoxyribonucleotide diphosphate can be used as a substrate. The reaction is reversible and occurs in two steps (ping-pong mechanism), with the formation of a phosphoenzyme intermediate (Parks & Agarwal, 1973; Almala et al., 1995).



The primary role of NDP kinase in the cell has been suggested to be the maintenance of a pool of nucleotide triphosphates for the synthesis of DNA and RNA. Furthermore, NDP kinase has been reported to be the only enzyme responsible for catalysing this reaction in *Salmonella typhimurium* (Ginther & Ingraham, 1974) and has also been found to be essential in *Myxococcus xanthus* (Muñoz-Dorado et al., 1990a,b). The *Drosophila awd* gene involved in larval development encodes an NDP kinase (Rosengard et al., 1989).

The enzyme has been implicated as a tumour suppressor candidate in studies of proliferating malignant human cells. NDP kinases have been reported to be associated with protein complexes *in vivo* and are believed to participate in the DNA replication machinery. NDP kinase has been found to be present in highly purified bacterial DNA polymerase preparations (Miller & Wells, 1971) and was reported to associate with ribonucleotide reductase (Allen *et al.*, 1983). NDP kinase has also been proposed as a novel protein kinase without sequence similarities to the classical protein serine-threonine kinases (Hanks *et al.*, 1988).

The crystal structure of *Myxococcus xanthus* nucleoside diphosphate kinase has been determined (Williams *et al.*, 1993) and would allow modelling of the *S. aureus* sequence. The *E. coli* enzyme has been modelled based on the *M. xanthus* structure and utilising the high identity that exists between Ndk enzymes (Almaula *et al.*, 1995).

The original observation that *aro* mutants of salmonellae were avirulent and conferred protection against challenge with a virulent strain has led to the production of *aro* mutants in a variety of bacterial species which are attenuated and stimulate protective immunity. To date these include: *Salmonella typhimurium* (Hoiseth & Stocker, 1981), *Salmonella typhi* (O'Callaghan *et al.*, 1988), *Salmonella choleraesuis* (Nhalue & Stocker, 1987), *Shigella flexneri* (Verma & Lindberg, 1991), *Bordetella pertussis* (Roberts *et al.*, 1990), *Yersinia enterocolitica* (Bowe *et al.*, 1989) *Aeromonas salmonicida* (Vaughan *et al.*, 1993) and *Bacillus anthracis* (Ivins *et al.*, 1990).

The production of an *aro* mutant of *Staphylococcus aureus* which was attenuated and which stimulated protection against challenge with a virulent strain would have obvious commercial benefit. The ever increasing problem of methicillin resistant *Staphylococcus aureus* (MRSA) strains in hospitals has significantly added to the spread of antibiotic resistance and reduced the number of antibiotics which can be used to successfully treat infected patients. In addition, the problem of staphylococcal mastitis is of concern to the dairy industry and efforts to produce a vaccine could significantly reduce the problem.

O' Connell *et al.* (1993) isolated *S. aureus* *aroA::Tc<sup>r</sup>* insertion mutants in an attempt to obtain attenuation of strain 8325-4. They succeeded in isolating an allelic replacement mutant which required aromatic amino acids for growth, however, the strain was able to grow in the absence of PABA. Integration of *aroA* deletion plasmids into the chromosome of strain 8325-4 produced a PABA and aromatic amino acid dependent

phenotype. These strains were unsuitable for *in vivo* virulence and growth experiments and were very unstable reverting at high frequency. The authors suggested that the inability to isolate stable replacement mutants which were PABA and aromatic amino acid dependent was possibly the result of such an insertion mutant being lethal. This is unprecedented to date for the pre-chorismate pathway. However, there is the possibility that some uncharacterised essential metabolic pathway that is required for growth branches from chorismate in *S. aureus*.

The characterisation of the *aroC* gene in this study, which is likely to form the first gene in an operon with *aroB* and *aroA*, would allow a further study of the ability to produce attenuation of *S. aureus* using *aro* mutants. It would be of very great interest to determine if the failure of O'Connell *et al.* (1993) to obtain stable PABA and aromatic amino acid dependent mutants was a consequence of an uncharacterised essential metabolic pathway or merely the instability of the integration mutants produced. There would now also be the possibility of producing integration mutants in multiple *aro* genes albeit at the same locus.

The *S. aureus aroC* gene was found to be expressed in *E. coli* presumably from a promoter on the inserts of both pMJH701 and pMJH702. Since the level of expression was poor the gene was amplified using the polymerase chain reaction (PCR) to facilitate its cloning, optimally spaced, downstream from the T7 promoter on pTB361. The *aroC* strain of *E. coli* was successfully lysogenized with the  $\lambda$ DE3 phage to produce a chorismate synthase free background for expression. This expression system resulted in the accumulation of very high levels of soluble *S. aureus* chorismate synthase. The N-terminus and an internal region of the enzyme were sequenced and found to match that predicted from the gene sequence. Chorismate synthase from *S. aureus* was purified to near homogeneity, producing 100mg of enzyme from 13g of cells. This quantity of enzyme was necessary for its analysis using steady-state and pre-steady-state kinetics and has allowed initial but as yet unsuccessful attempts at crystallising the enzyme.

The sequenced *S. aureus aroC* gene was found to encode a polypeptide of 388 amino acids with a predicted  $M_r$  of 43,027 as calculated by the PEPTIDESORT program of the GCG package, similar to the  $M_r$  of 43,024  $\pm$  3.8 determined for overexpressed chorismate synthase by electrospray mass spectrometry. The amino acid sequence of *S. aureus* chorismate synthase was found to have 61% identity (78% similarity) with the putative *aroF* gene product from *B. subtilis* and 37% identity (57% similarity) with chorismate synthase from *E. coli*. Little attention has been paid to the sequence from *B.*

*subtilis* previously due to its lower identity when compared with other chorismate synthases (excluding *S. aureus*) which typically share upwards of 50% identity (70% similarity) with each other.

Comparison of the *B. subtilis* and *S. aureus* sequences with the other chorismate synthases suggested that these two species may form a different sequence group, illustrated by the dendrogram produced from the PILEUP program of the GCG package (Figure 3.7). The formation of a separate sequence group was also supported using immunological analysis. Antibodies raised against chorismate synthase from *E. coli* and/or *Corydalis sempervirens* have been shown to possess strong inter-species cross-reactivity with chorismate synthases from higher plants, fungi and bacteria (Schaller *et al.*, 1990, 1991a,b; Schmidt *et al.*, 1993; Henstrand *et al.*, 1995b). This immunological cross-reactivity between the chorismate synthases has been reasoned to indicate that antigenic determinants of these enzymes were highly conserved during evolution (Schaller *et al.*, 1991a). This study, in contrast, has demonstrated that there was no detectable immunological cross-reactivity between *S. aureus* chorismate synthase and antibodies raised against *E. coli* chorismate synthase. While this indicates that there are structural differences between the chorismate synthases from *S. aureus* and *E. coli* the two enzymes must share essential functional identity since the *aroC* gene from *S. aureus* was cloned using its ability to complement an *aroC* strain of *E. coli*.

The subunit structure of *S. aureus* chorismate synthase was determined using both gel filtration and cross-linking with dimethyl-suberimidate. Both of these techniques demonstrated that the enzyme exists as a homotetramer. This subunit structure was also observed for the monofunctional *E. coli* chorismate synthase and the bifunctional *N. crassa* chorismate synthase (White *et al.*, 1988). Both the *B. subtilis* (Hasan & Nester, 1978b) and the *E. gracilis* enzymes (Schaller *et al.*, 1991a) have been suggested to be trimers with associated flavin reductase activity (not bifunctional) although in the latter case this has yet to be confirmed. Chorismate synthase from *Corydalis sempervirens* has been observed to be a homodimer, and it was suggested that this may be a consequence of interaction between chorismate synthase and a putative flavin reductase present in the plastid (Henstrand *et al.*, 1995a). This subject will be discussed further later.

The pH optimum determined for *S. aureus* chorismate synthase was found to be non-symmetrical in MOPS buffer with an optimum of activity around pH 7.0. Other chorismate synthases studied to date have been shown to have a pH optimum around

pH8 (Table 8.2) and their more symmetrical bell shaped profile taken as evidence that catalysis was not dependent on a single ionisable group (Fersht, 1985; Ramjee, 1992). This experiment with *S. aureus* chorismate synthase was designed merely to determine the optimum pH for activity and was not aimed at identifying possible groups involved in catalysis. Nevertheless, it is interesting to note the profile obtained and if time had permitted the  $V_{max}$  values for the enzyme across the pH range shown could have been determined with the aim of trying to measure the  $pK_a$  value of the amino-acid side chain(s) involved in catalysis. The  $pK_a$  of MOPS buffer is 7.15 at 25°C and as such this buffer solution only has useful buffer action in a range of one pH unit on either side of this value. A more detailed study would have typically involved a combination of buffers or the use of buffers of constant ionic strength to minimise possible buffer effects.

It should be noted that the pH dependence observed for *S. aureus* chorismate synthase activity may reflect the partial or complete ionisation of either the substrate or cofactor at the various pH values (Fersht, 1985). The interaction between the enzyme and substrate/cofactor might then have been altered such that this was the effect being observed.

*S. aureus* chorismate synthase was observed to exhibit maximum activity with reduced FMN as cofactor. FAD and riboflavin were capable of substituting FMN as cofactor but produced lower levels of activity than FMN, 13% and 2.4% respectively. This preference is common to all of the chorismate synthases which have been studied to date and in *N. crassa* and *B. subtilis* may reflect the properties of the associated flavin reductase. The *S. aureus* enzyme, while similar to other chorismate synthases with regard to its preferred flavin, exhibited considerably lower levels of activity with FAD and riboflavin. A comparison of the *E. gracilis*, *N. crassa*, *C. sempervirens* and *E. coli* chorismate synthases revealed activities for FAD and riboflavin relative to FMN of 73-84% and 14-39%, respectively when dithionite was used as reductant (Schaller *et al.*, 1991a). These values are around 6 times greater than the *S. aureus* enzyme.

Property	<i>E. gracilis</i>	<i>N. crassa</i>	<i>C. semperflorens</i>	<i>E. coli</i>	<i>B. subtilis</i> <sup>1</sup>	<i>S. aureus</i> <sup>2</sup>
Apparent K <sub>m</sub> (EPSP)	27μM	2.7μM	53μM	1.8μM <sup>3</sup>	nd	12.7μM
Apparent K <sub>m</sub> (FMN)	76nM	66nM	37nM	-	12.5μM	4.8μM
Cofactor specificity	FMN>FAD	FMN>FAD	FMN>FAD	FMN>FAD	FMN>FAD	FMN>FAD
Flavin reductase	Present	Present	Absent	Absent	Present	Absent
Apparent K <sub>m</sub> (NADPH)	7.4μM	21.4μM	-	-	78.5μM	-
M <sub>r</sub> (native)	110-138kD	198kD	80.1kD	162kD <sup>3</sup>	nd	182-186kD
M <sub>r</sub> (subunit)	41.7kD	46.4kD <sup>4</sup>	41.9kD	39.0kD <sup>3</sup>	39.9kD	43.0kD
No. of subunits	nd	4	2	4	3	4
isoelectric point	5.5	4.9	5.0	6.45 <sup>3</sup>	5.5	5.9
pH optimum	8.2	8.1	8.0	7.5-8.0 <sup>3</sup>	nd	7.0

nd, not determined.

**Table 8.2. Comparison of the properties of chorismate synthases studied to date.<sup>5</sup>**

The apparent K<sub>m</sub> for EPSP of the *S. aureus* enzyme in MOPS buffer pH 7.0 was determined to be 12.7 ± 0.5μM. This value is in accordance with the other chorismate synthases studied (see Table 8.2). The enzyme may also be substrate inhibited as evinced by the slight curvature in the points of the Lineweaver-Burke plot at low values of 1/S (Figure 5.8). This effect was also observed with the *C. semperflorens* and *E. gracilis* enzymes (Schaller *et al.*, 1991a). The apparent K<sub>m</sub> for FMN of the *S. aureus* enzyme in the same buffer was calculated to be 4.8 ± 0.5μM. This contrasts with apparent K<sub>m</sub> values for FMN of 76nM, 66nM, and 37nM for the *E. gracilis*, *N. crassa* and *C. semperflorens* enzymes, respectively. These are two orders of magnitude lower than the *S. aureus* enzyme.

<sup>1</sup> Hasan & Nester, 1978a,b.

<sup>2</sup> This study.

<sup>3</sup> Ramjee, 1992.

<sup>4</sup> Henstrand *et al.*, 1995b.

<sup>5</sup> Taken from Schaller *et al.*, 1991

Chorismate synthase from *E. coli* has been studied using pre-steady-state kinetics in an effort to obtain more information about the rates of individual steps on the enzyme reaction pathway and to detect transient intermediates. Kinetic studies under steady-state conditions reveal only very limited information and give an idea of rate constants for the slowest step only (Fersht, 1985). *S. aureus* chorismate synthase was investigated using pre-steady state kinetics. This work was not aimed at producing an in-depth analysis of the pre-steady state kinetics of the *S. aureus* enzyme but was instead more of a comparative exercise.

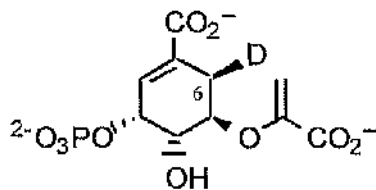
A feature of the work performed previously with *E. coli* chorismate synthase was the identification of transient absorbance changes during turnover. A difference spectrum of an enzyme-bound intermediate during the conversion of EPSP to chorismate was determined (Figure 1.4)(Ramjee *et al.*, 1991). The changes in the absorbance spectrum of FMNH<sub>2</sub> were reasoned to be consistent with the formation of a flavin-C4 adduct and a charge transfer complex. This was the first demonstration of the intimate involvement of the flavin cofactor in the catalytic cycle of a chorismate synthase although the exact nature of the intermediate is still unclear.

The *S. aureus* chorismate synthase reaction was investigated using rapid-scanning stopped-flow spectrophotometry to determine if similar transient absorbance changes were observed during EPSP turnover. A flavin intermediate was observed during turnover and the difference spectrum of this resembled that obtained with the *E. coli* enzyme. The spectral characteristics of the *S. aureus* flavin intermediate were different with respect to its maxima, minima and its overall shape (cf. Figures 1.4 & 5.9). However, in agreement with the *E. coli* enzyme was the absence of an increase in the amplitude at 580nm confirming that FMN semiquinone was not formed at detectable levels during turnover.

Single wavelength (390nm) stopped-flow experiments were carried out to more accurately measure the kinetics of the intermediate for comparison with the *E. coli* enzyme. This was complicated with the finding that the rate of formation of the intermediate was dependent on the substrate concentration (Figures 5.11, 5.12). Consequently, the rates of formation and decay could not be simply described by fitting two exponentials to the data without the introduction of large errors in the rate values. However, it was found that the latter part of flavin intermediate decay could be fitted to an exponential. This gave a rate ( $6.5\text{s}^{-1}$ ) (Figure 5.11) which was eight times slower

than that observed for the *E. coli* enzyme ( $52\text{s}^{-1}$ ) (Bornemann *et al.*, 1995) and this compares well with a 7 fold lower  $V_{\max}$ .

A further comparison of the kinetics of the *S. aureus* enzyme with the *E. coli* enzyme was carried out using analogues of EPSP under steady-state conditions and monitoring the formation of the product diene. As a means of investigating the reaction mechanism of both the *N. crassa* chorismate synthase and the *E. coli* chorismate synthase deuterated analogues of EPSP have been used.



(6R)-[6<sup>2</sup>H]EPSP

Primary kinetic isotope effects, which result from the cleavage of the bond to the atom which has been isotopically substituted, have been observed with both enzymes using (6R)-[6<sup>2</sup>H]EPSP. The presence of this primary kinetic isotope effect indicates that cleavage of the C-(6*pro*R)H bond of EPSP is rate limiting. A moderate primary kinetic isotope effect of  $\delta_{\text{pro}}\text{R}^2\text{HV}=2.7\pm 0.2$  for the *N. crassa* enzyme (Balasubramanian *et al.*, 1990) and a small and insignificant, primary kinetic isotope effect of  $\delta_{\text{pro}}\text{R}^2\text{HV}=1.13\pm 0.03$  for the *E. coli* enzyme (Bornemann *et al.*, 1995) have been detected. The *S. aureus* enzyme was investigated with quadruplicate assays and a very small kinetic isotope effect of  $\delta_{\text{pro}}\text{R}^2\text{HV}=1.02\pm 0.06$  was obtained. Further assays would be required to confirm this value given the error associated with the isotope effect. However, it would appear that there is no significant primary kinetic isotope effect associated with the *S. aureus* enzyme indicating that C(6)-H bond-breaking is not rate-limiting. The large value, by comparison, associated with the *N. crassa* enzyme may be a consequence of the bifunctional nature of this enzyme and may indicate that C-H bond breaking at the C-6 position is rate limiting with this particular enzyme.

The *S. aureus* enzyme was titrated with EPSP in the presence of approximately stoichiometric amounts of oxidised flavin and was found to bind one molecule of EPSP per subunit. Furthermore, the enzyme was observed to bind oxidised flavin both in the presence and absence of EPSP. The spectral characteristics of oxidised flavin were altered upon binding by the *S. aureus* enzyme. This contrasts with the *E. coli* enzyme which does not bind oxidised flavin as judged by the absence of spectral changes to the flavin upon addition of enzyme. As a consequence of the *S. aureus* chorismate synthase binding oxidised flavin the  $K_D$  for FMN<sub>ox</sub> was calculated. A value of  $K_D$ FMN<sub>ox</sub> = 7.15μM was determined and in the presence of 50μM EPSP this was reduced to 2.42μM. The presence of EPSP thus enhances the binding of FMN to the enzyme.

Further comparisons of *S. aureus* chorismate synthase with the *E. coli* enzyme were carried out with respect to flavosemiquinone formation. FMN bound to the *E. coli* enzyme has been observed to form a radical under conditions where EPSP was added to enzyme with reduced flavin bound. Similarly, a flavosemiquinone is formed under conditions where FMN is photoreduced when bound to the enzyme in the presence of (6R)-6F-EPSP (P. Macheroux, unpublished). A flavin radical was correspondingly detected when each of these experiments were performed using the *S. aureus* enzyme. There is as yet no explanation for the observation of this radical with EPSP and 6R-6F-EPSP other than the fact that the ligand is perturbing the FMN redox potential. In the case of EPSP it is not known whether the radical would be formed *in vivo*. Although the flavin radical can not yet be explained its observation during experiments with both the *E. coli* and the *S. aureus* enzymes suggests that it may be a feature of all chorismate synthases.

The chorismate synthase reaction is unusual due to its absolute requirement for a reduced flavin cofactor despite the absence of an overall change in redox state. As a means of further investigating the binding of reduced flavin to the *S. aureus* chorismate synthase site-directed mutagenesis was used. The possibility of using site-directed mutagenesis to analyse the enzyme was limited by the lack of structural information. However, examination of a number of flavoproteins using both crystallography and site-directed mutagenesis has demonstrated the involvement of residues, which are usually hydrophobic and often aromatic, in the binding of FMN (Shen *et al.*, 1989; Porter, 1991; Klein & Fulco, 1993; Oster *et al.*, 1991). These residues which are located above and below the isoalloxazine ring, help to maintain a hydrophobic environment for the flavin and may participate in stacking interactions with the isoalloxazine ring. In rat liver NADPH cytochrome P-450 oxidoreductase two tyrosine residues are involved in

binding of FMN to the protein (Shen *et al.*, 1989). The replacement of Tyr-148 in this enzyme with aspartate completely abolished FMN binding and cytochrome c activity. Replacement of Tyr-148 with the conservative replacement, phenylalanine did not substantially affect activity. Similarly crystallographic analysis of *Desulfovibrio vulgaris* flavodoxin has demonstrated the involvement of both tyrosine and tryptophan residues in binding FMN (Porter & Kasper, 1985).

The mutagenesis of tyrosine 121 of *S. aureus* chorismate synthase (130 in multiple sequence lineup, Figure 3.6) was therefore based upon the premise that tyrosine residues are known to be important for flavin binding in a number of flavin-cofactor requiring enzymes. Furthermore, a comparison of the chorismate synthase sequences known to date revealed only one completely conserved tyrosine residue. There are no tryptophan residues in *S. aureus* chorismate synthase. The conserved tyrosine was replaced with phenylalanine or alanine, using PCR, producing the two mutants Y121F and Y121A. The purification of these two mutants was hampered by precipitation after fractionation on DEAE-sephacel and their successful purification may ultimately require a different strategy from that of the wild-type. However, the enzymes were observed to be present in the soluble, supernatant fraction during crude extract preparation and this allowed the specific activities of the mutant enzymes to be demonstrated in an unpurified state. The phenylalanine mutant, Y121F was found to have around 10% activity compared to the 'wild-type' while the specific activity of the alanine mutant proved very difficult to measure in crude extracts but was determined to be at most 1% that of the 'wild-type'. A feature of the Y121A mutant was the dramatically less-yellow colour of the crude extract when compared to the 'wild-type' possibly indicating that less flavin was bound to the this mutant enzyme. The Y121F mutant crude extract was not visibly less yellow than the 'wild-type' although no absolute values for flavin absorbance were obtained for any of these enzymes.

While it may appear that the mutagenesis of tyrosine-121 of *S. aureus* chorismate synthase has altered flavin binding it is stressed that a more thorough analysis of these mutants would be required before such claims could be confirmed. There was an obvious effect on the activity of the enzyme, however, and techniques such as circular dichroism may be required to help establish that disturbance of the protein fold and structural characteristics of the enzyme have not resulted from the mutagenesis. The amino acid substitutions made have been suggested to be "safe" in site-directed mutagenesis (Bordo & Argos, 1991). However, the absence of conformational changes would need to be confirmed.

Another of the interesting features of chorismate synthase is its often intimate relationship with NAD(P)H-dependent flavin oxidoreductase activity. The *B. subtilis* and the *E. gracilis* chorismate synthases are isolated in complex form with separable flavin reductase activities while the *N. crassa* would appear to have flavin reductase activity embedded within the chorismate synthase sequence (Henstrand *et al.*, 1995b). The relationship of the monofunctional chorismate synthases with flavin reductase activity remains unexplored and it is often suggested that 'endogenous' flavin reductase activity is responsible for providing the reduced flavin cofactor required for catalysis. It is interesting to note that some chorismate synthases have become associated intrinsically or otherwise with flavin reductase activity during evolution while others have not.

Previous research with luciferase from *Vibrio harveyi* and *Photobacterium fischeri* has demonstrated that the kinetics of the luciferase were altered in the presence of flavin reductase activity (Duane & Hastings, 1975; Jablonski & DeLuca, 1978). For example, when luciferase was present in the flavin reductase assay the apparent  $K_m$  values for NADH, NADPH and FMN were lowered. The kinetic pattern of the NADPH-specific reductase was found to change from a ping-pong mechanism to a sequential mechanism. This was suggested to be evidence that the flavin reductase was an important source of reduced FMN to luciferase and that the transfer of reduced flavin from the reductase to luciferase occurs via a complex rather than diffusion of the reduced flavin through solvent (Duane & Hastings, 1975; Jablonski & DeLuca, 1978). However, the mechanism of transfer of the reduced flavin has not been unambiguously determined. The *Vibrio harveyi* NADPH:FMN oxidoreductase has been crystallised and this may help determine whether complex formation occurs (Tanner *et al.*, 1994).

As a means of investigating possible interactions between a monofunctional chorismate synthase and a flavin reductase the *fre* gene encoding flavin reductase in *E. coli*, as published previously (Spry *et al.*, 1991), was amplified by PCR and cloned into the expression vector pTB361. The enzyme was then purified to homogeneity using a modified procedure of Fontecave *et al.* (1987). The DNA sequence of the amplified gene was checked by sequencing and the purified enzyme had a mass of  $26,115 \pm 0.82$  similar to that of the translated gene sequence (26,113) with the N-terminal methionine removed as calculated by the PEPTIDESORT program of the GCG package. The kinetics of the flavin reductase were re-evaluated since the previous study of Fontecave *et al.* (1987) had used enzyme with a purity of around 25% and further analysis would require accurate determinations of the kinetic parameters of the enzyme.

The kinetic parameters of the purified *E. coli* flavin reductase were observed to be different from those published previously most likely as a result of the increased purity of the preparation. However, relative properties with regard to different flavins as substrates were the same. Maximal activity of the enzyme was observed with riboflavin as substrate followed by FMN then FAD and NADPH was preferred over NADH as the reduced pyridine nucleotide cofactor. As reported previously the enzyme was unable to utilise FAD as substrate when NADPH was cofactor and this was suggested to be a result of steric hindrance (Fontecave *et al.*, 1987). The  $K_m$  of the enzyme with respect to the flavin substrates and the reduced nucleotide cofactor were found to be lower than reported previously by Fontecave *et al.* The catalytic efficiency of the enzyme as judged by the value of  $K_{cat}/K_m$  was observed to be high when riboflavin was the substrate ( $1.8 \times 10^8 \text{ M}^{-1}\text{S}^{-1}$  and  $7.97 \times 10^7 \text{ M}^{-1}\text{S}^{-1}$  for NADH and NADPH as cofactor, respectively).

In order to replicate some of the kinetic experiments of the luciferase/flavin reductase system with chorismate synthase and flavin reductase a direct assay of flavin reductase activity in the presence of chorismate synthase and a chorismate synthase assay in the presence of flavin reductase was attempted. The presence of *E. coli* chorismate synthase, at stoichiometric levels, in the flavin reductase assay was observed to result in no change to the  $K_m$  of riboflavin or FMN when NADPH was reduced cofactor. An attempt to couple chorismate synthase activity with the flavin reductase activity proved unsuccessful. Chorismate formation observed at 275nm was obscured by the oxidation of  $\text{NADPH} \rightarrow \text{NADP}^+$  preventing a determination of whether chorismate formation was occurring and whether the  $K_m$  of flavin was changing.

One important feature of this coupled assay was the observation that oxidation of NADPH contributed to the absorbance change at 275nm when monitoring chorismate formation. The *N. crassa* enzyme which utilises NADPH as cofactor is assayed at 275nm and presumably this assay would also measure NADPH oxidation. The  $V_{max}$  of the *N. crassa* enzyme was determined using this assay to be 32.1 U/mg (Whitc *et al.*, 1988) which is larger than *E. coli* chorismate synthase and substantially larger than the other chorismate synthases. It remains to be determined whether this assay is suitable for bifunctional chorismate synthases as an accurate measurement of  $V_{max}$ .

The failure to observe a change in the  $K_m$  value for FMN with *E. coli* flavin reductase in the presence of *E. coli* chorismate synthase led to the examination of complex formation using BIACore. The technique of BIACore involves the immobilisation of one of the proteins of interest onto a sensor chip which is coated with a metal film and which is

illuminated with light. The binding of a second enzyme to the immobilised enzyme will produce a change in the refractive index close to the surface of the sensor chip and binding can be followed in terms of the change to the refractive index. In order to determine whether there was any interaction between the *E. coli* flavin reductase and the *E. coli* chorismate synthase the flavin reductase was immobilised to the sensor chip and binding of the chorismate synthase tested. No binding of the chorismate synthase to the flavin reductase was observed. When the order of the reaction was changed such that chorismate synthase was immobilised and the flavin reductase tested for binding a similar result was obtained. Therefore, using this system and with results of the limited kinetic work it is likely that *E. coli* flavin reductase encoded by the *fre* gene does not interact with *E. coli* chorismate synthase.

The flavin reductase (FRE) encoded by the *fre* gene in *E. coli* is known to be an essential component of a complex multiprotein system that catalyses the transformation of an inactive form of ribonucleotide reductase into an active enzyme. The function of the flavin reductase is to reduce the non-heme ferric centre of ribonucleotide reductase and may provide a mechanism for regulating ribonucleotide reductase. This flavin reductase is also proposed to play a role in iron metabolism in *E. coli*. It was not possible to determine in this study whether FRE provides the reduced flavin for the chorismate synthase reaction, however, if it does so it would appear that no complex forms between the two proteins. It should be noted that there are other flavin reductase activities in *E. coli* and these may also supply reduced flavin for the chorismate synthase reaction. The chorismate synthase reaction may easily obtain enough reduced flavin *in vivo* without complex formation in organisms such as *E. coli* where there are monofunctional chorismate synthases. Other organisms which have lower levels of endogenous flavin reductase activity may have compensated with the formation of complexes or bifunctional proteins.

**Future work.**

There are a number of areas which could be further investigated following the work presented in this thesis. The unambiguous determination that the *aroC*, *aroB* and *aroA* genes of *S. aureus* form an operon could be simply done using northern blot techniques. In addition, the confirmation that the *gerC* genes are present in their entirety and that they are expressed in *S. aureus* would be important together with the ability to ascribe a function to these genes in both *B. subtilis* and *S. aureus*. Further molecular biological work could involve extended analysis of the intriguing situation that the *aro* genes have been suggested to be essential in *S. aureus* (O'Connell *et al.*, 1993). This could be confirmed with the production of more integration mutants in the *aroC* and *aroB* genes and an analysis as to whether stable attenuated strains could be obtained.

The pH dependence of the *S. aureus* chorismate synthase could be further investigated to determine whether there is a single ionisable group involved in catalysis. This may lead to further study of the enzyme using chemical modification reagents to determine essential residues for catalysis and substrate/cofactor binding. The identification of such residues using chemical modification and subsequent peptide mapping techniques would allow for a more rational mutagenesis regime to be followed for the enzyme. The tyrosine mutants produced during this study definitely warrant further study to unambiguously determine whether the tyrosine residue is essential for catalysis and if it has a role in flavin binding to the enzyme.

The crystallisation of chorismate synthase from *S. aureus*, *E. coli* or *N. crassa* would provide a wealth of information on the enzyme and would facilitate a further study of the enzyme using site-directed mutagenesis. The availability of large quantities of chorismate synthase from *S. aureus* provides another source of the enzyme for attempts at crystallisation.

**REFERENCES.**

---

- Allen, J.R., Lasser, G.W., Goldman, D.A., Booth, J.W. & Mathews, C.K.** 1983. T4 phage deoxyribonucleotide-synthesizing enzyme complex. *J. Biol. Chem.* **258:** 5746-5753.
- Almaula, N., Lu, Q., Delgado, J., Belkin, S. & Inouye, M.** 1995. Nucleoside diphosphate kinase from *Escherichia coli*. *J. Bacteriol.* **177:** 2524-2529.
- Amrhein, N. Deus, B., Gehrke, P. & Steinrucken, H.C.** 1980. The site of inhibition of the shikimate pathway. II. Interference with chorismate formation *in vivo* and *in vitro*. *Plant Physiol.* **66:** 823-829.
- Anagnostopoulos, C., Pigget, P.J. & Hoch, J.A.** 1993. The genetic map of *Bacillus subtilis*. In *Bacillus subtilis* and other Gram-positive bacteria. pp425-462. Edited by A. Sonenschein, J.A. Hoch, R. Losick. American Society for Microbiology, Washington, D.C.
- Anton, I.A. & Coggins, J.R.** 1988. Sequencing and overexpression of the *Escherichia coli aroE* gene encoding shikimate dehydrogenase. *Biochem. J.* **249:** 319-326.
- Azevedo, V., Serokin, A., Ehrlich, D. & Serror, P.** 1993. The transcriptional organization of the *Bacillus subtilis* 168 chromosome region between the *spoVAF* and *serA* genetic loci. *Mol. Microbiol.* **10:** 397-405.
- Bacon, G.A., Burrows, T.W. & Yates, M.** 1951. The effects of biochemical mutation on the virulence of *Bacterium typhosum*. The loss of virulence of certain mutants. *Br. J. Exp. Pathol.* **382:** 85-96.
- Balasubramanian, S., Abell, C. & Coggins, J.R.** 1990. Observation of an isotope effect in the chorismate synthase reaction. *J. Am. Chem. Soc.* **112:** 8581-8583.
- Balasubramanian, S., Davies, G.M. Coggins, J.R. & Abell, C.** 1991. Inhibition of chorismate synthase by (6*R*)- and (6*S*)-6-Fluoro-5-enolpyruvylshikimate 3-phosphate. *J. Am. Chem. Soc.* **113:** 8945-8946.

- Balasubramanian, S., Coggins, J.R. & Abell, C.** 1995. Observation of a secondary tritium isotope effect in the chorismate synthase reaction. *Biochem.* **34:** 341-348.
- Banerji, S., Wakefield, A.E., Allen, A.G., Maskell, D., Peters, S.E. & Hopkin, J.M.** 1993. The cloning and characterisation of the arom gene of *Pneumocystis carinii*. *J. Gen. Microbiol.* **139:** 2901-2914.
- Bartlett, P.A., Maitra, U. & Chouinard, P.M.** 1986. Synthesis of "Iso-EPSP" and evaluation of its interaction with chorismate synthase. *J. Am. Chem. Soc.* **108:** 8068-8071.
- Bentley, R.** 1990. The shikimate pathway-a metabolic tree with many branches. *Crit. Rev. Biochem. Mol. Biol.* **25:** 307-384.
- Berlyn, M.B. & Giles, N.H.** 1969. Organisation of enzymes in the polyaromatic synthetic pathway: separability in bacteria. *J. Bacteriol.* **99:** 222-230.
- Biggs, J., Tripoulas, N., Hersperger, E., Dearolf, C. & Shearn, A.** Analysis of the lethal interaction between the *prune* and *killer of prune* mutations of *Drosophila*. *Genes Dev.* **2:** 1333-1343.
- Bolotin, A., Khazak, V., Stoyanova, N., Ratmanova, K., Yomantas, Y. & Kozlov, Y.** 1995. Identical amino acid sequences of the *AroA(G)* gene products of *Bacillus subtilis* 168 and *B. subtilis* Marburg strain. *Microbiology* **141:** 2219-2222.
- Boocock, M.** 1983. Ph.D. Thesis. University of Glasgow, Glasgow.
- Bordo, D. & Argos, P.** 1991. Suggestions for "safe" residue substitutions in site-directed mutagenesis. *J. Mol. Biol.* **217:** 721-729.
- Bornemann, S., Ramjee, M.N., Lowe, D.J., Thorneley, R.N.F., Coggins, J.R., Abell, C., Nichols, W.W. & Davies, G.M.** Studies on *Escherichia coli* chorismate synthase. In Proceedings of the Eleventh International Conference on Flavins and Flavoproteins. Edited by K. Yagi. 1993. Walter de Gruyter, Berlin.
- Bornemann, S., Balasubramanian, S., Coggins, J.R., Abell, C., Lowe, D.J. & Thorneley, R.N.F.** 1995. *Escherichia coli* chorismate synthase: a deuterium kinetic-isotope effect under single-turnover conditions shows that a flavin intermediate forms before the C-(6proR)-H bond is cleaved. *Biochem. J.* **305:** 707-710.

- Bowe, F., O'Gaora, P., Maskell, D., Cafferkey, M. & Dougan, G.** 1989. Virulence, persistence, and immunogenicity of *Yersinia enterocolitica* O:8 *aroA* mutants. *Infect. Immun.* **57:** 3234-3236.
- Brockbank, S.M.V. & Barth, P.T.** 1993. Cloning, sequencing and expression of the DNA gyrase genes from *Staphylococcus aureus*. *J. Bacteriol.* **175:** 3269-3277.
- Cease, K.B., Potcová, C.A., Lohff, C.J. & Zeigler, M.E.** 1994. Optimized PCR using Vent polymerase. *PCR Meth. Appl.* **3:** 298-300.
- Charles, LG., Lamb, H.K., Pickard, D., Dougan, G. & Hawkins, A.R.** 1990. Isolation, characterization and nucleotide sequences of the *aroC* genes encoding chorismate synthase from *Salmonella typhi* and *Escherichia coli*. *J. Gen. Micro.* **136:** 253-258.
- Chatfield, S., Li, J.L., Sydenham, M., Douce, G., Dougan, G.** 1992a. *Salmonella* genetics and vaccine development. In Molecular Biology of Bacterial Infection. pp 299-312. Edited by C. E. Hormaeche, C.W. Penn, C.J. Smyth Society for General Microbiology. Symposium 49. Cambridge University Press.
- Chatfield, S.N., Fairweather, N., Charles, I., Pickard, D., Levine, M., Hone, D., Posada, M., Strugnell, R.A. & Dougan, G.** 1992b. Construction of a genetically defined *Salmonella typhi* Ty2 *aroA*, *aroC* mutant for the engineering of a candidate oral typhoid-tetanus vaccine. *Vaccine* **10:** 53-60.
- Chaudhuri, S. & Coggins, J.R.** 1985. The purification of shikimate dehydrogenase from *Escherichia coli*. *Biochem. J.* **226:** 227-231.
- Chen, Q., Actis, L.A., Tolmasky, M.E. & Crosa, J.H.** 1994. Chromosome-mediated 2,3-dihydroxybenzoic acid is a precursor in the biosynthesis of plasmid-mediated siderophore anguibactin in *Vibrio anguillarum*. *J. Bacteriol.* **176:** 4226-4234.
- Coggins, J.R. & Boocock, M.R.** The *aroM* multifunctional enzyme. In *Multidomain Proteins*. Edited by D.G. Hardie and J.R. Coggins. 1986. Elsevier Science Publishers, Amsterdam.

- Coggins, J.R., Boocock, M.R., Campbell, M.S., Chaudhuri, S., Lambert, J.M., Lewendon, A., Mousdale, D.M., Smith, D.D.S.** 1985. Biochem Soc. Trans. **13**: 299-303.
- Coggins, J.R., Duncan, K., Anton, I.A., Boocock, M.R., Chaudhuri, S., Lambert, J.M., Lewendon, A., Millar, G., Mousdale, D.M., Smith, D.D.S.** 1987. Biochem Soc. Trans. **15**: 754-759.
- Cooper, G.L., Venables, L.M., Nicholas, R.A.J., Cullen, G.A & Hormaeche, C.E.** 1992. Vaccination of chickens with chicken-derived *Salmonella enteritidis* phage type 4 *aroA* live oral salmonella vaccines. Vaccine **10**: 247-254.
- Davies, G.M., Barrett-Bee, K.J., Jude, D.A., Lehan, M., Nichols, W.W., Pinder, P.E., Thain, J.L., Watkins, W.J. & Wilson, R.G.** 1994. (6S)-6-fluoroshikimic acid, an antibacterial agent acting on the aromatic biosynthetic pathway. Antimicrob. Agents Chemother. **38**: 403-406.
- Davis, B.D.** 1955. Intermediates in amino acid biosynthesis. Adv. Enzymol. **16**:287-295.
- Defeyter, R.C. & Pittard, A.J.** 1986. Genetic and molecular analysis of *aroL*, the gene for shikimate kinase II in *Escherichia coli* K-12. J. Bacteriol. **165**: 226-232.
- Deka, R.K., Anton, I.A., Dunbar, B. & Coggins, J.R.** 1994. The characterisation of the shikimate pathway enzyme dehydroquinase from *Pisum sativum*. FEBS Lett. **349**: 397-402.
- Dougan, G., Maskell, D., Pickard, D. & Hormaeche, C.** 1987. Isolation of stable *aroA* mutants of *Salmonella typhi* Ty2: properties and preliminary characterisation in mice. Mol. Gen. Genet. **207**: 402-405.
- Duane, W. & Hastings, J.W.** 1975. Flavin mononucleotide reductase of luminous bacteria. Mol. Cell. Biochem. **6**: 53-64
- Duncan, K., Lewendon, A. & Coggins, J.R.** 1984. The purification of 5-enolpyruvylshikimate 3-phosphate synthase from an overproducing strain of *Escherichia coli*. FEBS Lett. **165**: 121-126.

- Duncan, K., Chaudhuri, S., Campbell, M.S. & Coggins, J.R. 1986. The expression and complete amino acid sequence of *Escherichia coli* 3-dehydroquinase. Biochem J. **238**: 475-481.
- Duncan, K., Edwards, R.M. & Coggins, J.R. 1987. The pentafunctional *arom* enzyme of *Saccharomyces cerevisiae* is a mosaic of monofunctional domains. Biochem. J. **246**: 375-386.
- Ewart, C.D.C., Jude, D.A., Thain, J.L. & Nichols, W.W. 1995. Frequency and mechanism of resistance to antibacterial action of ZM 240401, (6S)-6-fluoro-shikimic acid. Antimicrob. Agents Chemother. **39**: 87-93.
- Fersht, A. 1985. Enzyme Structure and Function. W.H. Freeman & Co., New York.
- Floss, H.G., Onderka, D.K. & Carroll, M. 1972. Stereochemistry of the 3-Deoxy-D-arabino-heptulosonate 7-phosphate synthetase reaction and the chorismate synthetase reaction. J. Biol. Chem. **247**: 736-744.
- Fontecave, M., Eliasson, R. & Reichard, P. 1987. NAD(P)H:flavin oxidoreductase of *Escherichia coli*. J. Biol. Chem. **262**: 12325-12331.
- Fontecave, M., Eliasson, R. & Reichard, P. 1989. Enzymatic regulation of the radical content of the small subunit of *Escherichia coli* ribonucleotide reductase involving reduction of its redox centers. J. Biol. Chem. **264**: 9164-9170.
- Fontecave, M., Coves, J. & Pierre, J.L. 1994. Ferric reductases of flavin reductases? Biometals. **7**: 3-8.
- Frost, J.W., Bender, J.L., Kadonga, J.T. & Knowles, J.R. 1984. Dehydroquinate synthase from *Escherichia coli*: purification, cloning and construction of overproducers of the enzyme. Biochem. **23**: 4470-4475.
- Ganem, B. 1978. From glucose to aromatics: recent developments in natural products of the shikimic acid pathway. Tetrahedron Report. **34**: 3353-3383.
- Gaertner F.H. & K.W. Cole. 1973. Properties of chorismate synthase in *Neurospora crassa*. J. Biol. Chem. **248**: 4602-4909.
- Gaertner F.H. & K.W. Cole. 1977. A cluster gene: evidence for one gene, one polypeptide, five enzymes. Biochem. Biophys. Res. Comm. **75**: 259-264.

- Gaudu, P., Touati, D., Niviere, V. & Fontecave, M.** 1994. The NAD(P)H:flavin oxidoreductase from *Escherichia coli* as a source of superoxide radicals. *J. Biol. Chem.* **269:** 8182-8188.
- Ghisla, S. & Massey, V.** 1986. New flavins for old: artificial flavins as active site probes for flavoproteins. *Biochem. J.* **239:** 1-12.
- Ghisla, S. & Massey, V.** 1989. Mechanisms of flavoprotein-catalyzed reactions. *Eur. J. Biochem.* **181:** 1-17.
- Gibson, F.** 1970. Preparation of chorismic acid. *Methods Enzymol.* **17:** 362-364.
- Gill, S.C. & von Hippel, P.H.** 1989. Calculation of protein extinction coefficients from amino acid sequence data. *Anal. Biochem.* **182:** 319-326.
- Ginther, C.L. & Ingraham, J.L.** 1974. Cold-sensitive mutant of *Salmonella typhimurium* defective in nucleosidediphosphokinase. *J. Bacteriol.* **118:** 1020-1026.
- Gorlach, J., Schmid, J. & Amrhein, N.** 1993. Differential expression of tomato (*Lycopersicon esculentum* L.) genes encoding shikimate pathway enzymes. II. Chorismate synthase. *Plant Mol. Biol.* **23:** 707-716.
- Grantham, R., Gautier, C., Gouy, Mercier, R. & Pave, A.** 1981. Codon catalog usage and the genome hypothesis. *Nucleic Acids. Res.* **8:** 49-53.
- Griffin, H.G. & Barrow, P.A.** 1993. Construction of an *aroA* mutant of *Salmonella* serotype Gallinarum: its effectiveness in immunization against experimental fowl typhoid. *Vaccine* **11:** 457-461.
- Halle, F. & Meyer, J-M.** 1992. Ferrisiderophore reductases of *Pseudomonas*: purification, properties and cellular location of the *Pseudomonas aeruginosa* ferripyoverdine reductase. *Eur. J. Biochem.* **209:** 613-620.
- Hama, H., Almaula, N., Lerner, C.G., Inouye, S. & Inouye, M.** 1991. Nucleoside diphosphate kinase from *Escherichia coli* its overproduction and sequence comparison with eukaryotic enzymes. *Gene* **105:** 31-36.
- Hanks, S.K., Quinn, A.M. & Hunter, T.** 1988. The protein kinase family:conserved features and deduced phylogeny of the catalytic domains. *Science* **241:** 4342-4352.

- Harris, J., Kleanthous, C., Coggins, J.R., Hawkins, A.R. & Abell, C.** 1993. Different mechanistic and stereochemical courses for the reactions catalysed by type I and type II dehydroquinases. *J. Chem. Soc., Chem. Commun.* 1080-1081.
- Hasan, N. & Nester, E.W.** 1978a. Purification and characterisation of NADPH-dependent flavin reductase; an enzyme required for the activation of chorismate synthase in *Bacillus subtilis*. *J. Biol. Chem.* **253**: 4987-4992.
- Hasan, N. & Nester, E.W.** 1978b. Purification and properties of chorismate synthase from *Bacillus subtilis*. *J. Biol. Chem.* **253**: 4993-4998.
- Hasan, N. & Nester, E.W.** 1978c. Dehydroquinate synthase in *Bacillus subtilis*; an enzyme associated with chorismate synthase and flavin reductase. *J. Biol. Chem.* **253**: 4987-4992.
- Haslam, E.** 1993. Shikimic Acid: Metabolism and Metabolites. John Wiley & sons, Chichester, England.
- Hastings, J.W., Potrikus, C.J., Gupta, S.C., Kurkust, M. & Makenson, J.C.** 1985. Biochemistry and physiology of bioluminescent bacteria. *Adv. Microb. Physiology.* **26**: 235-291.
- Hawkes, T.R., Lewis, T., Coggins, J.R., Mousdale, D.M., Lowe D.J. & Thorneley, R.N.F.** 1990. Chorismate synthase; pre-steady-state kinetics of phosphate release from 5-enolpyruvylshikimate 3-phosphate. *Biochem. J.* **265**: 899-902.
- Henner, D.** (1991). Unpublished sequence data. *gerCAgerCBgerCC, ndk, cheR, aroFaroBaroH* nucleotide sequence. Genbank accession No. M80245.
- Henner, D.J., Band, L., Flaggs, G. & Chen, E.** 1986. The organization and nucleotide sequence of the *Bacillus subtilis hisH, tyrA, aroE* genes. *Gene* **49**: 147-152.
- Henner, D.J., Gollnick, P. & Moir, A.** 1990. Analysis of an 18 kilobase pair region of the *Bacillus subtilis* chromosome containing the *mtr* and *gerC* operons and the *aro-trp-aro* supraoperon. In 6th International Symposium on Genetics of Industrial Microorganisms p657-665. Edited by H. Heslot, J. Davies, J. Florent, L. Bobichon, G. Durand, L. Penasse. Societe Francaise de Microbiologie, Strasbourg, France.

**Henner, D. & Yanofsky, C.** 1993. Biosynthesis of aromatic amino acids. In *Bacillus subtilis* and other Gram-positive bacteria. pp269-280. Edited by A. Sonenshein, J.A. Hoch, R. Losick. American Society for Microbiology, Washington, D.C.

**Henstrand, J. M., Amrhein, N. & Schmid, J.** 1995a. Cloning and characterization of a heterologously expressed bifunctional chorismate synthase/flavin reductase from *Neurospora crassa*. *J. Biol. Chem.* **270**: 20447-20452.

**Henstrand, J. M., Schmid, J. & Amrhein, N.** 1995b. Only the mature form of the plastidic chorismate synthase is enzymatically active. *Plant Physiol.* **108**:

**Higuchi, R., Krummel, B. & Saiki, R.K.** 1988. A general method of in vitro preparation and specific mutagenesis of DNA fragments: study of protein:DNA interactions. *Nucleic Acids Res.* **208**: 7351-7383.

**Hill, R.K. & Bock, M.G.** 1978 Stereochemistry of 1,4-conjugate elimination reactions. *J. Am. Chem. Soc.* **100**: 637-639.

**Hill, R.K. & Newkome, G.R.** 1969. Stereochemistry of chorismic acid biosynthesis. *J. Am. Chem. Soc.* **91**: 5893-5894.

**Hoiseth, S.K. & Stocker, B.A.D.** 1981. Aromatic-dependent *Salmonella typhimurium* are non-virulent and are effective live vaccines. *Nature* **241**: 238-239.

**Homchampa, P., Strugnell, R.A. & B. Adler.** 1992. Molecular analysis of the *aroA* gene of *Pasteurella multocida* and vaccine potential of a constructed *aroA* mutant. *Mol. Microbiol.* **6**: 3585-3593.

**Huang, L., Montoya, A.L. & Nester, E.W.** 1974a. Characterization of the functional activities of the subunits of 3-deoxy-D-arabinoheptulosonate 7-phosphate synthase-chorismate mutase from *Bacillus subtilis* 168. *J. Biol. Chem.* **249**: 4473-4479.

**Huang, L., Nakatsukasa, W.M. & Nester, E.W.** 1974b. Regulation of aromatic biosynthesis in *Bacillus subtilis* 168. *J. Biol. Chem.* **249**: 4473-4479.

**Huang, L., Montoya, A.L. & Nester, E.W.** 1975. Purification and characterization of shikimate kinase enzyme activity in *Bacillus subtilis* 168. *J. Biol. Chem.* **250**: 7675-7681.

**Ikemura, T. & Ozeki, H.** 1983. Codon usage and transfer RNA contents: organism specific codon-choice patterns in reference to the isoacceptor contents. *Cold Spring Harbor Symp. Quant. Biol.* **47:** 1087-1097.

**Ivins, B.E., Welkos, S.L., Knudson, G.B. & Little, S.F.** 1990. Immunization against anthrax with aromatic compound-dependent (*Aro<sup>-</sup>*) mutants of *Bacillus anthracis* and with recombinant strains of *Bacillus subtilis* that produce anthrax protective antigen. *Infect. Immun.* **58:** 303-308.

**Jablonski, E. & DeLuca, M.** 1978. Studies of the control luminescence in *Beneckea harveyi*: properties of the NADH and NADPH:FMN oxidoreductases. *Biochem.* **17:** 672-678.

**Jensen, R. A. & Nester, E.W.** 1965. The regulatory significance of intermediary metabolites: control of aromatic acid biosynthesis by feedback inhibition in *Bacillus subtilis*. *J. Mol. Biol.* **12:** 468-481.

**Jensen, R. A., Nasser, D.S. & Nester, E.W.** 1967. Comparative control of a branch-point enzyme in microorganisms. *J. Bacteriol.* **94:** 1582-1593.

**Jensen, R.A. & Nester, E.W.** 1966. Regulatory enzymes of aromatic acid biosynthesis in *Bacillus subtilis*. I. Purification and properties of 3-deoxy-D-arabino-heptulosonate 7-phosphate synthetase. *J. Biol. Chem.* **241:** 3365-3371.

**Jones, D.G.L., Reusser, U. & Braus, G.H.** 1991. Molecular cloning, characterization and analysis of the regulation of the *ARO2* gene, encoding chorismate synthase, of *Saccharomyces cerevisiae*. *Mol. Microbiol.* **5:** 2143-2152.

**Jones, P.W., Dougan, G., Haywood, C., Mackensie, N., Collins, P. & Chatfield, S. N.** 1991. Oral vaccination of calves against experimental salmonellosis using a double *aro* mutant of *Salmonella typhimurium*. *Vaccine* **9:** 29-33.

**Jude, D.A., Ewart, C.D.C, Thain, J.L., Davies, G.M. & Nichols, W.W.** Transport of the antibacterial agent (6S)-6-fluoroshikimate and other shikimate analogues by the shikimate transport system of *Escherichia coli*. In press.

**Karnell, A., Cam, P.D., Verma, N. & Lindberg, A.A.** 1993. *AroD* deletion attenuates *Shigella flexneri* strain 2457T and makes it a safe and efficacious oral vaccine in monkeys. *Vaccine* **11:** 830-836.

- Kleanthous, C., Deka, R., Davis, K., Kelly, S.M., Cooper, A., Harding, S.E., Price, N.C., Hawkins, A.R. & Coggins, J.R.** 1992. A comparison of the enzymological and biophysical properties of two distinct classes of dehydroquinase enzymes. *Biochem. J.* **282**: 687-695.
- Klein, M.L. & Fulco, A.J.** 1993. Critical residues involved in FMN binding and catalytic activity in cytochrome P450<sub>BM-3</sub>. *J. Biol. Chem.* **268**: 7553-7561.
- Koike-Takehita, A., Koyama, T., Obata, S., Ogura, K.** 1995. Molecular cloning and nucleotide sequence of the genes for two essential proteins constituting a novel enzyme system for heptaprenyl diphosphate synthesis. *J. Biol. Chem.* **270**: 18396-18400.
- Koshiba, T.** 1978. Purification of two forms of the associated 3-dehydroquinate hydro-lyase and shikimate:NADP+ oxidoreductase in *Phaseolus mungo* seedlings. *Biochim. Biophys. Acta* **522**: 10-18.
- Lacombe, M., Wallet, V., Troll, H. & Veron, M.** 1990. Functional cloning of a nucleoside diphosphate kinase from *Dictyostelium discoideum*. *J. Biol. Chem.* **265**: 10012-10018.
- Laemmli, U.K.** 1970. Cleavage of structural proteins during the assembly of the head of bacteriophage T4. *Nature* **227**: 680-685.
- Lauhon, C.T. & Bartlett, P.A.** 1994. Substrate analogues as mechanistic probes for the bifunctional chorismate synthase from *Neurospora crassa*. *Biochem.* **33**: 14100-14108.
- Lei, B., Liu, M., Huang, S. & Tu, S.** 1994. *Vibrio harveyi* NADPH-flavin oxidoreductase: cloning, sequencing and overexpression of the gene and purification and characterization of the cloned enzyme. *J. Biol. Chem.* **176**: 3552-3558.
- De Ley, J.** 1970. Reexamination of the association between melting point, buoyant density, and chemical base composition of deoxyribonucleic acid. *J. Bacteriol.* **101**: 738-754.
- Llewellyn, D.J., Daday, A. & Smith, G.D.** 1980. Evidence for an artificially evolved bifunctional 3-deoxy-D-arabinoheptulosonate 7-phosphate synthase-chorismate mutase in *Bacillus subtilis*. *J. Biol. Chem.* **255**: 2077-2084.

- Lo, H-S. & Reeves, R.E.** 1980. Purification and properties of NADPH: flavin oxidoreductase from *Entamoeba histolytica*. *Mol. Biol. Parasitol.* **2**: 23-30.
- Luckner, M.** 1990. Secondary metabolism in microorganisms, plants and animals. Springer-Verlag, Berlin.
- Lumsden, J. & Coggins, J.R.** 1977. The subunit structure of the *arom* multienzyme complex of *Neurospora crassa*: a possible pentafunctional polypeptide chain. *Biochem. J.* **161**: 599-607.
- Lumsden, J. & Coggins, J.R.** 1978. The subunit structure of the *arom* multienzyme complex of *Neurospora crassa*: Evidence from peptide 'maps' for the identity of the subunits. *Biochem. J.* **169**: 441-444.
- Macheroux, P., Petersen, J., Bornemann, S., Lowe, D.J., Thorneley, R.N.F.** 1995. Binding of the oxidized, reduced and radical flavinsemiquinone species to chorismate synthase; an investigation by spectrophotometry, fluorimetry, EPR, and ENDOR spectroscopy. Unpublished.
- Majumder, K., Selvapandian, A., Fattah, F.A., Arora, N., Ahmad, S. & Bhatnagar, R.K.** 1995. 5-enolpyruvylshikimate 3-phosphate synthase of *Bacillus subtilis* is an allosteric enzyme. *Eur. J. Biochem.* **229**: 99-106.
- Matsudaira, P.** 1987. Sequence from picomole quantities of proteins electroblotted onto polyvinylidene difluoride membranes. *J. Biol. Chem.* **262**: 10035-38.
- Millar, G.** 1988. PhD Thesis. University of Glasgow, Glasgow.
- Millar, G., Lewendon, A., Hunter, M.G. & Coggins, J.R.** 1986. The cloning and expression of the *aroL* gene from *Escherichia coli* K12. *Biochem. J.* **237**: 427-437.
- Miller, L.K. & Wells, R.D.** 1971. Nucleoside diphosphokinase activity associated with DNA polymerases. *Proc. Natl. Acad. Sci.* **68**: 2298-2302.
- Moffat, B.A. & Studier, F.W.** 1987. T7 lysozyme inhibits transcription by T7 RNA polymerase. *Cell* **49**: 221-227.
- Mousdale, D.M. & Coggins, J.R.** 1986. Detection and subcellular localization of a higher plant chorismate synthase. *FEBS Lett.* **205**: 328-332.

- Muller, F., Brustlein, M., Hemmerich, P., Massey, V. & Walker, W.H.** 1972. Light-absorption studies on neutral flavin radicals. *Eur. J. Biochem.* **25**: 573-580.
- Munoz-Dorado, J., Inouye, M. & Inouye, S.** 1990. Nucleoside diphosphate kinase from *Myxococcus xanthus* I. cloning and sequencing the gene. *J. Biol. Chem.* **265**: 2702-2706.
- Munoz-Dorado, J., Inouye, S. & Inouye, M.** 1990. Nucleoside diphosphate kinase from *Myxococcus xanthus* II. Biochemical characterization. *J. Biol. Chem.* **265**: 2707-2712.
- Nakane, A., Ogawa, K., Nakamura, K. & Yamane, K.** 1994. Nucleotide sequence of the shikimate kinase gene (*aroI*) of *Bacillus subtilis*. *77*: 312-314.
- Nakatsukasa, W.M. & Nester, E.W.** 1972. Regulation of aromatic amino acid biosynthesis in *Bacillus subtilis* 168. *J. Biol. Chem.* **247**: 5972-5979.
- Nester, E.W., Jensen, R.A & Nasser, D.S.** 1969. Regulation of enzyme synthesis in the aromatic amino acid pathway of *Bacillus subtilis*. *97*: 83-90.
- Nnalue, N.A. & Stocker, B.A.D.** 1987. Tests of the virulence and live-vaccine efficacy of auxotrophic and *galE* derivatives of *Salmonella choleraesuis*. *Infect. Immun.* **55**: 955-962.
- Novick, R.P.** 1990. The *Staphylococcus* as a molecular genetic system. In Molecular Biology of the Staphylococci, pp1-37. Edited by R.P. Novick. VCH. New York.
- O'Callaghan, D., Maskell, D., Liew, F.Y., Easmon, C.S. & Dougan, G.** 1988. Characterization of aromatic- and purine-dependent *Salmonella typhimurium*: attenuation, persistence, and ability to induce protective immunity in BALB/c mice. *Infect. Immun.* **56**: 419-423.
- O'Connel, C., Pattee, P. & Foster, T.J.** 1993. Sequence and mapping of the *aroA* gene of *Staphylococcus aureus* 8325-4. *J. Gen. Microbiol.* **139**: 1449-1460.
- Onderka, D.K. & Floss, H.G.** 1969. Steric course of the chorismate synthetase reaction and the 3-deoxy-D-arabinoheptulosonate 7-phosphate synthetase reaction. *J. Amer. Chem. Soc.* **91**: 5894-5896.

- Oster, T., Boddupali, S.S. & Peterson, J.A.** 1991. Expression, purification and properties of the flavoprotein domain of cytochrome P450<sub>BM-3</sub>. *J. Biol. Chem.* **266**: 22718-22725.
- Parks, R.E. & Agarwal, R.P.** 1973. Nucleoside diphosphokinases pp307-333. *In The Enzyme*. Edited by P.D. Boyer. Academic Press, New York.
- Pattee, P.A.** 1981. Distribution of Tn551 Insertion sites responsible for auxotrophy on the *Staphylococcus aureus* chromosome. *J. Bacteriol.* **145**: 479-488.
- Pattee, P.A., Lee, H. & Bannantine & J.P.** 1990. Genetic and physical mapping of the chromosome of *Staphylococcus aureus*, pp. 41-58. *In Molecular biology of the staphylococci*. Edited by R.P. Novick, VCH publishers, New York.
- Pattee, P.A.** 1993. The genetic map of *Staphylococcus aureus*. pp489-496. *In Bacillus subtilis and other Gram-positive bacteria*. Edited by A.L. Sonenshein, J.A. Hoch, R.L. Losick. American Society for Microbiology, Washington, D.C.
- Pittard, A.J. & Wallace, B.J.** 1966. Distribution and function of genes concerned with aromatic biosynthesis in *Escherichia coli*. *J. Bacteriol.* **91**: 1494-1508.
- Pittard, A.J.** 1987. *In Escherichia coli and Salmonella typhimurium: Cellular and Molecular Biology*. Volume 1, pp 368-395. Edited by F.C. Niedhart. American Society for Microbiology, Washington, D.C.
- Polley, L.D.** 1978. Purification and characterization of 3-dehydroquinate hydrolase and shikimate oxidoreductase: evidence for a bifunctional enzyme. *Biochim. Biophys. Acta* **526**: 259-266.
- Poirier, T.P., Kehoe, M.A. & Beachey, E.H.** 1988. Protective immunity evoked by oral administration of attenuated *aroA* *Salmonella typhimurium* expressing cloned streptococcal M protein.. *J. Exp. Med.* **168**: 25-32.
- Porter, T. D.** 1991. An unusual yet strongly conserved flavoprotein reductase in bacteria and mammals. *TIBS*. **16**: 154-158.
- Porter, T.D. & Kasper, C.B.** 1985. Coding nucleotide sequence of rat NADPH-cytochrome P-450 oxidoreductase cDNA and identification of flavin-binding domains. *Proc. Natl. Acad. Sci.* **82**: 973-977.

- Ramjee, M.K., Coggins, J.R., Hawkes, T.R. Lowe, D.J. & Thorneley, R.N.F.** 1991. Spectrophotometric detection of a modified flavin mononucleotide intermediate formed during the catalytic cycle of chorismate synthase. *J. Am. Chem. Soc.* **113**: 8566-8567.
- Ramjee, M.K.** 1992. Ph.D. Thesis. University of Sussex, Brighton.
- Ramjee, M.K., Balasubramanian, S. Abell, C. Coggins, J.R. Davies, G.M. Hawkes, T.R. Lowe, D.J. & Thorneley, R.N.F.** 1992. Reaction of (6R)-6-F-EPSP with recombinant *Escherichia coli* chorismate synthase generates a stable flavin mononucleotide semiquinone radical. *J. Am. Chem. Soc.* **114**: 3151-3153.
- Ramjee, M.K., Coggins, J.R. & Thorneley, R.N.F.** 1994. A continuous, anaerobic spectrophotometric assay for chorismate synthase activity that utilizes photoreduced flavin mononucleotide. *Analyt. Biochem.* **220**: 137-141.
- Roberts, M., Maskell, D., Novotny, P. & Dougan, G.** 1990. Construction and characterization in vivo of *Bordetella pertussis aroA* mutants. *Infect. Immun.* **58**: 732-739.
- Rosengard, A.M., Krutzsch, H.C., Shearn, A., Biggs, J.R., Barker, E., Margulies, I.M.K., King, C.R., Liotta, L.A. & Steeg, P.S.** 1989. Reduced Nm23/Awd protein in tumour metastasis and aberrant *Drosophila* development. *Nature* **342**: 177-180.
- Sambrook, J., Fritsch, E.F. & Maniatis, T.** 1989. Molecular Cloning: a Laboratory Manual. 2nd edn. Cold Spring Harbor, NY: Cold Spring Harbor Laboratory.
- Schaller, A., Afferden, M., Windhofer, V., Bulow, S., Abel, C., Schmid, J. & Amrhein, N.** 1991. Purification and characterization of chorismate synthase from *Euglena gracilis*. *Plant Physiol.* **97**: 1271-1279.
- Schaller, A., Schmid, J., Leibinger U. & Amrhein, N.** 1991. Molecular cloning and analysis of a cDNA coding for chorismate synthase from the higher plant *Corydalis sempervirens* Pers. *J. Biol. Chem.* **266**: 21434-21438.

- Schaller, A., Windhofer, V. & Amrhein, N.** 1990. Purification of chorismate synthase from a cell culture of the higher plant *Corydalis sempervirens* Pers. Arch. Biochem. Biophys. **282**: 437-442.
- Schmidt, J., Bubunenko, M. & Subramanian A.R.** 1993. A novel operon organization involving the genes for chorismate synthase (aromatic biosynthesis pathway) and ribosomal GTPase center proteins (L11, L1, L10, L12: rplKAJL) in cyanobacterium *Synechocystis* PCC 6803. J. Biol. Chem. **268**: 27447-27457.
- Shen, A.L., Porter, T.D., Wilson, T.E. & Kasper, C.B.** 1989. Structural analysis of the FMN binding domain of NADPH-cytochrome P-450 oxidoreductase by site-directed mutagenesis. J. Biol. Chem. **264**: 7584-7589.
- Shneir, A., Harris, J., Kleanthous, C., Coggins, J.R., Hawkins, A.R. & Abell, C.** 1991. Evidence for opposite stereochemical courses for the reactions catalysed by type I and type II dehydroquinases. J. Am. Chem. Soc. **113**: 9416-9418.
- Short, J.M., Fernandez, J.M., Sorge, J.A. & W.D. Hause.** 1988.  $\lambda$ -ZAP: a bacteriophage  $\lambda$  expression vector with *in vivo* excision properties. Nucleic Acids Res. **16**: 7583-7600.
- Shuttleworth, W. A., Hough, C.D., Bertrand, K.P. & Evans, J.N.S.** 1992. Overproduction of 5-enolpyruvylshikimate-3-phosphate synthase in *Escherichia coli*: use of the T7 promoter. Protein Eng. **5**: 461-466
- Somerville, R.L.** 1983. Tryptophan: biosynthesis, regulation and large scale production. In *Amino Acids: Biosynthesis and Genetic Regulation*, edited by K.M. Hermann & R.L. Somerville. Addison-Wesley, Massachusetts.
- Sorokin, A., Zumstein, E., Azevedo, S., Ehrlich, D. & Serrr, P.** 1993. The organization of the *Bacillus subtilis* 168 chromosome region between the *spoVA* and *serA* genetic loci, based on sequence data. Mol. Microbiol. **10**: 385-395.
- Southern, E.** 1975. Detection of specific sequences among DNA fragments separated by gel electrophoresis. J. Mol. Biol. **98**: 503-517.
- Springer, D.B.** 1961. The biosynthesis of aromatic compounds from D-glucose Adv. Carbohydrate Chem. **15**: 235-252.

- Spryou, G., Haggard-Ljungquist, E., Krook, M., Jornvall, H., Nilsson, E. & Reichard, P. 1991. Characterization of the flavin reductase gene (*fre*) of *Escherichia coli* and construction of a plasmid for overproduction of the enzyme. *J. Bacteriol.* **173**: 3673-3679.
- Strugnell, R., Dougan, G., Chatfield, S., Charles, I., Fairweather, N., Tite, J., Li, J.L., Beesley, J. & Roberts, M. 1992. Characterization of a *Salmonella typhimurium* aro vaccine strain expressing the P.69 antigen of *Bordetella pertussis*. *Infect. Immun.* **60**: 3994-4002.
- Studier, F.W. and B.A. Moffatt. 1986. Use of bacteriophage T7 RNA polymerase to direct selective high-level expression of cloned genes. *J. Mol. Biol.* **189**: 113-130.
- Sutherland, J.K., Watkins, W.J., Bailey, J.P., A.K., Chapman, A.K. & Davies, G.M. 1989. The synthesis of 6 $\alpha$ - and 6 $\beta$ -fluoroshikimic acids. *J. Chem. Soc. Chem. Commun.*: 1386-1387.
- Takahashi, I., Ogura, K., Seto, S. 1980. Heptaprenyl diphosphate synthetase from *Bacillus subtilis*. *J. Biol. Chem.* **255**: 4539-4543.
- Tanner, J., Lei, B., Liu, M., Tu, S. & Krause, K.L. 1994. Crystallization and preliminary crystallographic analysis of NADPH:FMN oxidoreductase from *Vibrio harveyi*. *J. Mol. Biol.* **241**: 283-287.
- Tribe, D.E., Camakaris, H. & Pittard, J.A. 1979. Constitutive and repressible enzymes of the common pathway of aromatic biosynthesis in *E. coli* K-12: regulation of enzyme synthesis at different growth rates. *J. Bacteriol.* **127**: 1085-1091
- Troll, H., Winckler, T., Lascu, I., Muller, N., Saurin, W., Veron, M. & Mutzel, R. 1993. Separate nuclear genes encode cytosolic and mitochondrial nucleoside diphosphate kinase in *Dictyostelium discoideum*. *J. Biol. Chem.* **268**: 25469-25475.
- Vaughan, L.M., Smith, P.R. & Foster, T.J. 1993. An aromatic-dependent mutant of the fish pathogen *Aeromonas salmonicida* is attenuated in fish and is effective as a live vaccine against the salmonid disease furunculosis. *Infect. & Immun.* **61**, 2172-2181.

- Vellanoweth, R.L.** 1993. Translation and its regulation. In *Bacillus subtilis* and other Gram-positive bacteria. pp699-711. Edited by A.L. Sonenshein, J.A. Hoch, R.L. Losick. American Society for Microbiology, Washington, D.C.
- Verma, N.K. & Lindberg, A.A.** 1991. Construction of aromatic dependent *Shigella flexneri* 2a live vaccine candidate strains: deletion mutations in the *aroA* and the *aroD* genes. *Vaccine* **9**: 6-9.
- Voet, D. & Voet, J.G.** 1990. Biochemistry. John Wiley & Sons, USA.
- Warburg, R.J., Mahler, I., Tipper, D.J. & Halvorson, H.O.** 1984. Cloning of the *Bacillus subtilis* 168 *aroC* gene encoding dehydroquinase. *Gene* **32**: 57-66.
- Watanabe, H. & Hastings, J.W.** 1982. Specificities and properties of three reduced pyridine nucleotide-flavin mononucleotide reductases coupling to bacterial luciferase. *Mol. Cell. Biochem.* **44**: 181-187.
- Welch, G.R., Cole, K.W. & Gaertner, F.H.** 1974. Chorismate synthase of *Neurospora crassa*. *Arch. Biochem. Biophys.* **165**: 505-518.
- Whipp, M.J. & Pittard, A.J.** 1995. A reassessment of the relationship between *aroK*- and *aroL*-encoded shikimate kinase enzymes of *Escherichia coli*. *J. Bacteriol.* **177**: 1627-1629.
- White, P.J., Mousdale, D.M. & Coggins, J.R.** 1987. A simple anaerobic assay for chorismate synthase. *Biochem. Soc. Tans.* **15**: 144-145
- White, P.J., Millar, G. & Coggins, J.R.** 1988. The overexpression, purification and complete amino acid sequence of chorismate synthase from *Escherichia coli* K12 and its comparison with the enzyme from *Neurospora crassa*. *Biochem. J.* **251**: 313-322.
- Williams, R.L., Oren, D.A., Munoz-Dorado, J., Inouye, S., Inouye, M. & Arnold, E.** 1993. Crystal structure of *Myxococcus xanthus* nucleoside diphosphate kinase and its interaction with a nucleotide substrate at 2.0 Å resolution. *J. Mol. Biol.* **234**: 1230-1247.
- Willet, H.P.** 1988. In Zinsser Microbiology, pp128-161. Edited by Joklik, W., Willet, H.P., Amos, D.B., Wilfert, C.M. Prentice-Hall International Inc. USA.

- Yanisch-Peron, C., Vieira, J. & Messing, J.** 1985. Improved M13 phage cloning vectors and host strains : nucleotide sequences of the M13mp18 and pUC19 vectors. *Gene* **33**: 103-119.
- Yazdi, M. A.** 1991. Ph.D. Thesis. University of Sheffield, Sheffield.
- Zalkin, H. & Ebbole, D.J.** 1988. Organization and regulation of genes encoding biosynthetic enzymes in *Bacillus subtilis*. *J. Biol. Chem.* **263**: 1595-1598.
- Zenno, S. & Saigo, K.** 1994. Identification of the genes encoding NAD(P)H-flavin oxidoreductases that are similar in sequence to *Escherichia coli* Frb in four species of luminous bacteria: *Photorhabdus luminescens*, *Vibrio fischeri*, *Vibrio harveyi* and *Vibrio orientalis*. *J. Bacteriol.* **176**: 3544-3551.

